The Official Journal of Indian College of Cardiology, Kerala Chapter

Vol. 6, Issue - 1 September 2022

KJC 6

Kerala Journal of Cardiology

Focus Topic: **Imaging in Cardiology**

Cover image: ***Heart in Bloom***, Digital painting by Almaaz Anwer.

The artist is an architect and interior designer based at Australia. Her passion for creating abstract concepts using the digital medium is akin to how imaging adds colour to our understanding of the fascinating human heart.
E-mail: almaazanwer@gmail.com

KJC

Kerala Journal of Cardiology

The Official Journal of Indian College of Cardiology, Kerala Chapter

KJC

Journal lay-out and printing: Vision Grafix, Thiruvananthapuram-695 012. Phone: 9072340914, E-mail: visiongrafix@gmail.com

CONTENTS

Editorial

KJC Diamonds

Focus topic : Imaging in Cardiology

KJC Pearls

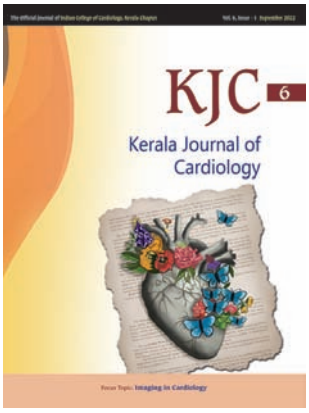

Through the Looking-Glass

Sajan Ahmad Z

Senior Consultant in Cardiology
Parumala Cardiovascular Centre, Thiruvalla, Kerala, India.

Seeing is believing, but feeling is the truth.
Thomas Fuller, 17th Century

Greetings from Kerala Journal of Cardiology (KJC) and Indian College of Cardiology (ICC), Kerala Chapter.

The word *image* has its roots in the Latin word *imitari,* meaning 'to copy, or imitate the subject or object of interest'. Imaging has transformed the science of Cardiology and added precision to diagnostic and therapeutic pathways, thus enhancing patient care and outcomes. After focus issues on congenital heart disease, valvular heart disease, interventions of the inter-atrial septum, pulmonary hypertension and hypertrophic cardiomyopathy, the 6th issue of Kerala Journal of Cardiology (KJC) is intended to throw light on the major imaging modalities that we use in clinical practice. Like Alice in Lewis Carroll's *Through the Looking-Glass,* we may find the true wonders of the heart.

KJC Diamonds section begins with Chest Xrays which continue to be used more than a century after the invention. Next on the list is Cardiac MRI which has revolutionised our understanding of myocardial diseases. Nuclear Cardiology has always been a grey area for cardiologists and merits more understanding for its optimal utilisation. Intracoronary imaging with IVUS and OCT have become ideal tools for coronary intervention. Intracardiac echo is becoming a useful adjunct in interventional procedures for structural heart disease and in electrophysiology practice. As in all fields, artificial intelligence has its share of application in imaging too, albeit in an evolving fashion.

KJC Pearls starts off with an international author in *Beyond the Heart,* with a transplant nephrologist's approach to hypertension management in post renal transplant patients. *Surgeon's Den* features an original article on minimally invasive beating heart closure of ASD. Zero contrast angioplasty and it's niche role are discussed in the *Case Report* section. After p value and confidence interval, *Statistics Simplified* marches on to the Kaplan – Meier curve and survival analysis. *KJC Classroom* talks about saline contrast echocardiography through a case based approach. *History of Cardiology* takes us on the interesting and inspiring journey of echocardiography. In *Resident's Corner,* we have a snapshot of LV non compaction and it's various diagnostic criteria. *Evidence Hub* presents the data on Bempedoic acid, the new arrival on the lipid scene.

The Editorial Board wishes to thank all the current and past office-bearers of ICC Kerala for the unflinching support. We are also happy that this issue is being released on the occasion of the 29th National ICC Conference and place on record our gratitude to the Organising Team and the office-bearers of National ICC.

A love for Cardiology was the key driving force for starting this journal and the KJC philosophy remains, as ever, in the celebration of the science, practice and art of this beautiful subject. We hope it will continue to be useful for post graduates and consultants alike as a medium for sharing information in a reader friendly manner.

With warm regards as always from the heart...

Team KJC

Address for correspondence: Dr. Sajan Ahmad Z, MD, DM, DNB, 16 FG, Skyline Edge, Thirumoolapuram, Thiruvalla, Kerala, India – 689115.
Ph: 9447097965, Email: sajanahmad@gmail.com

KJC Diamonds

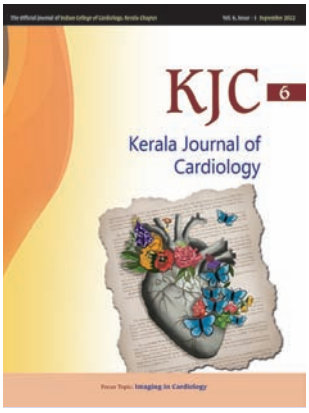

Primer on Chest X-Ray in Cardiac Diseases

M Sudhakar Rao
Associate Professor , Cardiology, KMC Manipal, MAHE Manipal.

Raghav Nagpal
Senior Resident, Cardiology, KMC Manipal, MAHE Manipal.

INTRODUCTION

Despite advances in various imaging modalities, the chest radiograph remains an important initial diagnostic tool in cardiac patients. Interpreting a chest radiograph involves checking the side markers, determining the projection(PA, AP or supine), assessing technical adequacy of the film(exposure, rotation, inspiratory or expiratory), identify and assess position of medical devices, categorising detected abnormalities, reviewing previous films and suspecting cardiac disease based on preformed criteria's. This article provides a guide to the systematic interpretation of a chest radiograph and a review of the classic radiological signs of cardiac disease.

OUTLINE OF THE ARTICLE

A. Differentiation between Inspiratory vs Expiratory Film/Structures seen in PA and Lateral view
B. Diagnosis of chamber enlargement
C. Diagnosis of PAH, PVH and vascularity
D. Diagnosis of cardiomyopathy and Pericardial diseases
E. Diagnosis of Pulmonary and Aortic diseases
F. X ray in congenital heart diseases

Address for correspondence: Dr M Sudhakar Rao, MD DM (Cardiology), Associate Professor, Department of Cardiology, KMC Manipal, Mahe.
Phone: +919902547712, Email Id: msudhakar88@gmail.com

A. DIFFERENTIATION BETWEEN PA VIEW AND AP VIEW AND STRUCTURES SEEN IN AP AND LATERAL VIEW

PA view	AP view
In erect patients	In supine patients
Vertebral spines morepromínent	Vertebral bodies clear
Scapulae clear of lungs	Scapulae overlap
Clavicles are horizontal	Clavicles are oblique
Gas bubble in fundus with a clear air fluid level	Gas bubble in antrum
No apparent cardiomegaly	Apparent cardiomegaly
Overriding of clavicle and first rib	Not prominent
Clavicle companion shadow	Absent

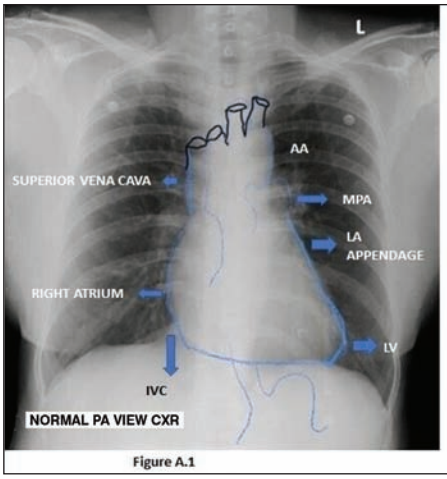

Figure A.1

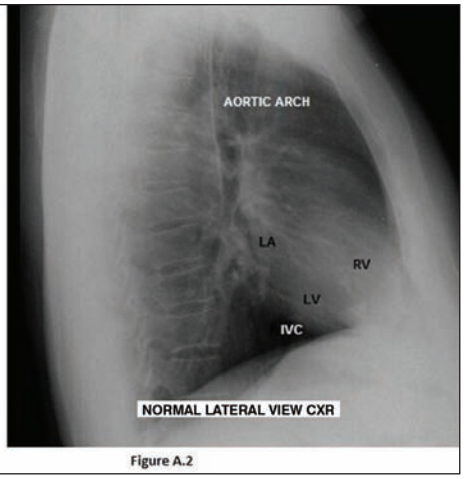

Figure A.2

B. ASSESSMENT OF CARDIOMEGALY AND CHAMBER ENLARGEMENT

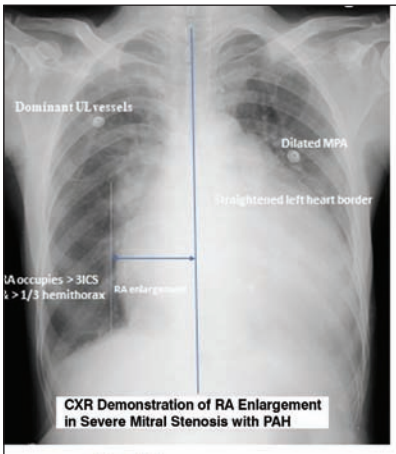

Figure B.1

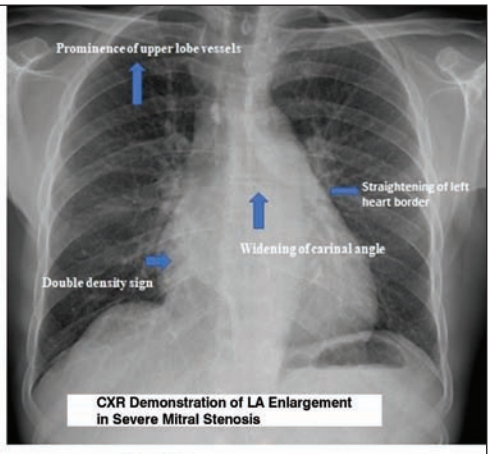

Figure B.2

1. Assessment of cardiomegaly

Normally less than 0.55
>0.55 in Adults – Cardiomegaly
>0.60 in Newborns – Cardiomegaly
Any increase in transcardiac diameter > 2 cm compared to old x-ray
In old age and emphysema a transcardiac diameter more than 15.5 cm in males &>12.5 cm in females

Clinical Vignette: Spurious causes of cardiac enlargement

Portable Film
Obesity
Pectus excavatum
Straight back syndrome
Ascites
Poor Inspiration
Large epicardial fat pad
Absence of pericardium

Clinical Vignette: Causes of Microcardia

Normal variants
Severe malnutrition and dehydration
Addisons disease
Emphysema
Constrictive pericarditis

2. Assessment of Right atrial enlargement

Vertical Criteria
(i). Rt. Atrial border extends >3 intercostal spaces
(ii). Rt. AtriWal border more than 50 percent of right heart border
Horizontal Criteria
(i). Rt. Atrial border extending 3.5 cm beyond lateral vertebral border
(ii). Rt. Atrial border extending 5.5 cm beyond mid vertebral line
(iii). Right Atrium occupying more than one third of right hemithorax
(iv). Right atrial convexity is more than 50% of the cardiovascular height

3. Assessment of Left atrial enlargement

(i). Widening of carina (normal 45-75 degree)
(ii). Elevation of left bronchus
(iii). Straightening of left border
(iv). Double atrial shadow (shadow within shadow)
Grade 1 - double cardiac contour
Grade 2 - LA touches RA border
Grade 3 - LA overshoots the Rt. Cardiac border (atrial escape sign)
(v). Displaces the descending aorta to the left and esophagus to right seen in barium swallow

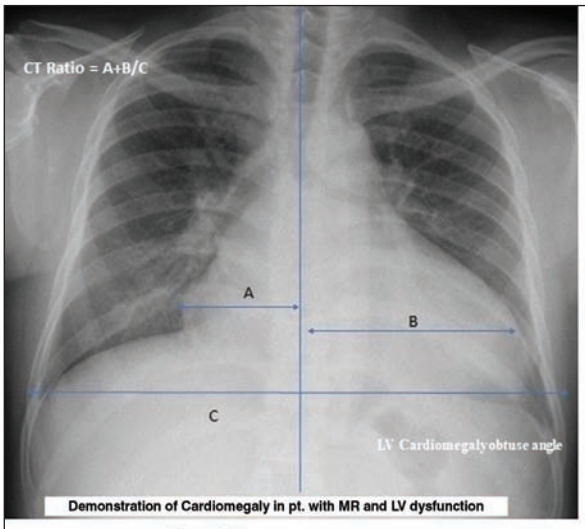

Figure B.3

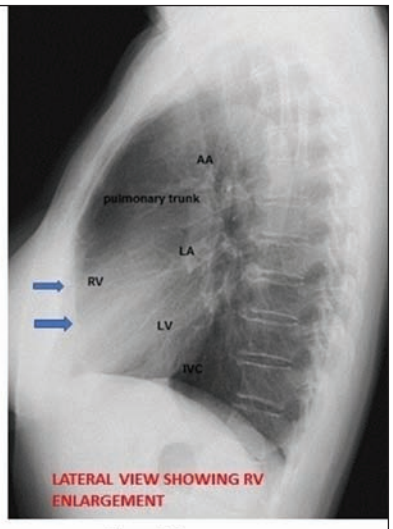

Figure B.4

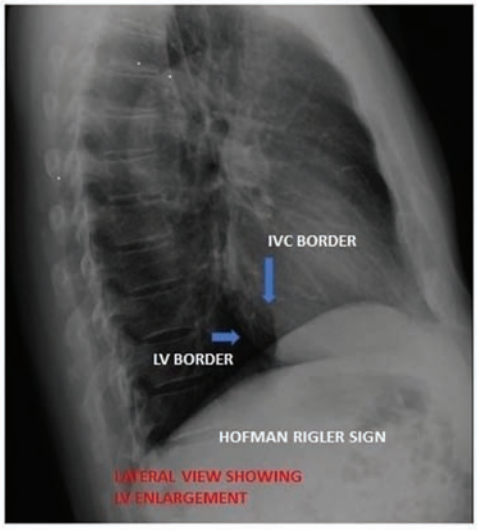

Figure B.5

4. Assessment of right ventricular enlargement

(i). PA view
1.Cardiophrenic angle is acute.
2.Clockwise rotation of heart causes RV to form the middle portion of the left heart border.
(ii). RIGHT LATERAL VIEW
1. Obliteration of retrosternal space
(iii). LEFT LATERAL VIEW
• Rigler's measurement will be 17mm or less
• Rigler's measurement will be 7.5mm or more
• Eyeler's ratio is 0.42 or less

5. Assessment of left ventricular enlargement

PA view
(a) Left cardiac border gets enlarged and becomes more convex resulting in cardiomegaly
(b) Lt. cardiac border dips into lt. dome of diaphragm
(c) rounded apical segment
(d) cardiophrenic angle is obtuse
Lateral view
(a) Left ventricle enlarges inferiorly and posteriorly
(b) Rigler's measurement A is >17 mm
(c) Rigler's measurement B is< 7.5 mm

(d) Eyeler's ratio becomes > 0.42
LA Oblique view
Mild lt. Ventricular enlargement-obliteration of retrocardiac space
mod. Lt.ventricular enlargement-cardiac shadow overlaps vertebral column
Marked Lt.ventricular enlargement-cardiac shadow overshoots vertebral column

Clinical Vignette: Differential Diagnosis of Retrosternal filling on Lateral CXR

RV Dilatation
TGA
Ascending Aortic Aneurysm
Non cardiovascular masses

C. ASSESSMENT OF PULMONARY ARTERY AND VENOUS HYPERTENSION AND VASCULARITY

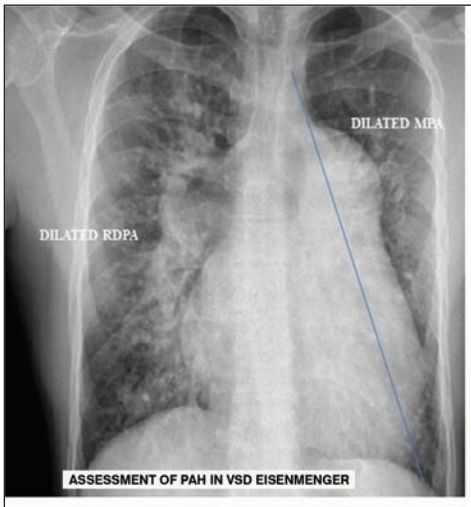

Figure C.1

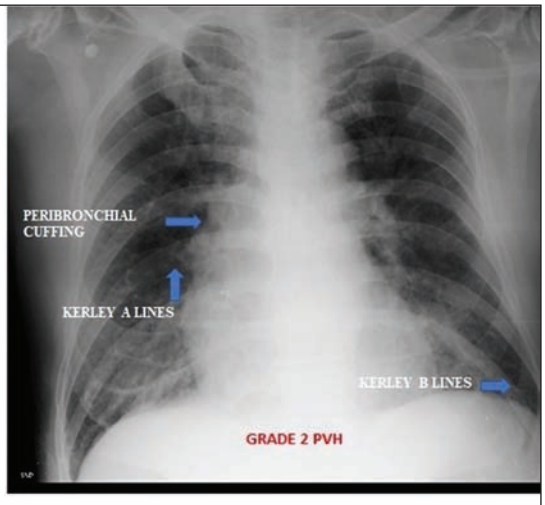

Figure C.2

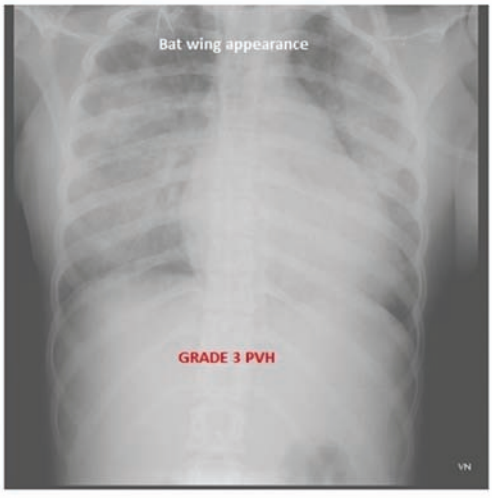

Figure C.3

1. Assessment of pulmonary artery hypertension

• Prominent Main pulmonary Artery
• Right descending pulmonary artery
> 17 mm in males and > 16 mm in females.
• Pruning of peripheral pulmonary artery.
• Reduced retro-sternal space on lateral views due to RV dilatation
Clinical Vignette
Echo criteria for dilated pulmonary artery > 22 mm
CT criteria for dilated pulmonary artery > 26 mm

2. Assessment of Pulmonary venous hypertension

LARRY ELLIOT'S CLASSIFICATION OF PVH		
Radiographic grade of PVH	Acute Disease PCWP (mm Hg)	Chronic disease PCWP (mm Hg)
Grade 1	13-17	13-17
Grade 2	18-25	18-30
Grade 3	>25	>30
Grade 4	Hemosiderosis and ossification	Long standing PVH

3. Grades of PCWP

GRADE 0 -PCWP <12 MM HG	**GRADE 1- PCWP 13-17MMHG**
Upper lobe pulmonary veins are less prominent than lower lobe veins	Redistribution of blood flow with cephalization' 'ANTLER SIGN' 1. increased resistance to flow due to interstitial odema 2. alveolar hypoxia in lower lobes causes reflex vasoconstriction 3. vasoconstriction of the arterioles due to LA or pulmonary vein reflex
GRADE 2-PCWP 18–25 mm Hg	**GRADE 3 – PCWP >25mm hg**
1. Interstitial edema 2. Peribronchial cuffing 3. Kerley A,B,C lines 4. Interlobular effusion 5. Pleural effusion 6. Hilar haze 7. Peribronchial	1. Alveolar odema 2. Bilateral diffuse patchy 3. Cotton wool opacities

Kerley A lines	**Kerley B lines**
Distended lymphatic channels within edematous septa coursing from peripheral lymphatics to central hilar nodes Towards the hilum Less specific for Pulmonary venous hypertension	Horizontal lines 1-3 mm thick Perpendicular to pleural surface Towards the costophrenic angle Accumulation of fluid in interlobular septa and lymphatics Highly specific for PVH

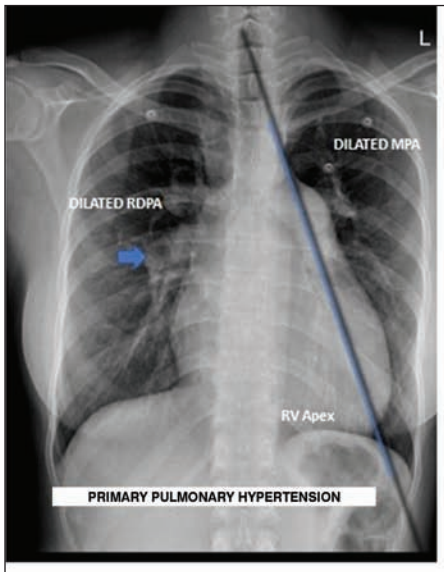

Figure C.4

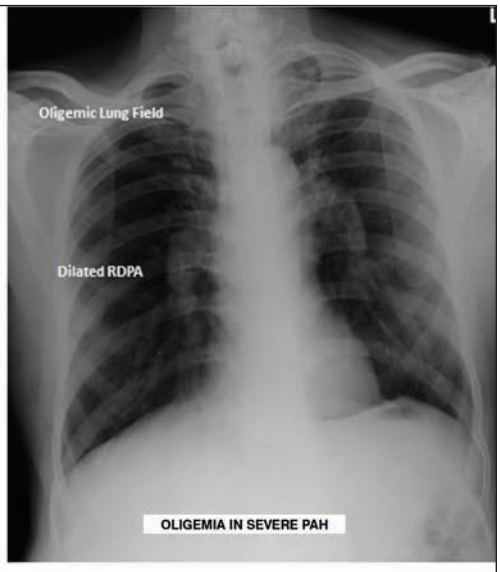

Figure C.5

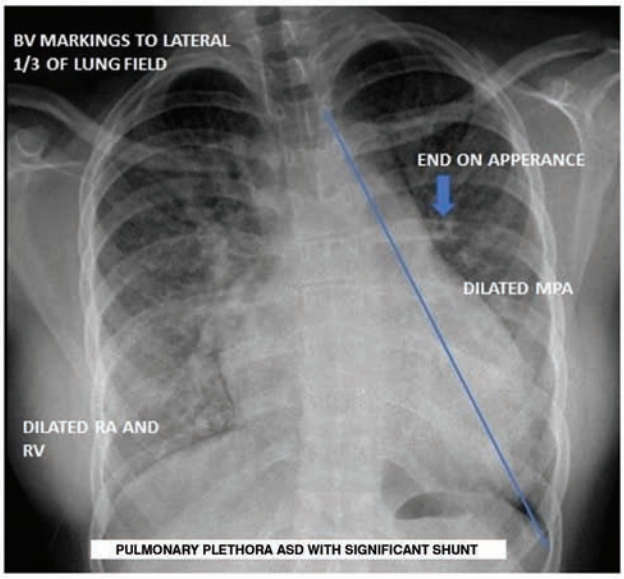

Figure C.6

4. Assessment of Pulmonary plethora

• pulmonary vessels are dilated and tortuous extending farther into the peripheral one-thirds of the lungs
• diameter of a pulmonary artery is greater than the accompanying bronchus
• Right descending pulmonary artery to tracheal diameter Ratio > 1
• End-on's > 3 in one lung field and >5 in both lung fields.

5. Assessment of pulmonary oligemia

• Small pulmonary artery
• Empty pulmonary bay
• Pulmonary vessels small
• Lung hyper translucent
• Lateral view shows diminution of hilar vessels

D. CARDIOMYOPATHY VS PERICARDIAL DISEASES

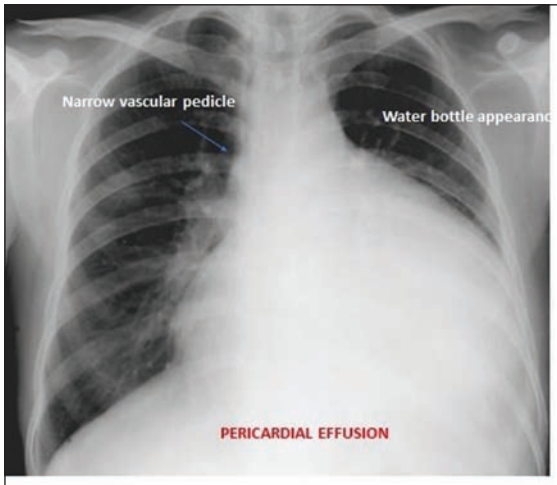

Figure D.1

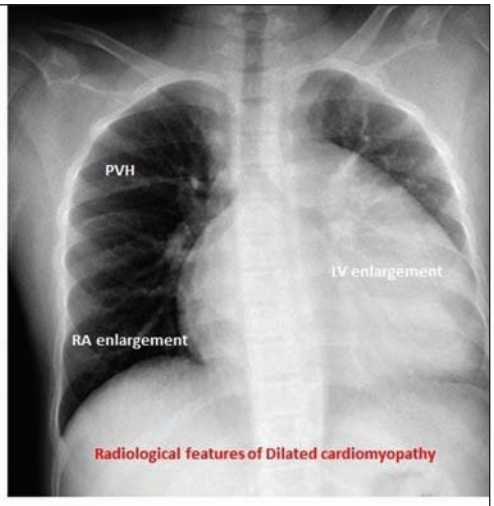

Figuree D.2

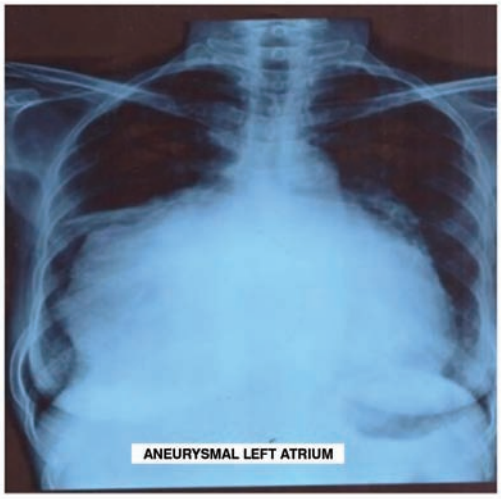

FigureD.3

1. Pericardial effusion

• Narrow vascular pedicle
• Cardiomegaly directly proportional to severity of pericardial effusion
• This shadow has a rounded, globular appearance with no particular chamber enlargement
• Cardiophrenic angle become more and more acute
• Oligaemic pulmonary vascular markings
• Marked change in cardiac silhouette in decubitus posture
• 'Epicardial fat pad sign'- anterior pericardial strip bordered by epicardial fat post. and mediastinal fat ant.>2mm

2. Dilated Cardiomyopathy

• Chambers can be identified
• Cardiophrenic angle is obtuse
• Increased pulmonary venous hypertension
• No change in cardiac silhouette in decubitus
• Vascular pedicle is dilated or normal

Clinical Vignette: Differential Diagnosis of Massive Cardiomegaly

1. Pericardial effusion
2. Dilated cardiomyopathy

3. Multivalvular heart ds(AR+MR with or without LV dysfunction)
4. Ebsteins anomaly
5. Aneurysmal left atrium(when LA enlarges right and left and approaches within an inch of lateral chest wall)

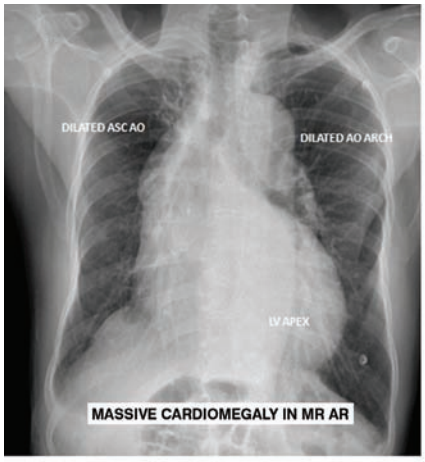

Figure D.4

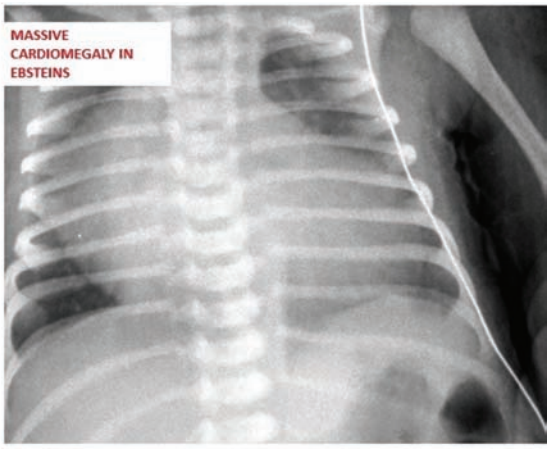

Figure D.5

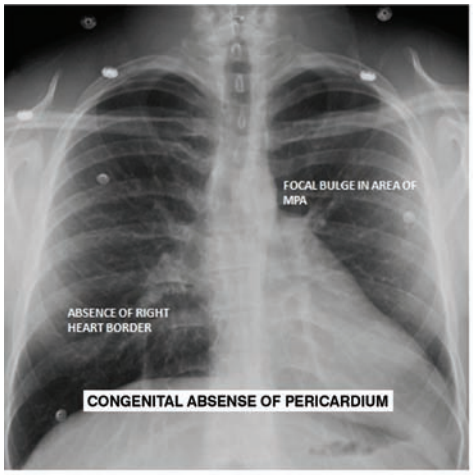

Figure D.6

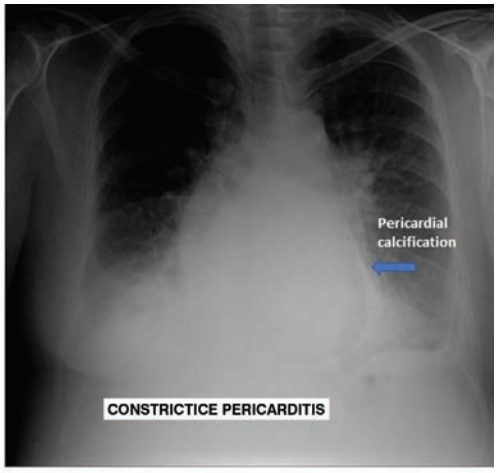

Figure D.7

3. Constrictive Pericarditis

Straightening of the right border
Pericardial thickening > 4 mm
Pericardial calcification (50% cases)
Dilatation of SVC and azygous vein

Clinical Vignette: Differential Diagnosis of Straightening of Right heart border

1. Congenital absence of pericardium Focal bulge in area of main pulmonary artery Sharply marginated Increased distance between sternum and heart due to absence of sterno pericardial ligament
2. Constrictive Pericarditis
3. Tricuspid Atresia (type IIb) with Juxtaposed atrial appendage (also seen in D -TGA)

Clinical Vignette: Differential Diagnosis of Straightening of Left heart border

RV dilatation
LA dilatation

cc-TGA
Congenital absence of left pericardium
Pericardial Effusion
Ebstein's anomaly

E. ASSESSMENT OF AORTIC AND PULMONARY DISEASES

1. Pulmonary embolism

Westermark sign - oligaemia (clarified area) distal to a large vessel that is occluded by a pulmonary embolus.
Hampton's hump - wedge- shaped opacity with a rounded convex apex directed towards the hilum

Fleischner's sign- prominent central pulmonary artery
Palla's sign- enlargement of the right descending pulmonary artery proximal to a cut off of the pulmonary artery due to acute pulmonary embolism
Chang's sign – dilatation and abrupt change in calibre of the rt. Descending PA

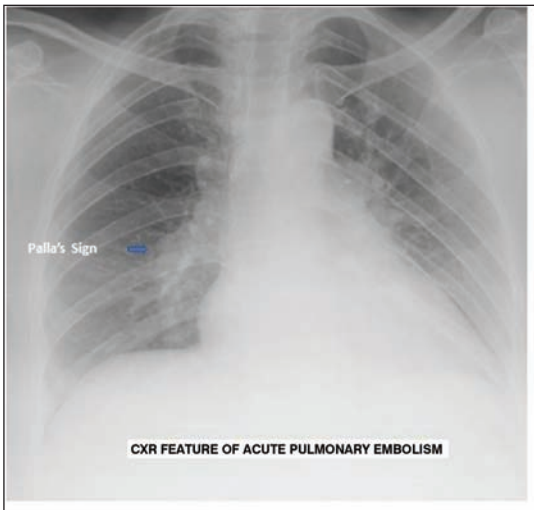

Figure E.1

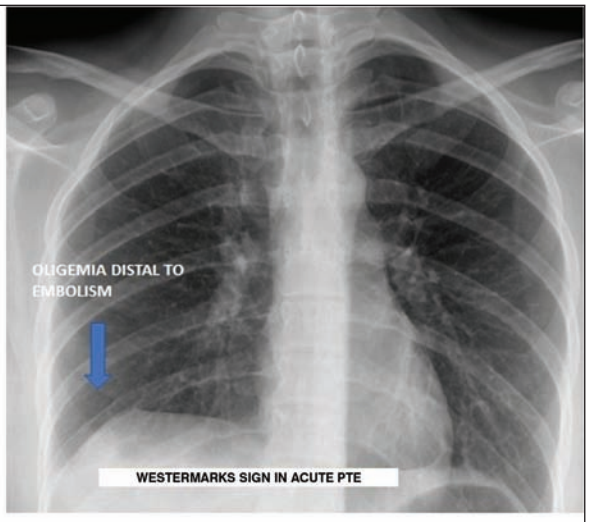

Figure E.2

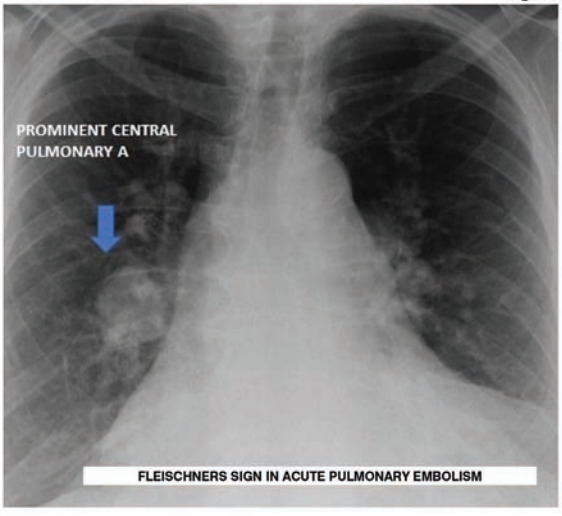

Figure E.3

2. Ascending aorta and Arch enlargement

PDA
CoA
Truncus Arteriosus
AS, AR, Hypertension
Ascending aortic aneurysm
Bicuspid aortic valve with/without AS

3. Aortic dissection

Widened mediastinum
Double/irregular aortic contour
Calcium sign (inward displacement of atherosclerotic calcification (>1 cm from the aortic margin)
Aortic kinking
Pleural effusion
Tracheal deviation

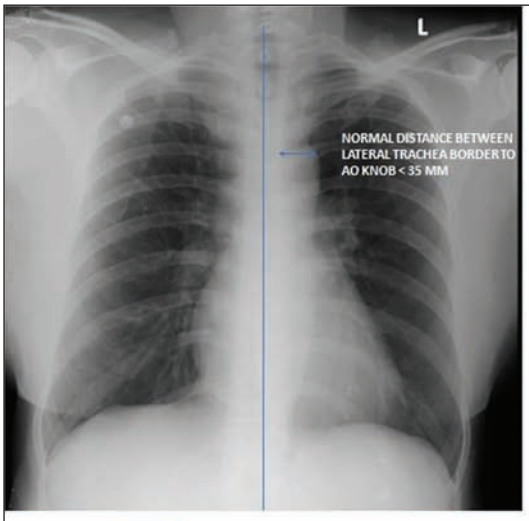

Figure E.4

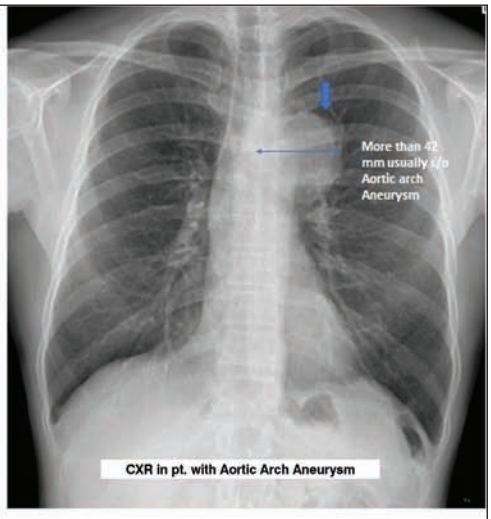

Figure E.5

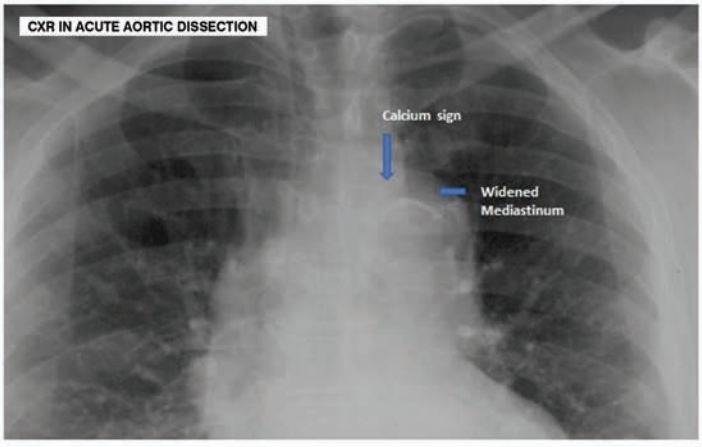

Figure E.6

F. CXR IN CONGENITAL HEART DISEASES

1. Acyanotic heart diseases

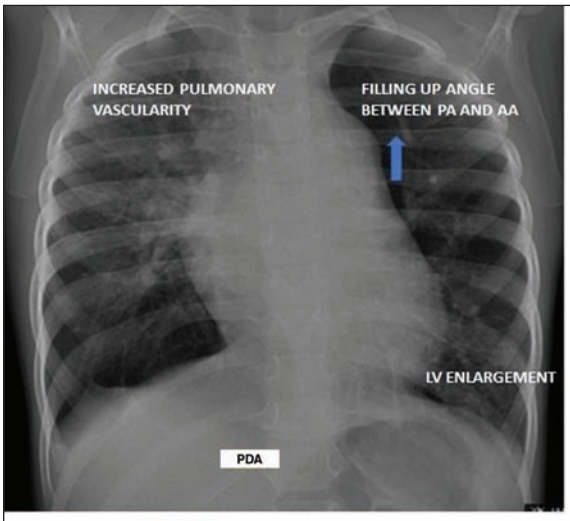

Figure F.1

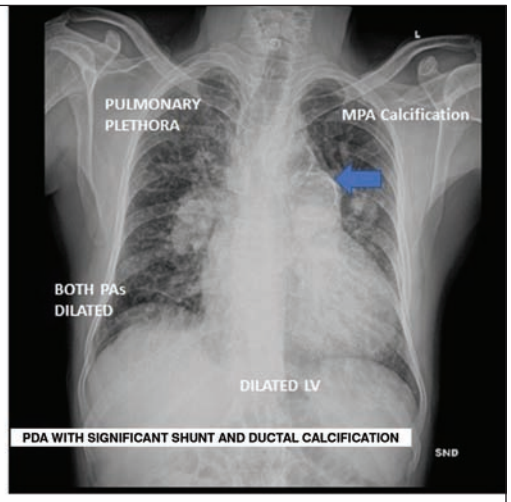

Figure F.2

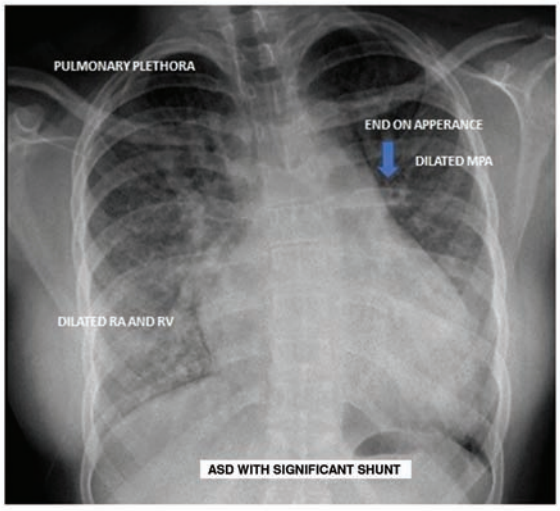

Figure F.3

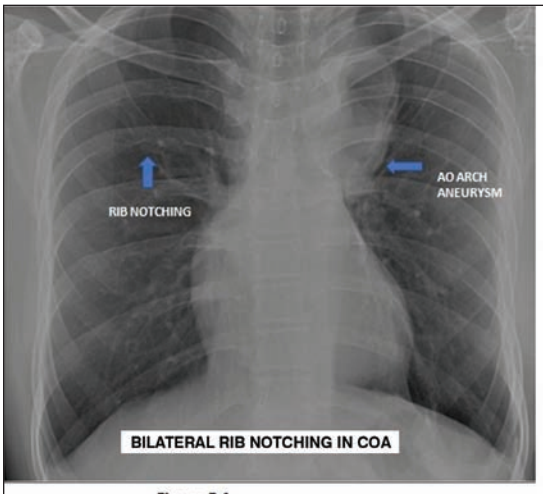

Figure F.4

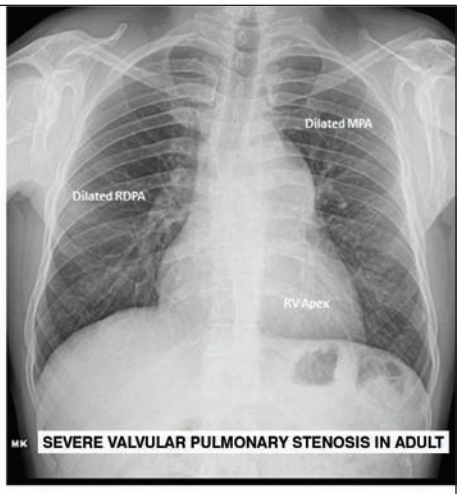

Figure F.5

ATRIAL SEPTAL DEFECT	OS ASD: Right atrium and ventricle enlargement Large pulmonary artery and increased pulmonary vascularity RPA>LPA = Jug handle appearance OP ASD: LV enlargement also SV ASD: Subtle localized dilatation of SVC
VENTRICULAR SEPTAL DEFECT	Small VSD – normal chest Xray Significant shunt – Qp/Qs>2: Cardiomegaly, LA/LV/ enlargement, increased pulmonary vascularity, both PAs are prominent Disproportionate RA enlargement→ suspect Gerbode defect
PATENT DUCTUS ARTERIOSUS	Cardiomegaly LA/LV enlargement Increased pulmonary vascularity/ both Pas equally dilated Filling up of angle between PA and AA(most specific sign) Unequal distribution of pulmonary arterial blood flow, especially sparing of left upper lobe Enlargement of aorta Ductal calcification (Cap of Zinn)
COARCTATION OF AORTA	Aortic figure- 3 configuration due to pre-stenotic dilatation of aorta, indentation of aorta caused by coarctation, post-stenotic dilatation Inferior rib notching involving ribs 3 to 8 Prominent left heart border due to left ventricular hypertrophy Normal pulmonary vascularity Critical CoA (neonates) PVH/pulmonary edema Cardiomegaly with LV enlargement No rib notching/aortic knob not characteristic Pulmonary plethora – no VSD/PDA
PULMONIC STENOSIS	Cardiomegaly Oligemic lung fields Dilated right ventricular outflow and right ventricle Post stenotic dilatation of MPA and LPA
AVSD	Cardiomegaly RA enlargement with left AVV regurgitation Left cardiac border straightened by prominent RVOT Increased pulmonary vascularity Other trisomy 21 findings :11 ribs, multiple manubrial ossification centres

Clinical Vignette on Rib Notching

Seen only in long standing cases, and therefore not seen in infancy (unusual in patients <5 years of age)
1st and 2nd posterior intercostal arteries arise from the costo-cervical trunk (a branch of the subclavian artery) and do not communicate with the aorta, these are not involved in collateral formation, and the 1st and 2nd ribs do not become notched
Anterior ribs are spared because anterior intercostal arteries do not run-in intercostal grooves.
if bilateral rib notching: the coarctation must be distal to the origin of both subclavian arteries, to enable bilateral collaterals to form
if unilateral right rib notching- a. the coarctation lies distal to the brachiocephalic trunk but proximal to the origin of the left subclavian artery b. there may be a right sided aortic arch with aberrant left subclavian artery distal to coarctation PS: collaterals cannot form on the left, as the left subclavian is distal to the coarctation
if unilateral left rib notching, then this suggests an associated aberrant right subclavian artery arising after the coarctation a. the coarctation is distal to the origin of the left subclavian artery, therefore collaterals form on the left b. collaterals cannot form on the right, as the aberrant right subclavian artery arises after the coarctation

Clinical Vignette: D/D's of Rib Notching

1. CoA (post subclavian)
2. Classical BT shunt (unilateral)

3. SVC obstruction (collateral intercostal venous dilatation)
4. Thrombosis of abdominal aorta (notching of lower ribs)
5. Neurofibromatosis
6. Intercostal AV fistula

1. Calcification in Main pulmonary artery

1. Eisenmenger syndrome
2. PDA (Cap of Zinn)
3. Severe Pulmonary artery hypertension (rarely)
4. Metastatic pulmonary artery calcification

2. Aneurysmal dilatation of MPA

1. Eisenmenger syndrome
2. TOF with Absent pulmonary valve
3. Idiopathic dilatation of pulmonary artery
4. Primary pulmonary hypertension
5. Connective tissue diseases, rheumatologic diseases (typically seen in Behcets diseases)
6. Infectious diseases like TB, Syphilis

3. CYANOTIC HEART DISEASE

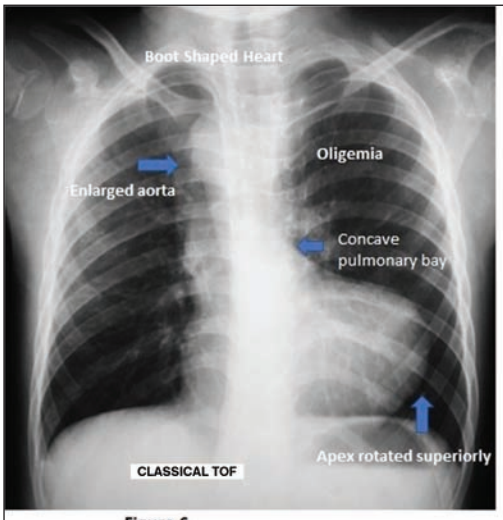

Figure 6

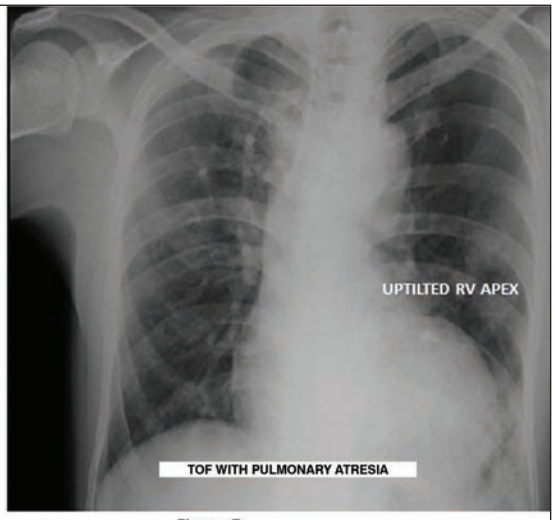

Figure 7

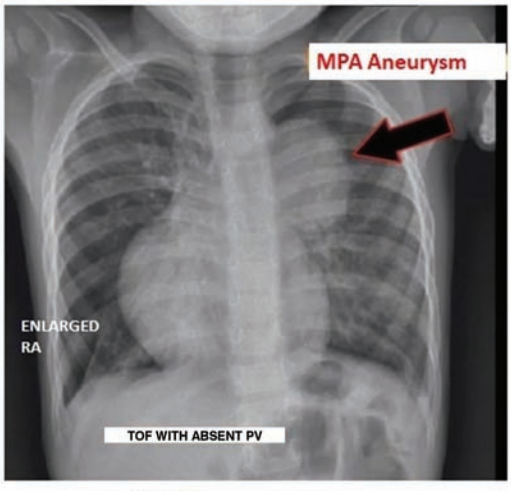

Figure 8

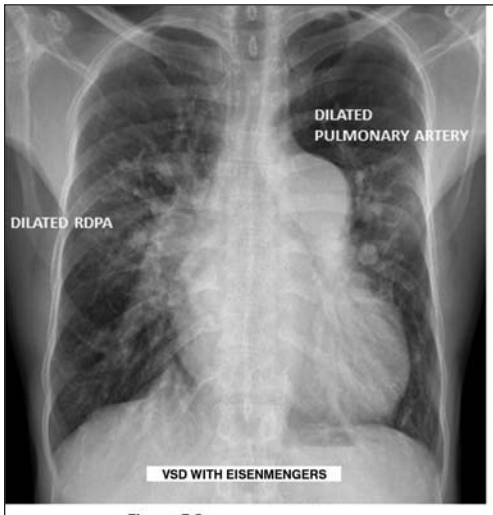

Figure F.9

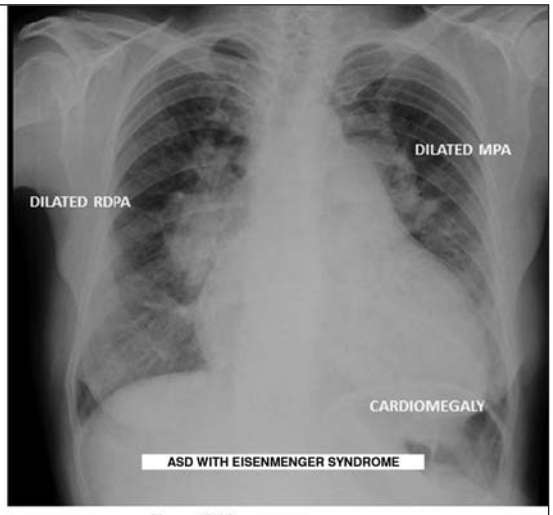

Figure F.10

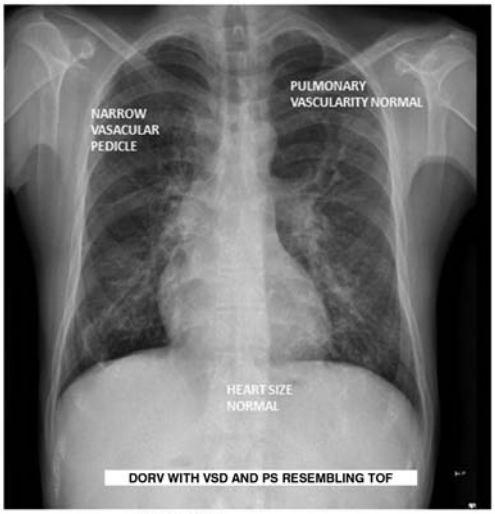

Figure F.11

EBSTEINS ANOMALY	Large 'square/box shaped' heart due to left side: horizontal position of RV outflow; right side: RA enlargement Small aortic knuckle Small pulmonary arteries and decreased vascularity
D-TGA	'Egg on side' contour: RA abnormally convex + convex left border (increased PBF) Narrow superior mediastinum Increased pulmonary vascularity Pulmonary trunk not visible due to posterior position Thymic shadow absent

L-TGA	Abnormal AA contour because of leftward position of the arch LA enlargement Right pulmonary hilus elevated over left pulmonary hilus(water-fall appearance) Pulmonary trunk and aorta are not apparent because of their posterior position Hump shaped appearance (prominent inverted infundibulum) Septal notch due to apical position of interventricular groove Dextrocardia in 20 % Abdominal situs solitus and dextrocardia should raise the suspicion of cc TGA

TRICUSPID ATRESIA	WITH TGA AND PS (Type 2b) Pointed bulge on the left border of the mediastinal shadow below the region where the pulmonary artery should be seen The right border of the right atrium is straight because the absence of right ventricle pulls the border towards the right atrium (Juxtaposed atrial appendage) Mediastinal pedicle is narrow because of TGA WITH RESTRICTIVE VSD AND NRGA(1b) Enlarged RA and flat receding inferior border reflecting absence of RV Enlarged LV occupies apex Inconspicuous MPA/enlarged Ao Pulmonary vascularity is reduced
TOTAL ANOMOLOUS PULMONARY VENOUS RETURN (TAPVC)	Figure of eight or Snowmans appearance The upper half of the figure of eight is formed by the dilated superior vena cava on the right side, the left brachiocephalic vein in the top and the dilated vertical vein on the left side The lower portion of the figure of eight is formed by the dilated right atrium and ventricle VSD with large thymus: Pseudo-snowman appearance
TETRALOGY OF FALLOT	Boot shaped heart- Coeur en sabot (enlarged RV + small or concave pulmonary artery) Normal cardiac size Decreased pulmonary vascularity Dilated Asc aorta 25 % Right aortic arch TOF with pulmonary atresia: B/L reticular formation due to broncho-pulmonary collaterals, cardiomegaly TOF with APV: Dilated RV with enlarged RA, decreased distal pulmonary vascularity, aneurysmal main pulmonary artery
TRUNCUS ARTERIOSUS	Enlargement of aortic shadow (which represents the truncus) All four chambers dilated(L>>R) Increased pulmonary vascularity 1/3rd cases – Right aortic Arch Absence of PA is same side as aortic arch in contrast to TOF
DOUBLE OUTLET RIGHT VENTRICLE	WITH SUBAORTIC VSD AND NO PS Prominent RA/dilated LV occupies the apex Pulmonary vascularity is increased PT is moderately convex WITH SUBAORTIC VSD AND PS Resembles TOF WITH SUBPULMONIC VSD (TAUSSIG-BING ANOMALY) Prominent RA/dilated LV occupies the apex Pulmonary vascularity is increased Vascular pedicle is narrow
SINGLE VENTRICLE	WITH INVERTED OUTLET CHAMBER SV and RA are dilated Outlet chamber forms a convex bulge and gives rise to Ao WITH NON-INVERTED OUTLET CHAMBER Dilated RA/dilated SV Narrow vascular pedicle

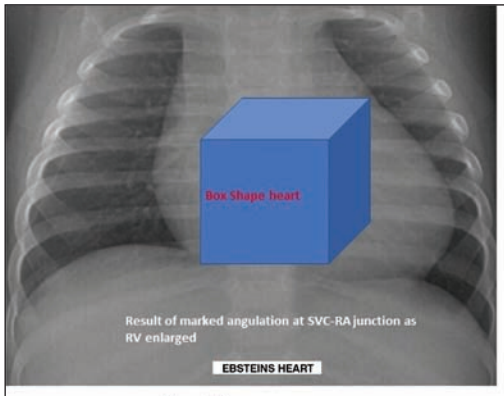

Figure F.12

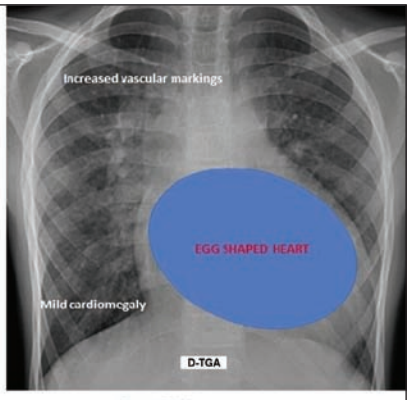

Figure F.13

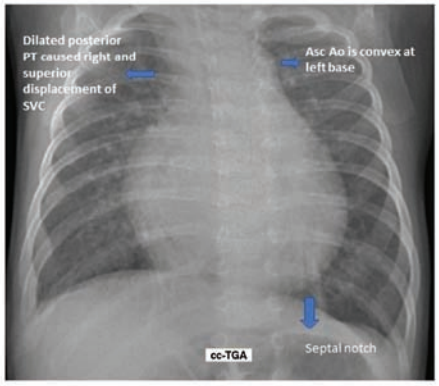

Figure F.14

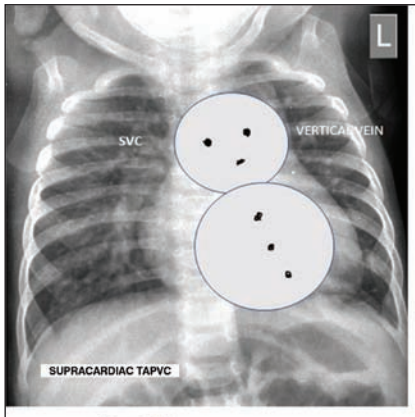

Figure F.15

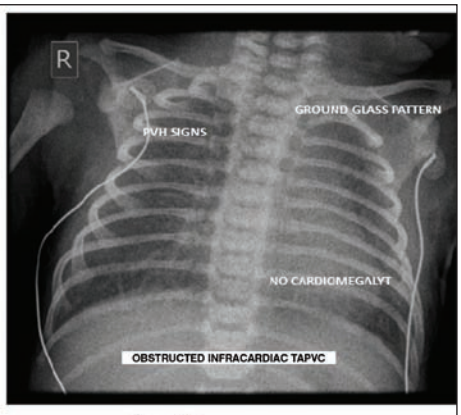

Figure F.16

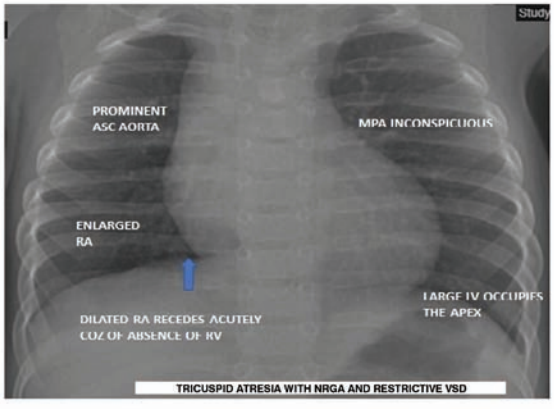

Figure F.17

Clinical Vignette: Narrow and Wide vascular pedicle

Wide	Narrow
DORV	Tricuspid atresia Type II
L-TGA	D-TGA
Single ventricle	TOF
Truncus A	Ebsteins anomaly

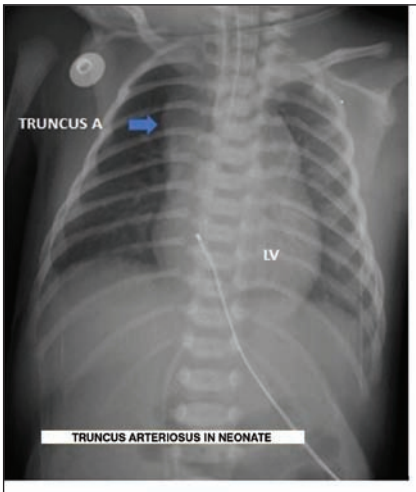

Figure F.18

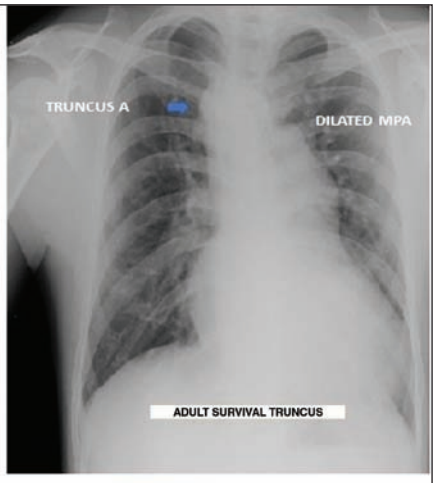

Figure F.19

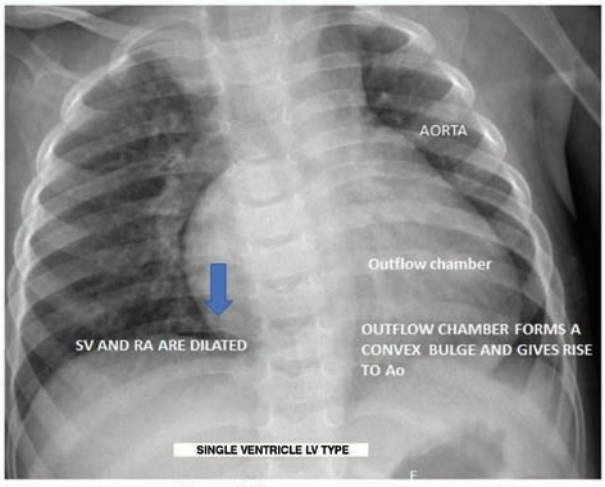

Figure F.20

CONCLUSION

A systematic approach is key to interpretation of chest radiograph in cardiac diseases. Careful assessment of cardiac and mediastinal contours and familiarity with normal chest radiograph including lateral projection at times is required to discern subtle features of cardiac chamber pathology and congenital heart disease.

SUGGESTED READINGS

1. Braunwald Heart Diseases 12th edition
2. Cardiac X-rays – V Chockalingam
3. Perloffs Clinical Recognition of Congenital heart disease.
4. Radiology and Imaging by Sutton 7th edition
5. Radiology of Congenital heart disease by Kurt Amplatz

Interpretation of Late Gadolinium Enhancement (LGE) images

Stigi Joseph

Senior Consultant Cardiologist and HOD,
Little Flower Hospital and Research Centre, Angamaly, Kerala.

Cardiac MRI, LGE images (otherwise named Delayed Hyperenhancement Images) help in myocardial tissue characterisation and the pattern of involvement is typical for different diseases. The commonest use of this modality in clinical practice is to assess myocardial viability, followed by the diagnosis of myocarditis.

LGE-Principle: The Gadolinium agents used in MRI are metabolically inert, large molecule which enters the extracellular space readily after intravascular injection. It will not cross into the intracellular space. In situations where there is an expansion of extracellular space (eg: Acute Myocardial infarction or any myocardial fibrosis, interstitial oedema as in Myocarditis), the Gadolinium agent (Gadolinium Based Contrast Agents-GBCA) accumulates in the extracellular space and its washout is delayed. These areas will give a bright signal compared to normal myocardium on T1-weighted images.[1]

Current Protocol: An initial non-contrast sequence followed by injection of 01. mmol/kg weight of GBCA and LGE imaging after 10 minutes of injection.[1]

Interpretation: The pattern and extent of bright images (LGE) have significance. The subendocardial involvement is typical of Infarct. The pattern of involvement in 17 segment model identifies the vessel involved and the extent of transmural involvement indicates viability.

ASSESSMENT OF VIABILITY

The routine Cardiac MRI methods to assess myocardial viability are 1) Left Ventricular End Diastolic Wall Thickness (LV EDWT), 2) Dobutamine Stress Cardiac MRI to assess contractile reserve, and 3) Late Gadolinium Enhancement imaging (LGE). The ability to predict functional recovery following revascularisation varies with these different modalities. LV EDWT (<5.5% >5.5 mm) has a sensitivity of 94% while low specificity 56%.[2]

LGE- As the myocardial involvement (transmural extend) progresses the chance of recovery after revascularisation decreases.[3] A near transmural involvement implies no chance for recovery after revascularization. If there is no LGE in an akinetic segment, the chance of recovery is almost total. Conventionally a > 50% transmural involvement is considered non-viable (the chance of recovery of contractility is<10%). If there is <50 % transmural involvement, the patient should be subjected to Dobutamine Stress MRI for better prediction of revascularisation results (especially in involvement 50-75%).

LGE has high sensitivity (95 %) but low specificity (51 %) while Dobutamine Stress MRI has a specificity of 91 %.[4] making the combined modality the ideal investigative tool for the detection of viability.

Address for correspondence: Dr Stigi Joseph MD.DM., Fellow ICPS (Paris), Senior Consultant Cardiologist and HOD, Little Flower Hospital and Research Centre, Angamaly. Email: drstigi@yahoo.com

MYOCARDITIS

In the late stages of myocarditis when necrosis and fibrosis set in, a typical LGE pattern of myocarditis sets in. The typical pattern is the epicardial hyperenhancement with sparing of subendocardium. Associated features like pericardial effusion, LV Dysfunction or LV thrombus may be present. The usual sites of DHE are the Inferolateral area and then the anteroseptal area. A hyperenhancement (LGE) involving LVOT, membraneous septum and the basal septum is likely to be false positive. The pattern of involvement is typical for certain viruses like,in Parvo B19 virus myocarditis, LGE is usually epicardial LV Lateral wall,while in Herpes Virus 6, it is the antero septal mid myocardial enhancement.[5]

Specific patterns are suggested for different conditions.

1. **Sarcoidosis-** Involvement of Septum, Left Ventricular and Right ventricular Free wall and papillary muscles. Associated features like thinning of basal septum and aneurysms may be seen.
2. **Eosinophilic myocarditis**-Endocardial Delayed Hyperenhancement.
3. **Chagas disease**-Apical Aneurysm.
4. **Amyloidosis-** subendocardial or transmural involvement, initial involvement of basal segments later becomes global, biventricular and transmural.
5. **Dilated Cardiomyopathy**-Septal mid myocardial hyperenhancement.

Now let us discuss a few images.

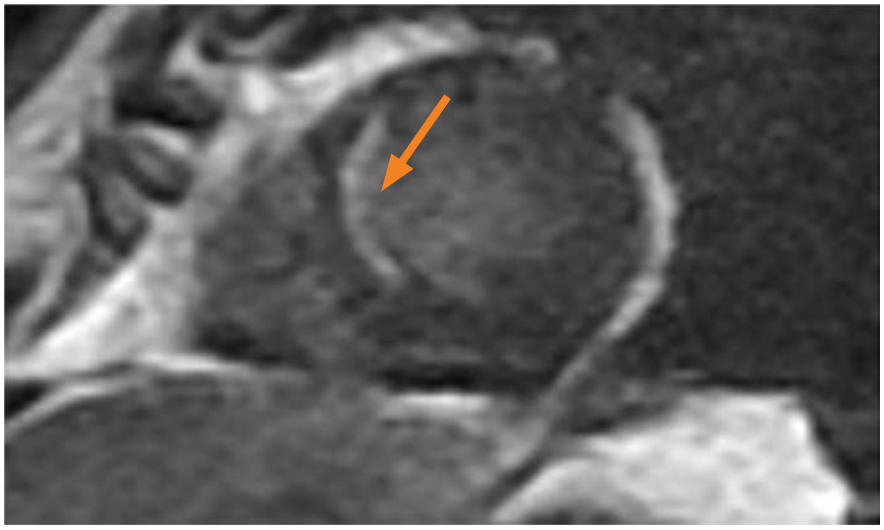

Figure:1
Subendocardial LGE images: White crescentic segment indicates areas of tissue necrosis. This is subendocardial, typical for ischemia/ infarct. There is <50 % thickness involved and so the myocardium is viable.

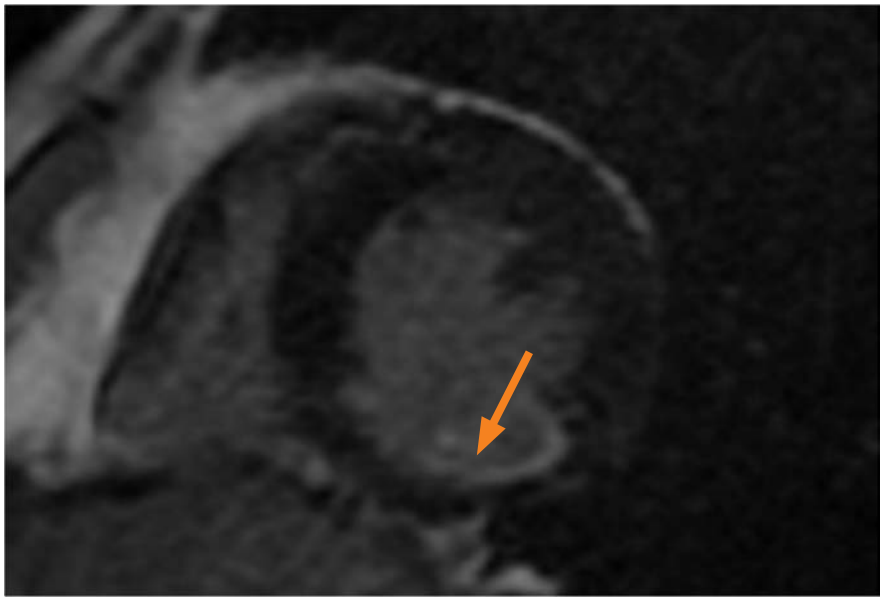

Figure:2
Short Axis LGE images - white curvilinear segment indicates areas of tissue necrosis. This is subendocardial, typical for ischemia/ infarct. The involvement is<50 % in the Inferior segment (viable). This patient is likely to have a good result after revascularization.

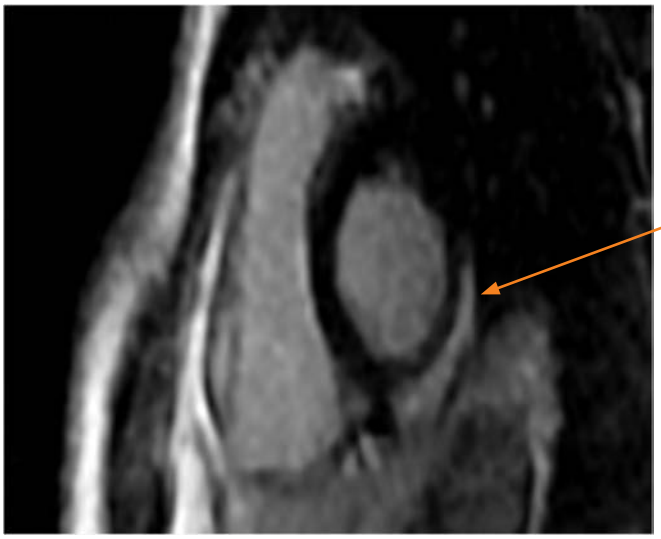

Figure:3
Typical Epicardialhyperenhancement pattern is seen in Myocarditis (Late stages when necrosis and fibrosis set in).

Now we shall go through certain common clinical scenarios and see how to interpret the images.

Clinical case-1

A 60-year-old male with H/o Extensive anterior wall Myocardialinfaction – delayed presentation – Cardiac Failure, medically stabilised underwent coronary angiogram which showed proximal total occlusion of LAD. A study was done to assess viability.

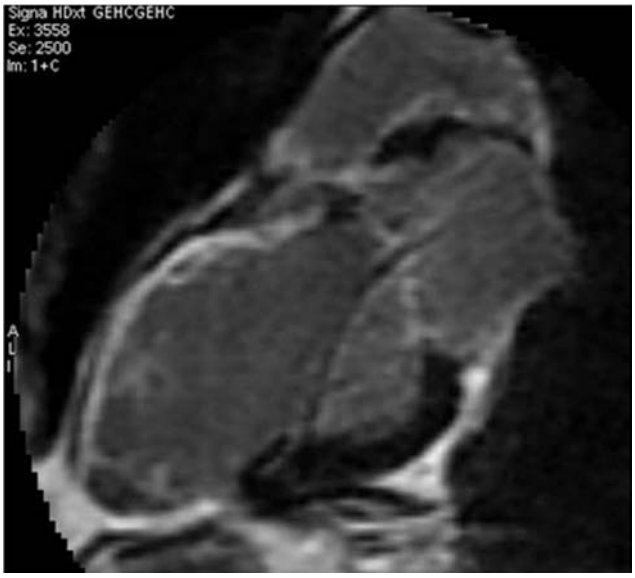

Clinical case-2

A 55-year-old female presented with Angina and breathing difficulty.

ECG was suggestive of Acute Anterior wall Myocardial infarction. Gives H/o Bronchial Asthma. A coronary Angiogram showed non-obstructive plaques. On repeat questioning, she stated that the events started after emotional stress in the family. Echocardiography was limited by poor echo window. She was stabilised and later did Cardiac MRI.

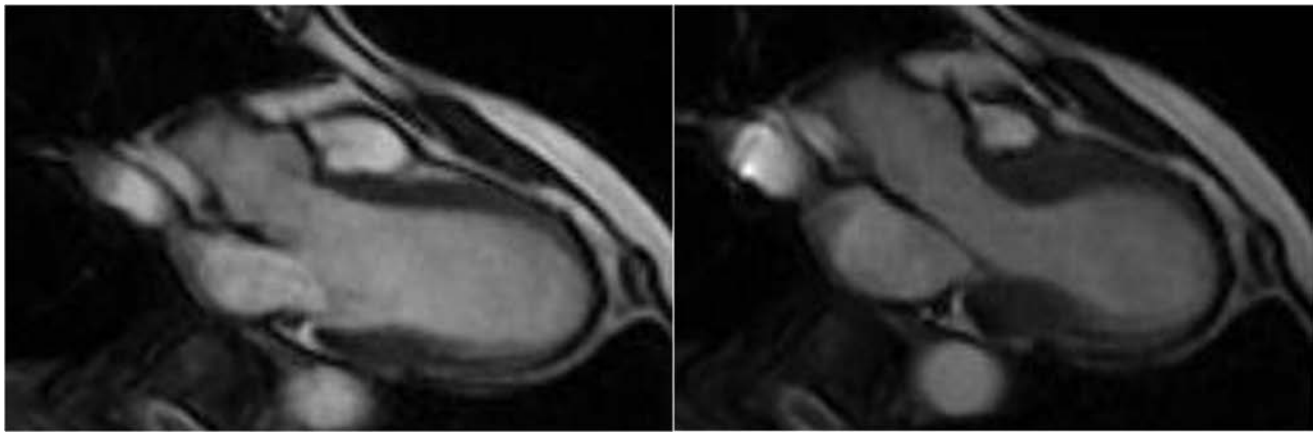

Image in Diastole **Image in Systole**

Clinical case-3

A 70-year-old male presented with acute onset breathlessness, ECG showed ST Depression T inversion in inferior leads, and Troponin was positive. He is not Diabetic nor hypertensive. Had fever the preceding week which was treated as Respiratory Infection from a nearby hospital. Bedside Echo study showed global hypokinesia with Moderate LVSystolic dysfunction. He was stabilised and underwent Cardiac MRI as Myocarditis was suspected.

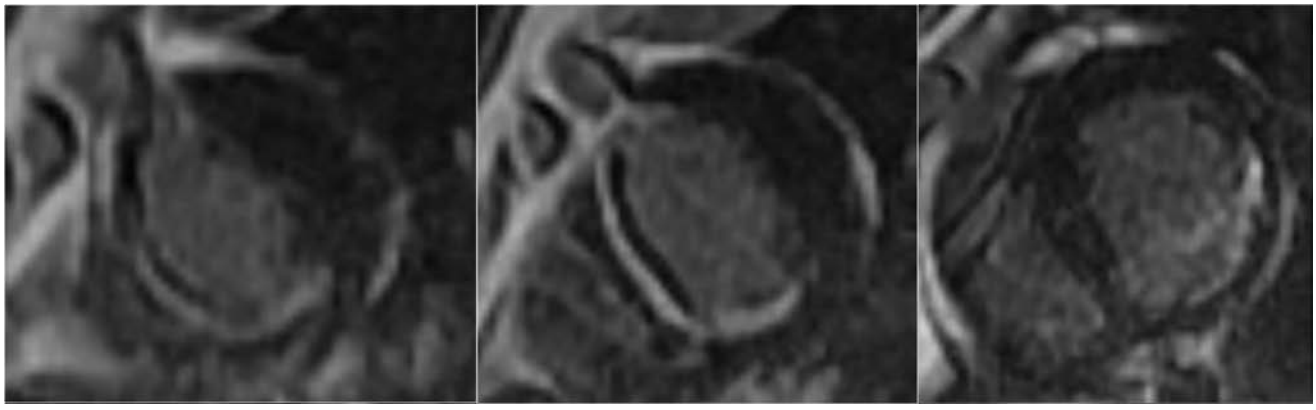

Clinical case-4

An 80-year-old female, previously diagnosed as HCM with mid cavity obstruction presented with Heart failure. She was stabilised and underwent a Cardiac LGE study.

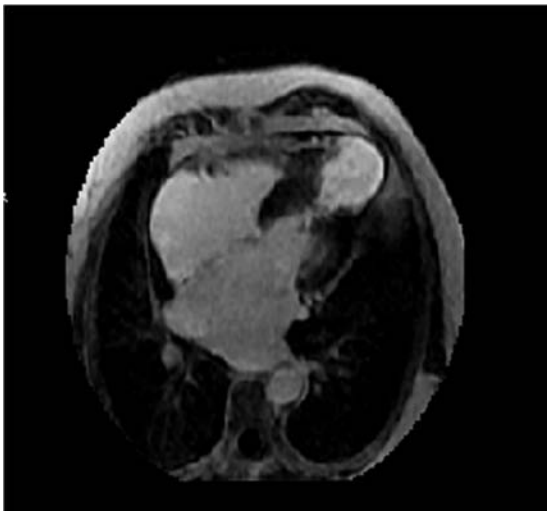

Clinical case-5

A 24-year-old male presented with non-anginal chest pain. His Echo study had the suspicion of non-obstructive HCM, probable Anteroseptal hypertrophy, and no family H/o HCM.What is seen in MRI?

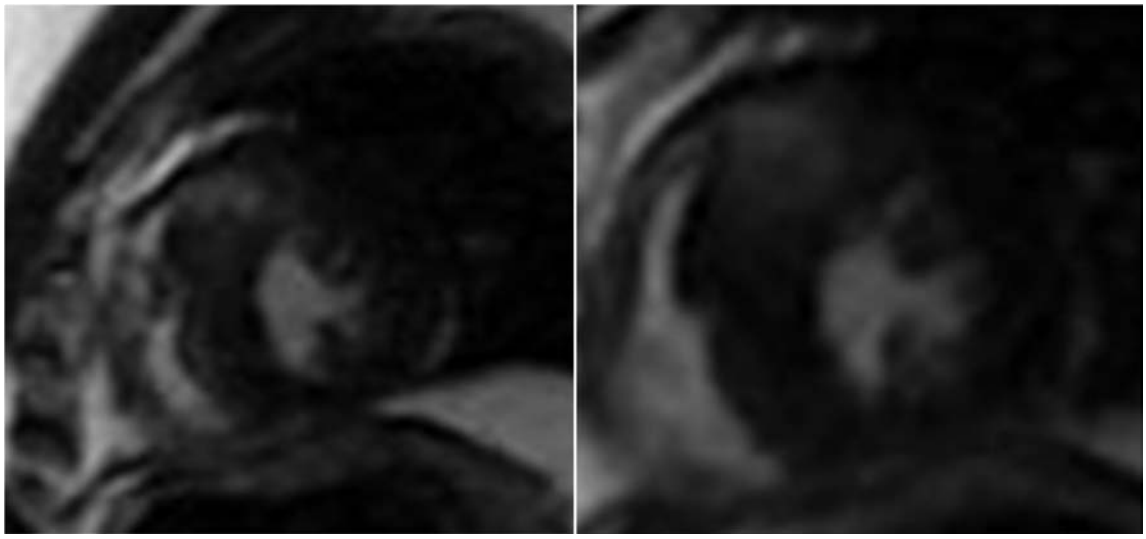

INTERPRETATION OF IMAGES

Clinical case-1: Interpretation

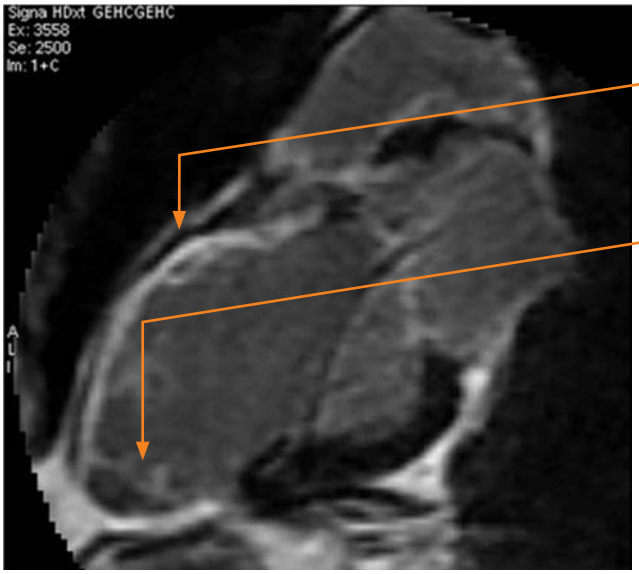

Subendocardial involvement

LV Apical clot

1. The LGE is subendocardial typical of an Infarct.
2. LGE is almost Transmural- Non-Viable.
3. LAD is Type III which wraps around the apex.
4. There is a fairly large organised LV Apical Clot.

The cine CMR and Contrast-enhanced CMR have a sensitivity of nearly 65 % in detecting intracardiac thrombus, while LGE (T1 600 msec) has maximum sensitivity and specificity (100 % sensitive and 99.2 % specific) **making it the diagnostic choice for the detection of intracardiac thrombus.**[6]

Clinical case-2

History is typical and there is no diagnostic confusion. Bronchial asthma patients have a higher prevalence of stress Cardiomyopathy, which may be due to a hyperadrenergic state. This patient had no subendocardial hyperenhancement in LGE and had an uneventful recovery.

Image in Diastole

Image in Systole

Clinical case-3

The images are interesting in that it shows all three patterns clubbed together, the septal mid myocardial hyperenhancement of Dilated Cardiomyopathy,[7] Epicardialhyperenhancement of Myocarditis sequel and Endocardial Hyper enhancement of Inferior and Inferno lateral segments consistent with ischemia-infarct. Subsequently, he underwent Coronary Angiogram which showed three-vessel disease and underwent elective CABG.

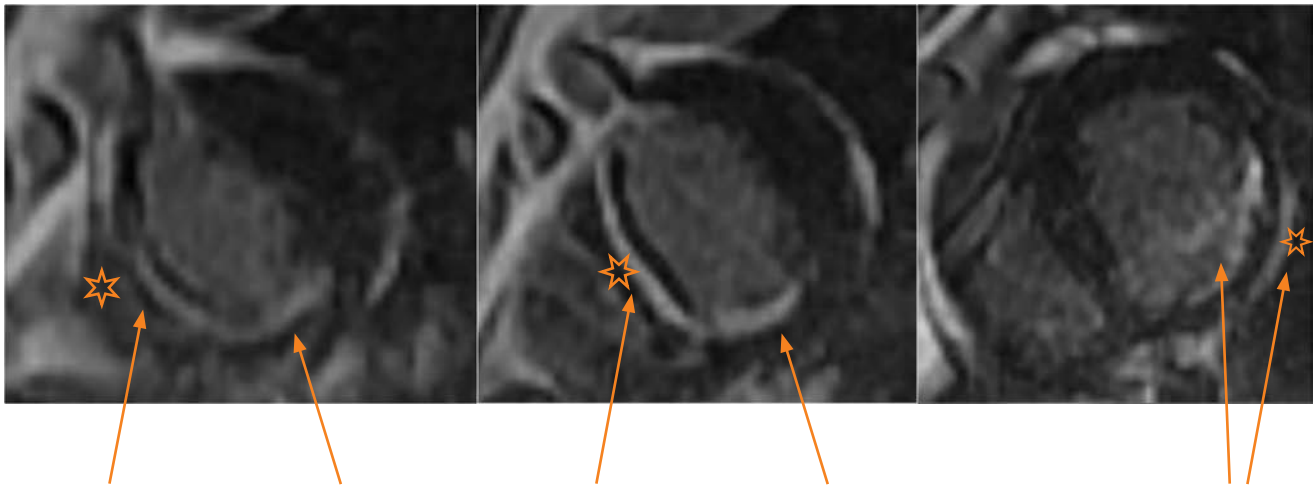

The Septalmid myocardial hyper enhancement (starred areas). The second arrow shows sub-endocardial hyper-enhancement.

The starred areas show sub-epicardial hyperenhancement.
The vertical short arrow indicates endocardial Hyper-enhancement.

Clinical case-4

The mid-ventricular obstruction results in Apical pressure overload and myocardial fibrosis resulting in "Burned out Apex"- a non-coronary cause of LV Apical Aneurysm.[8] Here almost trans mural Hyper enhancement of the apex is documented.

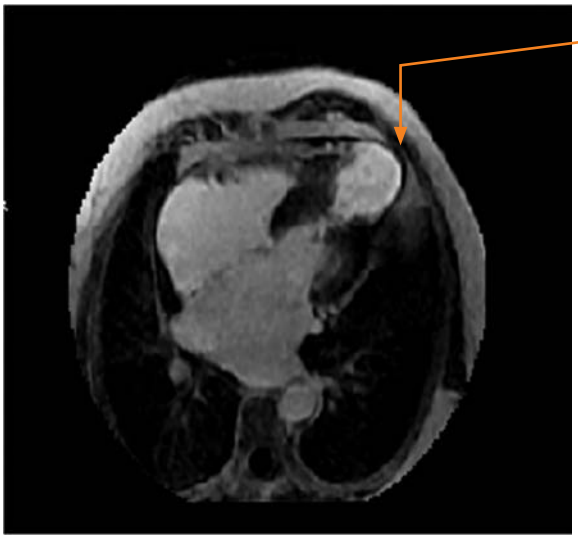

Clinical case-5

The LGE-Hyper enhancement at the RV insertion site is highly s/o HCM.[9]

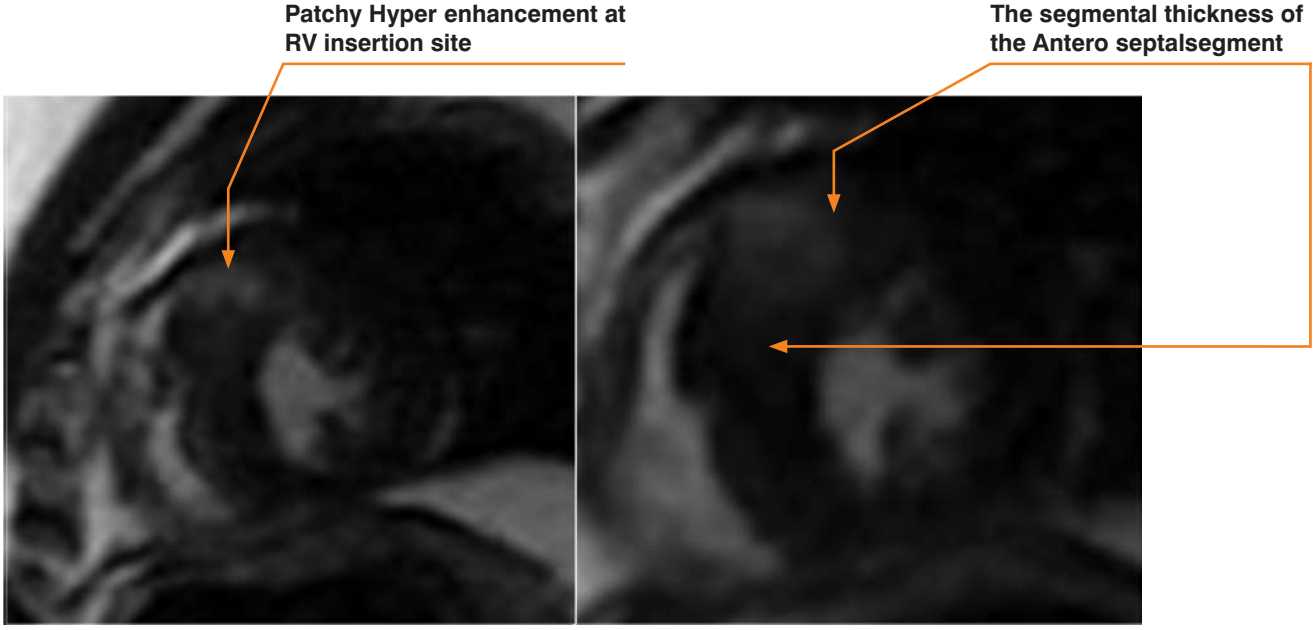

REFERENCES

1. Mario J. Garcia, MD et.al. State of the Art: Imaging for Myocardial Viability A Scientific Statement From the American Heart Association Endorsed by the Society for Cardiovascular Magnetic Resonance.CircCardiovasc Imaging. 2020;13:e000053. DOI: 10.1161/HCI.0000000000000053.

2. Frank M. Baer, MD, Peter Theissen, MD, Christian A. Schneider, MD, Eberhard Voth, MD, Udo Sechtem, MD, FACC, Harald Schicha, MD, Erland Erdmann, MD,FACC. Dobutamine Magnetic Resonance Imaging Predicts Contractile Recovery of Chronically Dysfunctional Myocardium After Successful Revascularization. JACC Vol. 31, No. 5 April 1998:1040–8.

3. Raymond J. Kim M.D, Edwin Wu MD, Allen Rafael MD, Enn-Ling Chen PH. D, Michele A. Parker MS, Orlando Simonetti, PH. D, Francis J. Klocke MD, Robert O. Bonow M.D, Robert M. Judd PH. D. The use of contrast-enhanced magnetic resonance imaging to identify reversible myocardial dysfunction. N Engl J Med. 2000; 343:1445–1453.doi: 10.1056/NEJM200011163432003.

4. Jorge Romero, MD, XiaonanXue, PHD, Waddy Gonzalez, MD, Mario J. Garcia, MD.CMR Imaging Assessing Viability in Patients With Chronic Ventricular Dysfunction Due to Coronary Artery Disease A Meta-Analysis of Prospective Trials. J Am CollCardiolImg 2012;5:494 –508.

5. Heiko Mahrholdt, MD; Anja Wagner, MD; Claudia C. Deluigi, MD; Eva Kispert, RN; Stefan Hager, MD; Gabriel Meinhardt, MD; Holger Vogelsberg, MD; Peter Fritz, MD; Juergen Dippon, PhD; C.-Thomas Bock, PhD; Karin Klingel, MD; Reinhard Kandolf, MD; Udo Sechtem, MD. Presentation, Patterns of Myocardial Damage, and Clinical Course of Viral Myocarditis. Circulation.2006; 114:1581-1590.

6. Kitkungvan D, Nabi F, Ghosn MG, Dave AS, Quinones M, Zoghbi WA, et al. Detection of LA and LAA Thrombus by CMR in patients referred for pulmonary vein isolation. JACC Cardiovasc Imaging 2016;9:809 18.

7. Marthe A.J. Becker, Cornelis P. Allaart, Alwin Zweerink, Jan H. Cornel, Peter M. van de Ven, Albert C. van Rossum, Tjeerd Germans. Correlation between septal mid wall late gadolinium enhancement on CMR and conduction delay on ECG in patients with non-ischemic dilated cardiomyopathy. JC Heart & Vasculature 26 (2020) 100474.

8. Elena Mershina, Olga Blagova, Valentin Sinitsyn and Ekaterina Pershina. A case of hypertrophic cardiomyopathy with “burned-out” apex of the left ventricle due to mid-ventricular obstruction. Clin Case Rep Rev, 2016 doi: 10.15761/CCRR.1000S2002.

9. Yasuo Amano, Mitsunobu Kitamura, Hitoshi Takano, Fumi Yanagisawa, Masaki Tachi, Yasuyuki Suzuki, Shinichiro Kumita, and Morimasa Takayama. Cardiac MR Imaging of Hypertrophic Cardiomyopathy: Techniques, Findings, and Clinical Relevance. Magn Reson Med Sci 2018; 17; 120–131 doi:10.2463/mrms.rev.2017-0145.

Stress Myocardial Perfusion Scintigraphy

Arun Sasikumar

Consultant and Head,
Dept of Nuclear Medicine, PET/CT and Radionuclide therapy,
St Gregorios International Cancer Care Centre,
Parumala, Thiruvalla, Pathanamthitta, Kerala.

Introduction

In conventional radiology we make use of X rays for imaging. For example, CT coronary angiogram makes use of X rays emitted from the CT machine for imaging. In contradistinction, in Nuclear Medicine we utilise gamma rays for imaging. Also, unlike in radiology, in Nuclear medicine we use medicines known as "radiopharmaceuticals" (usually in sub pharmacological doses) which are able to emit radiation (gamma rays). These gamma rays are then emitted from the body of the patient and detected by machines called as Gamma Cameras (**Image 1**). The gamma camera where the radiation detectors are able to move around the patient and acquire 3D images are called as SPECT cameras, where SPECT stands for Single Photon Emission Computed Tomography. Advanced hybrid imaging machines where CT is combined with the gamma camera with 3D rotational capabilities are known as SPECT/CT machines.

Dual head SPECT Gamma Camera

One of the most commonly used procedure in Nuclear Cardiology is Myocardial Perfusion Imaging (MPI). Myocardial perfusion imaging uses an intravenously administered radiopharmaceutical to depict the distribution of blood flow in the myocardium. MPI SPECT images provide a visual threedimensional image of the myocardium perfusion for assessment. The MPI SPECT images can be gated to the electrocardiogram (ECG) to provide Gated SPECT images, which also provide functional assessment of the perfusion images.

The aim of this article is to provide a comprehensive understanding of clinical aspects of MPI relevant for the clinician. The article also aims to provide a basic understanding of the technical aspects of MPI with relevance to its clinical interpretation.

History

The initial application of radioisotopes to cardiac studies started in the mid-1920s. Ventricular function was evaluated in the 1960s and 1970s by first pass and equilibrium techniques. Myocardial stress perfusion imaging was first performed by Dr Barry L. Zaret and Dr H. William Strauss (**images**) using potassium-43

Address for correspondence: Dr Arun Sasikumar MD (PGIMER), FEBNM, FANMB, MICNM, Consultant and Head of the Dept, Dept of Nuclear Medicine, PET/CT and Radionuclide therapy, St Gregorios International Cancer Care Centre, Parumala, Thiruvalla, Pathanamthitta, Kerala.
Email: drarunsgiccc@gmail.com, sasikumararun@gmail.com, Mob: +91-85 899 899 65

and exercise in 1973. Stress imaging rapidly evolved thereafter with new tracers and from revolutionary technological advancements.

Radiopharmaceuticals

Radiopharmaceuticals also called as radio-tracer or tracer is a pharmaceutical labelled with a small amount of radioactivity, which emits gamma rays. The addition of radioactivity does not alter the pharmacological properties of the drug. The major radiopharmaceuticals used for MPI can be divided into two – 201 Tl Thallous chloride and 99mTc based agents including ^{99m}Tc sestamibiand^{99m}Tc tetrofosmin. Initially 201 Tl Thallous chloride was the major agent used for MPI and hence in many older text books / articles, MPI is mentioned as Thallium imaging. However in modern day nuclear cardiology practice, 99mTc agents especially 99mTc Sestamibi is the preferred imaging agent for MPI. 99mTc Sestmibi is preferred over 201Thallous chloride owing to the much better image quality, less radiation exposure and lesser cost of 99mTc Sestamibi.^{13}N-ammonia and ^{82}Rb are radiopharmaceuticals used for PET myocardial perfusion imaging. Our discussion in this article would be restricted to SPECT MPI alone.

99mTc Sestamibi

Sestamibi is a lipophilic monovalent cation (an isonitrile compound). The uptake in myocardium is proportional to blood flow in the physiologic flow range. The myocardial uptake of ^{99m}Tc-sestamibi is dependent on multiple factors like mitochondrial-derived membrane electro-chemical gradient, intact energy production pathways and cellular PH. Sestamibi will not be extracted by non-viable myocardium.

99mTc Tetrofosmin

Tetrofosmin is a lipophilic, cationic compound, which is rapidly cleared from the blood following intravenous administration. The uptake mechanism is membrane-potential driven diffusion independent of cation channel transport. The agent accumulates within mitochondria similar to ^{99m}Tc-sestamibi. The biological half-life for tetrofosmin in normal myocardium is around 5 hours, which is shorter than sestamibi (11 hours) and is because of higher lipophilicity of tetrofosmin. The mean first pass extraction fraction is about 54%.

Indications

1. Symptomatic patients or patients with ECG suggestive of ischemia, with intermediate or high pre-test probability.
2. Symptomatic patients or patients with ECG suggestive of ischemia, with low pre-test probability and
   a. unable to perform a stress test
   b. an uninterpretable ECG (left branch block, preexcitation, etc)
3. Patients with known coronary anatomy, with need for identification of the vessel related to the ischemia (definition of the hemodynamic meaning of coronary lesions).
4. Moderate-risk pre-operative patients of non-cardiac surgery or vascular surgery with one or more risk factors* and poor functional capacity.
5. General surgery pre-operative stratification in patients with confirmed heart disease: recent acute myocardial infarction (AMI) – last six months, unstable angina, decompensated heart failure and severe valve disease.
6. High or intermediate risk general surgery pre-operative stratification in patients with functional capacity ≤ 4 METS, or patients whose functional capacity is impossible to assess when at least one of the risk factors*.
7. After coronary artery bypass surgery (>3 months) in symptomatic patients, if the surgery was incomplete, or if the procedure was over five years before.
8. Asymptomatic patients with high pre-test probability of coronary artery disease, calcium score between 100-400 or > 400 and intermediate risk.
9. For risk evaluation and stratification of known CAD patients undergoing medication therapy after 6 months of beginning and/or alteration of treatment.
10. Patients with suspected CAD who underwent previous exams with inconclusive or conflicting results.
    a. Patients with diabetes mellitus (for at least ten years or with diabetic microangiopathy or risk factors for CAD, such as systemic arterial hypertension, smoking, dyslipidemia, or family history of early onset CAD);
    b. Patients with evidence of documented atherosclerosis by complementary exams;
11. Patients with Framingham risk score ≥ 20% of events in 10 years.

**Clinical risk factors: previous history of coronary artery disease (CAD), history of heart failure, history of cerebrovascular disease, diabetes mellitus or kidney failure (serum creatinine over 2 mg/dL);*

Principle

MPI scans are acquired under conditions when the body is at rest and when stressed. The comparison of the stress and rest images makes it possible for the assessment of relative myocardial perfusion. The stress condition can be induced either physically by performing an exercise task, or pharmacologically by intra-venous injection of a vasoactive drug to the patient. During

periods of stress, areas of the myocardium supplied by normal healthy arteries will increase their blood supply however areas of myocardium supplied by permanently or temporarily stenosed coronary arteries cannot do so to the same extend as the normal myocardium. This difference in myocardial perfusion is mapped by the radiopharmaceutical.

The radiopharmaceutical delivery and uptake will be reduced in areas of myocardium supplied by permanently or temporarily stenosed arteries. If either the area or the severity of decreased tracer concentration (perfusion defect) is worse when the tracer is administered during stress than at rest; is called a reversible perfusion defect. This reversible perfusion defect is most likely due to ischemia (the ischemia induced by the stress) and hence it represents inducible ischemia. If the area of diminished tracer concentration remains unchanged from rest to stress (fixed perfusion defect), the defect most likely represents scar. The fixed perfusion defect although in some cases may represent viable, underperfused myocardium which can be identified with 18F-FDG PET cardiac viability study.

Preparation

Patient preparation instructions for stress MPI.

1. Patients should be fasting for at least 4 h.
2. If exercise stress testing is planned beta-blocking drugs and preferably (if clinical condition permits) calcium channel blocking drugs to be stopped 48 hrs before stress study.
3. If pharmacological stress testing using adenosine is planned then Caffeine-containing beverages (tea, coffee, cola and chocolates) and methylxanthine-containing medications that interfere with the coronary hyperemia produced by these drugs should be discontinued for at least 24hrs.
4. If pharmacological stress testing using dobutamine is planned then beta-blocking drugs to be stopped 48 hrs before stress study.

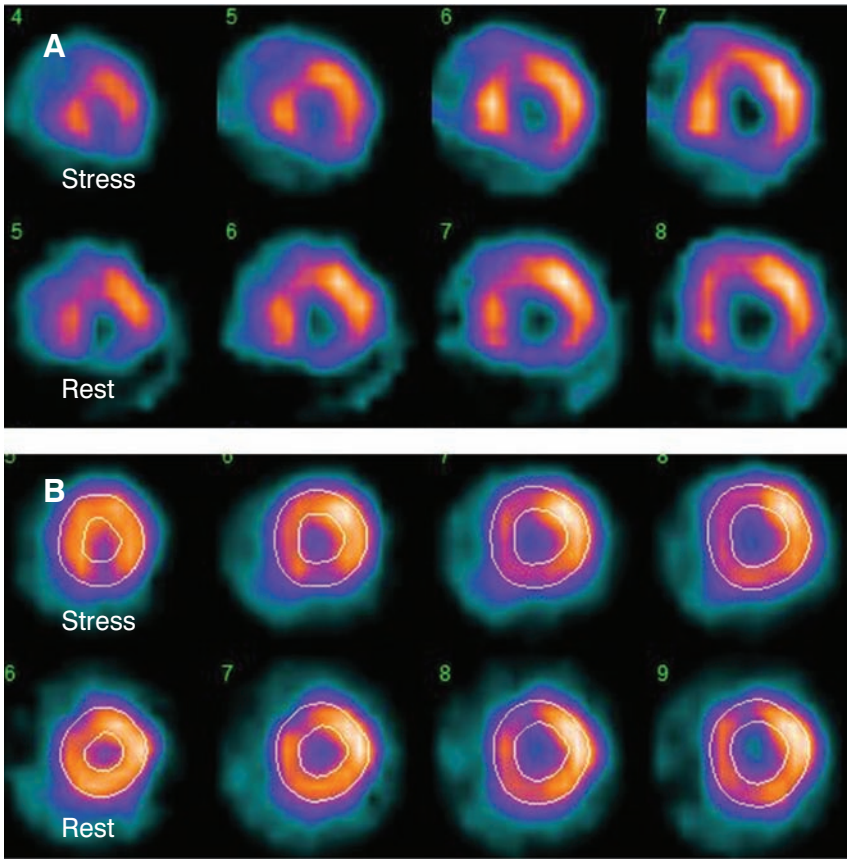

A: Fixed perfusion defect in inferior wall (black arrows, note that the significant reduction in inferior wall persists in stress and rest images).
B: Stress induced reversible perfusion defect / inducible ischemia in inferior wall (white arrows, note the improvement in tracer uptake in inferior wall in rest images compared to stress images).

Ensure the following prior to performing stress test:

1. Clinical history should be obtained, including the indication for the test, symptoms, risk factors, medication and prior diagnostic or therapeutic procedures.

2. In diabetic patients, diet and insulin dosing should be optimized on the day of examination. In selected, insulin treated patients, it may be useful to check blood sugar concentration before an exercise stress test.

3. Patients should be haemodynamically and clinically stable for a minimum of 48 h prior to the test.

Stress MPI

There are two forms of stress available for stress MPI namely exercise stress testing and pharmacological stress testing. Exercise stress testing is preferred modality in India over pharmacological stress test as it is cheaper and logistically easier to perform; and also because it provides additional prognostic information.

Exercise stress test: Graded exercise stress using treadmill (bicycle ergometer is an alternative option) is the most widely used exercise modality, with Bruce and modified Bruce being the most widely used exercise protocols. Exercise testing has a limited value in patients who cannot achieve an adequate heart rate and blood pressure response due to non-cardiac physical limitations such as pulmonary, peripheral vascular, musculoskeletal abnormalities or due to a lack of motivation. Pharmacological stress is to be considered for such patients. **Figure** represents the clinical algorithm to choose the mode of stress for a patient referred for MPI. Contraindications to different forms of stress have been summarised in **table**.

Algorithm to choose mode of stress for MPI

The pharmacological stress test has proven to be an excellent alternative to the physical exercise test. There are two forms of pharmacological stress agents available - vasodilator agents (such as Adenosine, Regadenoson or Dipyridamole) or inotropic agent - Dobutamine.

Adenosine is a direct coronary vasodilator and leads to a 3.5 to 4-fold increase in myocardial blood flow. The coronary vasodilatation is induced by the stimulation of adenosine A2A receptors, and the non-specific stimulation of the other receptors is thought to be the cause of the side effects. The plasma half-life of adenosine is approximately 2–10 seconds and hence needs a constant intravenous infusion during pharmacological stress test to maintain high plasma levels. It is routinely given as a continuous infusion at a rate of 140 μg/kg/min over 6 minutes (**figure**). Submaximal dynamic exercise may be coupled when tolerated (except in patients with LBBB)to reduce the frequency and severity of adverse effects encountered during infusion. Low level exercise attenuates the adenosine-induced drop in blood pressure and also improves image quality by decreasing the artefacts due to increased splanchnic activity. Common side effects observed during adenosine stress test are:- Chest pain, Dyspnoea, Flushing, Headache, SVT/ventricular arrhythmias, Bronchospasm, Palpitations, Dizziness, Hypotension and High degree AV block.Owing to short half life of adenosine these side effects are often short-lived and rarely require active intervention.

Adenosine infusion algorithm

Dipyridamole is an indirect coronary artery vasodilator that increases the tissue levels of adenosine by preventing the intracellular reuptake and deamination of adenosine. Side effect profile is similar to adenosine but owing to its longer half life may require administration of theophylline to reverse the side effects.Dipyridamole is not available in India.

Regadenoson is a A2A adenosine receptor agonist which acts as a direct coronary vasodilator like adenosine. Regadenson has a half life of 2 to 3 minutes which allows single bolus administration. Regadenoson is given as a slow bolus over 10 s followed by a 10 s flush of 5 to 10 ml NaCl 0.9%, 10 to 20 s later the radiopharmaceutical is injected. Regadenoson is administered independent of patient weight in a dose of 0.4 mg in 5 ml.

Vasodilator stress should be stopped early under the following circumstances:

- Severe hypotension (systolic blood pressure <80 mmHg)
- Persistent second-degree or sign of third-degree atrioventricular or sino-atrial block
- Wheezing
- Severe chest pain.

Dobutamine increases regional myocardial blood flow and results in direct β1 (beta) and β2 receptor stimulation, with a dose-related increase in heart rate, blood pressure and myocardial contractility. The increase in heart rate and myocardial contractility as a result of dobutamine infusion results in an increase in myocardial oxygen demand, with subsequent hyperaemia. This causes secondary dilatation of coronary arteries, resulting in increased blood flow through normal coronary arteries.

Dobutamine is infused incrementally starting at a dose of 5 to 10 μg/kg/min, which is increased at 3 minute intervals to 20, 30, and 40 μg/kg/min. (**Figure**) Carefully monitored titration is required throughout the test and is often time consuming and mostly performed under ICU setting or with adequate support from cardiology team. Common side effects of dobutamine include chest pain, dyspnoea, headache, palpitations, hypotension and SVT/ ventricular arrhythmias. Beta-blockers are the antidotes used to counteract the side effects/complications of dobutamine.

Some use atropine in patients where the heart rate fails to reach 85% of age predicted heart rate or THR, even with the maximum dose of dobutamine. Contraindications to atropine administration under dobutamine stress include narrow angle glaucoma, obstructive uropathy, including bladder neck obstruction from prostatic hypertrophy, atrial fibrillation with an uncontrolled heart rate and an obstructive gastrointestinal disease or paralytic ileus.

Dobutamine infusion algorithm

Imaging protocols: A myriad of imaging protocols are available including single isotope and dual isotope protocols and single day versus two day protocol and is quite confusing for the referring physician. Dual isotope protocols may be completely ignored as 201Tl based imaging is not performed these days.

The major imaging protocols thus to be considered are one day protocol and two day protocols. In one day protocol both stress and rest MPI is performed on the single day with a 3 to 4hrs gap between stress and rest MPI. Usually rest study is performed first in such scenarios. The stress study is performed on the same day using two to three times the dose of 99mTc sestamibi and hence the patients gets an additional radiation dose.

In two day protocol using the same low dose of 99mTc sestamibi injected on two separate days,stress and rest MPI images are obtained. Although this offers advantage of reduced radiation exposure it may be difficult from patient perspective as it requires two days of hospital visit. Now the question of whether to perform stress first or rest first is also debatable in various single day and two day protocols. A rest study is normally performed first as it rules out major defects and low functional capacity at rest itself, that may be preclude the stress study. However stress study may be performed first in busy departments and if the pre test probability for a normal study is more; because if stress study is absolutely normal a rest study can be avoided. To summarise the imaging protocol is chosen based on patients clinical condition and logistic requirements from both the patient side and the Nuclear Medicine department side.

Image acquisition and interpretation:

SPECT image acquisition is done on gamma camera with 3D rotation capabilities (SPECT gamma camera) and may take from 15-40 minutes depending on the gamma camera. The images are reconstructed using appropriate reconstruction algorithms to obtain images in various planes for interpretation. Most modern gamma cameras provide gated acquisition (G-SPECT) where the images are acquired in phases of ECG and this provides additional functional information including global EF, RWMA etc. Hybrid SPECT/CT machines are available which allow low dose CT for attenuation correction. The acquired images are segmented and represented in various formats including planar in axial, VLA and HLA sections, surface rendering, gated images etc. The Nuclear Medicine physician interprets the images after thorough analysis of all available image sub sets.

Data analysis of regional perfusion imaging

Adequate interpretation of MPI requires a systematic visual review of raw data and reconstructed images on a computer screen. The process is represented below:

Data analysis flow chart

Analysis of raw data is done for QC of acquired data including patient motion. Following features are assessed in raw images:

- LV dilatation, either permanent or transient after stress
- Increased lung uptake of tracer, particularly when 201Tl is used
- Clearly visible RV tracer uptake: RV hypertrophy or (occasionally) generalised low LV uptake
- Extra-cardiac abnormalities: focal breast or lung accumulations, duodenal-gastric reflux, or bile obstruction.

Analysis of Stress parameters is done to assess the adequacy of stress (optimal / suboptimal). If suboptimal then it should be mentioned in the report. Inadequate stress may result in underestimation of the presence, severity and extent of stress induced perfusion abnormalities. Lack of true rest in patients with critical coronary disease, may lead to underestimation of the presence, severity and extent of the reversibility of perfusion defects.

Analysis of Processed image data and Quantitative data to assess myocardial perfusion in stress and rest images based on segment based models.

Review of tomograms

Slices (**figure**) All three image planes should be inspected: short-axis, horizontal long-axis and vertical long- axis. Stress and rest images should be aligned in a way that the tomograms are carefully displayed with anatomically corresponding stress and rest slices under each other. The short-axis tomograms should be displayed with the apical slices to the left and the base to the right. The vertical long-axis tomograms should be displayed with septal slices to the left and the lateral slices to the right. Similarly, the horizontal long-axis tomograms should be displayed with inferior slices to the left and anterior slices to the right.

Polar maps (bull's eye) display: (**figure**) This display represents LV perfusion in a single two-dimensional image and facilitates the assessment of the presence, location, extent and severity of perfusion abnormalities. Ventricular size, however, is not represented in the polar map. By digitally subtracting the rest polar map from the stress polar map, the presence, location, extent and severity of stress induced perfusion defects are easily reviewed. It is critical that the rest and stress polar maps are based on identical delineation and orientation of the LV and no marked differences between possible extracardiac activity accumulations adjacent to the LV. If corresponding parts of the polar maps do not represent identical parts of the LV myocardium, it can lead to serious, falsely positive differences in stress induced perfusion changes in the polar maps. It should be emphasised that the polar map does not disclose possible artefacts such as false perfusion defects caused by attenuation from by intervening tissue or a pacemaker, intra- or extracardiac hot spots.

Three-dimensional display: This display may also facilitate the assessment of the presence, extent and location of LV perfusion abnormalities. LV size and configuration can be displayed. In addition it may be helpful for correlation of perfusion data with other examinations such as echocardiography and coronary

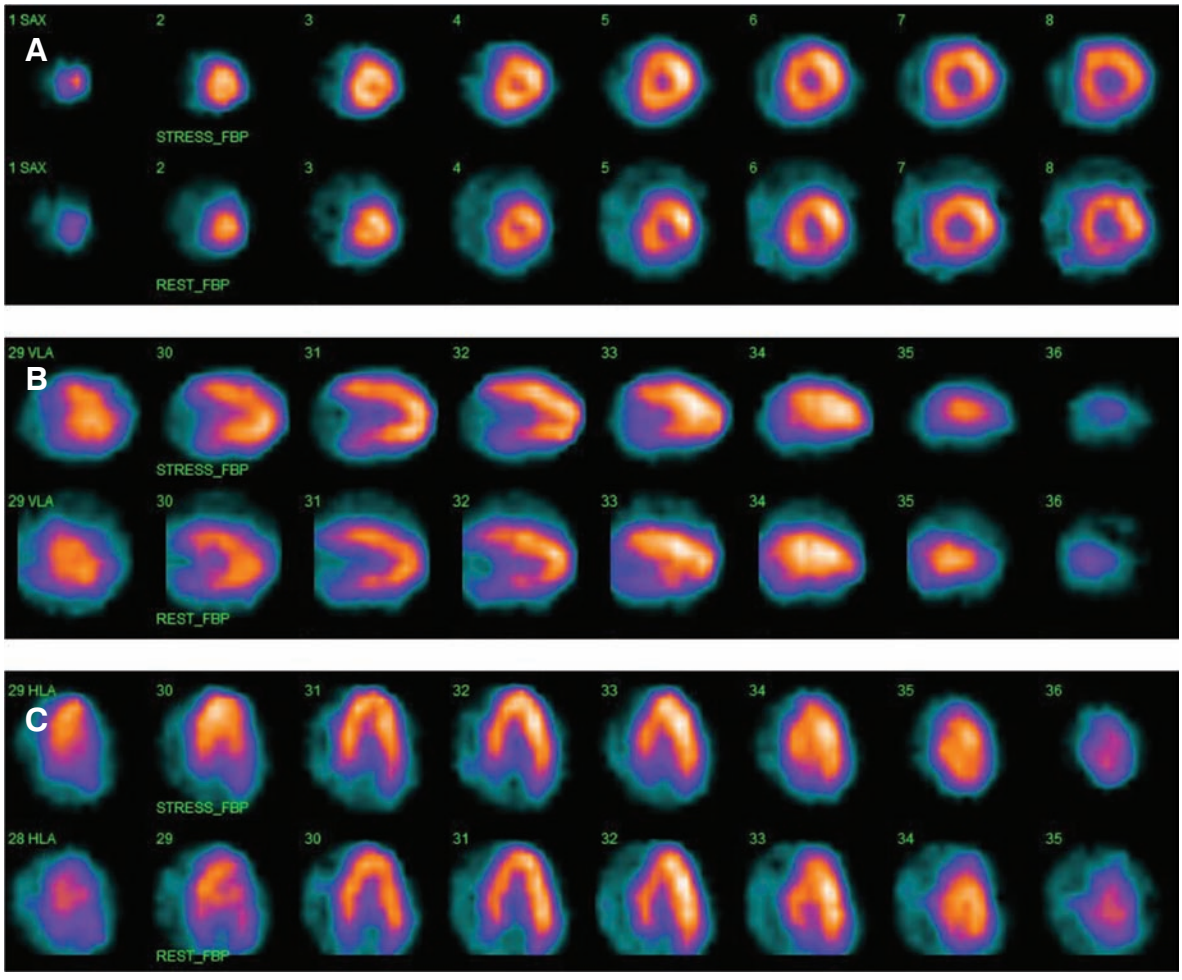

Adenosine stress rest MPI images. **A**: axial slices, **B**: Vertical long axis (VLA) slices, **C**: Horizontal long axis (HLA) slices.

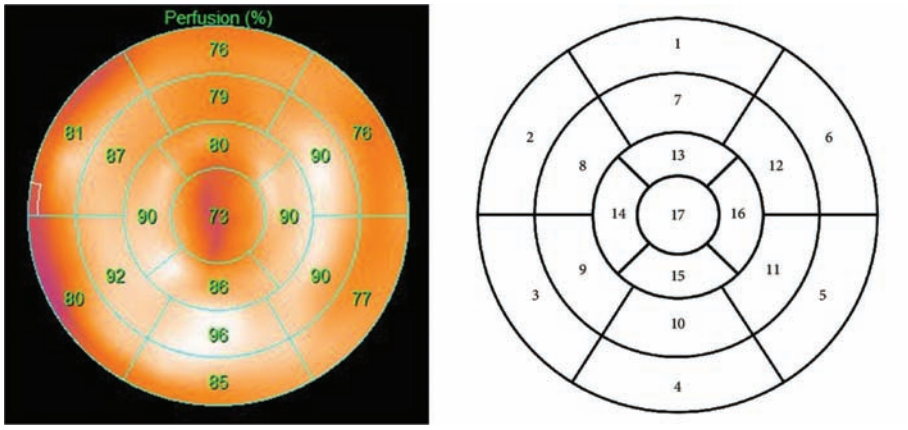

Bulls eye representation of stress myocardial perfusion images in 17 segment model.

angiography in particular in the communication with clinical cardiologists.

Visual analysis: An area of diminished uptake of the radiopharmaceutical has to be described with respect to localisation, severity and extent. If using a segmental model, the 17-segment model (**figure**) and the associated nomenclature is recommended, as this model provides the best agreement with other imaging modalities such as MRI, echocardiography and anatomical data.

Regional tracer uptake. The distribution of the perfusion tracer may be assessed in relation to the activity distribution in healthy, gender-stratified, reference populations for the same LV region as

- Normal: ≥70%
- Mildly reduced: 50-69%
- Moderately reduced: 30-49%
- Severely reduced: 10-29%
- Absent: <10%.

The percentages allow for the normal, regional variation of count rates, e.g. septal count rate to be lower than that in the lateral wall in healthy subjects.

Extent of a perfusion defect - The extent of a perfusion abnormality should not only be classified as small, intermediate or large. Quantitative data should be added.

LV size and function - A visual assessment of the LV cavity should be performed. With gated studies, quantitative measurements of volumes can be acquired like EDV and EF etc can be obtained.

Quantitative analysis

Absolute quantification of regional myocardial perfusion is still only possible with PET, but a number of validated, quantitative programs for SPECT analysis of the relative perfusion distribution and cardiac function are commercially available. These quantitative analysis should be used in combination with the visual review of the images since technical problems and most artefacts will not be recognised if only quantitative analysis is performed.Segmental models. One approach to quantify MPI is to first divide the myocardium into 17 segments. Each segment is scored separately using a 5-point model ranging from 0 (normal uptake) to 4 (uptake absent). The total scores of the LV are referred to as the summed stress score (SSS), summed rest score (SRS) and summed difference score (SDS: stress minus rest score). All scores have been shown to be of prognostic value. In addition, the scores should be expressed as normalized to percent of the total LV involved with stress, rest, and ischaemic defects by dividing the summed scores by 68, the maximum potential score in the 17-segment model (4x17), and multiplying by 100, respectively.

Score normalized to %LV = score (ie., SSS, SDS or SDS) * 100 / 68

Coronary artery supply and SPECT images. Some quantitative analysis programs may offer the option of assigning myocardial segments to a specific vascular territory. One has to bear in mind, however, that there is a large inter-individual variability in the territories subtended by the three main coronary arteries and their branches, and caution should be taken when assigning myocardial segments to specific vascular territories. Programs that allow matching of the angiographic data and perfusion data within one person are commercially available.

Mild reduction of regional tracer uptake may represent a mild perfusion reduction or an attenuation artefact. Information on wall motion and wall thickening in such regions may help to differentiate between these

Table: Artifacts during nuclear imaging.

	Artifact	Cause	Correction
1.	Patient motion	Patient motion during scan acquisition	Use motion correction algorithms for correction.
2.	Upward Creep artefact	Mostly seen with 201Tl scans	Use motion correction algorithms for correction.
3.	Soft tissue attenuation artefacts	Inferior wall, particular in men, Breast attenuation in women and Pectoral muscles in athletic subjects causing anterior / anteroseptal defects.	Use attenuation correction Mention in report the possible attenuation artefacts.
4.	Scatter	Adjacent activity in bowel, liver, gall-bladder	Use scatter correction
5.	Arrhythmias	Arrhythmias	Gated images should not be used for interpretation if significant rejection (>1/3) of cardiac cycles has occurred

possibilities. However, presence of regional wall motion and/or thickening does not exclude a stress-induced perfusion defect shown by ^{99m}Tc tracers, since the imaging is a reflection of post-stress (i.e. usually = resting) myocardial function. Moreover, LV function has been found to be an independent prognostic marker for cardiac events. The combined assessment of perfusion and function has major prognostic implications.

Technical artifacts

SPECT images may be affected by technical artifacts. Careful acquisition and adequate quality control measures can ensure minimisation of technical artifacts. Below given **table** summarises the technical artefacts and ways to reduce / correct it. If technical artefacts still persists after correction measures are used and if they interfere with interpretation of the study it should be mentioned in report or if required the study may be repeated.

Myocardial Perfusion Imaging for Risk Stratification in Suspected or Known Coronary Artery Disease:

Chronic stable angina: For patients with chronic chest pain syndromes, testing is directed towards establishing the presence or absence of CAD to guide therapy and determine prognosis. Pre-test probability of CAD based on the patient's history, physical examination and risk factor assessment is crucial. Those with an intermediate to high pre-test probability of CAD are considered the best candidates for MPI. MPI can act as a gate keeper to determine which patients need invasive procedures and who do not. Reported sensitivities (the percentage of abnormal images in patients with significant CAD) of exercise and vasodilator stress SPECT MPI are 87% and 89% respectively; while specificities (the percentage of normal images in patients without significant CAD) are 73% and 75%.

In patients with stable symptoms, a normal stress Tc-99m sestamibi SPECT MPI was associated with a very low risk of death or nonfatal myocardial infarction (0.6% annually) in contrast to a 12-fold higher event rate (7.4% annually) in patients with abnormal images (fixed or reversible defects). To note is the fact that a normal stress MPI carries similar satisfactory outcomes in stable angina patients with significant angiographic disease. The annual rate of cardiac death or nonfatal myocardial infarction in these patients, remains less than 1% per year, comparable with the overall event rate in patients with a normal scan who had documented CAD.

Patients with remote myocardial infarction may also benefit from stress MPI for prediction of subsequent cardiac events. Integration of the severity of ischemia, left ventricular functional status, lung-to-heart ratio and the presence of transient ischemic dilatation of the left ventricle (LV) improves post-test stratification of patients into low, intermediate, and high risk of cardiac death, and help guide clinical decision-making and referral for coronary angiography and revascularization procedures.

Acute Coronary Syndrome (ACS): In the emergency department (ED), the differentiation between cardiac

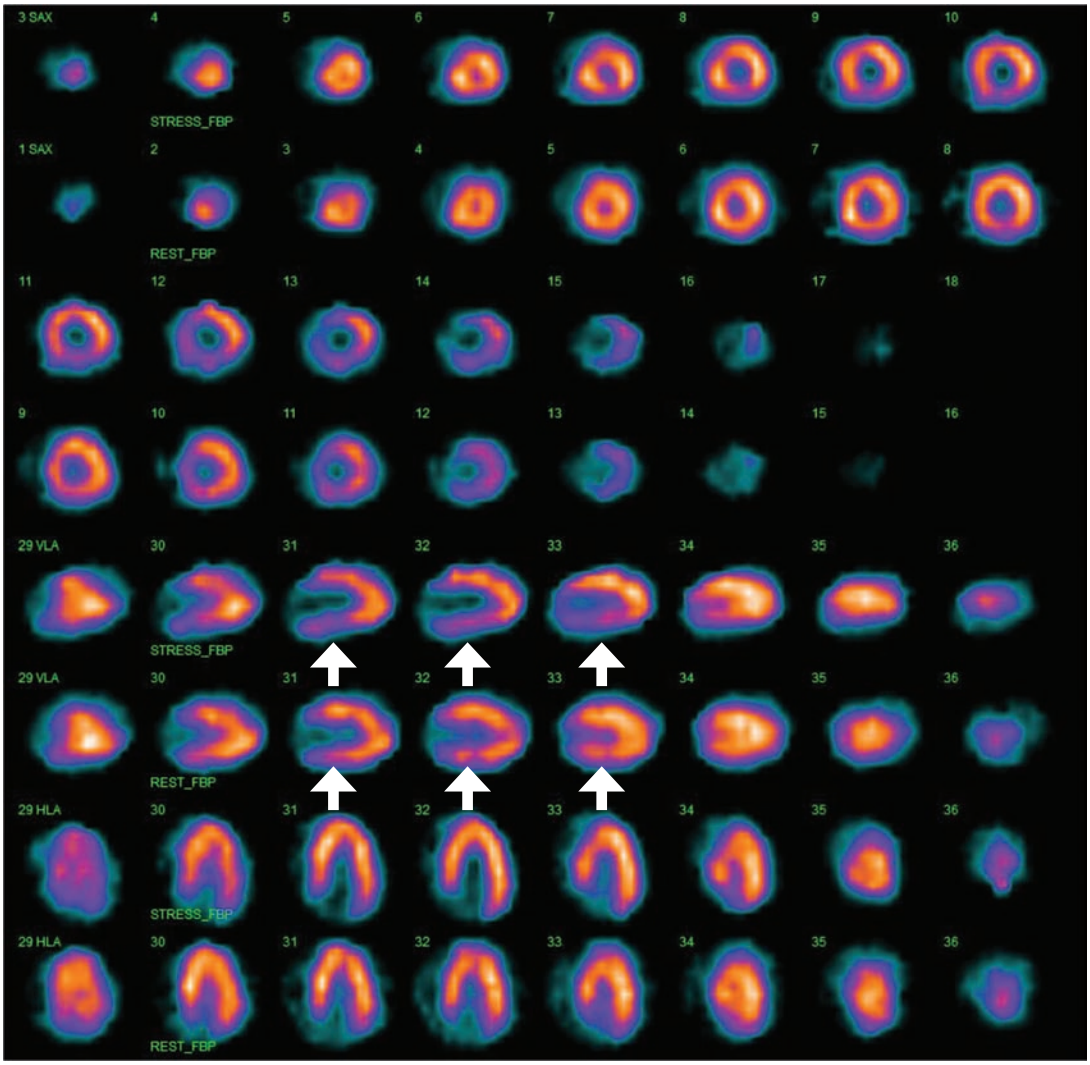

63 yr old male with stable chronic chest pain, CAG showed SVD with 70% ostial stenosis in RCA. MPI with exercise stress was done. Images show stress induced reversible perfusion defect (inducible ischemia) (best appreciated in VLA images - white arrows) of mild severity involving entire inferior wall (RCA territory) involving ~15-18% of LV myocardium.

and noncardiac chest pain is often difficult despite meticulous initial evaluation. Acute coronary syndrome refers to any constellation of clinical symptoms that are compatible with acute myocardial ischemia. It includes ST-segment elevation myocardial infarction (STEMI), non-ST-segment elevation myocardial infarction (NSTEMI), as well as unstable angina (UA).

Current practice favors using coronary angiography for delineation of coronary anatomy as the basis for decision management in acute coronary syndrome. In the absence of markers of ischemia or obvious abnormalities on initial ECG (possible ACS), rest Tc-99m sestamibi perfusion imaging is appropriate and can reduce unnecessary hospitalizations among patients without acute ischemia. Tc-99m-sestamibi or tetrofosmin are suitable for acute imaging at the ED as they remain trapped in the myocardium and thus enabling later imaging. The negative predictive value (NPV) of SPECT MPI to exclude myocardial infarction in these patients ranges from 99% to 100% and the NPV for excluding future cardiac events during medium-term follow-up is approximately 97%. While rest MPI is useful for diagnosis of an acute myocardial infarction by identifying perfusion defects, such defects do not distinguish between acute ischemia, acute infarction, or previous infarction.

In medically stabilized US/NSTEMI patients, stress gated SPECT MPI is appropriate for:

1. detection of inducible ischemia in the distribution of the "culprit lesion" or in remote areas in patients at intermediate or low risk for major adverse cardiac events.

2. recognition of the severity/extent of inducible ischemia.

3. identification of hemodynamic significance of coronary stenosis after coronary arteriography.

4. measurement of baseline LV function.

In patients with STEMI, MPI remains an accurate method for risk-stratifying patients after acute reperfusion therapy. Exercise and pharmacologic stress MPI can predict the outcome in patients following thrombolytic therapy. Travin et al. reported that the presence of either ischemia as seen on SPECT or defects in multiple vascular territories identified 92% of patients who subsequently experienced an event after hospital discharge. As post-thrombolysis patients who lack ischemia by noninvasive testing have an excellent prognosis, it seems unlikely that routine late coronary revascularization in this population would further improve outcomes.

Current guidelines recommend exercise or pharmacological MPI before or early after discharge in patients with STEMI who are not undergoing cardiac catheterization to look for inducible ischemia. MPI is also reasonable in hemodynamically and electrically stable patients 4 to 10 days after STEMI to assess myocardial viability when required to define the potential efficacy of revascularization. A small fixed perfusion defect indicates an excellent prognosis, and probably low benefit from revascularization. On the other hand, patients with markers of increased risk (number and severity of myocardial perfusion defects, transient LV dilation, and increased tracer lung uptake) could be referred for coronary angiography and revascularization.

Asymptomatic patients: The American College of Cardiology Foundation (ACCF) and the American Society of Nuclear Cardiology (ASNC) recommend against routine stress imaging studies in asymptomatic patients without chest pain syndrome. MPI is indicated in asymptomatic patients without chest pain syndrome in the following situations: - Patients with moderate to high CHD risk and the presence of new onset or diagnosed heart failure, new-onset atrial fibrillation and ventricular tachycardia; Patients with high-risk occupation (e.g., airline pilot) and for evaluation of ventricular function in patients using potentially cardiotoxic therapy (e.g., Doxorubicin). SPECT MPI is of particular importance in the evaluation of silent myocardial ischemia in moderate risk patients undergoing major vascular surgery, type II diabetics, chronic hemodialysis patients and transplant recipients.

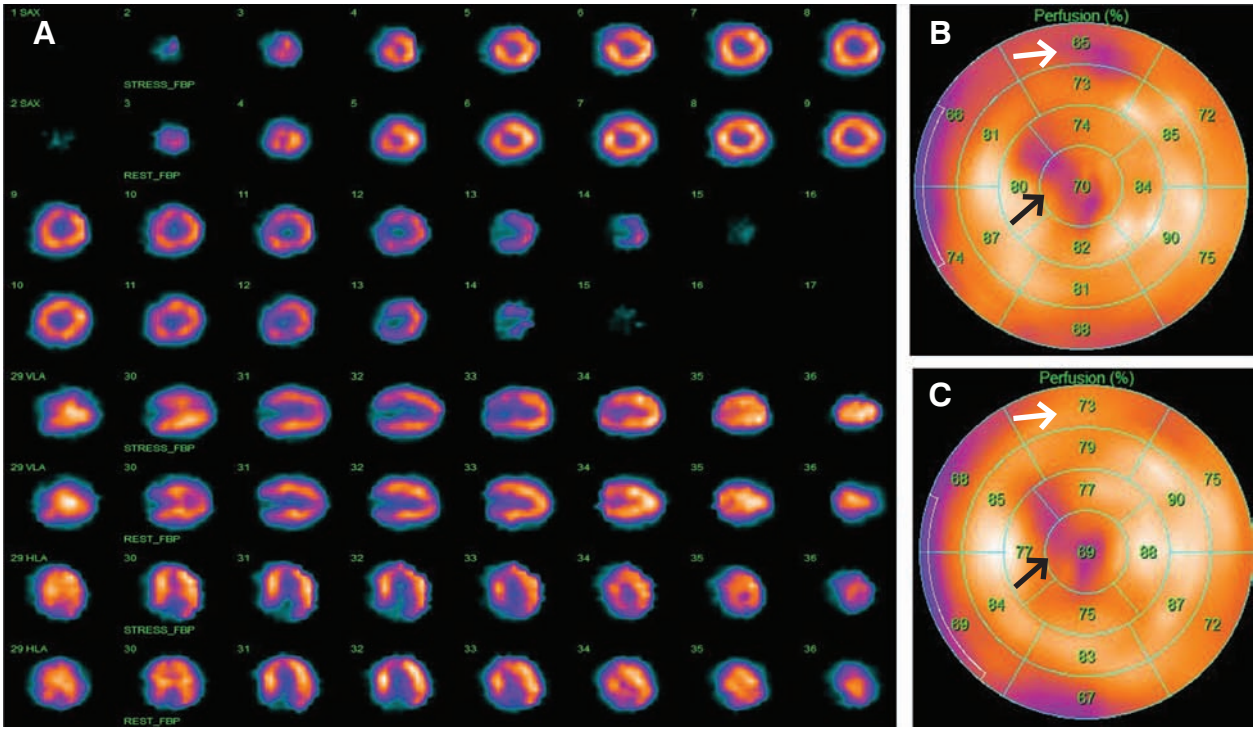

64 yr old male, known case of long standing diabetes with CKD and dyspnea on mild exertion. MPI using exercise stress test was done. Images A – slices, B bulls eye map of stress perfusion and C bulls eye map of rest perfusion. Images show stress induced mild reversible perfusion defect (**mild inducible ischemia**) in part of basal anterior segment (**white arrows**) involving **~5-6%** of the LV myocardium at the level of stress achieved in this study. Fixed perfusion defect of mild severity in part of apex and the apical septum (**black arrows**) involving **~8-10%** of the LV myocardium.

MPI in women: Exercise electrocardiography (ECG) has a perceived lower diagnostic accuracy in women, in particular because of the occurrence of ≥1 mm of ST segment depression. In women, exercise ECG has an average sensitivity and specificity of 61% and 70% respectively. There is potential additive benefit of stress MPI in women, particularly those with an intermediate–high pretest likelihood of CAD. In women undergoing exercise myocardial perfusion imaging, the number of abnormal territories remains the strongest correlate of mortality after adjustment for exercise variables. Women incapable of attaining a minimum of 5 METS of exercise should be considered candidates for myocardial perfusion imaging with pharmacologic stress.

LIMITATIONS

1. Technical artifacts:- Tissue attenuation artefacts, photon scatter, motion artefacts, and limited spatial resolution.

2. Medications such as beta-blockers, calcium channel blocking agents and long-acting nitrates may limit the development of ischemia during the exercise test or decrease the extent of perfusion defects

3. The level of exercise may also affect the sensitivity of SPECT MPI in the localization and evaluation of the extent of coronary artery disease and the detection of ischemia.

4. In the setting of ACS, the availability of alternative methods and the logistics and time demands of performing MPI in the setting of AMI have limited its widespread clinical application

5. STEMI patients treated with thrombolysis have a low overall mortality and as a result the ability of a positive early scan to predict poor outcomes may be inadequate

6. In extensive CAD, SPECT MPI may not show the typical pattern of multi-vessel disease and may not necessarily reflect involvement of more than one vessel. Some scintigraphy features such as transient ischemic dilatation and increased lung uptake of tracer represent useful predictors of extensive CAD in this setting.

Radiation exposure to relatives of patient and to hospital staff

Patient relatives

In general, radiation exposure to accompanying persons and relatives is very limited, and no special precautions are needed for studies with either ^{99m}Tc-labelled tracers or ^{201}Tl-chloride. Only close contact with infants should be restricted. One-day protocols for patients taking care of infants should be avoided.

Staff

The radiation exposure to staff working in nuclear medicine or nuclear cardiology departments varies widely depending on workload, local work procedures etc., but the effective dose to technologists/physicians are generally well below limits.

Pregnant patients

In general MPI should not be performed in pregnant women since a number of alternative methods are available for cardiac imaging giving less or no radiation exposure. This holds true not only when pregnancy is confirmed, but also for women in whom pregnancy is not excluded (e.g. a missed period or the period is known to be irregular).

Lactating patients

In general, elective diagnostic nuclear medicine procedures should be delayed until the patient is no longer breast-feeding. However, according to the ICRP 106, the interruption of breast-feeding is not essential for ^{99m}Tc-labeled compounds. But according to the principle of keeping exposure “as low as reasonably achievable”, following recommendations are made:

- Use 99mTc-labelled tracers rather than 201Tl
- Nurse the infant just before administration of the radiopharmaceutical
- Interrupt breastfeeding for 3 to 6 hours after the administration of dose
- Express the milk completely once and discard it
- Close contact with infants should be restricted for 6-12 hours.

CONCLUSION

MPI is one of the most powerful non invasive imaging tests available to assess myocardial perfusion. Gated SPECT studies provide additional functional information pertinent to perfusion abnormalities. Hybrid SPECT/CT minimises attenuation artifacts as well. Used in appropriate patients and for valid indications MPI provides great adjunct information in management of diagnosed or suspected CAD patients.

Adenosine algorithm

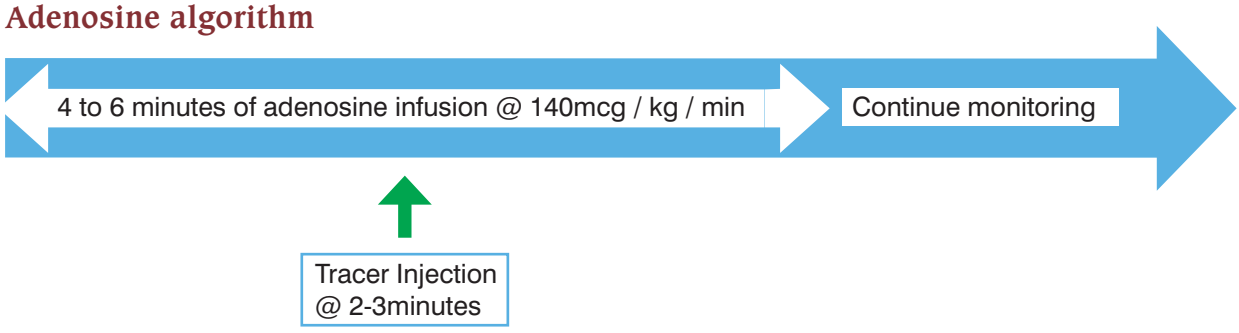

Dobutamine algorithm

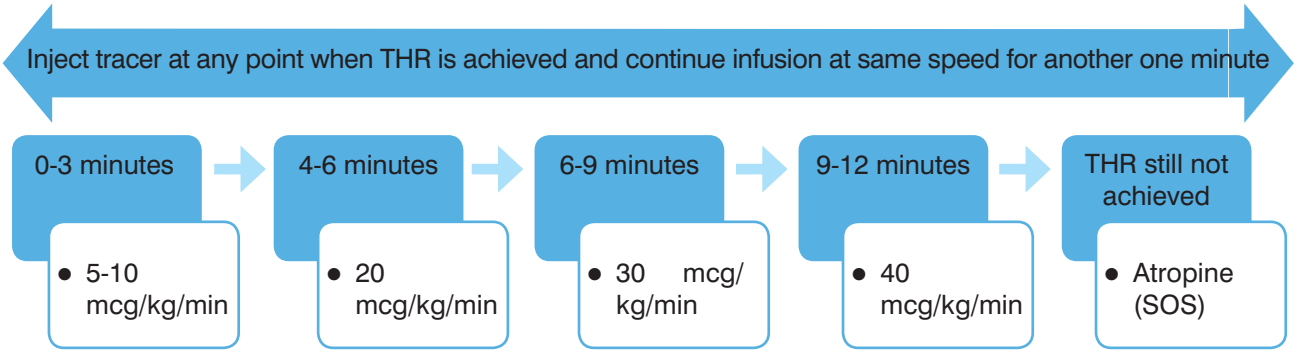

Algorithm to choose mode of stress for MPI

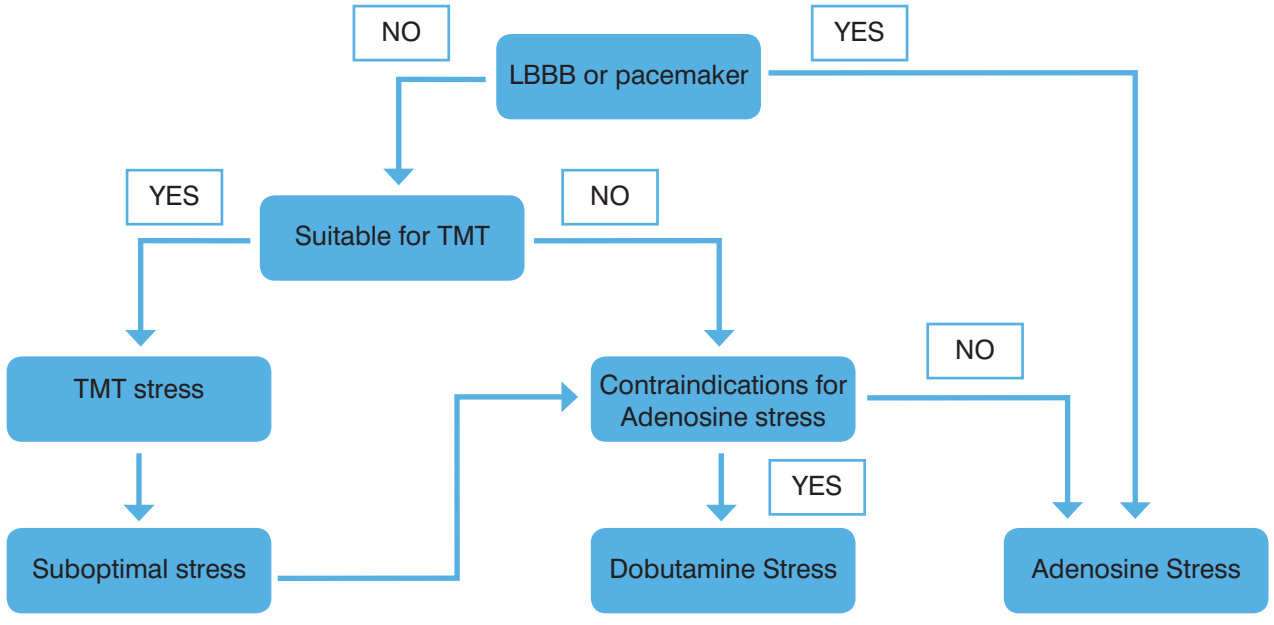

Data analysis flow chart

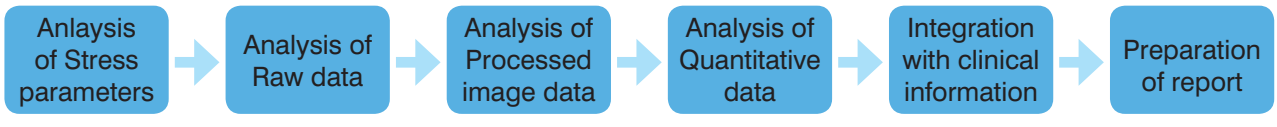

Table: Contraindications for stress

Type of stress	Absolute contraindication	Relative contraindication
Exercise stress test	• Acute coronary syndrome, until the patient has been stable for at least 48 h and the risk is clinically assessed as acceptable • Acute pulmonary embolism • Severe pulmonary hypertension • Acute aortic dissection • Symptomatic severe aortic stenosis • Hypertrophic, obstructive cardiomyopathy • Uncontrolled cardiac arrhythmias causing symptoms or haemodynamic instability • Acute myocarditis and pericarditis • Active endocarditis.	• Patients with decompensated or inadequately controlled congestive heart failure • Active deep vein thrombophlebitis or deep vein thrombosis • Left bundle branch block, ventricular paced rhythm • Hypertension with resting systolic or diastolic blood pressures > 200/110 mmHg • Recent stroke or transient ischaemic attack • Moderate to severe aortic stenosis.
Vasodilator stress (adenosine) test	• Same as for exercise as aboveand additionally the following: • Severe chronic obstructive (in particular bronchospastic) pulmonary disease (COPD) • Greater than first-degree heart block or sick sinus syndrome, without a pacemaker • Symptomatic aortic stenosis and hypertrophic obstructive cardiomyopathy • Systolic blood pressure <90 mmHg • Cerebral ischaemia.	• Same as for exercise as above and additionally the following: • Mild to moderate asthma and COPD • Severe sinus bradycardia (heart rate <40/min) • Severe atherosclerotic lesions of extracranial artery • Use of dipyridamole during the last 24 h (to avoid possible enhancement of the drug effect).
Dobutamine stress test	• Same as for exercise as above and additionally the following: • β-blocker medication that has not been or could not be discontinued sufficiently long.	• Same as for exercise as above:
Atropine administration as part of dobutamine stress	• Narrow angle glaucoma • Obstructive uropathy, including bladder neck obstruction from prostatic hypertrophy • Atrial fibrillation with an uncontrolled heart rate • Obstructive gastrointestinal disease or paralytic ileus	

REFERENCES

1. Nuclear Cardiac Imaging: Principles and Applications (5 ed.). Nuclear Cardiology: History and Milestones Chapter: Nuclear Cardiology: History and Milestones Author(s): Barry L. Zaret DOI:10.1093/med/9780199392094.003.0001
2. Strauss HW, Miller DD, Wittry MD, Cerqueira MD, Garcia EV, Iskandrian AS, et al. Procedure guideline for myocardial perfusion imaging 3.3. J Nucl Med Technol. 2008 Sep;36(3):155-61. DOI: 10.2967/jnmt.108.056465. Epub 2008 Aug 14. PMID: 18703619.
3. Verberne HJ, Acampa W, Anagnostopoulos C, Ballinger J, Bengel F, De Bondt P, et al. European Association of Nuclear Medicine (EANM). EANM procedural guidelines for radionuclide myocardial perfusion imaging with SPECT and SPECT/CT: 2015 revision. Eur J Nucl Med Mol Imaging. 2015 Nov;42(12):1929-40. DOI: 10.1007/s00259-015-3139-x. Epub 2015 Aug 21. PMID: 26290421; PMCID: PMC4589547.
4. Klocke FJ, Baird MG, Lorell BH, Bateman TM, Messer JV, Berman DS, et al; American College of Cardiology; American Heart Association; American Society for Nuclear Cardiology. ACC/AHA/ASNC guidelines for the clinical use of cardiac radionuclide imaging--executive summary: a report of the American College of Cardiology/American Heart Association Task Force on Practice Guidelines (ACC/AHA/ASNC Committee to Revise the 1995 Guidelines for the Clinical Use of Cardiac Radionuclide Imaging). J Am Coll Cardiol. 2003 Oct 1;42(7):1318-33. DOI: 10.1016/j.jacc.2003.08.011. PMID: 14522503.
5. Assad Movahed, Gopinath Gnanasegaran, John R. Buscombe, Margaret Hall Integrating Cardiology for Nuclear Medicine Physicians. Springer. ISBN 978-3-540-78673-3. DOI: 10.1007/978-3-540-78674-0
6. Clinical nuclear cardiology: state of the art and future directions/[edited by] Barry L. Zaret, George A. Beller. — 4th ed. Mosby Elsevier

Intravascular Ultrasound: Basics of Image Analysis & Interpretation

Sajan Narayanan

Senior Consultant & Interventional Cardiologist,
Little Flower Hospital & Research Institute,
Kochi, Kerala.

INTRODUCTION

- Atherosclerosis is the main cause of coronary heart disease and is the leading cause of morbidity and mortality worldwide.
- In early stages, lipid deposition starts in vessel wall as a fatty streak, which progresses overtime to more complex forms of atherosclerotic plaque. Complicated plaques have necrotic core, infiltration by inflammatory cells, thin cap and high lipid content.
- In earlier stages of atherosclerosis, vessel remodelling prevents encroachment of plaque into lumen and angiographic assessment may not recognize the lesion. Hence intravascular ultrasound (IVUS) has emerged as the prime tool to assess atherosclerotic plaque characteristics in defining prognosis and treatment strategies.
- Certain pathologies like spontaneous coronary dissection mimic acute coronary syndrome (ACS) and is difficult to distinguish on coronary angiogram (CAG). IVUS is very helpful in identifying these pathobiological mimics and helps in tailoring the treatment.
- IVUS optimized percutaneous intervention (PCI) – Refers to the achievement of set targets which define optimal stent deployment and improves long term outcomes.

Rationale for Intravascular ultrasound examination

1. Coronary angiogram provides information about coronary lumen and hence cannot detect pathological changes in the vessel wall.
2. Assessment of lesion by coronary angiogram assumes that segments adjacent to the lesion are 'normal', which is most often not the case, since atherosclerosis is a diffuse disease.
3. Lesion assessment by coronary angiogram has high inter and intra observer variability.
4. IVUS provides complete information about vessel wall both axially and longitudinally.
5. By analysing different acoustic impedence properties

Address for correspondence: Dr. Sajan Narayanan MD, DM, FESC, Senior consultant & Interventional Cardiologist, Little Flower Hospital & Research Institute, Kochi, Kerala. Email: sajannarayanan@gmail.com

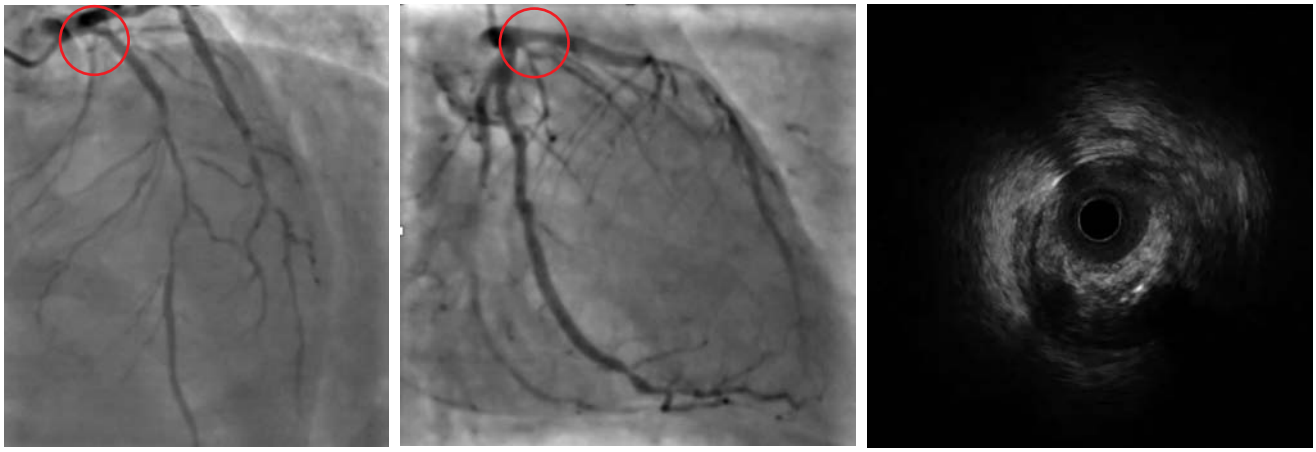

Importance of intravascular imaging: A case with NSTE ACS. Angiogram showed mid LAD diffuse 90% lesion. IVUS pullback showed a lesion in proximal LAD which had high plaque burden and significant luminal narrowing which appeared insignificant on diagnostic angiogram (red circle).

of lesions, IVUS would be able to provide information about atherosclerotic plaques succinctly.

Basic principles of IVUS

- IVUS transducer is mounted at the tip of a coronary catheter, where it emits and receives high ultrasound signals, centered at 20 – 60MHz.
- For some distance, ultrasound waves travel in parallel has better image and then begin to diverge ('far field').
- Tissues reflect and absorb ultrasound waves differently. According to mechanical impedance and acoustic properties, ultrasound beam is partially reflected and partially transmitted depending on tissue composition. Analysis of this difference becomes the basis of identification of pathological subtypes of lesions that affect the vessel wall.
- Axial resolution is about 100 microns. Longitudinal resolution is about 200 – 250 microns.

Catheter designs

- Mechanical IVUS probes has a single piezoelectrical system which rotate at around 1800 rpm and creates a sector of image, which is analysed and displayed on console.
- Electronic phase array probes have 64 transducer elements in an annular array, that are activated sequentially to generate a cross sectional image.
- Autoregressive spectral analysis of IVUS backscattered data has been incorporated to IVUS systems to facilitate image interpretation of different tissue components. Color coding is provided which helps in identification of different tissue components (eg: necrotic core in red, dense calcium in white, fibrofatty plaque in light green and fibrous plaque in dark green).

IVUS examination procedure

- IVUS catheters are to be introduced only through a guide catheter.
- ACT to be maintained > 250 s.
- Intracoronary vasodilators (eg: nitroglycerine 100 - 200μg) to be administered to avoid vasospam while introducing catheter inside the coronaries.
- Mechanical system should be properly cleared off airbubbles, inside the sheath covering the transducer by flushing with heparinised saline.
- IVUS catheter to be introduced under fluoroscopic guidance. Examination must start 10mm distal to intended area of interest and end 10mm proximal to the lesion.

QUALITATIVE IMAGE INTERPRETATION

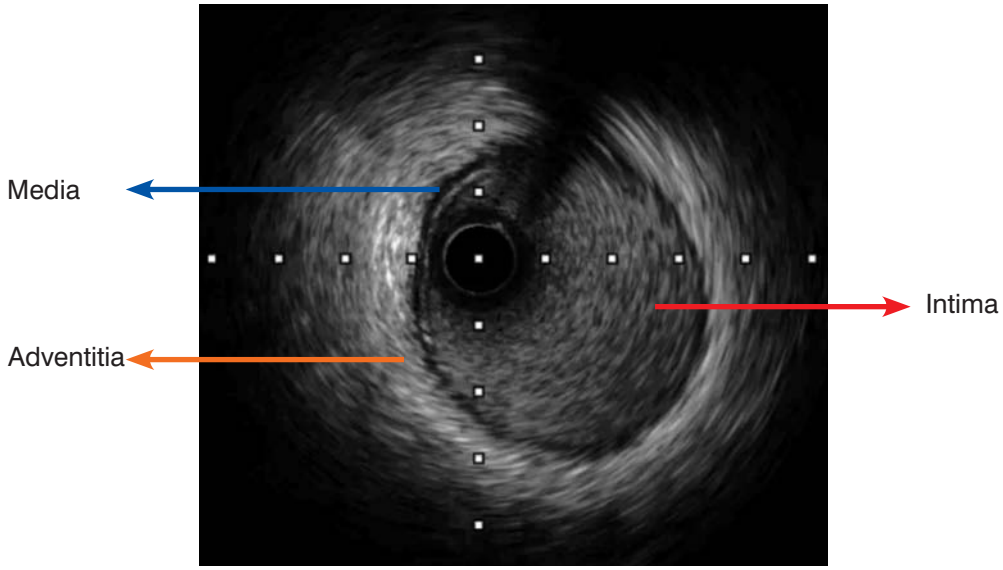

Normal arterial structure

Normal vessel wall on IVUS appear trilaminar in structure. Blood may be visualized as speckles. Intima is composed of single layer of endothelial cells and is in direct contact with blood in the lumen (red arrow).

Intima is separated from media by internal elastic lamina which is not visualized on IVUS. Media is composed of smooth muscle cells and is less echogenic than intima, but may appear thick due to signal attenuation and weak reflectivity of internal elastic lamina (blue arrow).

Adventitia is separated from media by external elastic membrane (EEM). Adventitia contain abundant collagen fibrils, fibroblasts, vasa vasorum and nerve endings. Due to presence of collagen, they reflect ultrasound and appear bright (orange arrow).

The border between media & adventitia, i.e external elastic lamina is the most well defined landmark visualized on IVUS and is used as reference to determine vessel size and plaque area.

Atherosclerotic plaques

Atherosclerosis evolves through various stages of endothelial dysfunction, lipid accumulation, inflammatory cell recruitment, smooth muscle migration and proliferation, expansion of extracellular matrix and tissue necrosis. IVUS images reflect these changes and help to characterize the stage of plaque.

Soft plaque

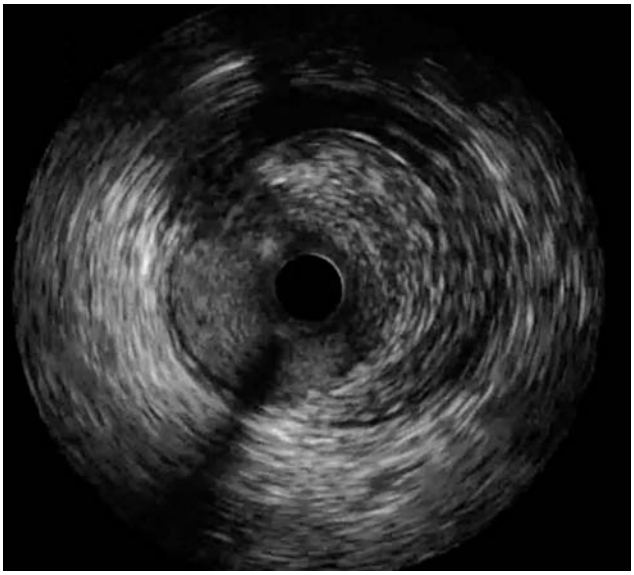

Echogenicity of plaque is lower than that of adventitia. Soft plaques are lipid rich.

Fibrous plaque

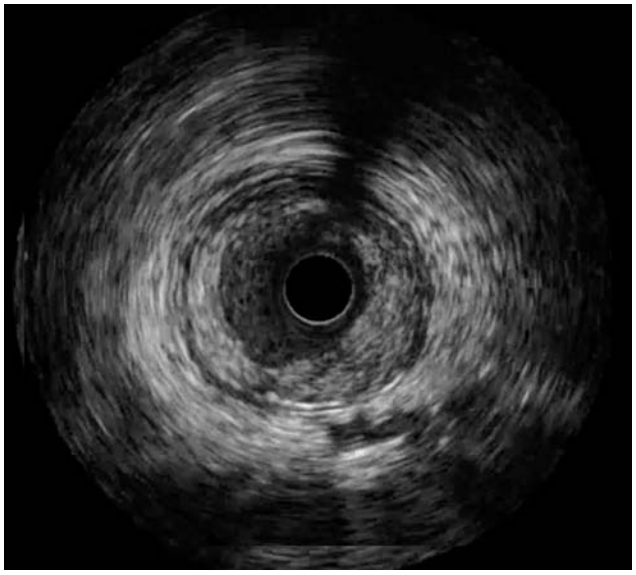

Fibrous plaque have intermediate echogenicity between soft echolucent plaque and highly echogenic calcified plaques.

Attenuated plaque

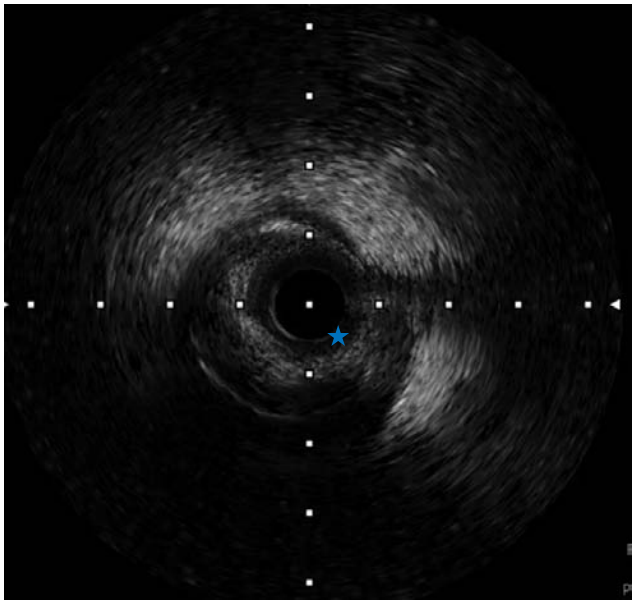

Attenuated plaque visualized between 4 – 10 o' clock position (star). Defined as deep area of ultrasound attenuation with no overlying fibrous tissue / calcium. Attenuated plaque signifies lipid rich plaque with confluent lipid pools.

Calcified plaque

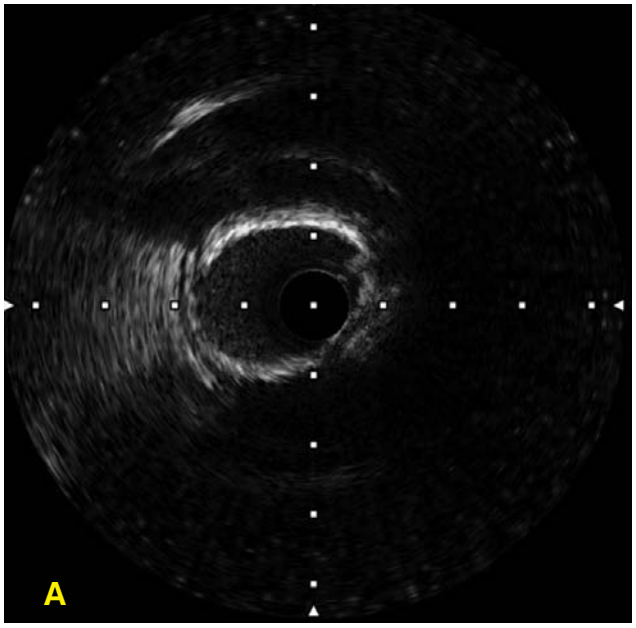

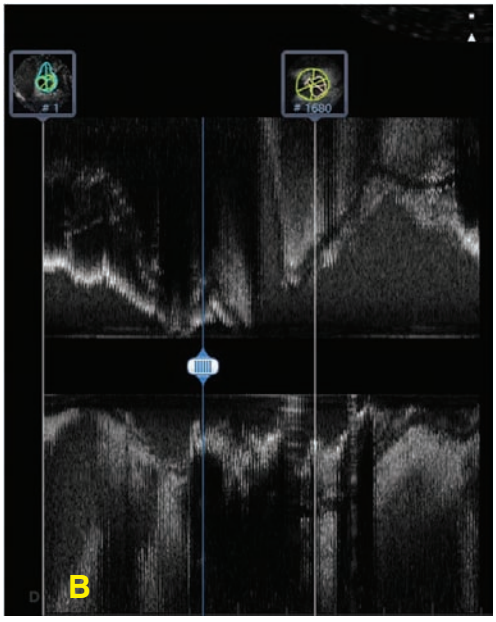

Calcified plaques appear highly echogenic (figure A). We cannot visualize structures behind the plaque since calcium reflects entire ultrasound beam and does'nt allow penetration. We can define the degree of calcium by noting the number of quadrants occupied by the plaque (eg: in figure A, there is concentric calcium and hence 360°). In Longitudinally reconstructed view (L-mode) we can estimate length of calcified plaque (figure B). Calcium reflects ultrasound and hence depth of calcification cannot be assessed on IVUS.

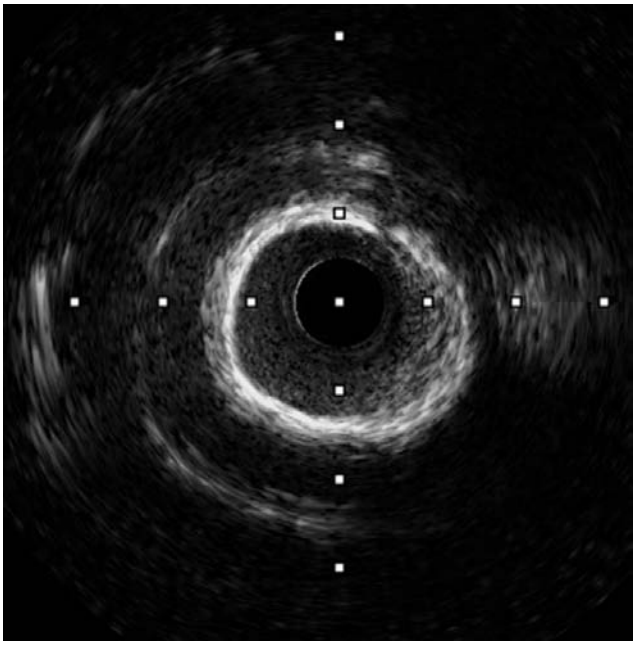

Reverberation: Appear as ripples around the calcified plaque. Reverberations around calcified plaque signifies thin calcium.

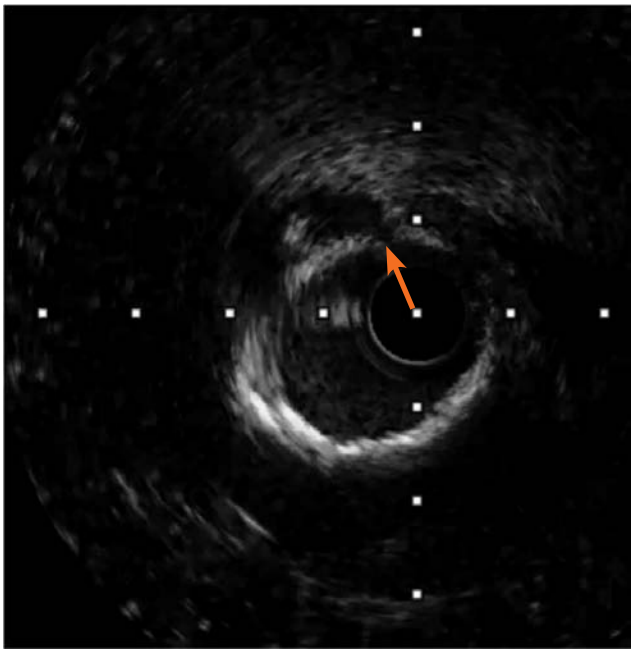

Ruptured plaque: Note the breach in intima with blood (black) inside the cavity extending into media.

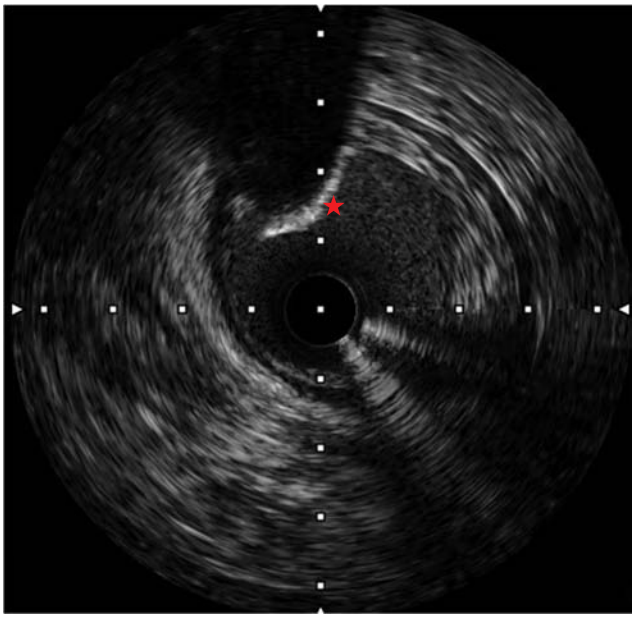

Calcified nodule: Nodular protrusion seen arising from vessel wall.

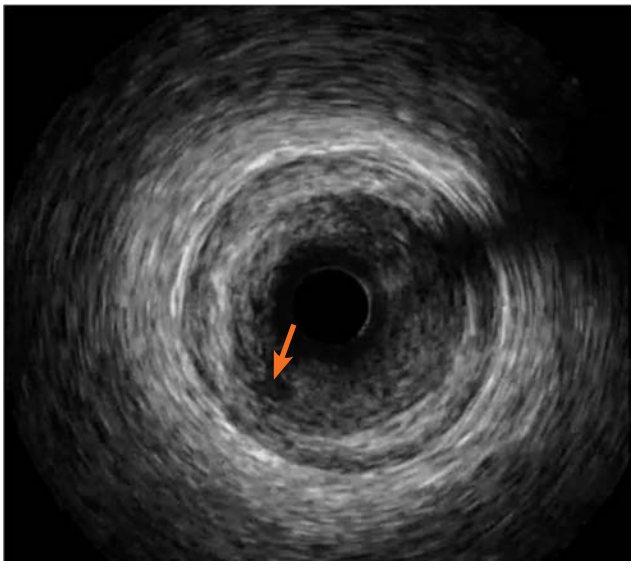

Plaque erosion: Note the breach limited to intima without extension into media.

Thrombus

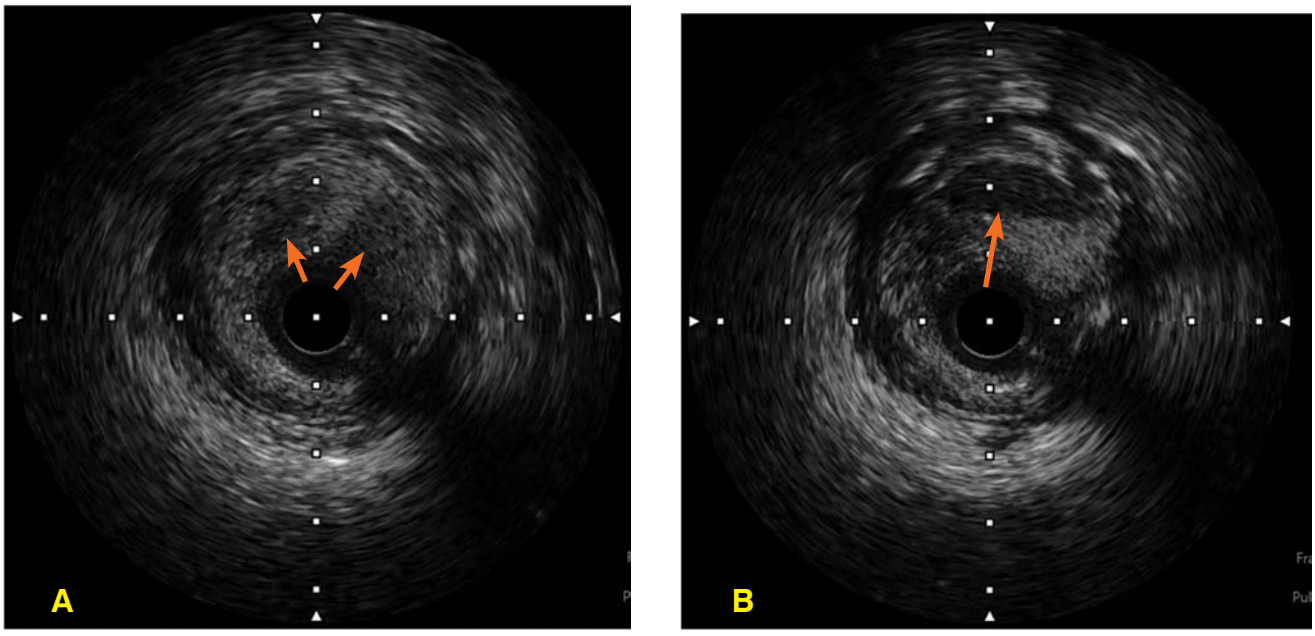

Subacute thrombus on left (figure A) –light to dark grey appearance and less clear delineation. Organised thrombus on right (figure B) has homogenous dark appearance and is delienated from lumen wall.

CLINICAL APPLICATIONS OF INTRAVASCULAR IMAGING

Determination of severity and extend of atherosclerosis

Quantitative determination of severity and extent of atherosclerosis is one of the main diagnostic and clinical application of IVUS. Luminal area of stenosis describes the relative decrease in luminal cross sectional area (CSA) at site of disease, in percentage, compared to lumen CSA in a 'normal appearing' reference segment of coronary artery. The lumen area relative to reference lumen area is analogous to the angiographic definition of diameter of stenosis.

Reference vessel

Reference segment of the vessel is the area of vessel where there are no major side branches and plaque burden is minimal. This segment is used as reference to assess measurements at lesion site and taken as benchmark for results of intervention at the stenosed portion of the vessel.

Proximal reference

The site with the largest lumen proximal to a stenosis but within the same segment within 10mm of stenosis with no major intervening branches and plaque burden of less than 50%.

Distal reference

The site with largest lumen distal to a stenosis but within the same segment within 10mm of stenosis with no major intervening branches and plaque burden of less than 50%.

Average reference lumen size

The average value of lumen size at proximal and distal reference sites.

Stenosis

A stenosis is a lesion that compromises the lumen by atleast 50% by CSA compared with a predefined reference segment lumen (usually distal reference segment / average of proximal & distal reference segment).

Worst stenosis (T-1)

The stenosis with smallest lumen size.

Secondary stenoses (T-2, T-3 etc)

lesions meeting definition of stenosis, but with lumen sizes larger than the worst stenosis

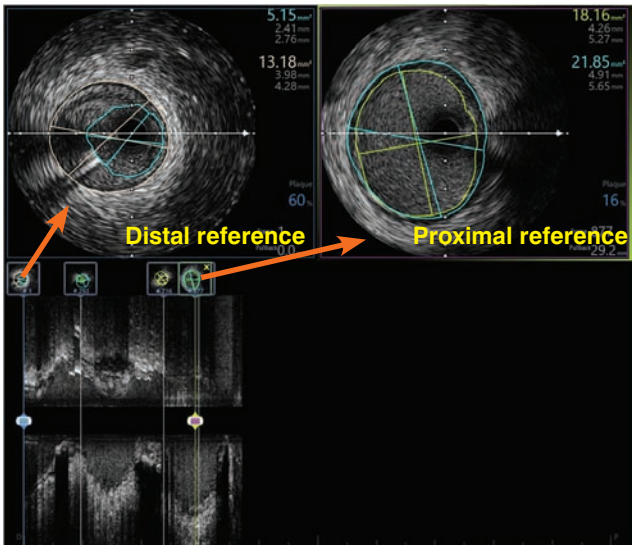

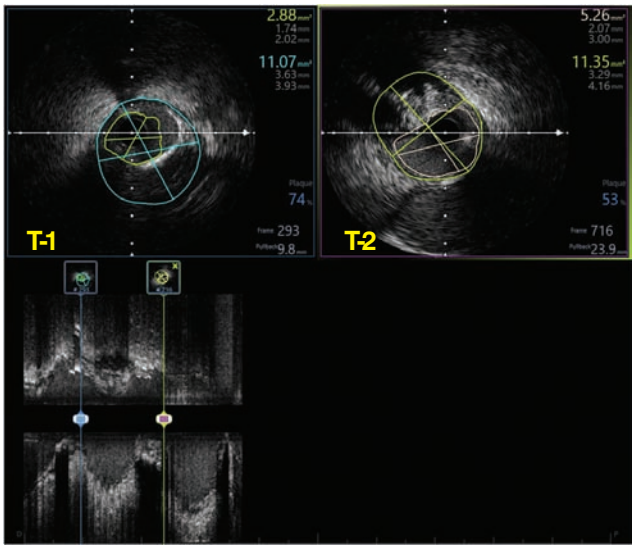

Image on left showing distal & proximal reference segments. Longitudinal view provides entire lesion length assessment. Distal reference segment minimal lumen area (MLA) was 5.15mm^2. Proximal reference segment MLA was 18.16mm^2. Hence average MLA was 11.66mm^2. Image on right provides assessment of stenosis. T-1 has minimal lumen area (MLA) of 2.88mm^2 (worst stenosis; hence T-1) and T-2 has MLA of 5.26mm^2.

Plaque Burden

Quantification of atheroma or plaque area in cross sectional IVUS images is performed by subtracting lumen area from EEM area. Since plaque itself is not directly quantifiable, it is derived by subtracting lumen area from total vessel area. Figure illustrates calculation of plaque burden (PB).

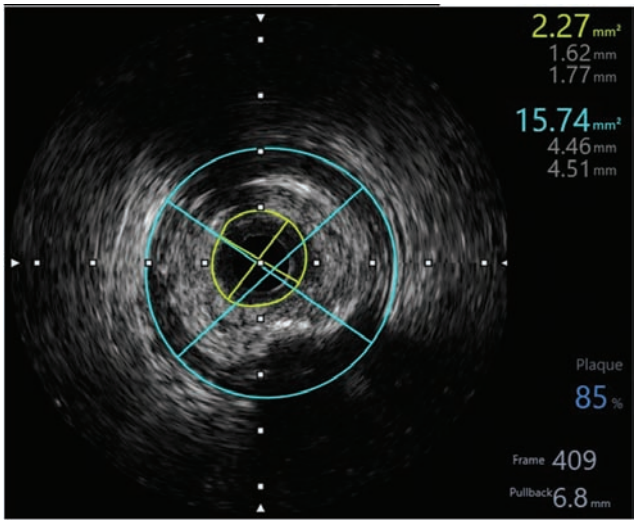

PB = (EEM CSA – Lumen CSA) ÷ EEM CSA X 100
In the example sited above PB = (15.74 - 2.27) ÷ 15.74 X 100 = 85%.

Post stent IVUS assessment

Assessment of stent results becomes one of most useful applications of IVUS in interventional practice. IVUS provides cross sectional views of the stent and its interaction with the vessel wall enabling unique assessment of expansion, apposition, vessel dissection and residual untreated disease that cannot be properly defined by angiography.

- Optimal stent expansion as laid down by different criteria predict future stent related outcomes.
- Minimal stent area (MSA): >5.5mm2 / >90% of distal reference MLA.
- Plaque burden within 5mm of stent edges (proximal & distal) <50%.
- No edge dissection involving media and extending axially >3mm.
- Malapposition (gap between stent struts and vessel wall) must be <400μ and < 1mm axially).

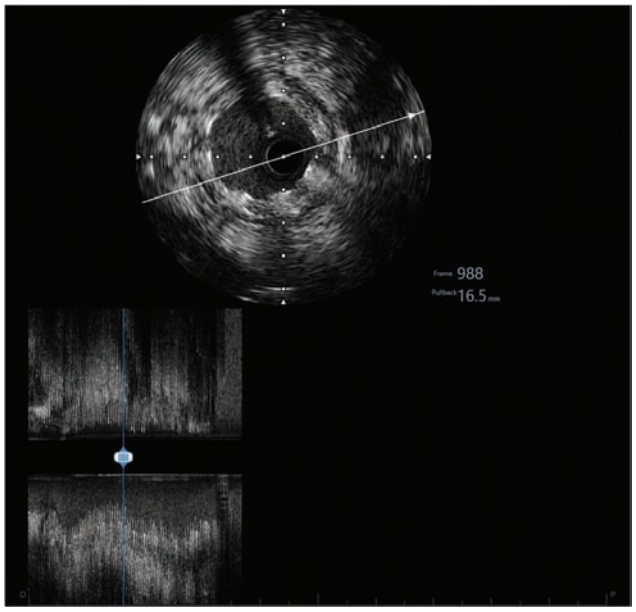

Well expanded stent: Note the uniform expansion with no gap between stent struts and the vessel wall. L view provides longitudinal estimate of stent expansion along entire length.

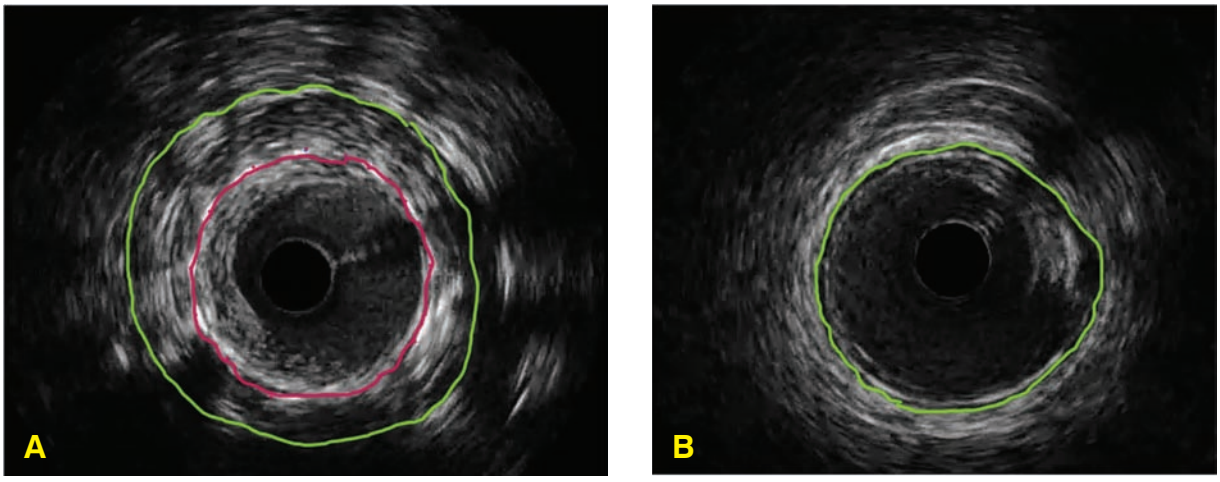

Underexpanded stent (figure A): Note the stent borders (red) and vessel borders (green). Distal reference vessel (figure B) size is highlighted. Stent is undersized for the vessel diameter and MSA was < 90% of distal reference. Underexpanded stent must be corrected with adequate sized non compliant balloon (determined by EEM – EEM diameter) at high pressures.

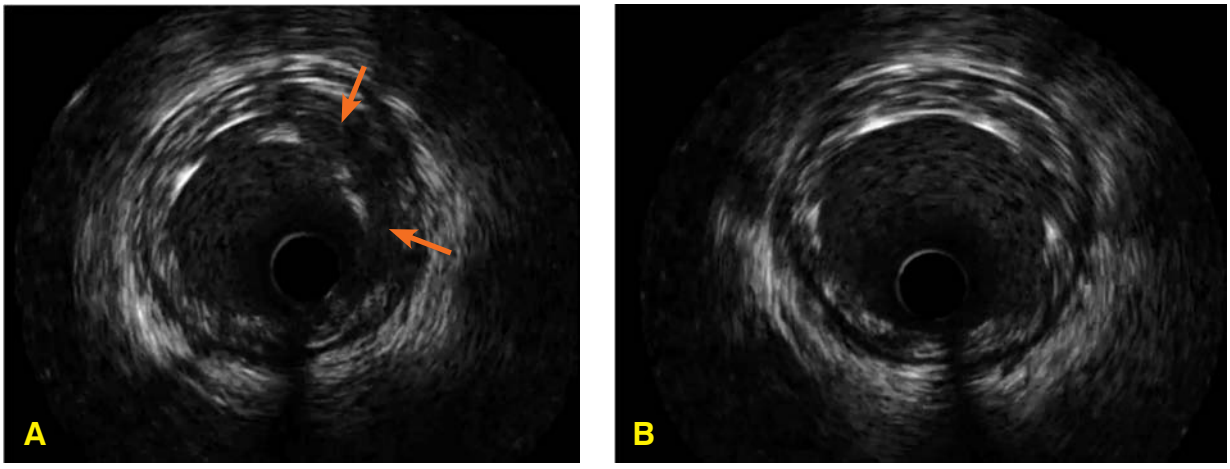

Malapposition: Note the gap between stent struts and the vessel wall (figure A – arrows). Malapposition must be corrected with adequately sized semi compliant balloon at nominal pressures (figure B – after correction of malaposition)

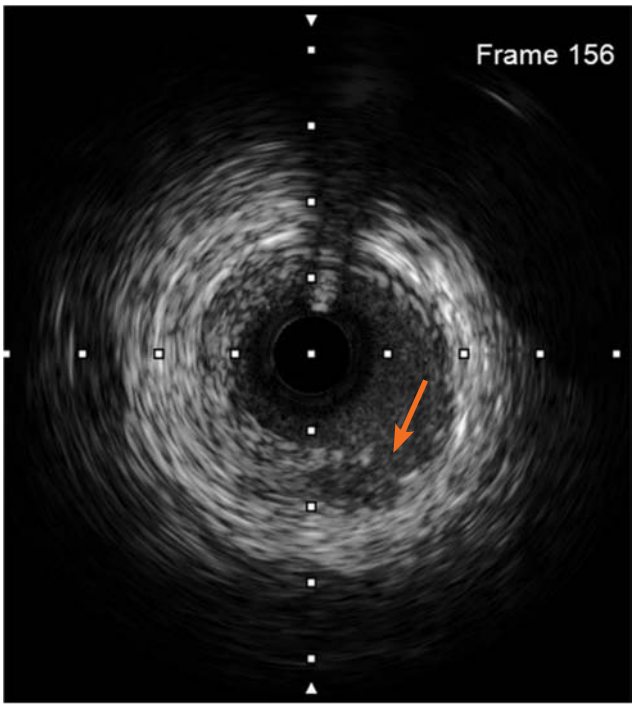

Edge dissection: IVUS pullback after placement of stent must start atleast 5mm distal and end 5mm proximally. Edge dissections extending to media or occupying >60° or extending axially ≥ 3mm needs further treatment.

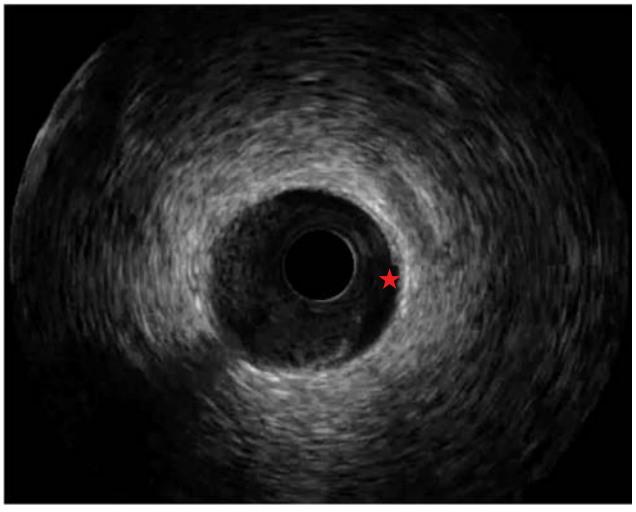

Hematoma: A case of spontaneous coronary artery dissection (SCAD). Note the presence of blood within media (star).

Perivascular structures

IVUS penetrates vessel wall and can display structures beyond the vessel wall. Some structures are clinically relevant during image interpretation.

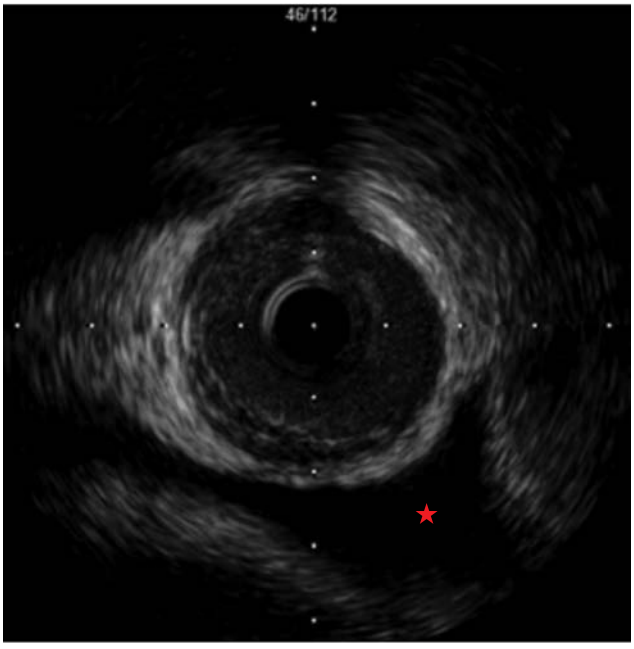

Pericardial space: echo free space denoted by star

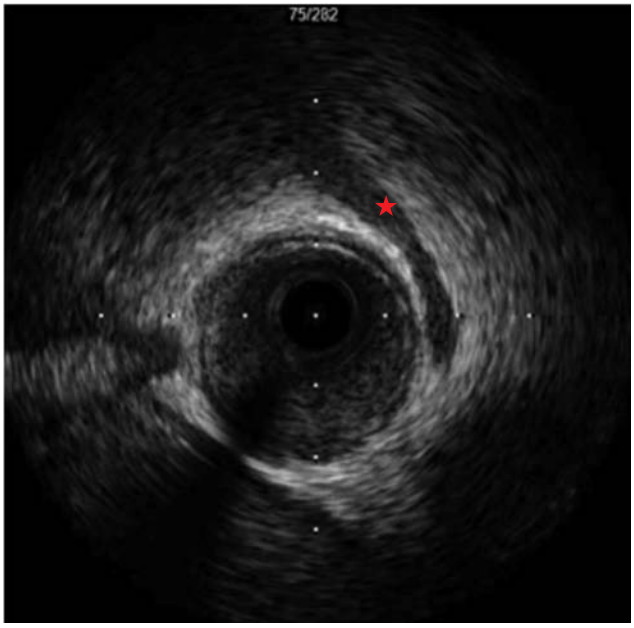

Cardiac veins: Linear echo free structures seen travelling parallel to the vessel interrogated

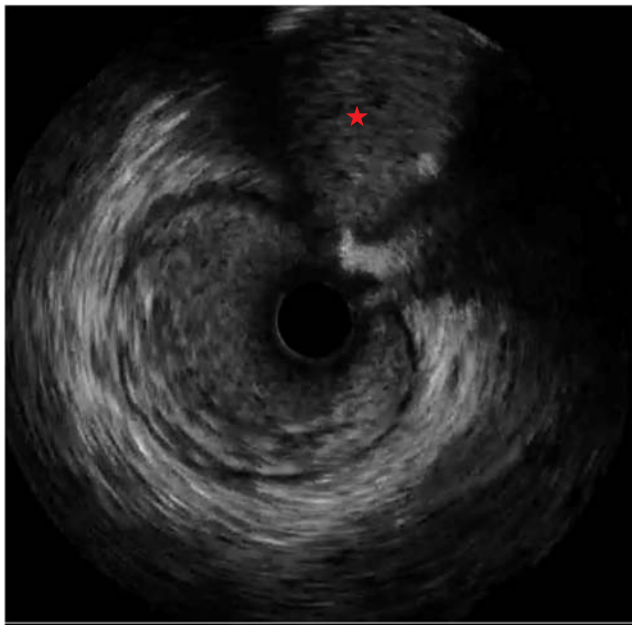

Side branches: Echo free spaces which run and eventually join the parent vessel. Cardiac veins run parallel and don't join the parent vessel.

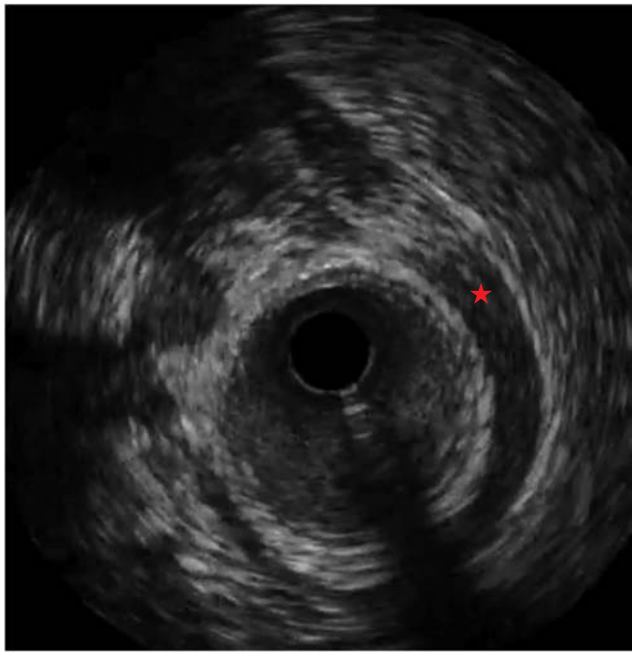

Myocardial bridge: Linear echo free space which squeeze the vessel during systole. The spaces appear like a semi circle or otherwise called "half moon sign"

Artifacts

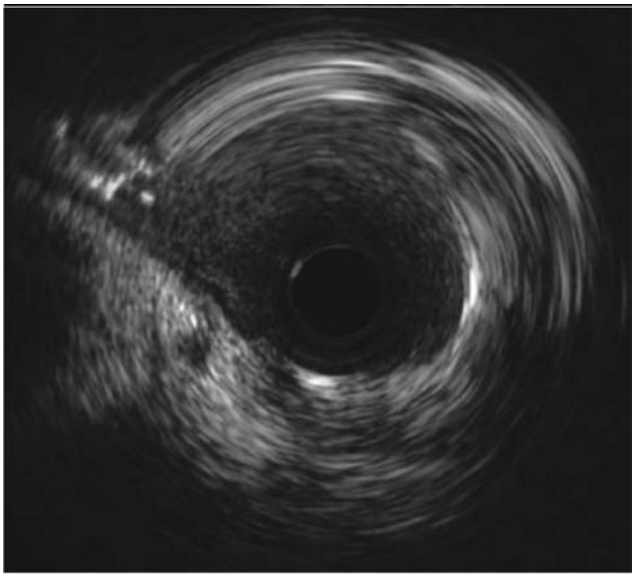

Non uniform rotational distortion (NURD): Image distortion where it appears like onion peel. This arises due to uneven drag on drive cable of mechanical catheters resulting in cyclical oscillations of rotational transducer speed, which appear as visible distortion of the image.

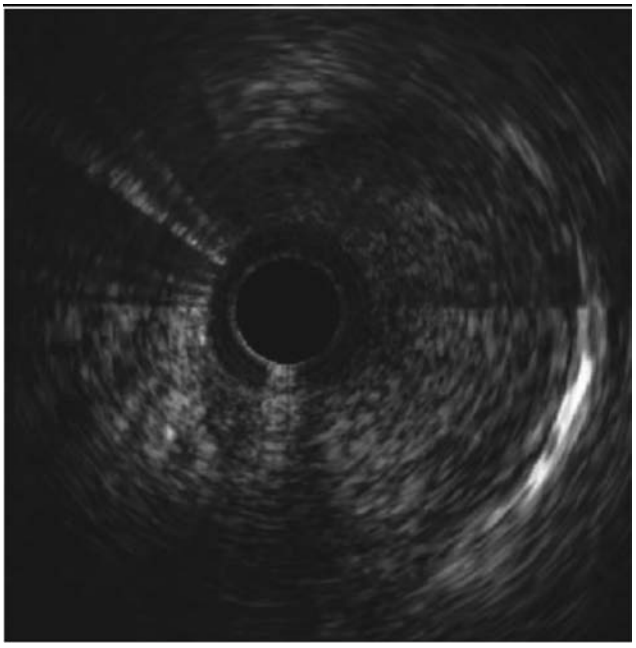

Airbubbles: Presence of air bubbles between sheath and transducer (mechanical catheters) will scatter ultrasound and interfere with image interpretation. Its important to properly flush the catheter and clear off airbubble to prevent the image distortion.

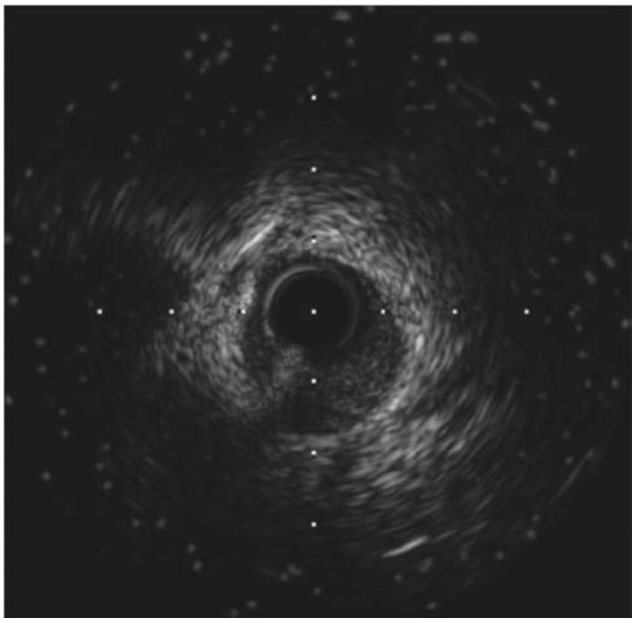

Background noise: starry sky like appearance which interfere with image interpretation. This happens due to radio frequency interference – most commonly from other electrical equipments within the cathlab. Sometimes presence of same power source for both IVUS console and other equipment (eg : ECG monitors) can cause this interference.

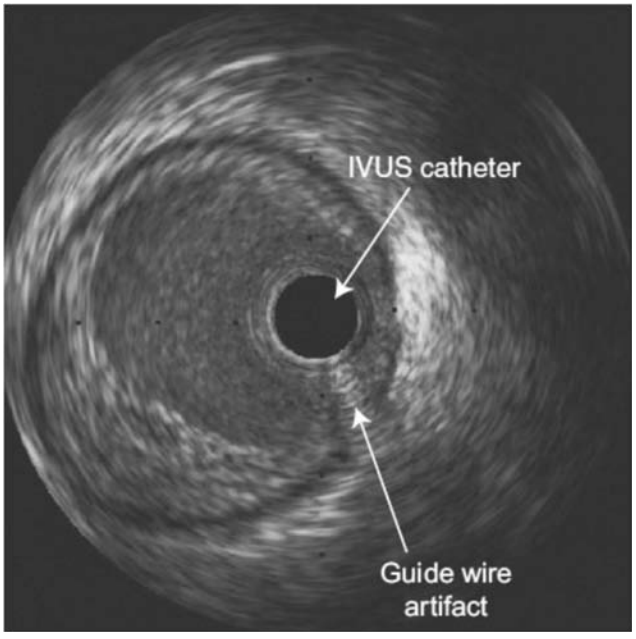

Guidewire artifact: This is seen exclusively with mechanical catheter systems. Using monorail technology, guidewire lies outside the transducer and causes a narrow angled shadow.

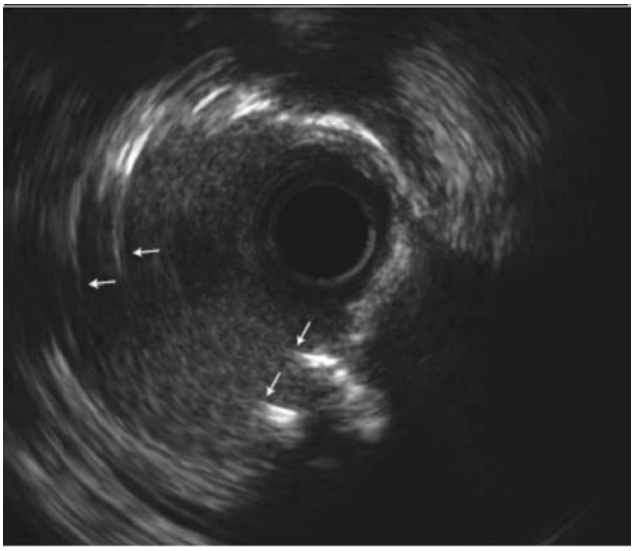

Side lobe artifact: side lobe artifact arises due to intense reflections from luminal structures, most commonly stent struts and edges of a calcified plaque. Side lobe artifacts interfere with luminal area measurements.

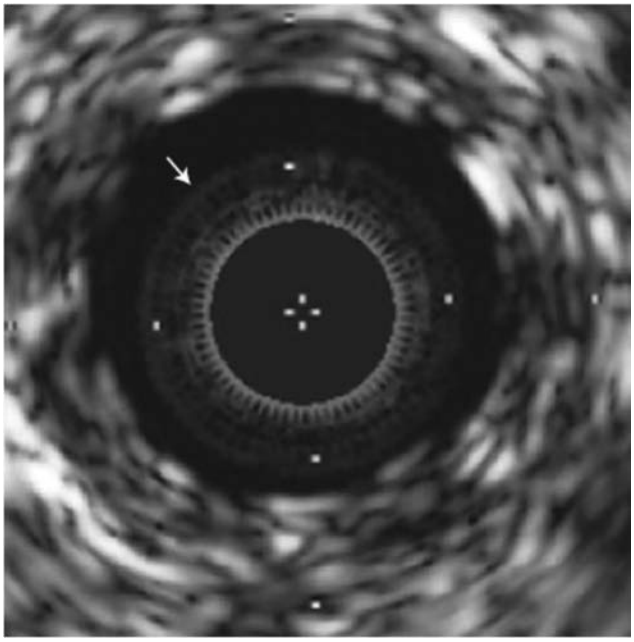

Ring down artifacts: These are bright halos of variable thickness surrounding the catheter, They are caused by acoustic oscillations in the transducer, which result in high amplitude ultrasound signals that obscure the area immediately adjacent to the catheter. Ring down artifacts seen with electronic catheter systems.

CONCLUDING REMARKS

- Intravascular ultrasound provides superior resolution of vessel wall.
- Helps in identification of lesions which are not evident on diagnostic angiogram.
- Qualitative evaluation of atherosclerotic plaques helps in diagnosing and planning PCI.
- IVUS optimized PCI i.e, performing and achieving set IVUS targets improves long term outcomes after intervention.

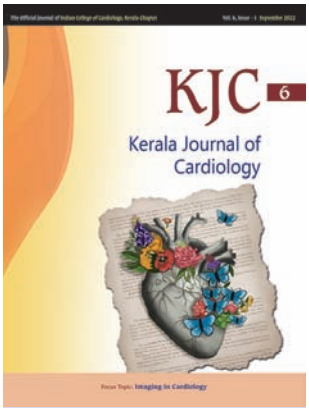

Coronary OCT – A Short Atlas

Mahesh Nalin Kumar

Senior Consultant and Head,
Dept. of Cardiology, Parumala Cardiovascular Centre,
Pathanamthitta, Kerala.

Principles of Intracoronary Optical Coherence Tomography (OCT)

- Near-infrared light with a wavelength of approximately 1.3 micrometers generates high-resolution intra-coronary images of approximately 10-20 micrometers which is an order of magnitude higher than IVUS.
- Blood attenuates near infrared light therefore OCT requires clearing of blood from the lumen.
- Measures the echo time delay and intensity of the light reflected from internal structures within tissues to generate cross sectional images.
- Light beam from OCT is separated into two arms: sample arm and reference arm.
    - SAMPLE arm light travels to sample tissue then it is reflected, refracted or absorbed by the tissue and travels back to interferometer.
    - REFERENCE arm light is directed to a mirror which it reflects off of and goes to interferometer where it combines with the sample arm light and then is detected by the detector.
- Two types of OCT systems:
    - TD-OCT (First Generation Time Domain) – reference arm is mechanically scanned by a moving mirror to produce time varying time delay.
    - FD-OCT (Second Generation Time Domain) – light source is swept therefore the interference of the light beam from the tissue and reference oscillates according to the frequency difference.
- Limitation of TD-OCT is need for an occlusion balloon to remove blood from vessel for imaging.
- FD-OCT uses a fixed reference mirror and adjustable laser light source and can reach relatively higher imaging speeds.

Address for correspondence: Mahesh N.K., MD (Med), DNB (Card), Senior Consultant and Head, Dept. of Cardiology, Parumala Cardiovascular Centre, Pathanamthitta, Kerala. Email: drnkmahesh@gmail.com

IMAGE INTERPRETATION

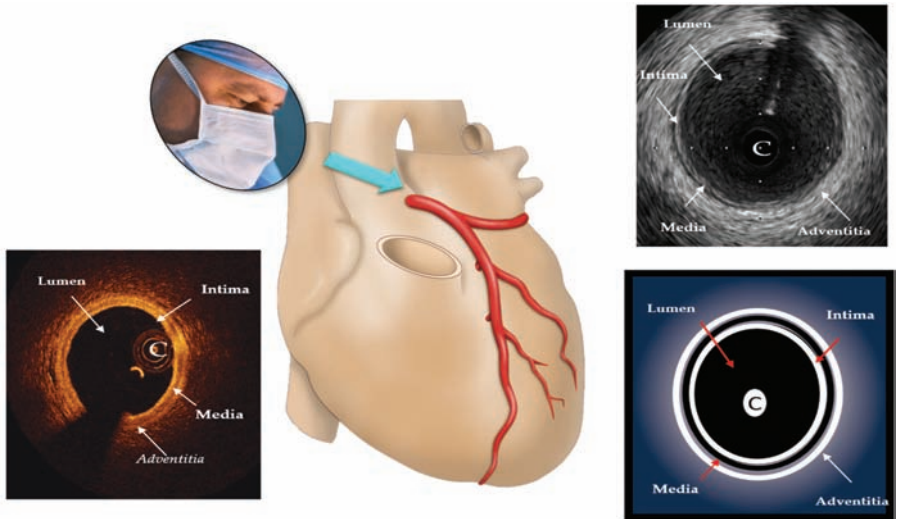

Images are oriented as if viewing from the ostium of the coronary artery.

Catheter in the center surrounded by the signal lumen. Then three layered vessel architecture – bright intima, dark media and bright adventitia.

Echoreflectivity of adventitia and periadventitial tissue are same with IVUS, clearly differentiated in OCT.

TERMINOLOGY

Backscatter

- The reflection of light waves off the tissue and back to the OCT catheter.
- High backscatter means a brighter pixel.
- Also described as a "signal rich" region.
- Low backscatter means a darker pixel.
- Also described as a "signal poor" region.

Attenuation

- The reduction in intensity of the light waves as they pass through tissue due to absorption or scattering.
- High attenuation means the light cannot penetrate very deep.
- Low attenuation means the light can pass through to allow visualization of deeper tissue.
- Blood attenuates the OCT light before it reached the artery wall therefore OCT images must be acquired as the blood is flushed from the field of view.

Low Attenuation	High attenuation
Calcific	Lipid
Fibrous	Red thrombus
White Thrombus	

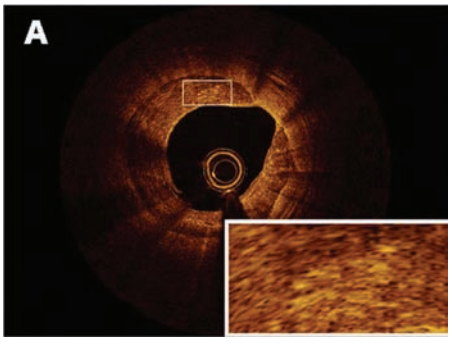

A. Calcific tissue has a low attenuation

Composition: A. Homogeneous means Uniform in structure.

Texture: A. Coarse

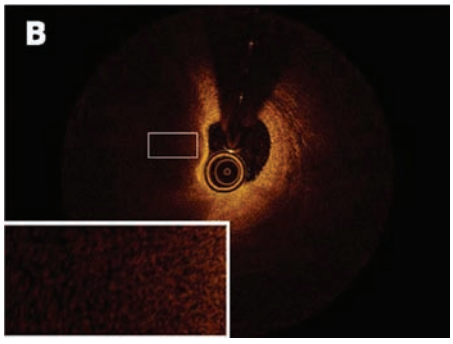

B. Lipid is a highly attenuating tissue

B. Heterogeneous means Structure consists of dissimilar elements.

B. Fine

EQUIPMENT

- OCT CATHETER: contains rotating optical fiber with a lens and refractor element.
- REFLECTOR ELEMENT: focuses the beam and directs it into the vessel wall.
- MOTOR UNIT: connects catheter to a rotary junction and rotates the fiber.
- IMAGING PROBES:
  - TD-OCT imaging probes: contain single mode fiberoptic core within a translucent sheath with maximal outer diameter of 0.019 inches.
  - FD-OCT imaging probes: integrated in a short monorail catheter comparable to conventional 0.014 inch angioplasty guidewire.
- OCT CONSOLE: detection of reflected light signal and conversion into digital signals.
  - Console is used to control rotational and pullback speed of the catheter.
  - Performs calibration prior to each OCT image acquisition and allows adjustment of the Z-offset in order to allow variation in the optical path length of the optical fiber to avoid errors in OCT measurements.

OPTIS

OPTIS Angio Co-Registration Module – allows user to visualize linkage between anatomic OCT image data on angiography image.

INTEGRATED System –fully integrated cath lab OCT and FFR system that provides physicians with increased control and ease of use with angio co-registration.

MOBILE System- combines OCT and FFR on a mobile system for seamless integration into multiple cath labs.

IMAGE ACQUISITION: A STEP BY STEP APPROACH

- SYSTEMIC ANTICOAGULATION: with heparin prior to guidewire insertion into vessel.
- INTRACORONARY NITROGLYCERIN: to avoid catheter induced vasospasm.
- OCT is INDICATED in vessels 2.0 – 3.5 mm in diameter.
- USE CAUTION IF:
  - Severe left ventricular dysfunction
  - Renal impairment
  - Single remaining vessel
  - Contrast Allergy

- BLOOD CLEARING: needed during image acquisition as infrared light cannot penetrate blood.
  *For vessels with near complete stenosis or total occlusion, it is recommended that the blood flow be restored prior to OCT so that the contrast media can adequately clear from the artery.
- Patient should receive systemic anticoagulation with heparin or bivalirudin with an ACT>250 sec.
- Conventional guiding catheters and 0.014'' intracoronary guidewire can be used to cross the target lesion. The monorail rapid exchange OCT catheter is compatible with a ≥6Fr guiding catheter.
- Open the OCT catheter from the package and flush the OCT catheter with the attached 3 cc syringe using 100% contrast. Make certain all the air has been purged from the catheter.
- Connect the catheter to the controller unit and

administer 200 μg of intracoronary nitroglycerin.
- Backload the guidewire through the OCT catheter and advance the distal tip of the catheter past the region of interest.
- Pullback may be performed manually or automatically (10-40 mm/sec) with simultaneous injection of contrast though the guiding catheter with a pre-set infusion rate of 2-4 mL/sec.
  - If Automatic Pullback: Set the power injector according to the manufacturer's instructions (typically at least 3cc/sec for a total volume of 12 cc for RCA and 4 cc/sec for a total volume of 14 cc for left coronary with no more than 450 PSI).
- Check catheter position with a test injection.
- Activate imaging catheter and injection 100% contrast.
- Assess acquired images and if clear and adequate then the OCT catheter may be removed.

OCT OVERVIEW - UPPER PANEL

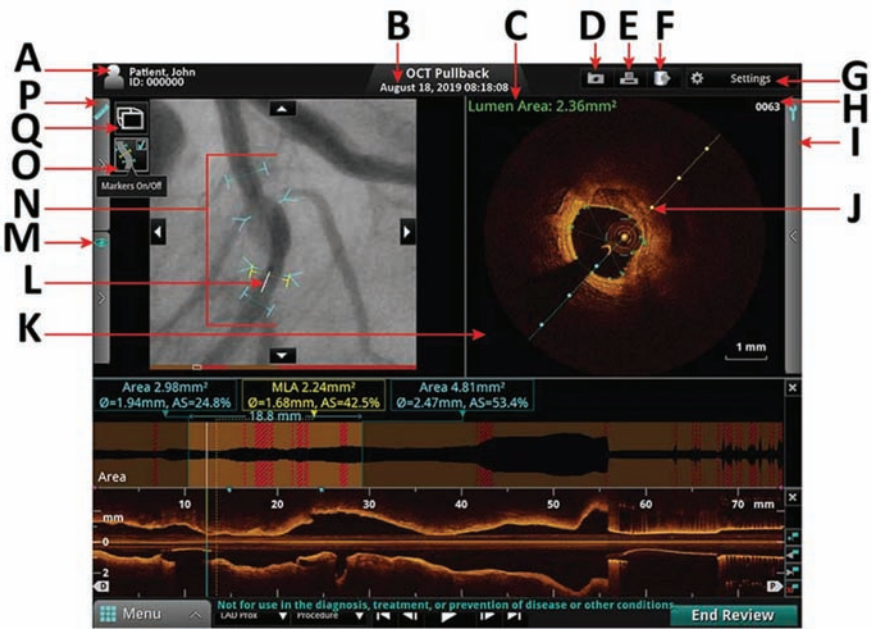

Labeled patient information, toolbar, coronary angiography and cross sectional OCT image retrieved during a routine OCT pullback.

A Patient name and ID.
B Recording date and time.
C **Lumen Contour Measurements:** Displays either **Mean Diameter** or **Area** of the cross section.
D **Capture button:** Available on a still frame or paused recording.
E **Print button:** Available when a USB drive is connected and the system is displaying a still frame or paused recording.
F **Export button:** Click to open the **Export Wizard**.
G **Settings button:** Click to open the (Playback) **Settings** menu.
H **Frame number:** Only visible on a paused recording when Tool Panel is closed.
I Tool Panel containing Measurement and Annotation tools: Use these to add measurements, calculations, and add text to recordings and still images.
J **Cut-Plane Indicator:** The cut-plane is shown as a solid line in the cross-sectional view. Click and drag this to change the lateral view shown in the L-Mode display.
K **Image Window:** A cross-sectional view of the current location of the pullback.
L **OCT Frame Indicator** (Angio Co-Registration view): Representation in the Angiography Window of the L-Mode **Current Frame Indicator**.
M **View Menu:** Includes the **Advanced Display, Lumen Profile** and **Rendered Stent** submenus.
N **Stent Roadmap:** This group of markers comprises the **Proximal Marker, Distal Marker, MLA Marker,** and **Bookmarks**.
O **Markers On/Off Button:** Click to turn on and off all indicators in Ango Co-Registration view with the exception of the **OCT Frame Indicator**.

OCT OVERVIEW - LOWER PANEL

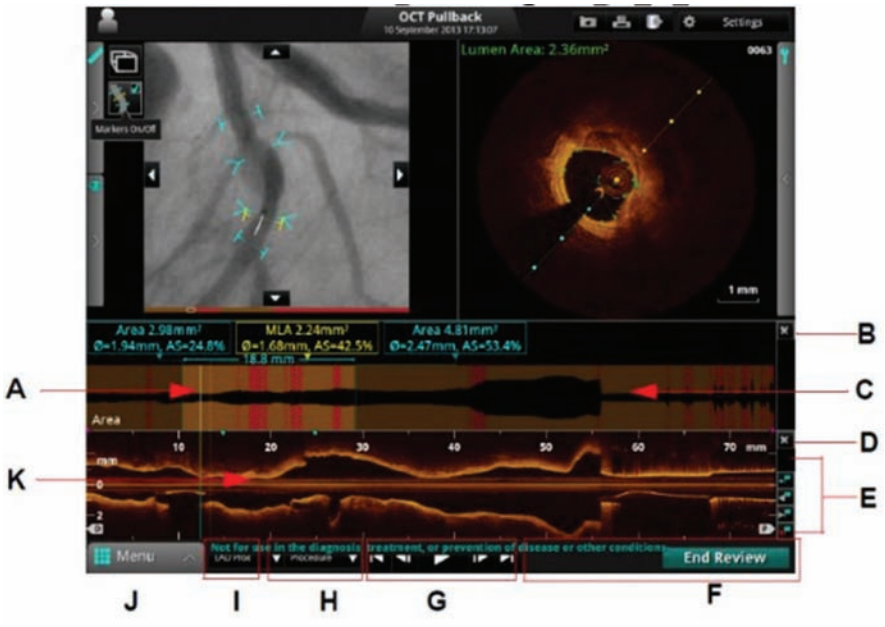

Labeled longitudinal OCT image and play function toolbar retrieved during a routine OCT pullback. Click on the letter to see the display function.

A **Current Frame Indicator** (L-Mode View): Click and drag to change the frame shown.

B **Lumen Profile View Close Box:** Click this to close the Lumen Profile view.

C **Lumen Profile:** Displays the lumen profile as either a diameter graph or an area graph.

D **L-Mode View Close Box:** Click this to close the L-Mode view.

E **Bookmark controls:** Add or remove bookmarks to the L-Mode view.

F **End Review:** Click the **End Review** button to close this window and return to the Patient Summary menu.

G **Playback controls:** Control the playback of the OCT recording. Not available with still images.

H **Procedure list:** Click to open a drop-down list of procedures to describe this recording.

I **Vessel list:** Click to open a drop-down list of vessels to describe this recording.

J **Menu:** Displays the context-sensitive menu. Click to access the **Setup** and playback **Calibration** controls.

K **L-Mode view:** An approximate lateral representation of the vessel for this recording. Not available with still images.

LESION MORPHOLOGY

1. Normal Vessel

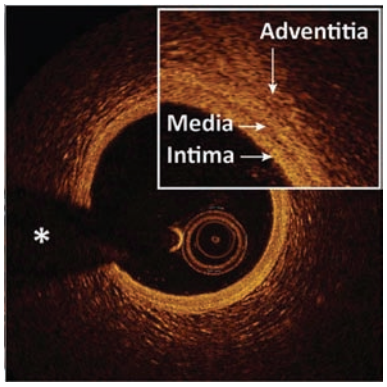

Three-layered structure: INTIMA, MEDIA, ADVENTITIA.

Signal-poor muscular MEDIA layer positioned between the thin high backscattering INTIMA layer and a heterogeneous high backscattering ADVENTITIA layer.

The dark band of media is surrounded by the internal elastic membrane and external elastic membrane, two thin layers of elastic fibers at the border between the intima and media, the media and adventitia.

2. Fibrous Plaque

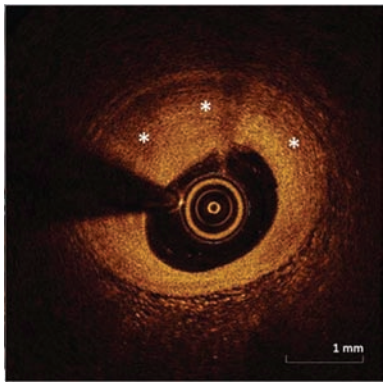

Fibrous plaque is represented by a high backscattering area with a relatively homogenous signal

3. Fibrocalcific plaque

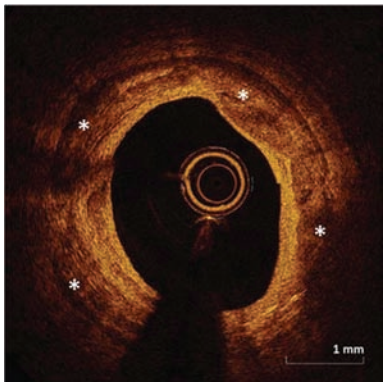

Contains fibrous tissue and calcification (asterisks) which appears as a signal-poor or heterogeneous region with a sharply well delineated border.

4. Fibroatheroma

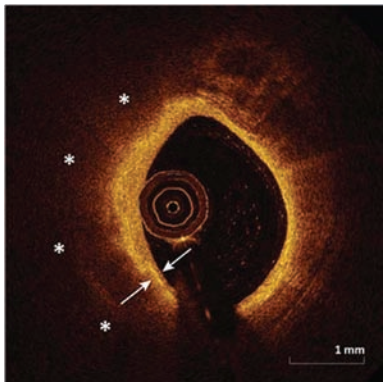

A fibroatheroma is a combination of a fibrous cap (arrows) and a necrotic core (asterisks). A fibrous cap is a signal-rich tissue layer overlaying a signal-poor region. The necrotic core is a signal-poor region within an atherosclerotic plaque with poorly delineated borders, a rapid signal drop-off and little or no signal backscattering within a lesion that is covered by a fibrous cap. It is imperative to note the distinction between signal-poor regions of calcium which have sharply delineated borders and signal-poor regions of necrotic core which have poorly defined borders.

5. Thin Capped Fibroatheroma

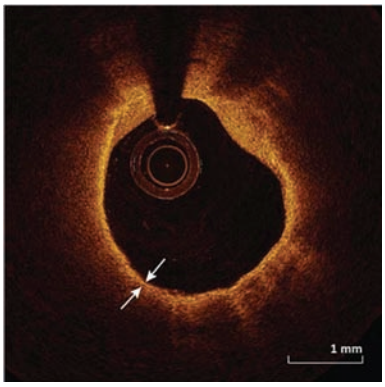

A thin cap fibroatheroma is defined as a delineated necrotic core with an overlying fibrous cap where the minimal cap thickness (arrows) is less than a predetermined threshold (usually <65 μm). Other data suggests a cap thickness threshold of <55 μm associated with plaque rupture and >85 μm associated with plaque stability

6. Macrophages

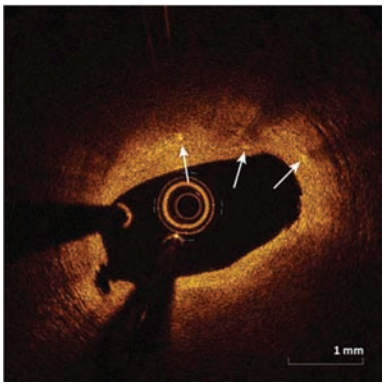

Macrophages appear as signal-rich, distinct or confluent punctate focal regions (arrows) that exceed the background intensity speckle noise. Macrophages attenuate the OCT light significantly and as a result superficial macrophages can shadow underlying tissue giving the appearance of a necrotic core

7. Intimal vasculature

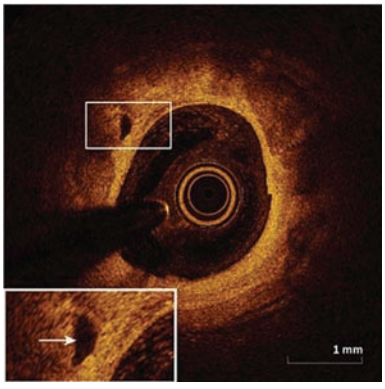

Appear as signal-poor voids seen within the intima that are sharply delineated and represent vessels (arrow) and can be visualized in multiple contiguous frames.

8. Cholesterol crystals

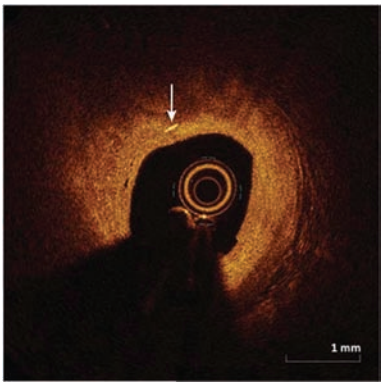

Cholesterol crystals (arrow) appear as high intensity thin linear regions usually associated with a fibrous cap or necrotic core.

9. Red Thrombus

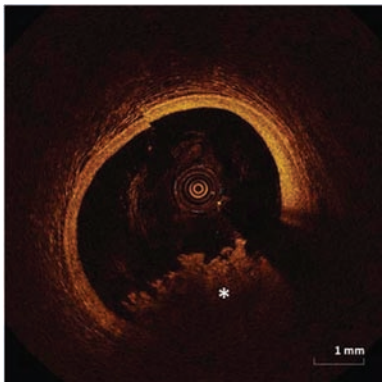

Red thrombus appears as a highly backscattering and highly attenuating mass (asterisk) attached to the luminal surface or floating within the lumen.

10. White thrombus

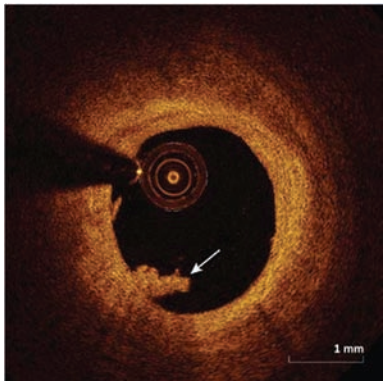

White thrombus appears as a homogenous mass (arrow) attached to the luminal surface or floating within the lumen with relatively less backscattering and very little signal attenuation.

11. Plaque rupture

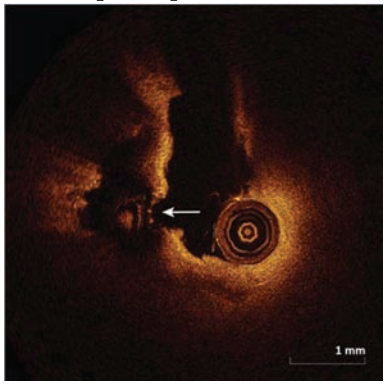

Plaque rupture frequently occurs in the setting of a thin cap fibroatheroma and appears as intimal tearing, disruption or dissection of the fibrous cap (arrow)

12. Plaque erosion

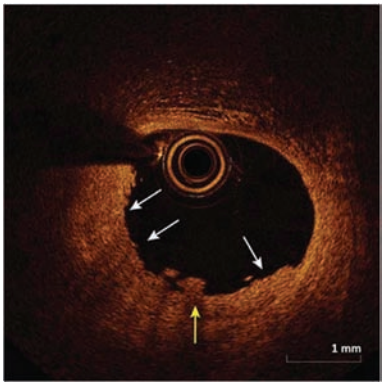

Plaque erosion appears as a presence of thrombus (yellow arrow) on an irregular luminal surface with no evidence of plaque rupture (white arrows) when evaluated in multiple adjacent frames.

13. Calcific Nodules

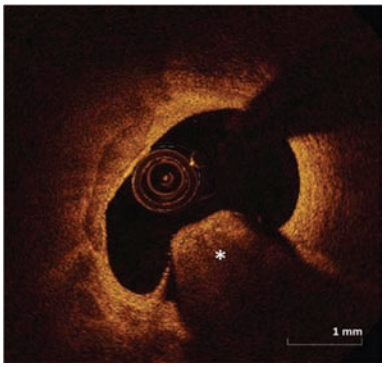

Single or multiple regions of calcium (asterisk) protruding into the intracoronary lumen forming sharp angles.

14. Difference between Fibrous, Lipid, Calcium

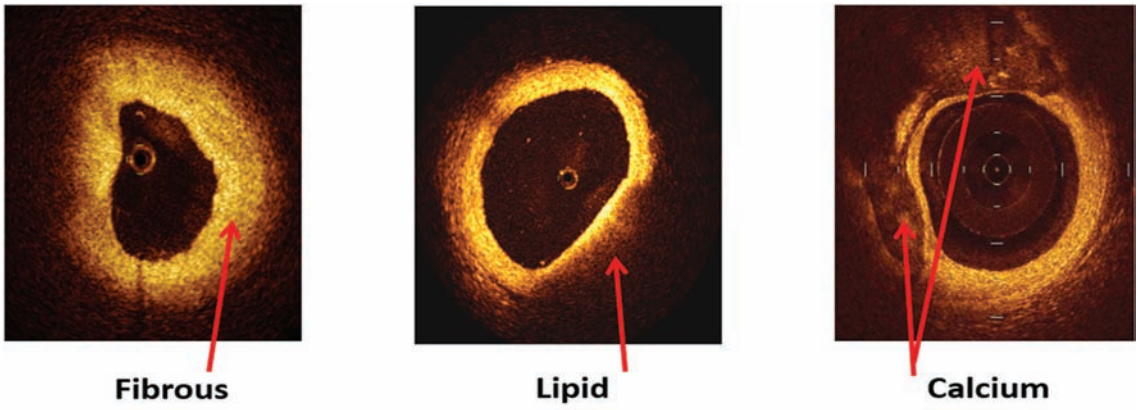

Fibrous	Bright pixels	Finely textured	Deep penetration	Homogeneous
Lipid	Dark pixels	Diffuse edge	Low penetration	Homogeneous
Calcium	Dark pixels	Sharp edge	Deep penetration	Homogeneous

STENT ASSESSMENT

1. Malapposition

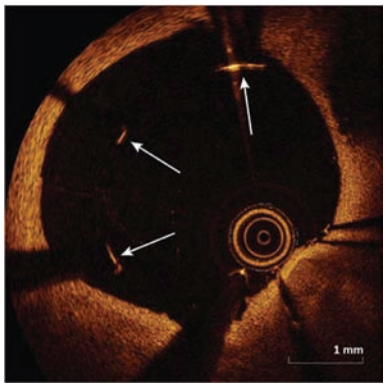

Malapposition (arrows) occurs when the axial distance between the stent strut's surface to the luminal surface is greater than the strut thickness (including the polymer if present). If this distance is less than the strut thickness, then the strut is considered apposed. Two forms of apposition have been described: protruding, where the endoluminal strut boundary is located above the level of the luminal surface, and embedded, where the endoluminal strut boundary is below the level of the luminal surface.

2. In-Stent Dissection

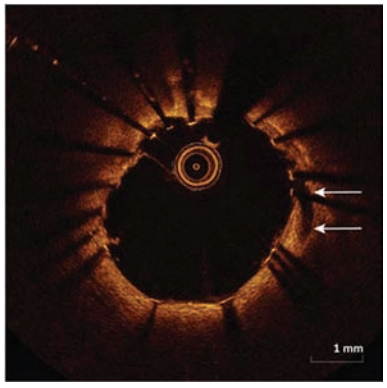

Disruption of the luminal vessel surface within the stented segment (arrows).

3. Stent edge Dissection

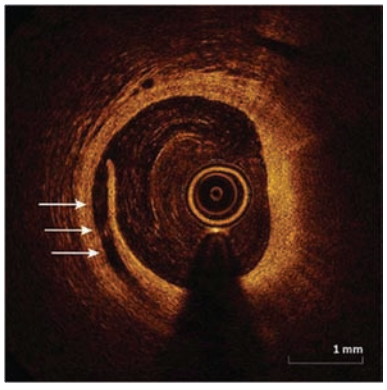

Appears as a disruption of the lumen surface (arrows) at the edge of the stent.

4. Tissue Prolapse

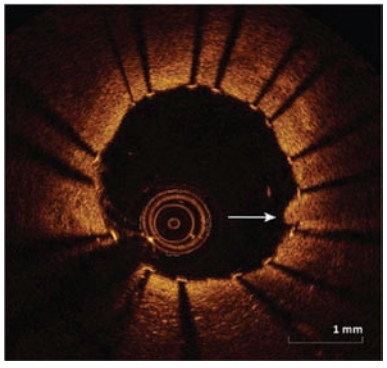

Protrusion/projection of tissue into the lumen between the stent struts (arrow) after implantation.

5. In-stent Restenosis

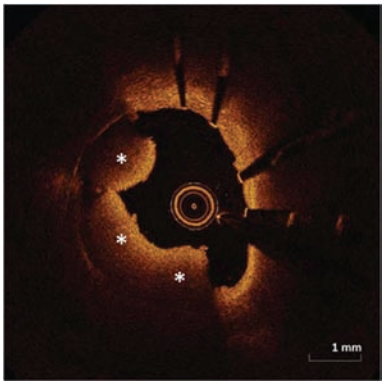

Thrombus protruding into the lumen (asterisks) in-between or over the stent struts. Within the stent there may be red thrombus (as depicted above) which appears as a highly backscattering and highly attenuating mass or white thrombus which appears as relatively less backscattering with very little signal attenuation after implantation.

6. Covered Stent Struts

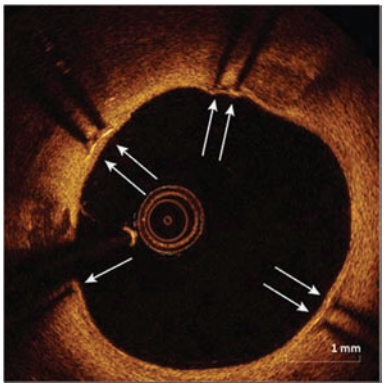

Stent struts are termed covered if overlying tissue (arrows) can be seen above the strut after implantation.

7. Uncovered Stent Struts

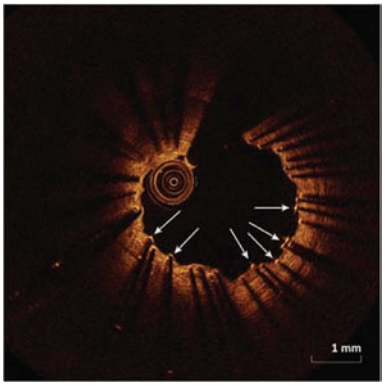

Stent struts with termed uncovered if there is no evidence of tissue (arrows) which can be seen above the strut.

8. In Stent Restenosis

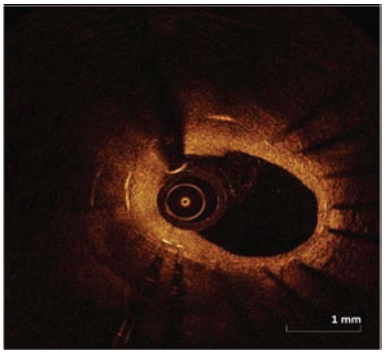

Appears as a shadow (asterisk) from the guidewire which can mask the underlying image.

ARTIFACTS

1. Guidewire Artefact

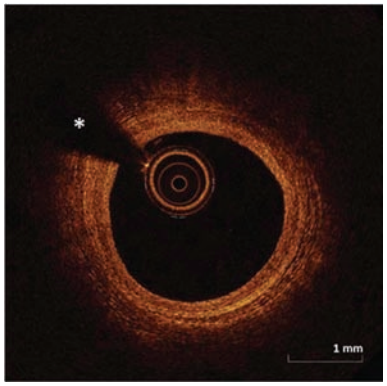

Appears as a shadow (asterisk) from the guidewire which can mask the underlying image.

2. Shadowing Artefact

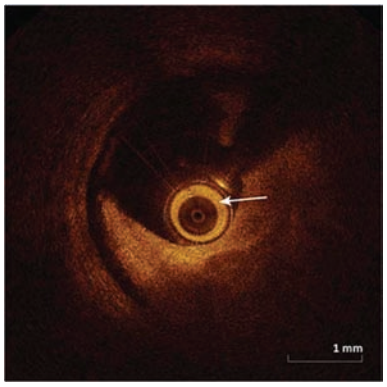

Appear as a drop in the signal on the abluminal side of the vessel by opaque object. Shadows can completely occlude or may diminish the image intensity of deeper structures. Common objects that create shadows are opaque and include the guidewire and metallic stent struts. Blood in the catheter (arrow) can also cause.

3. Multiple Reflections

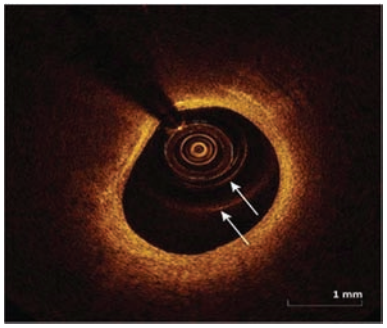

Circular lines (arrows) are created within the image which appear as a result of light reflection from the catheter surface which can lead to erroneous measurements when these lines are inappropriately used for calibration instead of the catheter edge.

4. Saturation Artefact

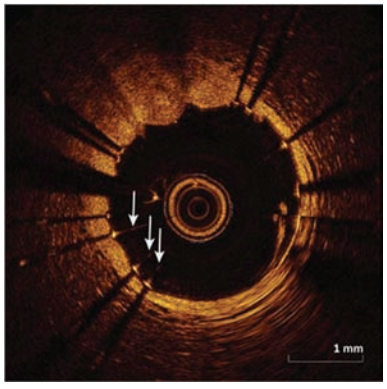

Reflection of a light source off a reflective surface such as the wire or stent strut cause a backscattered signal which is too high to be detected by the detector resulting in streaking scan lines of varying intensity (arrows) along the axial direction.

5. **Sew up Artefact**

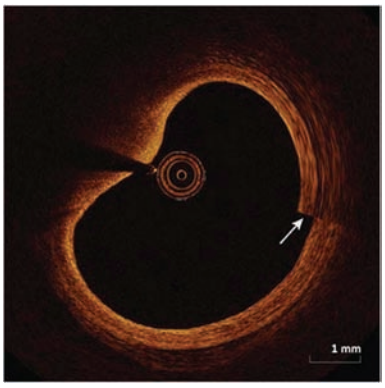

Misalignment of the intimal border (arrow) occurs as a result of movement of the vessel, wire or catheter during a single cross-sectional acquisition.

6. Fold over Artefact

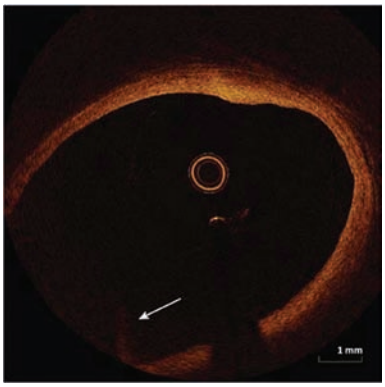

Appears as a portion of the vessel folded over (arrow) and occurs when the vessel is larger than the ranging depth. Fold-over artifact is most commonly seen in large caliber vessels adjacent to the respective side branch.

7. Residual Blood Artefact

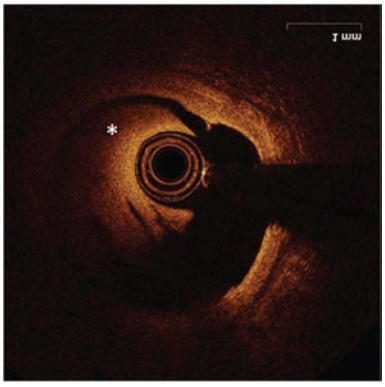

Appears as intraluminal residual blood (asterisk) which results in scatter and an unfocused image and occurs as a result of sub-optimal vessel flushing. Blood within the lumen may be misinterpreted as a thrombus in some cases.

8. **Tangential Signal Drop out Artefact**

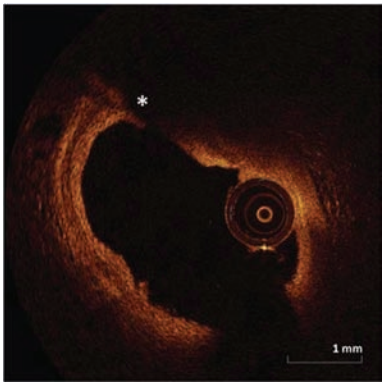

Signal-poor area (asterisk) within the artery as a result of catheter position near or touching the vessel wall. The catheter position causes the optical beam to be parallel to the tissue surface causing attenuation as it passes along the wall and as result there is an area of signal dropout.

OCT GUIDED PERCUTANEOUS CORONARY INTERVENTION

Pre PCI Assessment
Morphology , Length, Diameter (MLD)

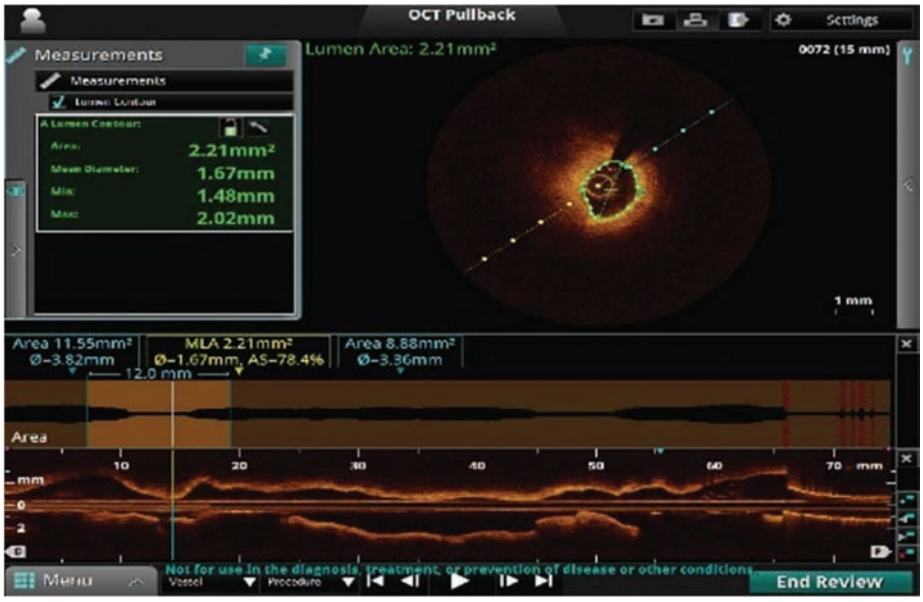

Prior to stent implantation OCT can provide quick and accurate measurements of the minimal luminal area (MLA), distal and proximal reference areas, diameters and lesion length. OCT can be used to determine landing zones to estimate the optimal stent length

There are two types of pullback modes: the 75 mm Survey Mode and the 54 mm High Resolution Mode:

- The 75 mm Survey Mode – fast and efficient and utilizes minimal contrast.
- The 54 mm High Resolution Mode – has twice the frame density producing a relatively sharper image.

MORPHOLOGY

Calcium Assessment Scoring system

The rule of 5's. "5"0 percent of the circumference, "5"mm long, 0."5"mm thick is like a brick

OCT-BASED CALCIUM SCORE		
1. Maximum calcium angle (°)	≤ 180° →	0 points
	≥ 180° →	2 points
2. Maximum calcium thickness (mm)	≤ 0.5 mm →	0 points
	≥ 0.5 mm →	1 points
3. Calcium length (mm)	≤ 5.0 mm →	0 points
	≥ 5.0 mm →	1 points
Total score	**0 to 4 points**	

Low Calcium

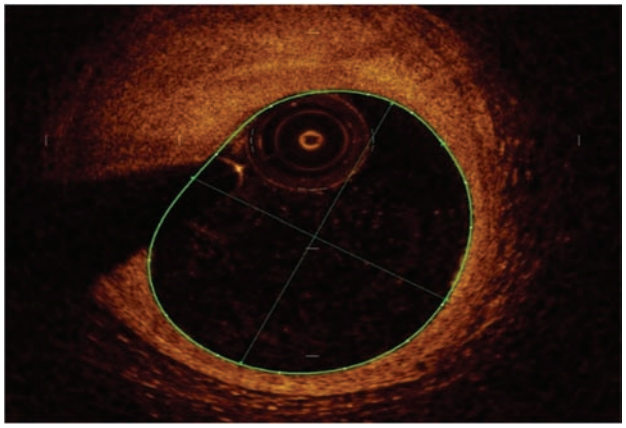

High Calcium

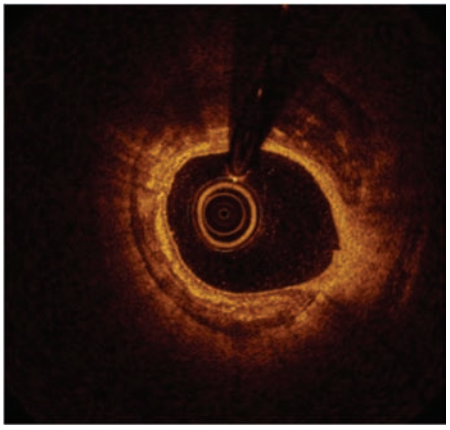

STENT LENGTH SIZING

- Select Landing Zones.
- Visually scan for largest luminal area.
- Place landing zones in healthy tissue (i.e. EEL visualization).
- In the absence of EEL to represent healthy tissue find the largest lumen to avoid areas of TCFA or lipid pools so as to not land your stent edge in these high risk areas.
- Adjust to stent length.

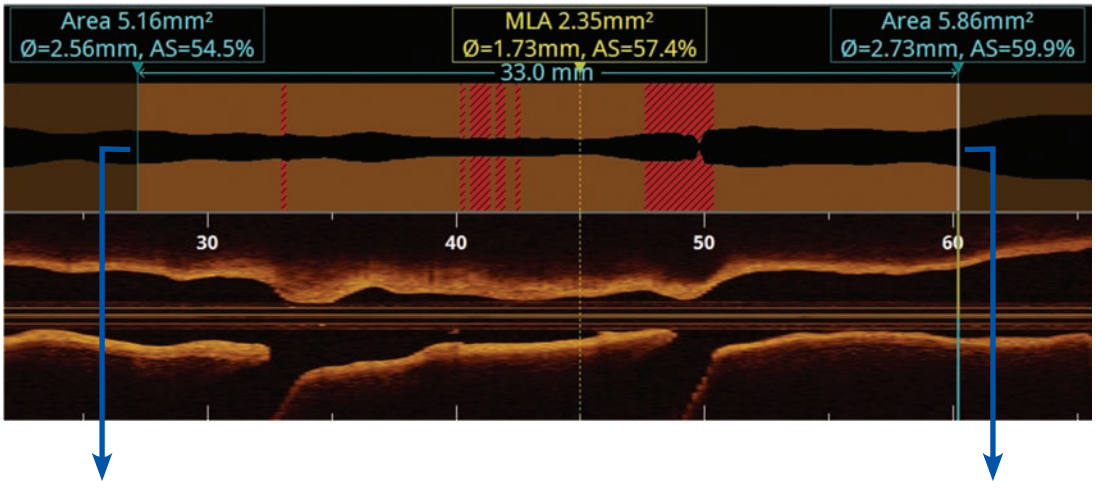

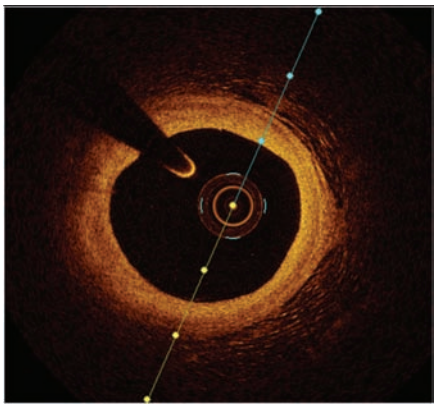

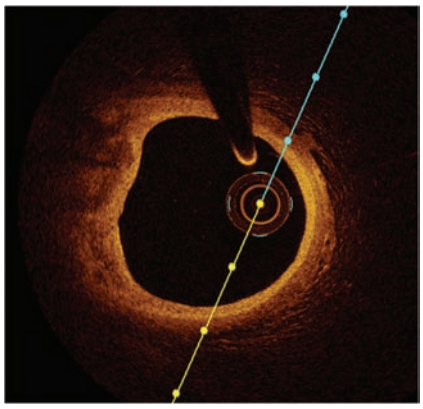

STENT DIAMETER SIZING

- Measure Vessel Diameter.
- Take EEL measurements at each reference (lumen if EEL not visible).
- Choose Stent Diameter.
- Use the distal reference measurement to select stent diameter.
- EEL: round down to nearest stent size. Lumen: round up.
- Choose Post Dilation Balloon Diameter.
- Distal Balloon: Use distal reference measurement Proximal Balloon: Use proximal reference measurement.

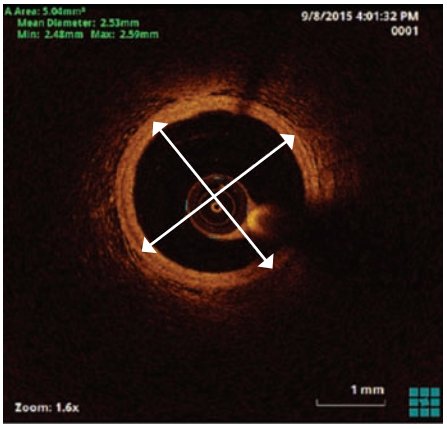

EEL Measurements
Average two perpendicular EEL measurements **Round down** to the next quarter size, **unless** already at a stent size.

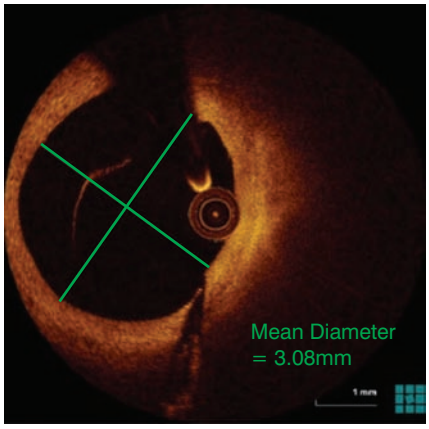

LUMEN Measurements
Use Automatic measurements at distal reference round upto next quarter size always.

POST STENT ASSESSMENT/OPTIMISATION

Medial dissection, Apposition, expansion (MAX)

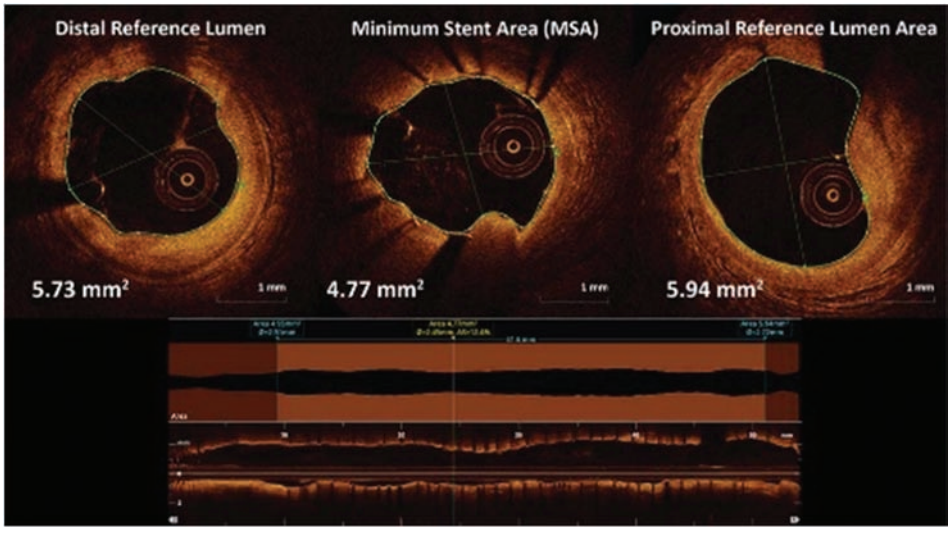

Stent Expansion = MSA/Average Reference Lumen Area * 100

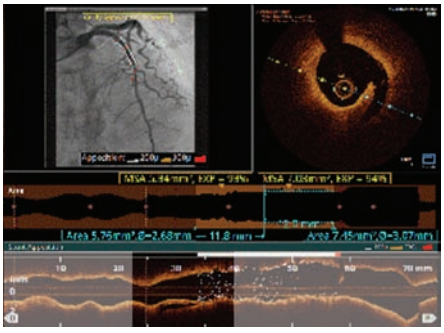

Medial Dissection
Dissection penetrates medial layer, and is greater than 1 quadrant arc

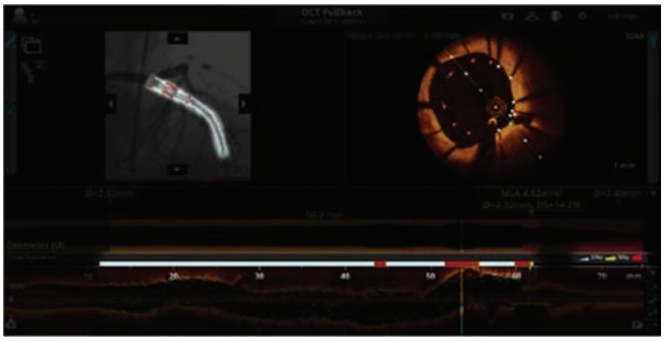

Malapposition
Longer than 3 mm[5] and ≥0.3 mm from wall[6]

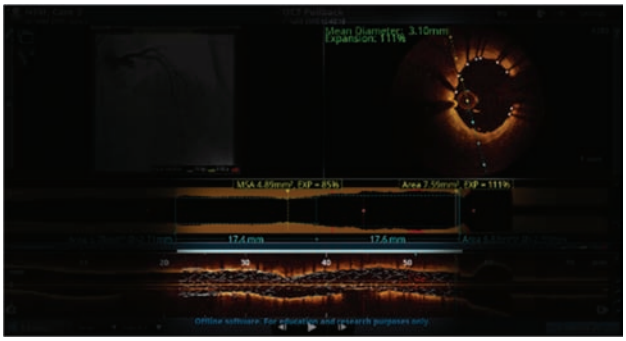

Expansion
≥80% acceptable (≥90% optimal)

3D OCT OPTIONS

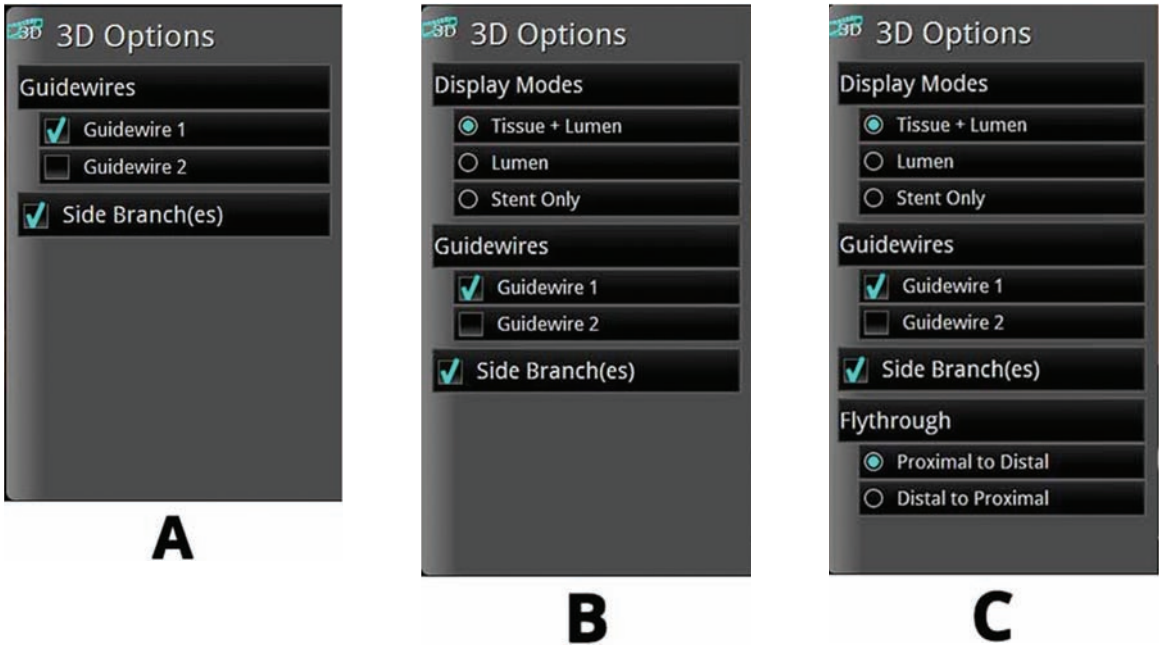

A 3D Bifurcation.
B 3D Navigation with Rendered Stent on.
C 3D Navigation with Rendered Stent and Flythrough on 3D Rendering of OCT is a new software feature which can be performed real time. The 3D Navigation 3D Rendering is an excellent function to use to visualize vessel geometry and the ostium of the side branch as seen below. The Segmental Lumen function is a helpful tool to use if visualization within the lumen is desired.

3 D BIFURCATION OSTIAL VIEW DISPLAY

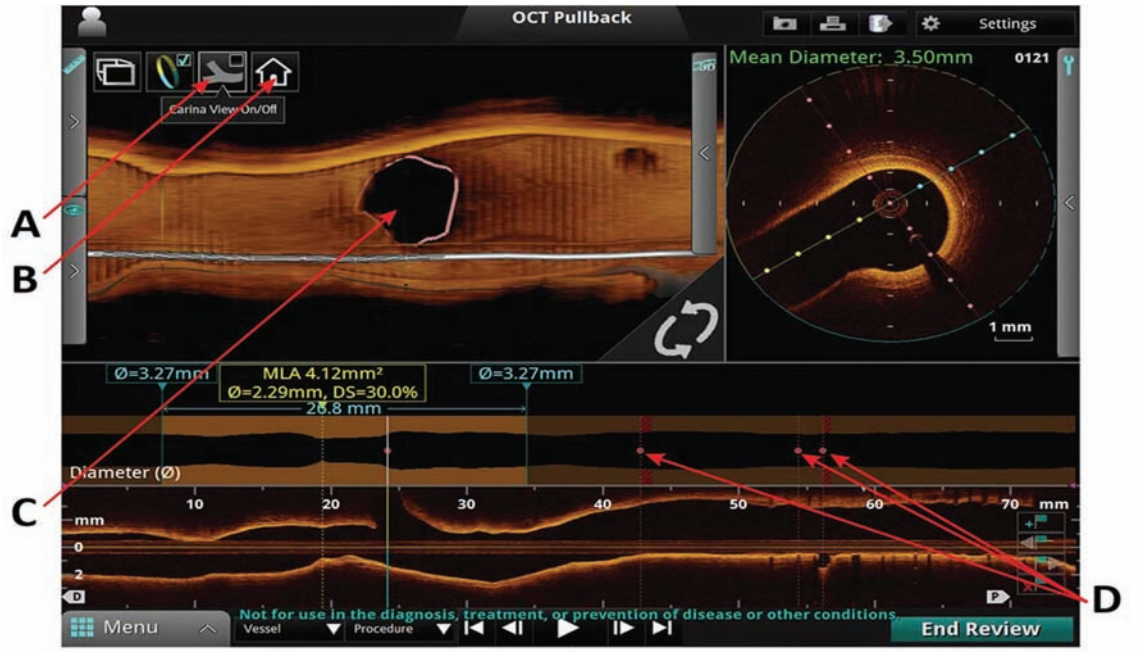

A. Carina View Button **B**. Reset Button View **C**. Sidebranch Ostium **D**. Detected sidebranch location

3 D BIFURCATION CARINA VIEW DISPLAY

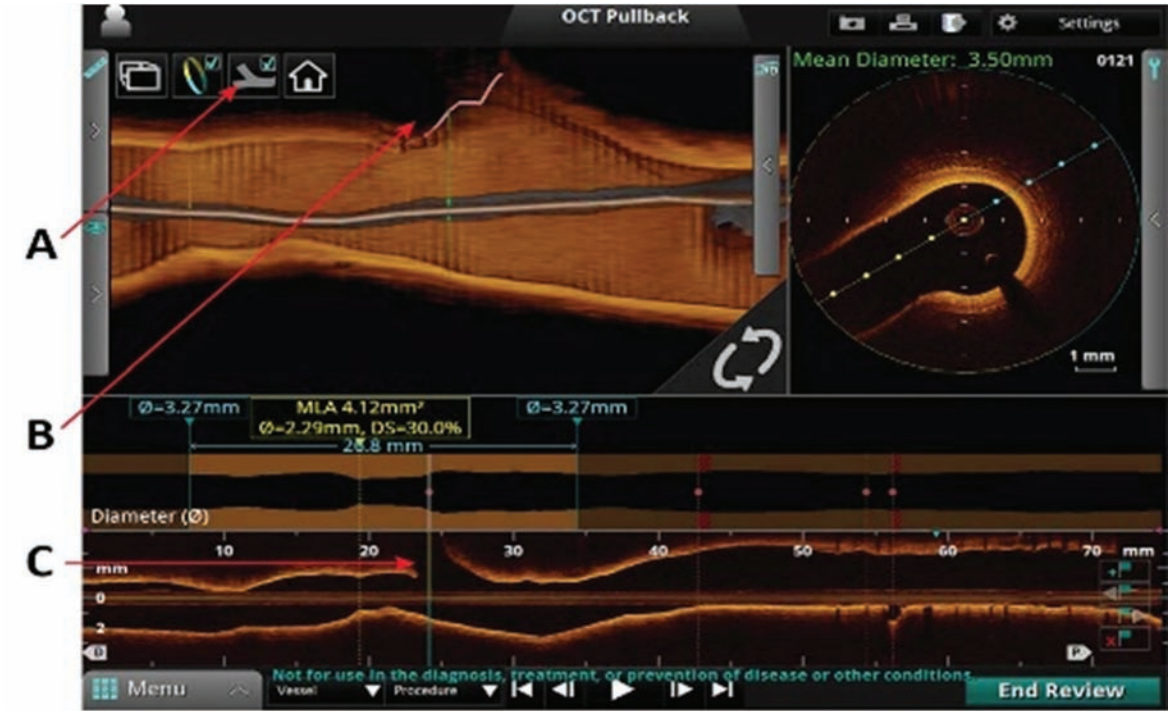

A. ACarina View Button **B**. Carina (displayed in 3D image region) **C**. Carina (displayed in L-Mode)

SALINE OCT

Study revealed heparinised saline does not affect the measured coronary dimensions when compared with contrast and may be used as a contrast alternative for coronary FD-OCT during PCI optimisation. Thus, an obligatory extra contrast load and associated risk of CIN can be avoided during OCT-guided PCI optimisation. Coronary FD-OCT using heparinised saline as flushing media yields images of same quality as that of contrast.

Comparison between Contrast and Saline OCT

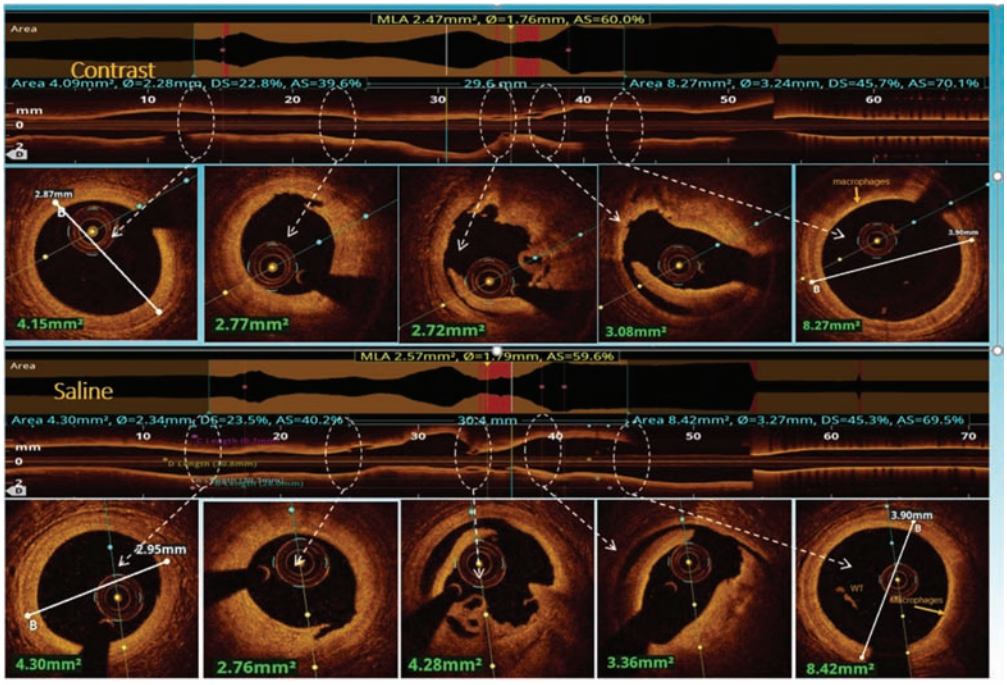

Hybrid IVUS-OCT Catheter

Intravascular ultrasound (IVUS) and optical coherence tomography (OCT) have been developed and improved as both diagnostic and guidance tools for interventional procedures over the past three decades. IVUS has a resolution of 100μm with a high tissue penetration and capability of assessing the entire structure of a coronary artery including the external elastic membrane, whereas OCT has a higher resolution of 10–20μm to assess endoluminal structures with a limited tissue penetration compared to IVUS. Recently, two companies, CONAVI and TERUMO, integrated IVUS and OCT into a single catheter system. With their inherent strength and limitations, the combined IVUS and OCT probes are complementary and work synergistically to enable a comprehensive depiction of coronary artery.

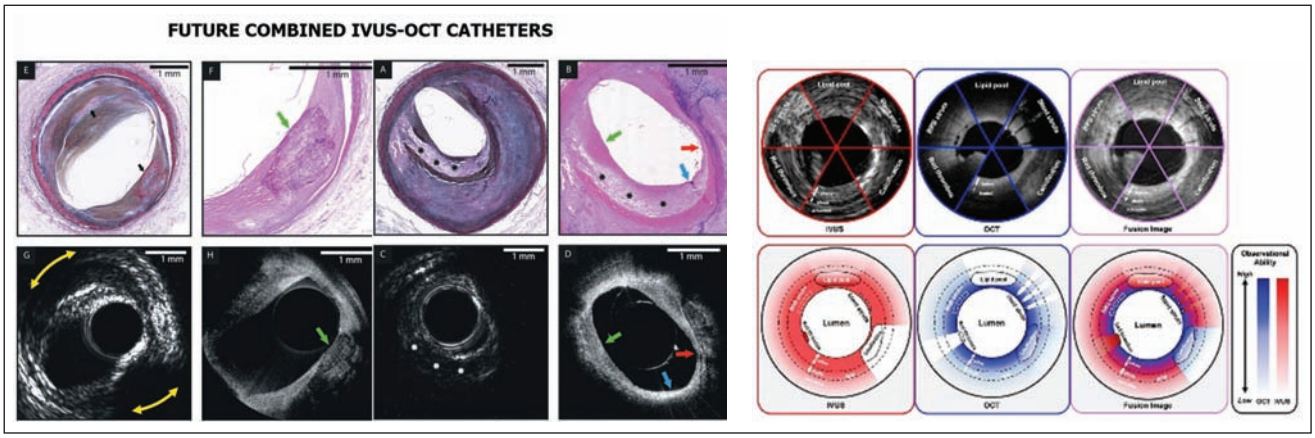

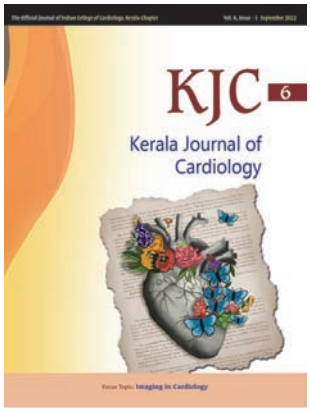

Intracardiac Echo – Clinical Applications

Arun Gopi
Senior Consultant Interventional Cardiologist and Electrophysiologist, Metromed International Cardiac Centre, Calicut, Kerala.

Sharath Kumar
Cardiac Electrophysiology Fellow, Halifax Infirmary, QEII Health Sciences Centre, Halifax, Nova Scotia, Canada.

Intracardiac echocardiography (ICE) is a very promising technique able to provide high-resolution real-time visualization of cardiac structures, continuous monitoring of catheter location within the heart, and early recognition of procedural complications. For interventional procedures it serves as an alternative for the trans oesophagealechocardiography, which is semi-invasive and requires anaesthesia. Cardiac electrophysiology armed with 3D mapping and ICE has emerged as a major force in reducing and eliminating fluoroscopy in modern day practice. Knowing and understanding ICE imaging is pivotal to the performance of complex ablations and interventions. The use of ICE is almost universal for complex ablations like atrial fibrillation (AF) ablation and ventricular tachycardia (VT) ablation in western centers. The use of ICE has expanded in recent times and the objective of this review is to provide the reader with information on the basics of ICE and its most common uses.

ICE Catheters

ICE catheters are of two types, They are:

1. **Radial or Rotational ICE:** These have a single ultrasound crystal mounted on a 6-10 F catheter. This has frequencies of 9 to 12 MHz and the rotating transducer produces 360º images in the long axis of the transducer. Most of these catheters have been non-steerable and they have poor tissue penetration and far field resolution. Its seldom used in clinical practice .

2. **Phased array ICE:** Here a 64-element transducer is mounted on a 6-10 F catheter and these catheters are deflectable in 4 directions. (anterior, posterior, right and left). The image produced is wedge shaped as viewed by the tip of the catheter. These catheters are easily maneuverable and offer better images with a depth of 15 cm. They also haveDoppler compatibility and can provide images on par with transesophageal echocardiography.[1]

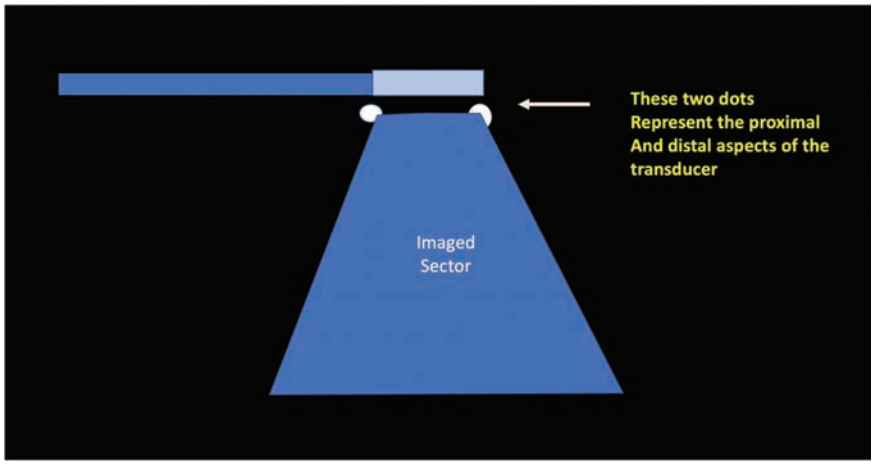

Address for correspondence: Dr. Arun Gopi, Senior Consultant, MD, DM, DNB, PDF (EP), CEPS-AC, CCDS, Interventional Cardiologist and Electrophysiologist, Metromed International Cardiac Centre, Thondayad Bypass Road, Kozhikode, Kerala - 673014, E-mail: arungopi@gmail.com

The two commonly used ICE catheters are the Abbott View Flex Extra (Abbott) and the AcuNav/Soundstar ICE catheters from Biosense Webster. Both catheters that are in common use are excellent and have their own advantages and disadvantages. The View Flex ICE catheter is a 8F side-looking 64-element phased-array and has 4-way steerability along with grayscale and color Doppler. The AcuNav is a 8 and 10 F Side-viewing 64-element phased-array along with 4-way steerability, with grayscale and Doppler. The Soundstar offers the same AcuNav catheter with a magnetic sensor at its tip and is integrated to the CARTO mapping system.

The View Flex ICE catheter (Abbott) has crisper and better image quality but is stiffer and needs a larger sheath. Due to its stiffer nature, it may sometimes be difficult to navigate this though tortuous femoral veins. The other aspect of this catheter is that we can anteroflex and posteroflex the catheter and do a left and right tilt, but it does not come back to neutral when we release the knob. The AcuNav ICE (Biosense Webster) catheter is a smaller catheter and goes through a smaller sheath and is more flexible. It goes back to neutral immediately when the rotating mechanism is released. The image quality may not be as good as the View Flex ICE catheter but the major advantage of the AcuNav ICE catheter is its compatibility with the CARTOSOUND module of the CARTO mapping system.

There are newer technologies like the Conavi Foresight ICE system which can provide us with a 360° view of the heart.

IMAGING THE ATRIA

The fundamental steps in ICE imaging include:

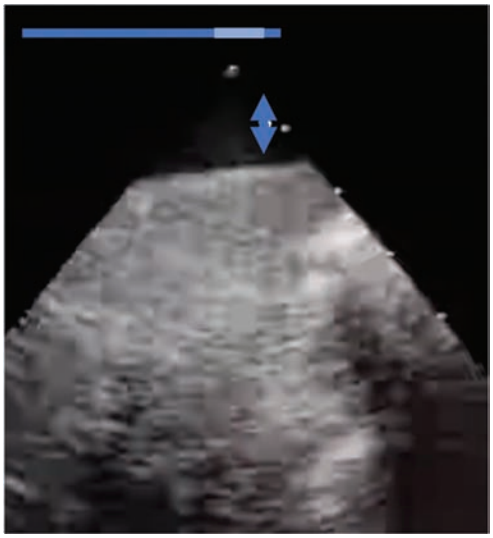

1. The ICE catheter is advanced up into the right atrium (RA) through the iliac vein and inferior vena cava (IVC). While advancing the ICE catheter through the femoral veins occasionally one may encounter difficulties such as tortuosity or the catheter entering the branches of the vein. It is important to maintain an echo free space at the tip of the transducer and the vascular wall at the leading-edgeduring advancement of the catheter. This is seen usually at the left iliac vein and IVC junction and deflecting the ICE catheter may be useful to subvert this problem. If one has inserted another catheter into the heart, this catheter or wire can be followed on the ICE to ensure the correct course of the ICE catheter. As the ICE catheter is moved upwards, we can see the liver which is a landmark that tells us we are close to the heart and then eustachian ridge is the first structure that is observed as we approach the IVC – RA junction. The ICE catheter can be usually maneuvered into the heart without fluoroscopy in most instances.
2. "Home view" from the RA: This is the most fundamental view that one acquires when we enter the RA. The ICE catheter is in the neutral position in the mid – RA. In this view, the segments of the RA, Tricuspid valve and RV are visualized. The aortic valve with the ascending aorta is also seen in this view.

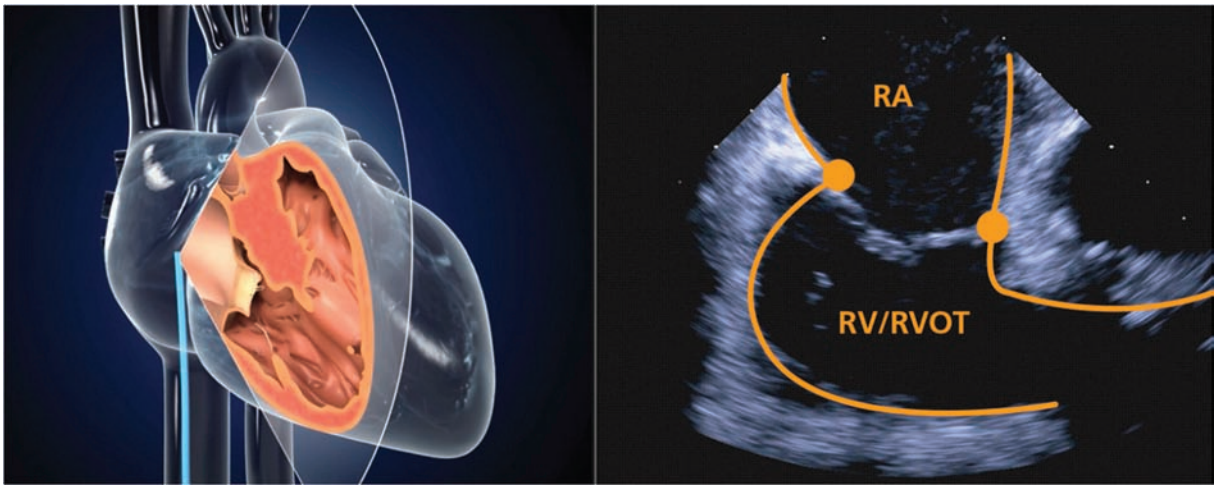

3. Further clockwise rotation from the "home view" brings the Aorta, RVOT and RV in view. In this view the Noncoronary cusp (NCC) is close to the RA and the left coronary cusp (LCC) can be seen superior and left of the NCC. During this rotation the coronary sinus may also be visualized.

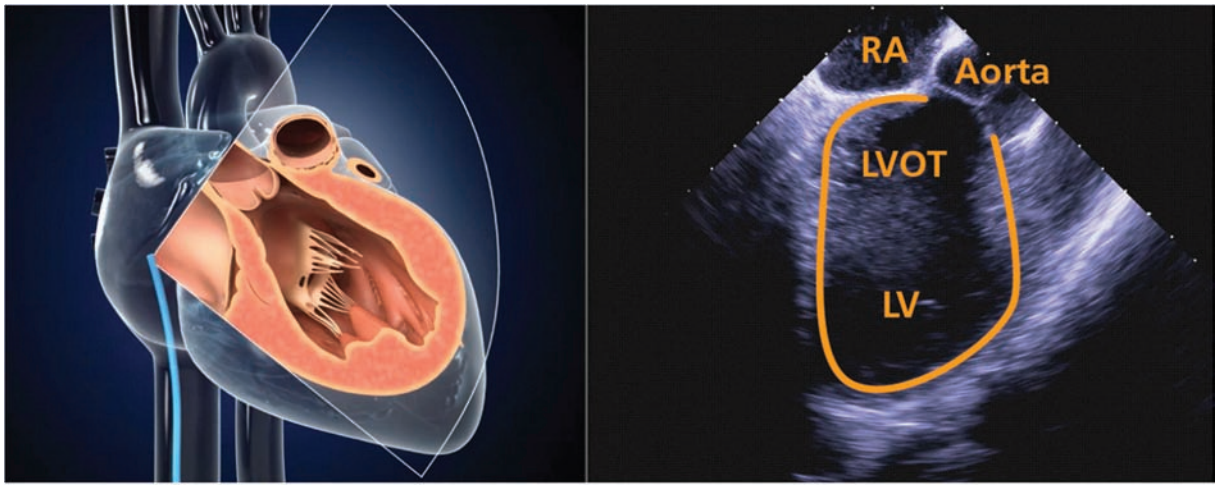

4. Further clockwise rotation of the ICE catheter gets us past the coronary sinus body and we are able to perceive the left atrial appendage(LAA) as an outpouching along with the mitral valve.

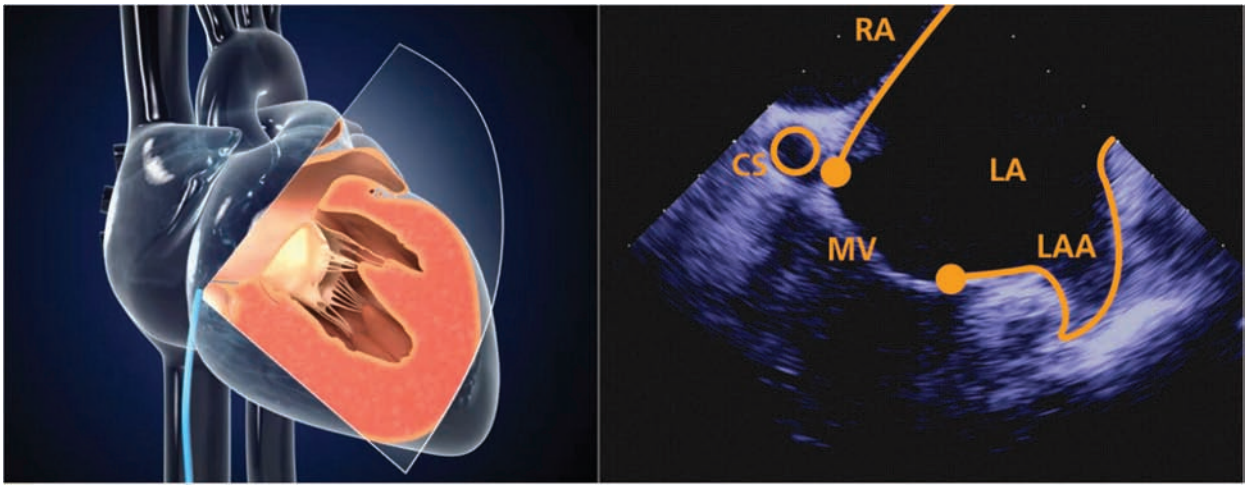

5. As we proceed clockwise further, we get the left superior (LSPV) and inferior pulmonary (LIPV). Veins usually in the same view.

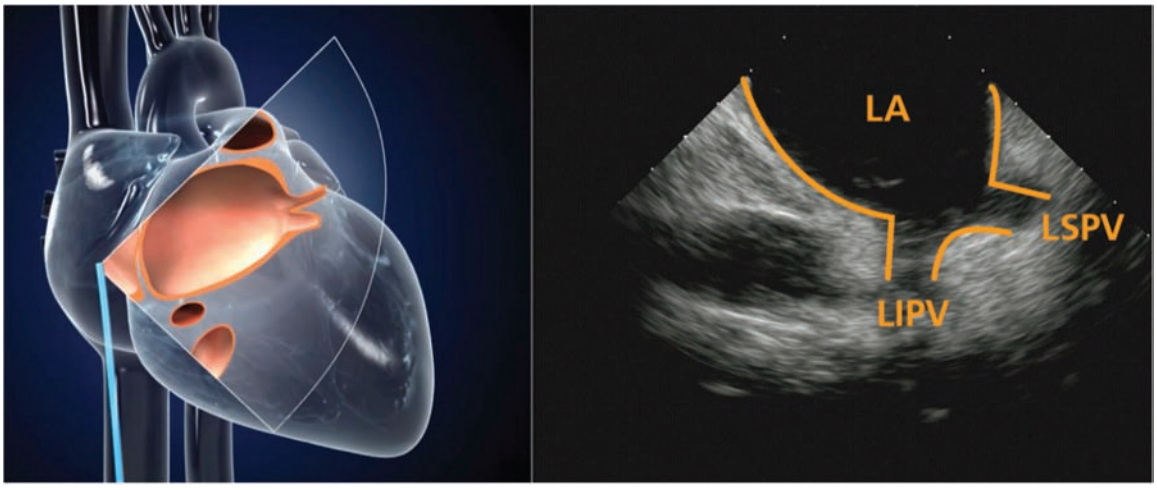

6. Continuing the clockwise rotation, we get a view of the posterior wall of LA and the esophagus along with descending thoracic aorta. It is important to mark the esophagus position on Cartosound here.

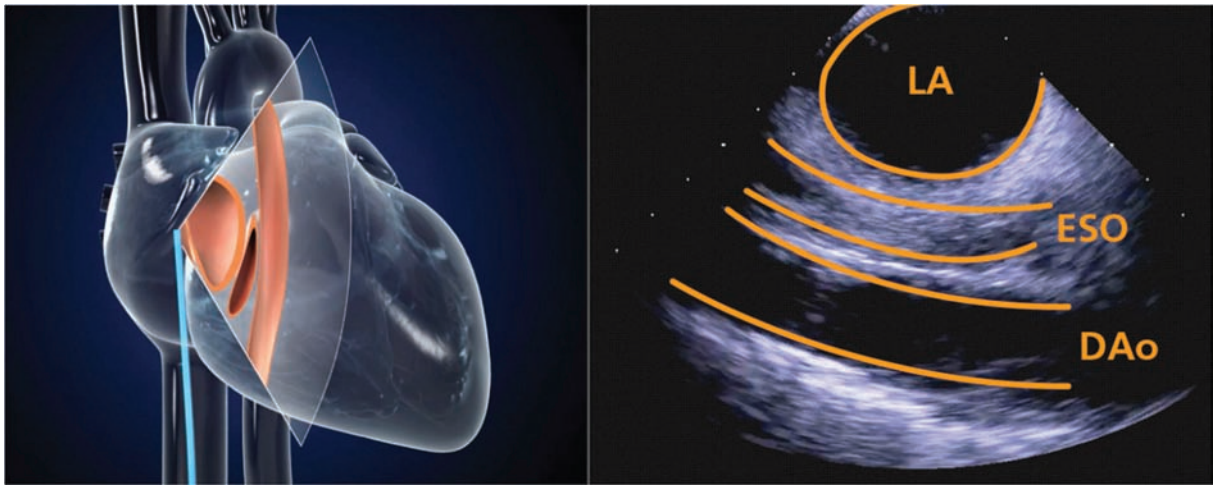

7. Clockwise torquing past the esophagus view with a slight cranial advancement brings the right inferior pulmonary vein (RIPV) at 7 o clock.

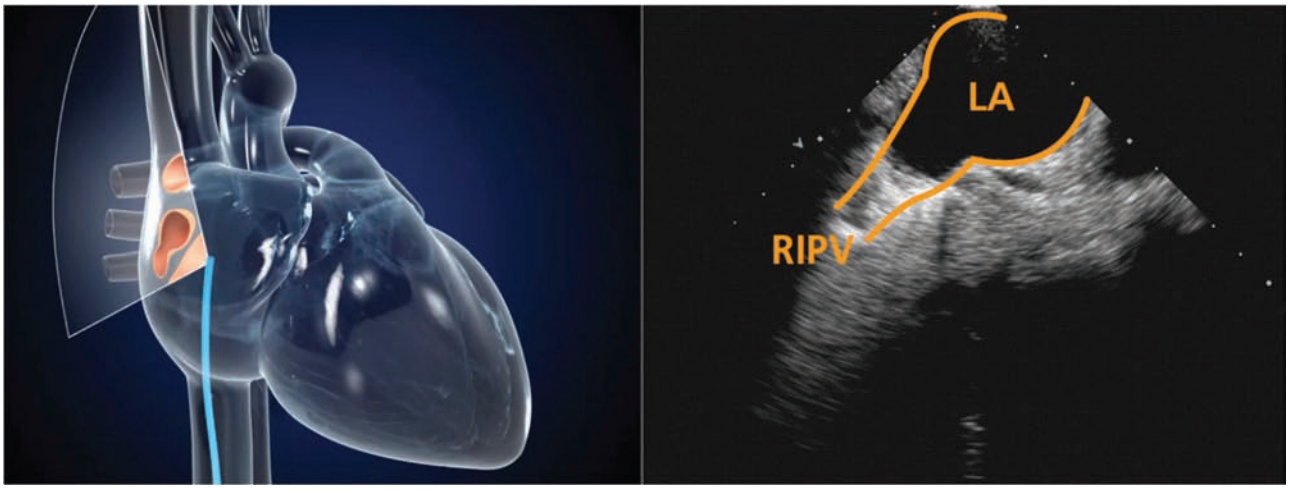

8. Imaging the Right superior pulmonary vein (RSPV) – This requires further clockwise rotation, and one may need to advance and posterior flex the catheter to get a good view of the RSPV. This can be tricky at times requiring maneuvers additional to clockwise torquing.

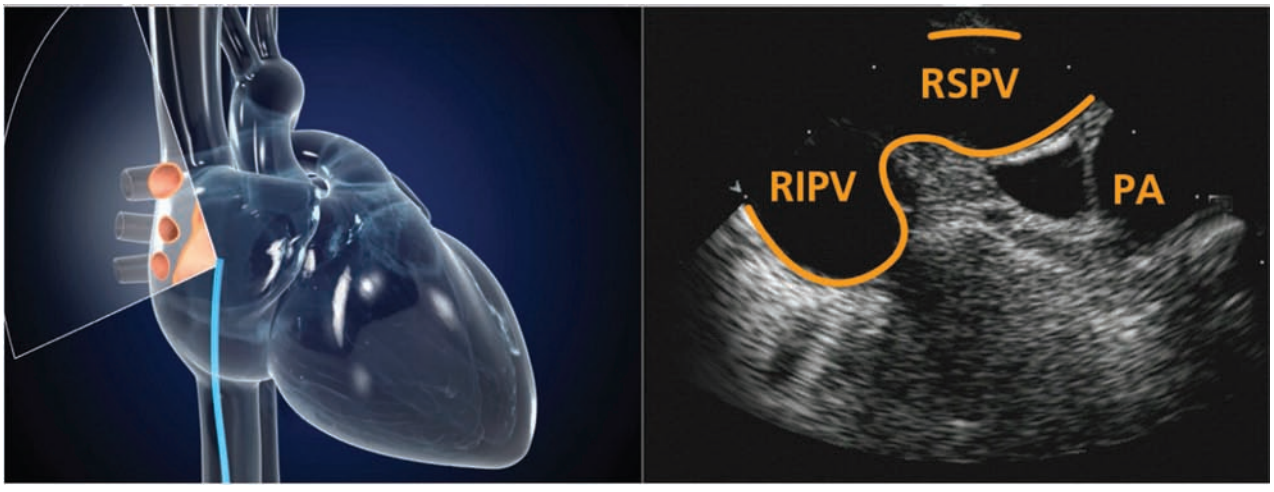

Imaging the ventricles

From the home view the catheter is slightly counterclockwise rotated to bring the tricuspid valve in view. Once the tricuspid valve is visible, the catheter is flexed anteriorly to cross the tricuspid valve and enter the RV. The ICE catheter is then carefully advanced into the RV. During this manipulation one may be able to RV structures such as the Moderator band and RV papillary muscles. Once we are in the RV the anterior flexion on the ICE catheter is removed. Rotating the catheter clockwise from this position helps in imaging LV anatomy.[2] The following structures are seen sequentially as we clockwise rotate the ICE catheter:

1. RV intracavitary structures: Moderator band and papillary muscle, the RV structures can be quite variable.

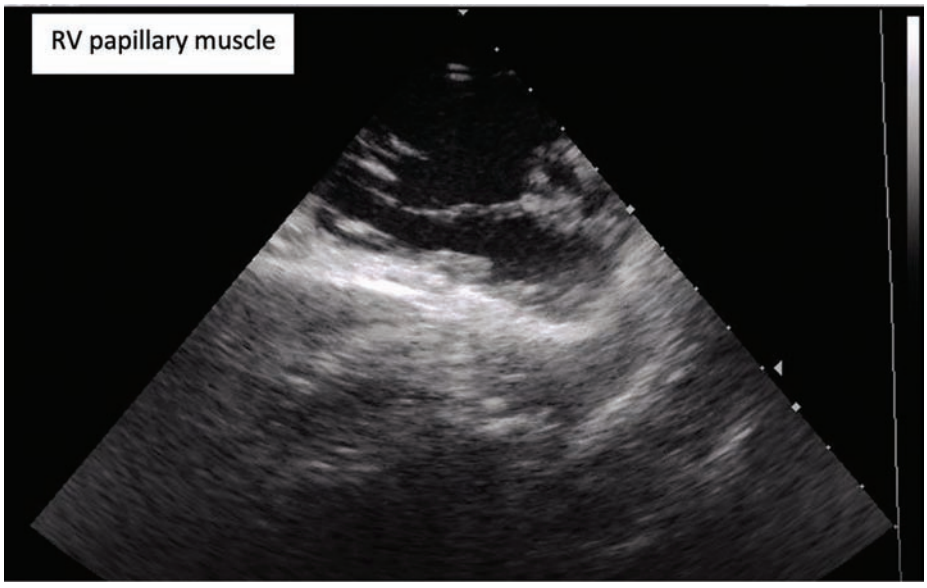

2. Intraventricular septum is seen on further clockwise rotation.
3. As clockwise rotation is continued, we can see the LV anterior and inferior wall along with the postero-medial papillary muscle.

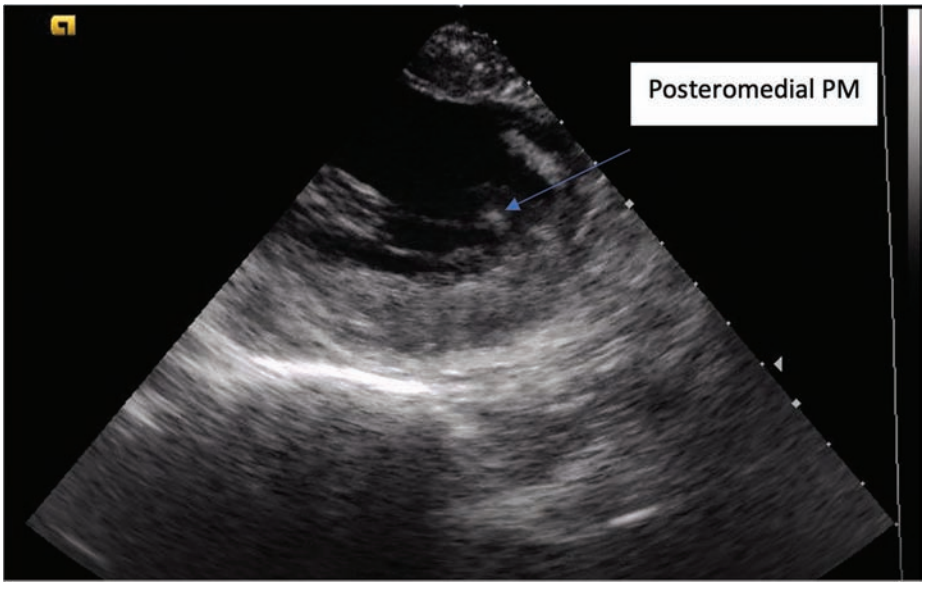

4. Further clockwise rotation reveals the Anterolateral papillary muscle and the lateral and septal LV valves. This is followed by the mitral valve and LV outflow.

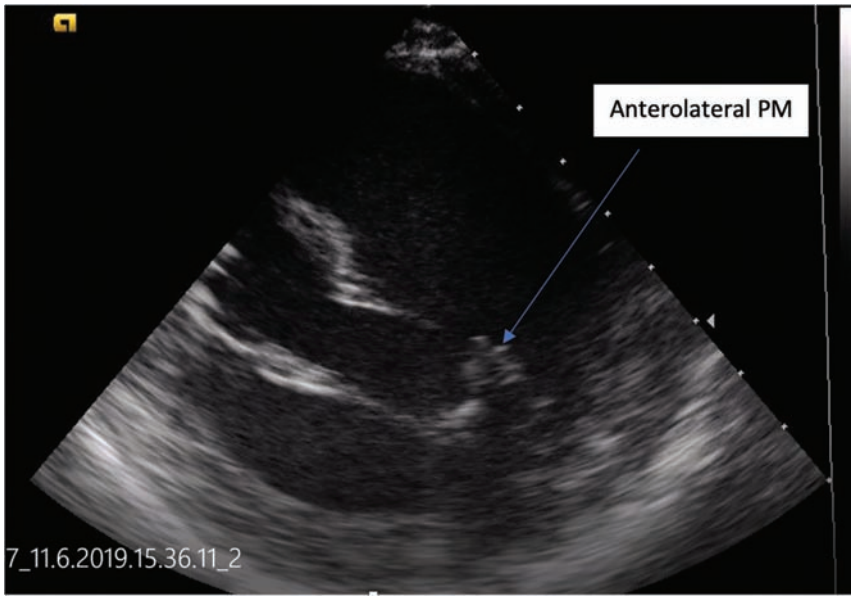

5. The aortic cusps are seen on further clockwise rotation with the RCC closest to the RV and LCC away from it. This is an important view to mark the coronaries during aortic sinus ablations and this can be marked on CARTOSOUND. The LAA can also be seen in the short axis view of the aortic valve.

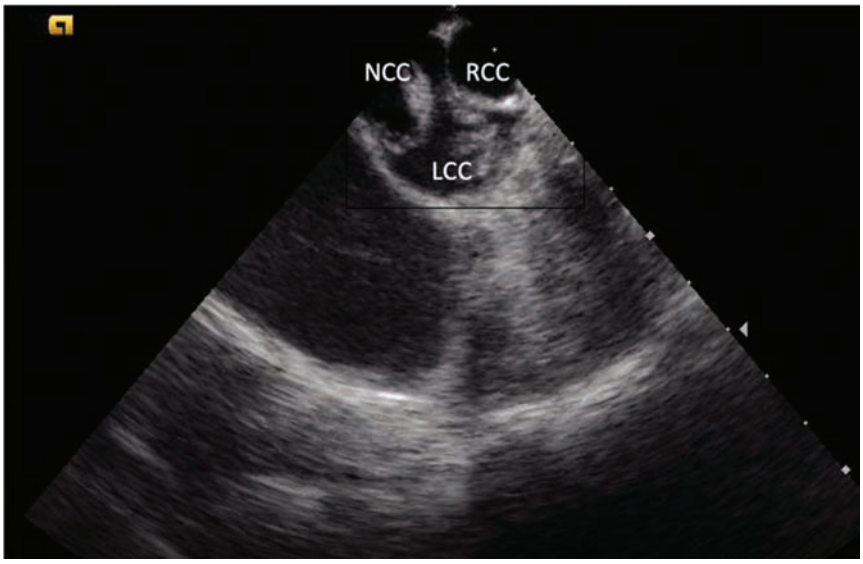

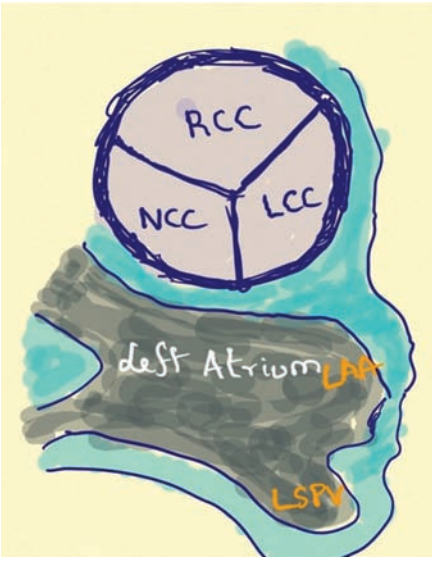

6. Finally, we can see the RVOT and a long axis of the aorta with further rotation.
7. Insertion of the ICE catheter into the pulmonary artery is useful to visualize the LAA, but this maneuver can be demanding and needs to be attempted by experienced operators.

Transseptal Puncture (TSP)

Doing a safe transseptal puncture is one of the key steps in most complex ablations. ICE can be used to direct the wire into the superior vena cava (SVC), define the right plane to perform the transseptal puncture, and to advance the sheath into the left atrium (LA).

The initial part of the TSP involves the placement of the guidewire into the SVC, this is conventionally performed

with fluoroscopy. In fluoroless procedures, the ICE is pivotal in imaging the SVC to guide the wire into it. This may be achieved by posterior tilt and counterclockwise rotation of the ICE catheter.The plane of TSP is different for different procedures, generally for AF ablations we choose the ICE view at the level of the left pulmonary veins or slightly anterior to it. For VT ablations a plane more anterior closer to mitral valve may be preferred. One should not use a view with aortic root in view due to the risk of aortic puncture. Similarly, a view with right sided pulmonary veins in view could be too posterior for TSP. Getting the optimal view for TSP may be difficult and may need slight posterior tilt to move the ICE catheter away from the septum. After the performance of the TSP, the ICE images can be used to maneuver the sheath into the LA.

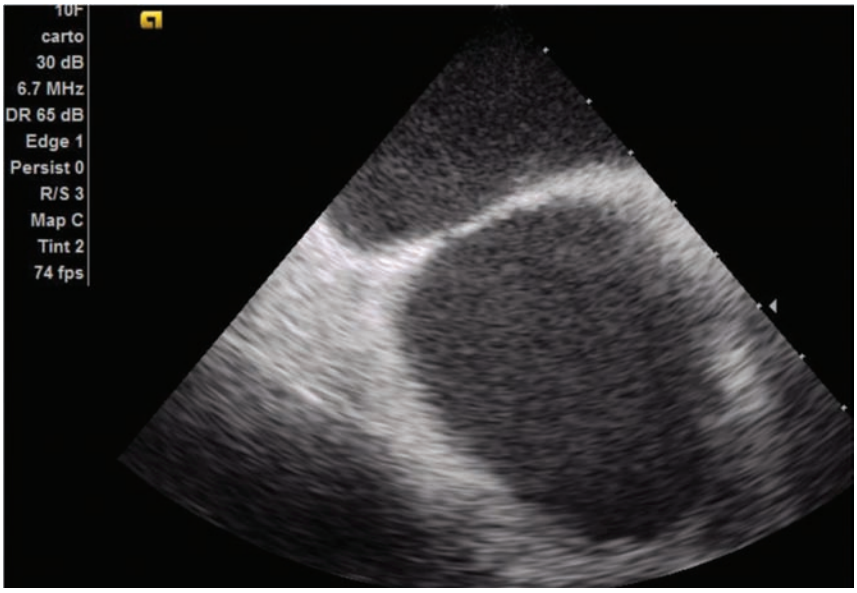

Figure: Showing the plane of Transseptal puncture in the thin portion of septum without aorta and a PV in view.

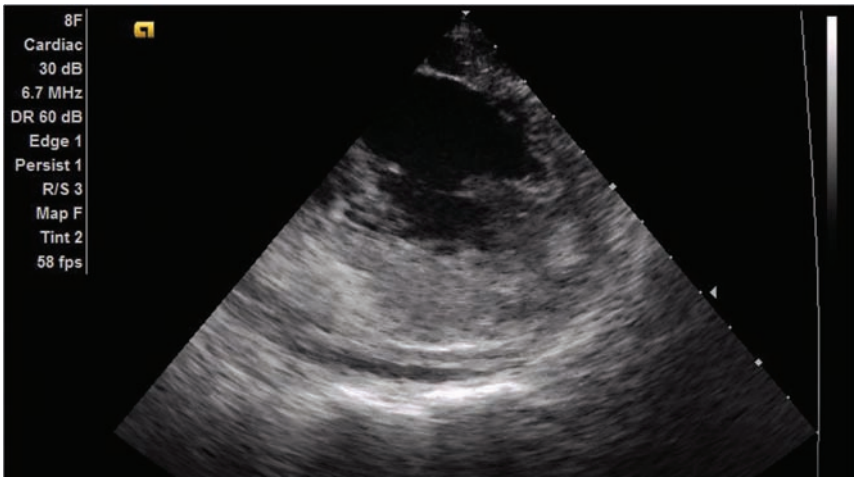

Figure: View of the LV showing a mild pericardial effusion.

Table 1

ICE utility in AF ablation
1. CARTOSOUND to create LA anatomy before the TSP
2. ICE to define PV anatomy
3. Imaging the LAA for thrombus.

4. ICE to guide TSP
5. During ablation to identify the PV antrum and to ensure contact
6. Monitor for steam pops and complications such as perforation/pericardial effusion, air embolism and thrombosis.
ICE utility in VT ablation
1. Create ventricular anatomy by CARTOSOUND – this is very useful for intracavitary structure such as papillary muscles and moderator band.
2. Define Anatomy of the cusps, LV summit and coronary arteries.
3. Appreciate the location of scar substrate.
4. Look for scars that appear hyperlucent on echo.
5. Monitor formation of thermal ablation lesions and contact of catheter with tissue.
6. Surveillance for complications such as thrombosis, Pericardial effusions

CONCLUSION

With the expanding development of percutaneous interventional procedures in the catheterisation laboratory, accurate online identification of intracardiac structures, catheters, and devices by ICE is very handy. ICE is an integral part of every complex ablation today and helps us understand the anatomy and monitor for complications. It is important to get acquainted with the fundamental ICE views and anatomy to get a good understanding of this technology. Direct detection of intraprocedural complications, such as cardiac tamponade, is possible with ICE, allowing immediate intervention.. Multimodality image integration with ICE is emerging as an excellent tool in interventional electrophysiology. Integration of ICE in procedures is likely to result in reduction of fluoroscopy and procedure times and improved outcome

REFERENCES

1. Enriquez A, Saenz LC, Rosso R, Silvestry FE, Callans D, Marchlinski FE, Garcia F. Use of Intracardiac Echocardiography in Interventional Cardiology: Working With the Anatomy Rather Than Fighting It. Circulation. 2018 May 22;137(21):2278-2294. doi: 10.1161/CIRCULATIONAHA.117.031343. PMID: 29784681.

2. Ehdaie A, Liu F, Cingolani E, Wang X, Chugh SS, Shehata M. How to use intracardiac echocardiography to guide catheter ablation of outflow tract ventricular arrhythmias. Heart Rhythm. 2020 Aug;17(8):1405-1410. doi: 10.1016/j.hrthm.2020.02.037. Epub 2020 Mar 6. PMID: 32151741.

Acknowledgment *– we acknowledge BIOSENSE WEBSTER for providing us with the illustrative pictures used in this article.*

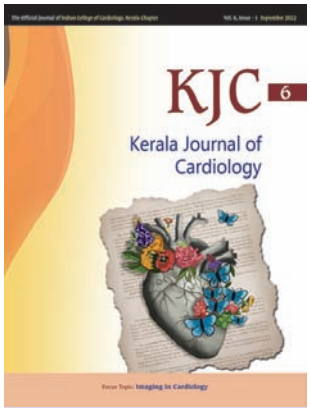

AI for the Cardiologist's Eye: Artificial Intelligence Integrating Cardiac Imaging

Jostol Pinto
Associate Professor and Interventional Cardiologist,
Father Muller Medical College, Mangalore, Karnataka.

Eye-Opener (Introduction)

All of us cardiologists have looked at electrocardiograms (ECGs) garnished with computerized values and even attempted diagnoses printed alongside. This is done by a few lines of code that reads and calculates the durations of P, QRS and T waves, PR and QTc intervals, amplitudes of R and patterns of ST elevations or depressions. They are also compared with set formulae/criteria for chamber hypertrophy or enlargement and with basic patterns of acute coronary syndromes or paced rhythms. But the software assistance often ends there. While untrained eyes, more so those of curious patients, find this more appealing than a plain graph, many physicians and cardiologists notice inaccuracies in these measurements and even wrongly diagnosed or missed coronary syndromes. These errors make it challenging to trust these computer-generated interpretations and at times even induce condescension. But these 'measurements' in no way involve any artificial intelligence (AI).

Let us look at another scenario: We are well aware how an ECG with poor R-amplitude progression or an ECG with a QS pattern in V1-V4 suggests left ventricular (LV) dysfunction. However, we are unable to conclusively determine the value of LV ejection fraction (EF) as there is no such formula. Again, we are also unable to numerically predict the LVEF of an 'apparently normal' ECG, and have not uncommonly detected reduced EF accompanied by a normal ECG in our clinical practice. Now let us consider this ECG is scanned and the computer notifies the EF rather accurately with a minimal margin of error. This is AI. But how could this be calculated without a known formula?

The Concept of AI

Many concepts tend to be insignificant or lack application when newly introduced: be it electric vehicles, cryptocurrency or AI. The above-mentioned ECG scenario tries to elucidate a core concept. AI uses not just defined code but statistics, logic and set algorithms to think like a human being, to self-correct, to modulate data interpretation coupled with a computer's massive capacity to calculate and store data. Enormous volumes of data tend to maximize accuracy. For example, predicting the time of sunrise would be fairly accurate if the sunrise times of the past 5 years are known. Now this accuracy increases exponentially (and not just 100-fold), if the past 500 years are considered. The quantum of necessary computation then goes beyond human capacity, but handling this remains equally simple for the computer. But what is interesting is that even when there is no conceivable algorithm or definite mathematical formula derivable, artificial intelligence still analyses data and provides information by a cryptic, and at times, an unknown method. This is subjected to further self-learning when errors are pointed out by real world studies. An example for this would be the ability to recognize an individual's

Address for correspondence: Dr. Jostol Pinto MBBS, MD (Medicine), DM (Cardiology), DNB (Cardiology), MNAMS.,
2-2-109/4, The Crystal House, Ladyhill Main Road, Urea Chilimbi, Mangalore, Karnataka - 575006. E-mail: drjostolcardio@gmail.com, Phone: 9880145676.

handwriting, voice or face even beyond human capacity. Despite the confidence of interpreting ECGs by human experts, it would be rather naïve to reject the possibility of machine identification of numerous details and patterns indiscernible to the human eye.

Artificial intelligence is when machines learn from their own experience and self-modulate as newer data is procured. One of its components is 'deep learning', in which a machine extracts far more features from raw information than just observation. This differentiates mere computation from AI. For example, simple image processing records the pixels and colours in an image, but deep learning would enable the machine to not only recognize that it is a picture of a face, but also estimate the age of the person and the mood or expression. This is not processed by just referring to a database of faces in memory, but rather by the machine being able to differentiate a face from another object by abstract algorithms.

Already Applied AI in Cardiology

Using standard software, each ECG is interpreted using standard rules / parameters coded by a human being. In AI, extremely large volumes of ECG and loop recordings are fed into the machine along with other phenotypic data like echocardiographic, angiographic and even clinical and biochemical data. The AI is then allowed to make correlations on its own and bring out features in the ECG that then predicts other phenotypic data. These results could include both intended and unintended correlations. Of note, the method by which AI arrives at this may not be clear; but its accuracy is proportional to the quantum of input data.

AI in cardiology is still in its early stages, and most models aren't as accurate as we would wish them to be. However, the path is set to predict phenotypes beyond human capacity for the same. With wearable devices now continuously recording (even normal) ECGs, this provides AI with the much-needed volumes of data it needs to improve this accuracy. The AI ECG of today works on predicting ejection fractions, propensity to develop future atrial fibrillation (AF) (in an ECG of sinus rhythm), grade of hyperkalemia, hypertrophic cardiomyopathy, cardiac amyloidosis, valvular heart disease (especially aortic stenosis and mitral regurgitation) and age and sex of the person.[1,2] An AI ECG could thus provide domiciliary follow up of LVEF for those on ongoing therapy for heart failure or for those on chemotherapy. It would also predict future disease in apparently normal individuals ('previvors') like the likelihood of developing LV dysfunction or AF. Studies following up patients with AI ECGs have shown how the increasing probability of impending AF has been predicted over years in a given patient until the patient actually develops AF. Here, the AI might have observed manifestations of fractionated signals on the ECG, probably not dissimilar to those recorded by an intracardiac electrogram, but indeed not visible to the human eye. AI-enabled atrial fibrillation sensing watches (AFSWs) have been shown to be highly sensitive even when compared to insertable cardiac monitors and have received Food and Drug Administration (FDA) clearance for detection of atrial fibrillation since 2018.[3]

Left ventricular dysfunction is present asymptomatically in 3-9% of adults.[2] The EAGLE (ECG AI-Guided screening for Low Ejection fraction) trial involving over 20000 adults and 350 clinicians studied the role of the AI ECG in such individuals and showed significant capability of the AI ECG in this regard.[4] The AI algorithm however is not yet publicly available as it is patent-pending proprietary intellectual property. A recent study compared detection of digoxin toxicity using the AI ECG: human-machine competition using over 35000 ECGs revealed a sensitivity of 84.6% and a specificity of 94.6%.[5] Of note, the deep learning system could offer comparable accuracy by only reading lead I compared to analyzing all 12 leads. AI also reduces false-positives and false-negatives during treadmill testing, thus improving pre-angiographic pretest probability.

If the AI capabilities of harnessing predictable health information from an ECG could exceed that of human observation, then it only means that similar, if not better, results could be expected from the interpretation of advanced cardiac imaging: echocardiography, nuclear imaging, cardiac and coronary computed tomography (CT) and cardiac magnetic resonance imaging (MRI), especially by mitigating interobserver variability. However, this is in a more nascent stage of development than the AI ECG and necessitates a large quantum of cardiac imaging data stored prior to validation. This is enhanced nowadays by handheld/bedside echocardiographic imaging, often smartphone-linked, and by cloud-based systems for hospital data. Training of even unskilled echocardiographers for this purpose may help upscale data acquisition. In fact, recognition of 15 standard echocardiographic and doppler views even with low-resolution images was shown to be more accurate by deep learning enabled echocardiography than that by board-certified echocardiographers (92% vs 84%).[6] Echocardiography using AI algorithms have shown to provide LVEF and longitudinal strain in under 8 seconds which reduces reporting time.[7] AI-echocardiography was shown to successfully differentiate between concentric LV hypertrophy and hypertrophic cardiomyopathy with a sensitivity of 96%.[8] Valvular heart disease and regional wall motion are also fields of ongoing study with regards to AI assessment. Mitral regurgitation has been diagnosed with over 99% accuracy for each

grade of severity,[9] while myocardial infarction has been diagnosed with 87% accuracy.[10] A more recent study noted that a deep learning algorithm detected wall motion abnormality as accurately as cardiologists would and better than resident echocardiographers.[11] High-risk phenotypes among those with heart failure with preserved EF (HFpEF) were also identified which could better predict all-cause and cardiac mortality.[12]

In the case of cardiac CT and MRI, the role of AI at present mainly involves reducing time for interpretation, bring uniformity in reporting, overcoming motion artefacts and noise and improving reconstruction. Certain subtle findings missed by the human eye tend to get picked up with AI, although this advantage is an ongoing field of refinement. Machine learning attempts to procure fractional flow reserve from CT coronary angiography. In the days to come, AI may minimize the necessity of using pressure wires and even intravascular ultrasound during conventional angiograms and it may also suggest appropriate stent sizes. Further, AI in interventional cardiology may pave the way for robotic cardiac interventions.[13]

Keeping an Eye on AI

Far from fiction, and way ahead from just being a 'journal article' or a 'chapter in theory', AI has already made its practical presence well felt over the past few years. However, what it lacks at present is its validation beyond human supervision and its recognition and application by those less adaptable to accept inevitable change. Machine learning needs proper validation prior to being applied to decision making in healthcare. The data fed into the system will need to be enormous in order to minimize errors and this process is ongoing through both hospital databases and data from wearables. Troubleshooting algorithms may be significantly challenging when they are cryptic and when the formulae used by AI remain unknown. Randomized trials between various deep learning algorithms may prove to be difficult for the same reason. The deployment of AI applications may face ethical issues especially when deciding whether data input is institutional or cloud-based. Algorithms used by individual institutions would grossly limit machine learning due to limited data and lower computational power. On the other hand, cloud-based computing necessitates sharing of inter-institutional data which may need formal policies in place considering both patient privacy and institutional practices. Use of such data by third parties brings in financial and social concerns and could raise large conflicts if not planned well in advance. AI could find far too many inferences beyond what it is primarily designed for and as self-learning algorithms are not exactly defined in code, it may not be within human control to regulate the ramifications of such algorithms, which may seem inapparent in the early phases of AI.

REFERENCES

1. Somani S, Russak AJ, Richter F, et al. Deep learning and the electrocardiogram: review of the current state-of-the-art. Europace. 2021;23:1179-91. doi:10.1093/ europace/ euaa377
2. Attia Z, Kapa S, Noseworthy P, et al. Artificial Intelligence in Cardiovascular Medicine. In: Libby P, Bonow RO, Mann DL, editors. Braunwald's Heart Disease: A Textbook of Cardiovascular Medicine. 12th ed. Philadelphia. Elsevier; 2022
3. Wasserlauf J, You C, Patel R, et al. Smartwatch Performance for the Detection and Quantification of Atrial Fibrillation. Circ Arrhythm Electrophysiol. 2019;12:e006834. doi:10.1161/CIRCEP.118.006834
4. Yao X, Rushlow DR, Inselman JW, et al. Artificial intelligence–enabled electrocardiograms for identification of patients with low ejection fraction: a pragmatic, randomized clinical trial. Nat Med. 2021;27:815-9. doi:10.1038/s41591-021-01335-4
5. Chang DW, Lin CS, Tsao TP, et al. Detecting Digoxin Toxicity by Artificial Intelligence-Assisted Electrocardiography. Int J Environ Res Public Health. 2021;18:3839. doi:10.3390/ ijerph18073839
6. Madani A, Arnaout R, Mofrad M, et al. Fast and accurate view classification of echocardiograms using deep learning. NPJ Digit Med. 2018;1:6. doi:10.1038/s41746-017-0013-1
7. Knackstedt C, Bekkers SC, Schummers G, et al. Fully Automated Versus Standard Tracking of Left Ventricular Ejection Fraction and Longitudinal Strain: The FAST-EFs Multicenter Study. J Am Coll Cardiol. 2015;66:1456-66
8. Narula S, Shameer K, Salem Omar AM, et al. Machine-Learning Algorithms to Automate Morphological and Functional Assessments in 2D Echocardiography. J Am Coll Cardiol. 2016;68:2287-95
9. Moghaddasi H, Nourian S. Automatic assessment of mitral regurgitation severity based on extensive textural features on 2D echocardiography videos. Comput Biol Med. 2016;73:47-55
10. Tabassian M, Alessandrini M, Herbots L, et al. Machine learning of the spatio-temporal characteristics of echocardiographic deformation curves for infarct classification. Int J Cardiovasc Imaging. 2017;33:1159–67
11. Kusunose K, Abe T, Haga A, et al. A Deep Learning Approach for Assessment of Regional Wall Motion Abnormality From Echocardiographic Images. JACC Cardiovasc Imaging. 2020;13:374–81
12. Lancaster MC, Omar AMS, Narula S, et al. Phenotypic Clustering of Left Ventricular Diastolic Function Parameters: Patterns and Prognostic Relevance. JACC Cardiovasc Imaging. 2019;12:1149–61
13. Sardar P, Abbott JD, Kundu A, et al. Impact of artificial intelligence on interventional cardiology: from decision-making aid to advanced interventional procedure assistance. JACC Cardiovasc Interv. 2019;12:1293-303

KJC Pearls

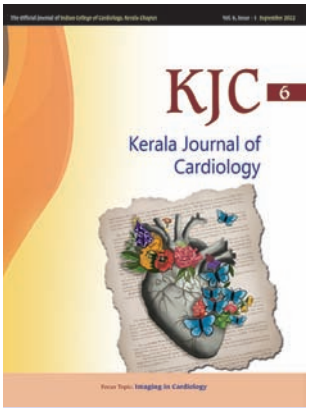

Hypertension in Kidney Transplant Recipients

Sumi Sukumaran Nair
Assistant Professor, Mayo Clinic College of Medicine.
Program Director, Transplant Nephrology Fellowship, Mayo Clinic Graduate School of Medicine.
Assistant Director, Renal Block, Mayo Clinic School of Medicine
Consultant, Division of Nephrology, Mayo Clinic.

CASE

A 57-year-old Hispanic male with end-stage kidney disease secondary to IgA nephropathy, on hemodialysis for 2 years, received a deceased donor kidney transplant. He had immediate graft function with a serum creatinine nadir of 1.3 mg/dL by the second week after transplant. His immunosuppression induction was with alemtuzumab, Solu-Medrol and he was maintained on tacrolimus and mycophenolate mofetil. He was on lisinopril and amlodipine prior to transplant and he did not require any antihypertensives medications on discharge from the hospital, and as his blood pressure (BP) was consistently < 130 /80 mmHg in the initial months. At 3 months post-transplant his blood pressure started to increase, and he had to be initiated on 10 mg of amlodipine daily, and 25 mg of carvedilol twice a day. However, his BP remained high at 172/98 mmHg at a follow-up clinic visit. He also had worsening allograft function with a creatinine of 1.9 mg/dl in the setting of a normal tacrolimus level. How will you evaluate this patient?

INTRODUCTION

Atherosclerotic cardiovascular disease is the leading cause of death in kidney transplant recipients. Hypertension is a potentially modifiable cardiovascular risk factor. It remains one of the most common comorbidities post-transplant with a reported prevalence of up to 80-90%. Uncontrolled hypertension can decrease allograft survival and increase the cardiovascular morbidity and mortality.

DEFINITION

American College of Cardiology/American Heart Association (ACC/AHA) guidelines recommend a target BP of <130/80 mmHg for patients with kidney disease. However optimal target for kidney transplant patients have not been defined. In the absence of strong evidence kidney transplant recipients, a BP ≥130/80 mmHg may be a reasonable definition for hypertension.

PATHOGENESIS

The etiology hypertension after transplant can be categorized into traditional risk factors seen in general population and transplant specific risk factors. Transplant specific risk factor may be further classified depending on the time after surgery. (**Figure 1**)

IMMEDIATE POST-TRANSPLANT

Intravenous Fluids

Patients receive significant intravenous fluid repletion during surgery and the immediate postoperative period which can lead to increased salt and water retention causing hypertension.

Address for correspondence: Dr. Sumi Sukumaran Nair, MD, Assistant Professor, Mayo Clinic College of Medicine, Program Director, Transplant Nephrology Fellowship, Mayo Clinic Graduate School of Medicine. Assistant Director, Renal Block, Mayo Clinic School of Medicine, Consultant, Division of Nephrology, Mayo Clinic. 5777 E, Mayo Blvd, AZ 85054, 480.342.1010, Fax: 480.342.2324, Pager: 480.301.5063, E-mail: nair.sumi@mayo.edu

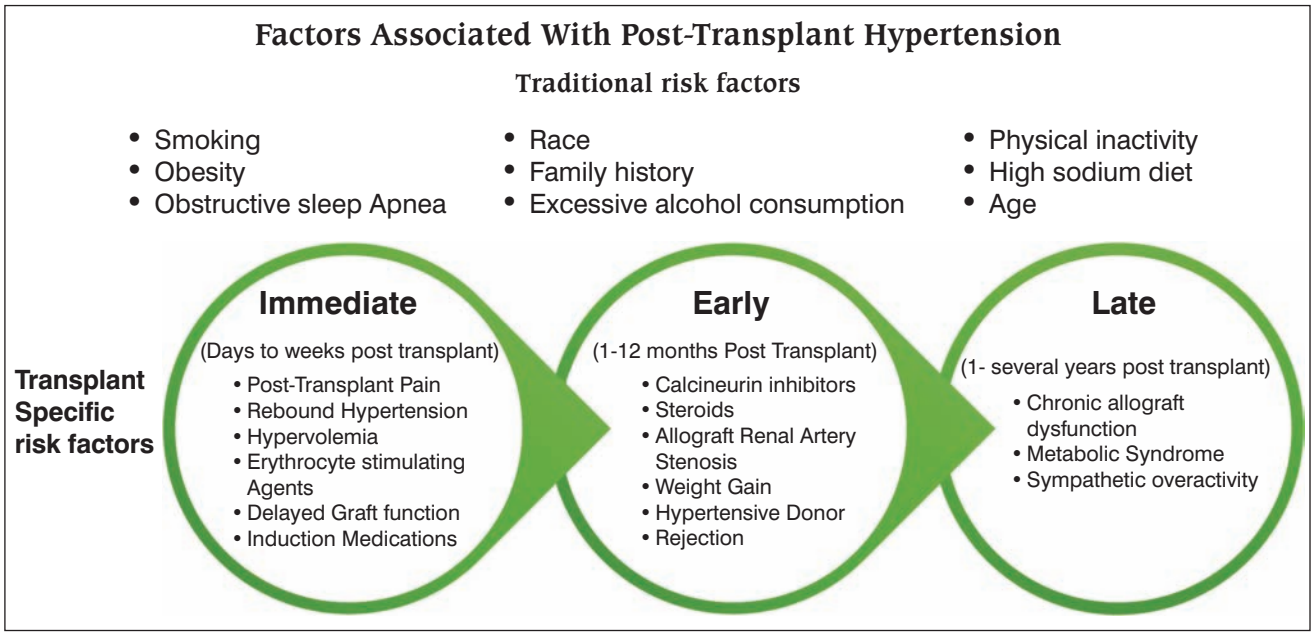

Figure 1: Factors Associated with Post-Transplant Hypertension

Steroids

Patients receive induction with high-dose intravenous steroids which can lead to hypertension. The exact mechanism is unclear but thought to be a result of increased arterial vascular resistance from alteration in intrinsic pressor response.

Pain

Inadequately controlled postsurgical pain can cause increased sympathetic response leading to increased heart rate, stroke volume and peripheral vascular resistance.

Rebound Hypertension

Withholding the pre-transplant antihypertensive regimen can cause a rebound hypertension

EARLY POST-TRANSPLANT

Use of Calcineurin Inhibitors (CNIs)

Figure 2 depicts the mechanisms by which CNIs causes hypertension. Cyclosporine has a much more pronounced effect than tacrolimus. CNIs causes renal vasoconstriction, mainly from its effect on increased

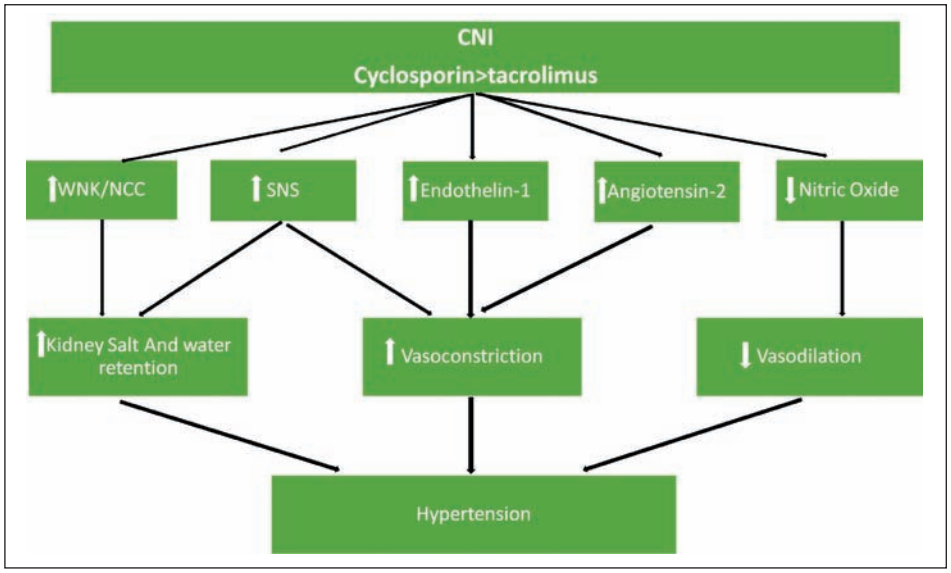

Figure 2: Mechanism of Calcineurin Inhibitors causing Hypertension

endothelin -1. It also has some effect on increasing angiotensin 2, leading to vasoconstriction. In addition, they reduce the production of nitric oxide which impairs renal vasodilation. CNI causes increased sympathetic nervous system activation which can lead to vasoconstriction and increased salt and water absorption from the renal tubules. CNI also increases salt and water absorption at the distal convoluted tubule of nephron by upregulating the activity of the sodium chloride channel.

Donor Factors

Pre-existing donor hypertension, older donor, smaller size kidney, poor allograft quality has been associated with posttransplant hypertension. There is evidence that shows that normotensive recipients receiving a kidney from a donor with hypertensive family had a higher association with hypertension.

Angiotensin II type 1-receptor activating antibodies (AT1R antibodies)

AT1R antibodies are one of the non-HLA antibodies that can affect the allograft and present with accelerated hypertension and/or antibody mediated rejection.

Transplant Renal artery stenosis (TRAS)

TRAS is the most common etiology of secondary hypertension after transplant. It typically presents between 3 months to 2 years post-transplant. The risk factors associated with TRAS are delayed graft function, cytomegalovirus infection, any vascular damage at anastomosis site -trauma/ difficulty with procurement, suturing difficulties.

Pathogenesis: Renal Hypoperfusion leads to increased renin release which subsequently activates angiotensin-2, aldosterone leading to systemic vasoconstriction, salt and water retention.

Presentation: May present with hypertension, increased creatinine, peripheral edema, and may sometimes present with congestive heart failure and flash pulmonary edema. Hypokalemia may be seen due to increased aldosterone. Bruit over the transplant kidney is a classic sign however not all bruits are from TRAS. Arteriovenous anastomosis from prior kidney biopsies can also present with bruit.

Diagnosis

Doppler Ultrasound: May show increased renal artery velocity, decreased resistive indices and tardus parvus waveform.

CTA/ MRA: Can be reliably used. But concerns exist about contrast induced nephropathy with CTA and gadolinium related nephrogenic systemic fibrosis (if GFR <30).

Newer modality MR with ferumoxytol is now being increasingly used.

Renal artery angiography remains the gold standard. CO2 angiography can significantly reduce contrast load.

Treatment: Stenting. However, it is less successful in the patient with arterial kinking, anastomotic structures, and long lesions. Surgical revascularization can be considered in those cases.

LATE POST-TRANSPLANT

Any injury to the allograft is associated with hypertension. Antibody mediated rejection recurrent glomerular disease and chronic allograft dysfunction can all cause increased blood pressure.

In addition to the above-mentioned allograft related factors, secondary causes of hypertension seen in general population should also be considered in the right setting. Presence of Hypokalemia, resistant hypertension, accelerated target organ involvement, or declining allograft function are indications for work up of secondary hypertension.

MANAGEMENT

Nonpharmacologic Management

Dietary and lifestyle modifications

- Reduction of salt intake (optimal goal <1500mg/ day)
- Diet high in fruits, vegetables, whole grains, and protein from plant sources and low in saturated fat and cholesterol (such as Dietary Approaches to Stop Hypertension- DASH Diet)
- 90-150 minutes/week min moderate daily physical or aerobic activity,
- Weight loss and maintenance of body mass index between 18-25 kg/m2
- Abstinence from smoking and reduction of excessive alcohol consumption (2 standard drinks for male and 1 for female per day).

Pharmacological management

The antihypertensive medication choice should be determined by the efficacy, interaction with the transplant medications, other patient comorbidities, and side effects. **Table 1** lists the commonly used medications.

Calcium Channel Blockers (CCBs)

They act by inhibiting the voltage-gated calcium channels in vascular smooth muscle and cardiac myocytes causing vasodilatation and reduced contractility. Dihydropyridine CCBs (amlodipine, nifedipine) are the 1st line of therapy. It can counteract the vasoconstrictive effect of CNI, which, in turn, decreases renal vasoconstriction and increases GFR.

Note: Non-dihydropyridine CCBs, such as verapamil and diltiazem, interact with cytochrome P450 to increase blood levels of CNI and mTOR inhibitors. So, if used for other indications, the levels of the CNI/mTOR inhibitors will need to be carefully monitored.

Diuretics

Thiazides and loop diuretics are helpful for treatment for hypertension when it is volume related. Loop diuretics can be especially helpful in the immediate postoperative period to counteract volume depletion and CNI related hyperkalemia. However, they can cause volume depletion and worsening kidney function. It may also worsen hypomagnesemia which is present due to urinary magnesium losses from CNI. Thiazides act on the sodium chloride channel (NCC) in distal convoluted tubules and help in counteracting the CNI induced hypertension. They can also cause electrolyte disturbances, especially hyperuricemia, hypercalcemia, and hyponatremia.

Angiotensin-converting enzyme inhibitors and Angiotensin 2 receptor blockers (ACEi & ARBs)

They are seldom used in the immediate/ early posttransplant period due to its effect on decreasing the GFR. Although this decrease is reversible, it may confound the detection of other causes of allograft dysfunction including rejection. ACE-I inhibitors and ARBs can potentiate the hyperkalemia induced by CNIs. They can also cause anemia in transplant patients in conjunction with CNIs. Consider initiation at around 3 months post-transplant, especially if patients have left ventricular hypertrophy, congestive heart failure, proteinuria, post-transplant erythrocytosis. ARBs are used in the treatment of angiotensin 2 type 1 receptor antibody (AT1R) related rejection.

Beta adrenergic blockers

β-blocker therapy has cardioprotective effects and has shown to have some survival benefit in transplant patients. Lipophilic β-blockers that undergo hepatic metabolism are preferred (labetalol carvedilol, metoprolol). Of these, carvedilol is preferred if patients have delayed graft function and require dialysis as it is mainly protein bound and does not get dialyzed.

Alpha1-Antagonists, centrally acting alpha2 agonists and Vasodilators are usually used as an adjunctive /last-line therapy.

OUR PATIENT

The doppler ultrasound of his allograft showed significantly elevated velocities in the renal artery. He underwent a CO2 renal angiogram which showed transplant renal artery stenosis, which was then successfully stented. In 2 weeks, the creatinine improved to his baseline, his antihypertensives were successfully withdrawn his BP remained within goal.

Renal Artery Angiogram of Allograft kidney

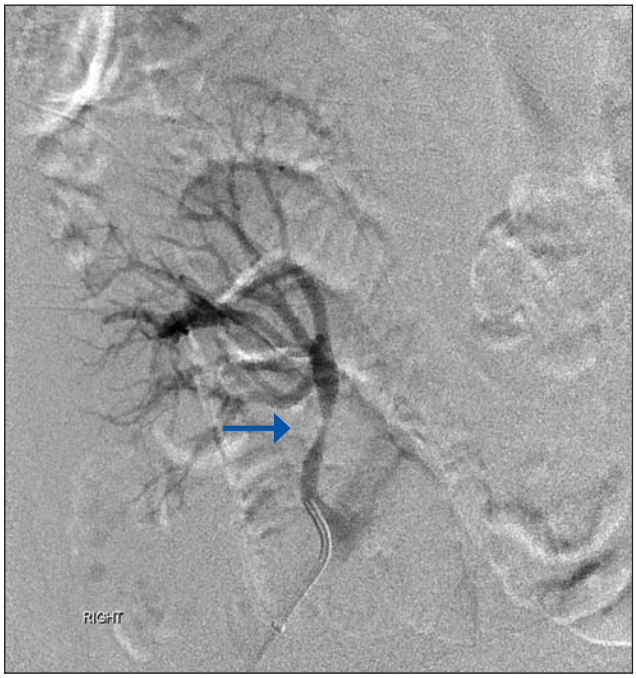

A. Carbon dioxide angiography demonstrating a moderate narrowing

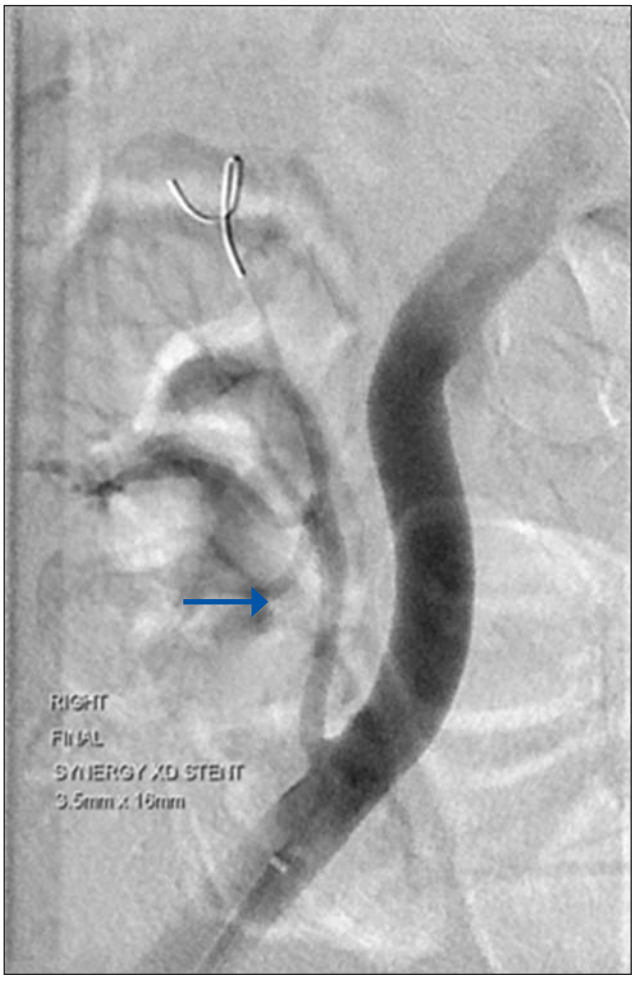

B. Stenosis resolved with drug-eluting stent placement

CONCLUSION

The pathogenesis of hypertension after transplant is multifactorial and CNIs plays an important role. Consider potential drug interactions and side effects when choosing the treatment. TRAS is the most common cause of secondary hypertension in this population.

REFERENCES

1. Whelton PK, Carey RM, Aronow WS, et al. 2017 ACC/AHA/AAPA/ABC/ACPM/AGS/APhA/ASH/ASPC/NMA/PCNA Guideline for the Prevention, Detection, Evaluation, and Management of High Blood Pressure in Adults: A Report of the American College of Cardiology/American Heart Association Task Force on Clinical Practice Guidelines. J Am Coll Cardiol. 2018;71(19):e127-e248.
2. Kasiske BL, Anjum S, Shah R, et al. Hypertension after kidney transplantation. Am J Kidney Dis. 2004;43(6):1071-1081.
3. Hoorn EJ, Walsh SB, McCormick JA, Zietse R, Unwin RJ, Ellison DH. Pathogenesis of calcineurin inhibitor-induced hypertension. J Nephrol. 2012;25(3):269-275.
4. Textor SC, Canzanello VJ, Taler SJ, et al. Cyclosporine-induced hypertension after transplantation. Mayo Clin Proc. 1994;69(12):1182-1193.
5. Weir MR, Burgess ED, Cooper JE, et al. Assessment and management of hypertension in transplant patients. J Am Soc Nephrol. 2015;26(6):1248-1260.
6. Loutradis C, Sarafidis P, Marinaki S, et al. Role of hypertension in kidney transplant recipients. J Hum Hypertens. 2021;35(11):958-969.
7. Tantisattamo E, Molnar MZ, Ho BT, et al. Approach and Management of Hypertension After Kidney Transplantation. Front Med (Lausanne). 2020;7:229.

Table 1. Antihypertensives commonly in Transplant patients

Class of Anti-hypertensive	Examples	Mode of Action	Therapeutic use	Side Effect
Dihydropyri-dine CCBs	Amlodipine Nifedipine	Vasodilation	Counteracts CNI-induced HTN Raynaud's phenomenon, Angina, Migraine	Edema
ACEi	Lisinopril	Iinhibits conversion of Ang I to Ang II	Useful in posttransplant erythrocytosis, proteinuria	Hyperkalemia, AKI, anemia, cough, Angioedema Avoid in pregnancy
ARBs	Losartan	Antagonist for AT1 and AT2 receptors	Treatment of AT1R related AMR, proteinuria	Hyperkalemia, AKI, anemia Avoid in pregnancy
Diuretics Loop	Furosemide, torsemide, Bumetanide	Salt & water excretion Blocks NKCC channel In loop of henle	For treatment of edema and hyperkalemia	Volume depletion, hypokalemia, Hyperuricemia, Hypomagnesemia

Diuretics Thiazides & Thiazide- type	Hydrochlorothiazide chlorthalidone, metolazone	Salt & water excretion Blocks NCC channel in distal convoluted tubule	For treatment of edema Urolithiasis- calcium stones	Volume depletion, hyponatremia, hypomagnesemia, hypercalcemia, hyperuricemia
Potassium-sparing diuretics	Mineralocorticoid receptor blockers- Spironolactone, Eplerenone ENaC blockers- Amiloride, Triamterene	Inhibits aldosterone receptor Inhibits aldosterone-induced sodium resorption	Useful if hyperaldosteronism suspected, if patient has hypokalemia, helps with proteinuria	Hyperkalemia, gynecomastia with spironolactone
β-Blockers	Carvedilol, metoprolol, labetalol	β-1adrenergic receptor antagonist	Angina pectoris, Heart Failure Rate control in Atrial fibrillation, Atrial Flutter, Migraine	Bradycardia, fatigue, hyperkalemia Bronchospasm Depression
α-1Blockers	Doxazosin, Prazosin, terazosin	α-1adrenergic receptors Antagonist	Helps with BPH	Orthostasis
Central α2 agonist	Clonidine	Stimulation of central α2 receptors causing decreased sympathetic flow		Potential rebound HTN Bradycardia
Direct Vasodilators	Hydralazine Minoxidil	Dilates peripheral vessels		Causes salt and water retention- use with diuretic, can cause reflex tachycardia- use with B blocker Hydralazine- Drug induced lupus at high dose Minoxidil - Hirsutism, pericardial effusion

Table 1. Antihypertensives commonly in Transplant patients
Abbreviations: CCB-calcium channel blocker, ACEi angiotensin-converting enzyme inhibitor; ARB, angiotensin receptor blocker; AT- angiotensin, NKCC- sodium potassium 2 chloride channel, NCC- sodium chloride channel, ENaC - epithelial sodium channel, BPH- benign prostatic hyperplasia; HTN- hypertension

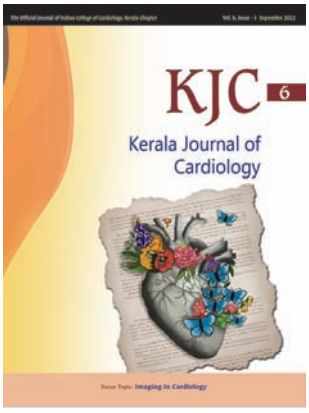

Minimally Invasive Beating Heart Closure of Atrial Septal Defect: *An Improvised Technique Useful in Paediatric Patients*

Sunil Agrawal

Consultant Cardiothoracic & Vascular Surgeon,
Dr K M Cherian Institute of Medical Sciences, Kallissery,
Chengannur, Kerala.

*Sunil Agrawal[1], Saji Phillip[2], Rakhi Kochupurayil Ratnamma[3], Nikhil George[3], Geevarghese Kalayaraezhithu Mathew[1], Ayyappa Das[1], Kotturathu Mamman Cherian[1].

[1]Department of Cardio Thoracic Surgery, [2, 3]Department of Anaesthesiology, K.M.Cherian Institute of Medical Sciences Sciences, Kallissery, Chenganoor, Kerala.

ABSTRACT

Objective: *Atrial septal defects (ASD) are among the third most common types of congenital heart disease (CHD). All those ASDs which are not suitable for device closure need surgical intervention. Currently, minimally invasive approach for ASD closure with smaller incision has been more popular. This approach in paediatric patients is difficult. We modified our technique of ASD closure through anterior mini-thoracotomy under beating heart procedure without cardioplegia and clamping of aorta. This technique provided extra space to work with small incision in paediatric population.*

Methods: *111 patients of ASD with age range of 15 months to 58 years were operated between Jan.2012 to Feb. 2020. 13 patients had sinus venosus type defect (SVC ASD) while 98 patients had secundum type of ASD. We used direct aortic and venous cannulation in paediatric patients through the incision. We did not cross clamp the aorta and all ASD were closed on beating heart. We took appropriate measures to avoid any air embolism. Glutereldehyde treated autologous pericardial patch closure of ASD was done in 104 patients while 7 patients had direct closure of ASD.*

Result: *There was no hospital mortality and air embolism. One patient needed conversion to median sternotomy due to injury of coronary sinus and one patient had minor stroke due to embolism of a piece of muscle after sinus venosus ASD was enlarged. In one patient IVC got routed to LA which was corrected immediately. The mean operating time was 210±36 minutes. Mean ventilation time was 156 ±162 minutes and mean ICU and hospital stay was 24.5±7.2 hours and 3.0±1.4 days respectively.*

Conclusion: *Our result shows that beating heart ASD closure is feasible in paediatric patients with acceptable results. With proper care, the risk of air embolism can be avoided.*

Key words: *Atrial septal defect, Beating heart ASD closure, Minimally invasive technique.*

Abbreviations: *Atrial septal defect (ASD), Congenital heart Disease (CHD), Sinus venosus Atrial septal defect (SVC ASD), Right atrium (RA), Inferior vena cava (IVC), Inter-costal space (ICS), Cardiopulmonary bypass (CPB), Carbon di-oxide (CO2), Left ventricle (LV), Trans-thoracic Echo (TTE), Trans-oesophageal echo (TEE), Sino-atrial node (SA node), Right ventricle (RV), Minimally invasive surgery (MIS), Internal Jugular Vein (IJV).*

Address for correspondence: *Dr. Sunil Agrawal MS, MCh (CVTS), DNB (CVTS), Consultant Cardiothoracic & Vascular Surgeon, Cardiothoracic Surgery Department, Dr K M Cherian Institute of Medical Sciences, Kallissery, Chengannur, Kerala -689124. E-mail: sunilagra@yahoo.com, Phone: +91 9446918250.

INTRODUCTION

Atrial septal defect (ASD) is one of the most common congenital heart diseases accounting for 1 in every 1500 live births.[1] Majority of the secundum ASDs can be closed by trans-catheter technique with nearly 98% success rate and acceptable complications related to this technique.[2] There are still some ASDs which needs to be closed surgically. Earlier median sternotomy approach was considered as a standard approach but in recent past various other approaches have been described.[3-4]

Minimally invasive approach through anterior mini-thoracotomy with 5-6 cm. length of incision has been more popular in recent time. This technique works for adult patients but challenge comes with paediatric populations in whom femoral vessels are not big enough for cannulation. Direct trans-incision aortic and bi-caval cannulation with cardioplegia and aortic cross clamp hardly leaves enough space for the surgeon to operate through small incision.

Aim of Study

ASD closure through minimally invasive approach is being done for more than last 10 years. This study is aimed to report the ASD closure through mini-thoracotomy approach with beating heart in paediatric age group which is being done at our centre since 2012. The primary aim of this study is to look for feasibility of this technique even in smaller paediatric patients. The secondary aim of this technique is to evaluate the safety and outcome of the procedure.

Inclusion Criteria

All cases of Ostium Secundum ASD and Sinus Venosus ASD were included in the study.

Exclusion Criteria

Ostium primum ASD, unroofed coronary sinus ASDs, presence of left superior vena cava , unusual drainage of partial anomalous pulmonary venous blood except in right SVC and ASDs with other associated defects were excluded for this approach. Patients with history of prior cardiac surgery or surgery on right side of chest were also excluded from the study.

Material and Methods

Between January 2012 and February 2020 we operated 111 patients with age range of 15 months to 58 years and weight range between 7-74kg. at our centre. There were 43 male and 68 female patients. Out of 111 patients 104 patients were operated through anterior mini- thoracotomy incision and 7 patients were operated through vertical incision along anterior axillary line. 98 patients had ostium secundum defect and 13 patients had sinus venosus defect **[Table-1]**. The project was approved by hospital ethics committee for performing the procedure and study. Informed consent was obtained from all patients.

Table 1: Baseline Characteristics of Patients (111 patients)

Age in years	(Range 1.4 - 58)
(a) < 12	78
(b) 12-18	7
(c) >18	26
Gender (M: F)	44:67
Weight (Kg)	7-74
BMI	16.2 ± 4.2 (Range 9.9 - 30.4)
ASD Type:	
Secundum	98
Sinus Venosus	13

All cases were diagnosed by trans-thoracic echo (TTE) with standard views by our paediatric cardiologist. Trans-oesophageal echo (TEE) was done among patients with SVC defect in whom ASD was not very well visualised in TTE. As per our hospital protocol all SVC ASD patients underwent CT angiogram to evaluate the anatomy and site of drainage of right anomalous pulmonary vein into SVC. This was done for the feasibility of procedure in these patients

Surgical Technique

Patients were operated under general anaesthesia with 20-30-degree elevation of right chest using a rolled pad under the chest. The right arm was extended for 45 degree away from the chest for easy access to the side of the right chest. About 5-7 cm long incision was made in the anterior chest wall with 3/4th of the incision lateral to the nipple. The incision was made in 6th intercostal space in female children to avoid interfering with the breast development. In all male patients incision was made directly over the 4th inter-costal space just under the nipple. Chest was entered through 3rdintercostal space (ICS). Pericardium was incised vertically about 1.5cm away from the right phrenic nerve and depending upon the size of ASD a piece of pericardium was harvested and treated with 0.6% glutereldehyde solution for 8 minutes to be used later for ASD closure. Extra amount of pericardium was removed for all SVC ASDs

to enlarge the superior vena cava (SVC) and SVC-RA junction by a separate pericardial patch.

Lower half of SVC was dissected out to pass a double loop of no.2 silk ligature for snaring. Aorta was cannulated just above the mid part of ascending aorta. SVC was cannulated about 1cm above the SVC-RA junction in all secundum ASD or as high as possible in SVC (almost at the junction of two innominate veins) for all SVC ASDs. IVC was cannulated using angled cannula on partial CPB. SVC and IVC were snared before opening the RA. Patient's head was lowered with continuous monitoring of LA and LV by TEE. We insufflate the pericardial cavity with Carbon di-oxide (CO2)(1litre/min) prior to opening of RA. A mean perfusion pressure of around 60-70 mm Hg was maintained throughout to keep the aortic valve closed. RA was opened in the mid part by vertical incision. Extreme care was taken to keep the LA filled with blood all the time and when needed cardiotomy sucker was placed close to coronary sinus opening to get easy visibility of ASD margin. If inferior rim was deficient we took the bite from the floor of left atrium. During this process of ASD closure anaesthesiologist has to keep an eye on LA and LV through TEE for any air entering into it due to manipulation of ASD edge during the suturing process. RA was closed using 6/0 polypropylene. During the whole process of repair, normothermia was maintained. For secundum ASDs we did not place epicardial pacing wire routinely. Right ventricular (RV) Pacing wire was placed routinely in all sinus venosus ASDs. Only a single right pleural drain was used in all patients.

Statistical Analysis

The data obtained from the records were entered into a computerised excel data sheet. The data was analysed using SPSS Statistics for windows, Version 20.0. The distribution of data related to clinical conditions and complications are mentioned as frequency. Data related to operative and post-operative results are mentioned as mean with standard deviation.

RESULT

All patients selected for the procedure were operated through mini-thoracotomy incision. Out of 111patients 104 patients were operated with anterior mini-thoracotomy and 7 patients were operated with vertical mini thoracotomy incision along anterior axillary line. 104 patients had glutereldehyde treated autologous pericardial patch closure of ASD. Direct closure of ASD was done in 7 patients. The mean operating time was 210 ± 36 minutes. The median CPB time was 55 minutes with CPB time ranging between 28-166 minutes. Most of the patients got extubated within 2-4 hours (156±162minutes). None of them needed any inotropic support. Postoperative drainage was 50±35 ml and only 13 patients needed blood for priming of CPB circuit mainly due to low body weight or low preoperative haemoglobin. Median ICU stay was one day and median hospital stay 3 days. Routine analgesic was used for two days only and all patients returned to normal life in 2-3 weeks (Table-2).

There was no postoperative mortality. In our study only one patient needed conversion to median sternotomy due to coronary sinus injury. In this patient ASD was very close to coronary sinus and he also had large left SVC which was missed in our preoperative echo assessment. It was not possible to cannulate the left SVC through the mini-thoracotomy incision. The left SVC drainage was being managed by keeping the cardiotomy sucker into the coronary sinus. The posterior wall of coronary sinus got sucked into the cardiotomy sucker which was not realised and manipulation of cardiotomy sucker led to the injury of posterior wall about 2cm away from the orifice. The bleeding site was inaccessible through the thoracotomy incision and we had to convert it into median sternotomy to get the bleeding under control. Repair of coronary sinus led into intractable arrhythmia in the postoperative period for 4 days before it got controlled with amiodarone infusion. One child had minor stroke which recovered slowly over a period of 6 months. In this patient ASD was SVC type and small in size. It was enlarged and we feel that probably a tiny piece of muscle got embolized during the enlargement process leading to minor stroke. In one patient IVC got routed to LA which was recognised due to low oxygen saturation and on TEE after completion of patch closure. It was corrected immediately. It happened due to absent IVC rim and large Eustachian valve which was missed as IVC rim. No patient needed permanent pace maker after the surgery.

Follow-up of these patients was on 1st week, 1 month and 6months after surgery and thereafter every 2 years. Post-discharge echo was done on first visit to assess the repair and to rule out any pericardial or pleural collection. 2nd echo was repeated at 6 months and thereafter every two years. No residual or recurrence of ASD was found in any patient in follow-up echo.

DISCUSSION

ASD is one of the most common congenital heart diseases with female preponderance in 2:1 ratio.[5] So for median sternotomy with aortic cross clamping with antegrade cardioplegia has been the standard surgical treatment. Due to cosmetic reasons alternate approaches have been used to avoid the median sternotomy scar.[3-4] Minimally invasive approaches have been known

to provide better cosmetic effect, less post-operative pain, less ICU and hospital stay and faster return to normal life and activity. Among all the described approaches anterior mini thoracotomy has been more popular approach for ASD closure. Among most of the adolescent and adult patients it is easy to cannulate femoral vessels along with percutaneous cannulation of RIJV to get enough working space but challenge comes in paediatric population where femoral vessels are not adequate enough to permit femoral cannulation without compromising the lumen.

We tried to overcome this difficulty by modifying our technique and performing the surgery on beating heart without cardioplegia and aortic cross clamping. Avoidance of aortic cross clamp and cardioplegia needle provides additional working space while keeping the length of incision small. However there is theoretical risk of air embolism as heart is beating and aorta is not clamped. To avoid this complication we took certain measures. We routinely insufflate the pericardial cavity with CO2 with 1 litre/min. It has certain advantages. CO2 replaces the air in the pericardial cavity, and being more soluble in blood it reduces the risk of air embolism[6] and reduces de-airing time. We also lower the head end of the operating table and keep the mean perfusion pressure no less than 60mm Hg. Precaution was taken to keep the left atrium filled with blood during ASD closure and anaesthesiologist constantly watch LA, LV and aorta through TEE for any air bubbles. We believe that even though left side of the heart is filled with blood and LV is contracting, it does not generate enough pressure to open the aortic valve to eject the blood into the aorta which is supported by high perfusion pressure. Mo et al in their study mentioned that high arterial pressure prevents the air from LV to enter into the aorta[7]. Our effort during the surgery is to get only that part of the ASD margin into view from where we have to take the next bite. We avoided active suction of blood in RA. As majority (104 patients) patients had pericardial patch closure of ASD we had a median CPB time of 55 minutes.

Reason for patch closure was, because we operated only those ASDs which were not suitable for device closure due to large size or inadequate rims. Special precaution was taken when IVC rim of ASD was either very small or absent. In these cases we took the bite from the floor of LA to avoid IVC drainage getting routed into LA. While operating on beating heart it is easy to recognise any rhythm disturbance and is very useful in SVC type defect due to the proximity of SA node. Due to this we did not come across any rhythm issues except in one case where we had injury to coronary sinus and arrhythmia after its repair.

Cremer et al in their study described three different minimally invasive techniques without aortic cross clamping and they observed that small anterior mini-thoracotomy incision is most preferred technique.[4] His all patients were adult with mean age of 35±11 years. We used mini vertical incision in 7 paediatric patients which were made along anterior axillary line. These 7 children had secundum ASD. There was no problem in access to aorta and vena cavae through this incision. We abandoned this incision due to significant hypertrophy of scar in 2 patients. This was considered due to the incision crossing the natural line of Langer.

Dang et al[9] in their study of totally endoscopic ASD closure on beating heart concluded that beating heart ASD closure can be safely performed. Mean age of their patients were 21.1 ± 13.9 years with range between 3–58 years and their minimum weight patient was 13.5kg. The mean operating time in first 15 patients was 279.3 ± 41.1 (210–350) and in next 10 patient was 225 ± 18.7 (200–250) with CPB time of 163.7 ± 32.4 (115–220) and 125 ± 24.9 (100–166) respectively. Xiao et al[6] in their study of Robotically assisted ASD closure in 160 patients over a period of 7 years concluded that arrested or beating heart ASD closure can be safely and effectively performed. Their mean operating and CPB time was 254 ± 57.1 and 61 ± 17.0 minutes respectively. Their smallest patient was 11 years old. Thapmongkol S. el al[10] in their study of ASD closure on beating heart through median sternotomy incision expressed that it is a safe procedure and their results were not different than the conventional technique. Our beating heart technique helped us to extend this procedure among paediatric population through mini-thoracotomy incision where we don't have the advantage of femoral cannulation. Due to absence of aortic cross clamp and cardioplegia needle we had the advantage of cannulation of aorta in the mid part. Direct aortic and venous cannulation through the incision also avoided any additional scar on the chest wall. Multiple entry scars in thoracoscopic or Robotic assisted surgery is not as cosmetic as a single small scar. We also have the advantage of short operating time (210±36 minutes) and CPB time (60.2±22.4 minutes) as compared to the totally thoracoscopic or robotically assisted ASD closure.

Cosmetically mini-thoracotomy scar was well accepted by patients. We did not observe a gross disparity in breast size among female patients. Some children did show the tendency of scar getting hypertrophied but it regressed over the period of time. We observed that the length of scar was nearly 5-10 mm longer in female children than male patients because we had to make the incision at a lower level to avoid any breast deformity and then we had to dissect up to the 3rd intercostal space. Among male patients we made the incision just under the nipple

and could manage to make small incision. Invariably in all children 3rd ICS was corresponding to the mid part of RA. It was important as entering the chest either a space below or above was making the access of either SVC or IVC difficult. In children we did not require long instruments.

Most of the complications **[Table-2]** happened in the beginning of the study. They were all avoidable complications. Each procedure has its own learning curve. As we gained experience we got more aware and careful. Even the operating time was longer in first two years. In last 6 years we have not come across any complications. We found the procedure to be safe and reproducible. This technique is especially useful in paediatric patients as minimally invasive ASD closure on beating heart could make it possible to make small incision which is difficult with cardioplegia and aortic cross clamp where incision is invariably long. A proper team work, preoperative work up, surgical planning and co-ordination is mandatory to achieve a good and safe repair.

Table 2: Operative and Postoperative results

	Mean ± SD	Range
Mean Operating Time (Minutes)	210±36	120-300
CPB Time (Minutes)	60.2±22.4	28-166
Patch Closure	104	
Direct Closure	07	
Blood Transfusion (ml)	14.0 ± 28.8	0-100
Drainage (ml)	46.8 ± 21.7	20-125
Post-op. Ventilation time (Minutes)	156±162	36-1152
ICU stay (Hours)	24.5 ± 7.2	10-74
Hospital Stay (Days)	3.0 ±1.4	2-15
Mortality	Nil	
Conversion to sternotomy	01	
Patch revision	01	
Post-operative arrhythmia	01	
Minor stroke	01	
Injury to coronary Sinus	01	
Wound infection	Nil	

Conclusion: Minimally invasive beating heart ASD closure is a safe and effective procedure without any additional cost and can be easily performed in children. Beating heart technique can be used even in selected cases of SVC type ASDs. The risk of air embolism can be avoided completely by taking appropriate measures. Cosmetically females are more benefitted with this modified technique.

Limitations of the Study

This is single centre nonrandomized study and could have the selection bias. Also sample size is small. A randomized multi-centre study with larger sample size is needed to prove the importance of the technique. A comparison with conventional approach will also help to prove or disprove the superiority of this technique.

Acknowledgements

Authors are thankful to Mr. Rajeev, the physician assistant and secretary Mrs. Jisha Santhosh for their help in collecting the data and preparation of the manuscript.

Compliance with ethical standards

Conflict of interest: All authors declare that there is no conflict of interests.

Ethical approval: The procedure performed in this study involving human participants were in accordance with the ethical standard of the institution and/or national research committee and with the 1964 Helsinki declaration and its later amendments or comparable ethical standards.

Informed Consent: Informed consent was obtained from all the patients after explaining the procedure in detail. Among the paediatric cases consent was obtained from the parents.

Funding: No special funding was required for the study.

Author's contribution: All authors listed meet the authorship criteria according to the latest guidelines of the international committee of medical journal editors and all authors are in agreement with the manuscript. All authors of this manuscript have participated in the planning, execution and analysis of this study.

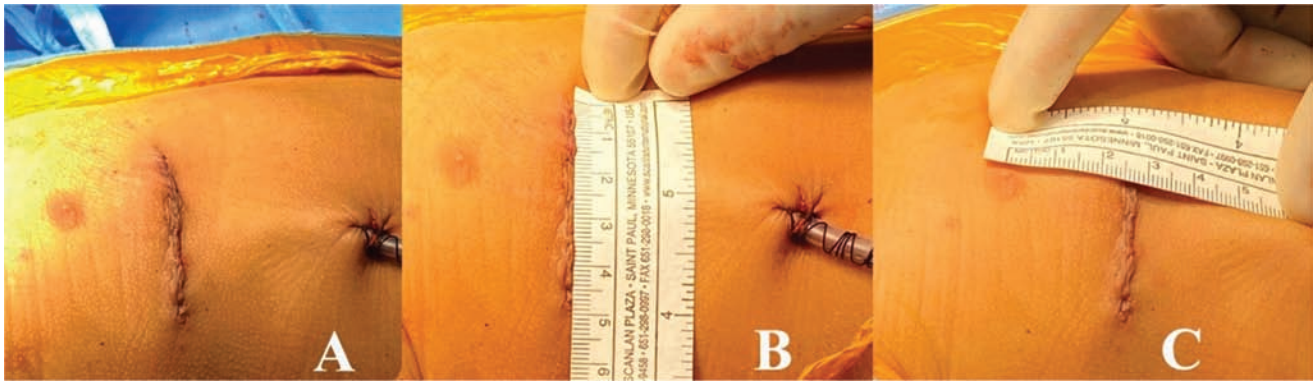

Figure 1 A-C: Intra operative incision scar measuring 4.8cm transversally and 2.2cm verically from the areola and 2.7mm from the nipple in an 18-months old female child diagnosed with large high type secundum ASD measured 18 x 22mm with tiny SVC rim.

REFERENCES

1. Kaplan S. Congenital heart disease in adolescents and adults. Natural and postoperative history across age groups. Cardiol. Clin. 1993;11: 543-56.
2. Yang MC, Wu JR. Recent review of transcatheter closure of atrial septal defects. Kaohsiung Journal of Medical Sciences 2018;34: 363-369.
3. Rosengart TK, Stark JF. Repair of atrial septal defect through a right thoracotomy. Ann. Thorac. Surg. 1993;55:1138-40.
4. Jochen T. Cremer, Andreas Boning, Marcel B, Anssar, Peter Y, Kim Klaus Pethig, Wolfgang Harrnger& Axel Haverich. Different approaches for minimally invasive closure of atrial septal defects. Ann. Thorasc. Surg. 1999;67:1648-52.
5. Van der Linde D, Konings EE, Slager MA, Witsenburg M, Helbing WA, Takkenberg JJM and Roos-Hesselink JW. Birth prevalence of congenital heart disease worldwide: a systematic review and meta analysis. J Am. Coll. Cardiol. 2011;58:2241-47.
6. Xiao C, Gao C, Yang M, Wang G, Wu Y, Wang J, Wang R, Yao M. Totally robotic atrial septal defect closure: 7 years single- institution experience and follow-up. Interact Cardiovasc Thorasc Surg. 2014;19:933-37.
7. Mo A, Lin H, WenZ, LuW, Long X, Zhou Y. Efficacy and safety of on–pump beating heart surgery. Ann. Thorac. Surg. 2008;86:1914-18.
8. Liu YL, Zhang HJ, Sun HS, Li SJ, Su JW, Yu CT. Correction of cardiac defects through a right thoracotomy in children. J Thorac Cardiovasc Surg. 1998;116:359–361
9. Dang QH, Le NT, Nguyen CH, Tran DD, Nguyen DH, Nguyen TH and Ngo TH. Totally endoscopic cardiac surgery for atrial septal defect repair on beating heart without robotic assistance in 25 patients. Innovations (Phila). 2017;12(6): 446-52.
10. Thapmongkol S, Sayasathid J, Methrujpanont J, Namchaisiri J. Beating heart as an alternative for closure of secundum atrial septal defect. Asian Cardiovasc Thorac Ann. 2012; 20:141-145.

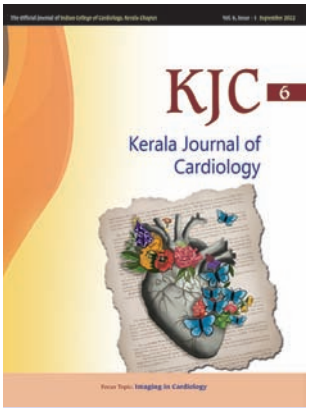

Zero Contrast Left Main Bifurcation Percutaneous Coronary Intervention *– It Always Seems Impossible Until It's Done*

*Prathap Kumar N., Blessvin Jino, Manu Rajendran

*Chairman and Managing Director, Consultant Cardiologists
Meditrina Hospital, Kollam, Kerala.



INTRODUCTION

Contrast induced acute kidney injury (CI-AKI) is a serious complication of percutaneous coronary intervention (PCI) and it is often underdiagnosed. KDIGO defines it as an increase in serum creatinine by ≥ 0.3mgs% within 48 hours of contrast administration or ≥ 50% increase within 7 days[1]. The incidence of CI-AKI ranges between 3-20%[2] and it is associated with increased short-term and long-term mortality. Important risk factors include cardiogenic shock, STEMI, advanced age, pre-existing renal dysfunction and diabetes mellitus. Adequate pre-procedural hydration, administration of statins and reduction in contrast volume are the predominant strategies to prevent CI-AKI following PCI. The MOZART trial showed that the IVUS guidance in PCI decreases the contrast volume requirement during PCI. Moreover, recent studies have shown that ultra-low contrast (Contrast volume < eGFR) reduces the CI-AKI risk. Zero-contrast PCI is a novel method that requires extremely skilled PCI operators and meticulous analysis of intra-coronary imaging for its successful clinical application and it is a high potential strategy to prevent CI-AKI and to improve survival after PCI.

CASE REPORT

A 59-year-old male, with a long-standing history of hypertension, diabetes mellitus and dyslipidemia, was admitted in our hospital with rest angina for 3 days. His serum troponin level was elevated and the serum creatinine and eGFR were 1.3mgs% and 56.5ml/min/1.73m^2 respectively. His coronary angiogram showed significant LMCA stenosis with 3-vessel disease and the SYNTAX score was 24. Since the patient was not willing to go for CABG, staged PCI was planned. Initially, PCI to RCA was done with 2 DES. Post procedure, the serum creatinine increased to 2.8mgs% and he was managed conservatively for CI-AKI. He recovered from the renal injury over a period of 2 weeks and the serum creatinine level came down to 1.6 mgs%. In view of this CI-AKI, further PCI to left system was planned as IVUS guided zero-contrast procedure. Furthermore, the LMCA bifurcation had medina (1,1,1) lesion (**Figure 1**) and hence an upfront 2-stent strategy with DK-crush technique was planned for LMCA bifurcation. Through right femoral artery access, a 7F EBU 3.5 guiding catheter was used to engage LMCA. Then, keeping the previous angiogram as a roadmap, both LAD and LCX

Address for correspondence: Prathap Kumar N. MD, DM, FIC, Chairman and Managing Director, Senior Consultant Cardiologist and Head, Meditrina Hospital, Kollam, Kerala. Email: prathapndr@gmail.com

Figure 1: Procedural steps of zero-contrast LMCA bifurcation PCI

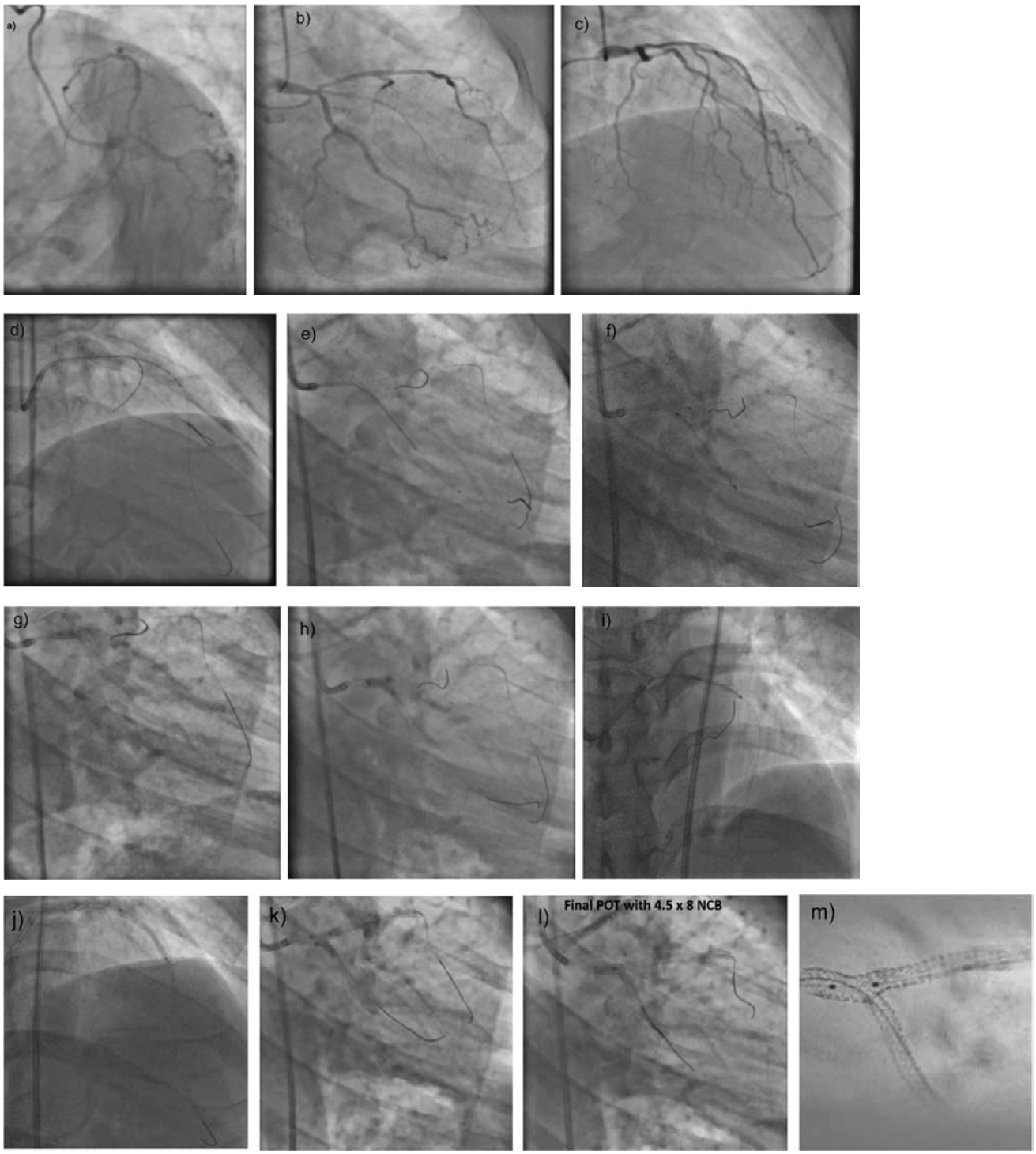

Figure 1: Procedural steps of zero-contrast LMCA bifurcation PCI. **a,b,c**): Angiographic images show significant LMCA bifurcation lesion with medina (1,1,1). **d)** Both LAD & LCX were wired and a marker wire was kept in septal artery. IVUS run from LAD-LMCA was done. **e**) IVUS run from OM-LMCA was done. **f**) LCX-OM stenting was done with 3x33mm DES. A 3.5 x 12mm NC balloon was kept in LAD for crush. **g**) 4 x 8mm NC balloon was used for repeat crushing. **h**) First kissing balloon inflation was done with 3.5 x 12mm & 3.5 x 8mm NC balloons. **i**) A floating wire was kept in left aortic sinus as a marker for LMCA ostium. A 3.5 x 38mm DES was deployed from LMCA ostium to septal marker wire. **j**) Mid LAD was stented with 3 x 28mm DES overlapping the first stent. **k**) Second kissing balloon inflation was done with 4 x 8mm & 3.5 x 8mm NC balloons. **l**) Final POT was done with 4.5 x 8mm NC balloon. **m**) 'Clear stent' image of LMCA bifurcation stenting.

were wired with the Fielder-FC guidewires in the same angiographic projections. Another Fielder-FC wire was parked in a septal artery as a marker wire. Then IVUS runs were done from LAD-LMCA and major OM-LMCA and the parameters are given below (**Table 1 & Figure 2**).

Table 1: IVUS analysis before stenting:

LMCA diameter	4.6mm
Proximal LAD diameter	3.6mm
Distal reference segment diameter at LAD	3.1mm
Distal reference segment diameter at major OM	3.1mm
Distal LMCA luminal area	3.18mm^2
Ostial LAD luminal area	3.27mm^2
Ostial LCX luminal area	2.6mm^2
Length between ostial LMCA to septal marker wire	36mm
Length between septal marker wire to distal LAD reference segment	25.6mm
Length between ostial LCX and Distal OM reference segment	30.1mm

IVUS runs confirmed the luminal position of both LAD and LCX guidewires. Then the LAD lesion was pre-dilated with a 2.5x12mm NC balloon and a 3x6mm cutting balloon was used at the ostial LAD and distal LMCA. Similarly, the LCX lesion was pre-dilated with 2x9mm NC balloon and 3x6mm cutting balloon was

Figure 2: IVUS analysis before stenting

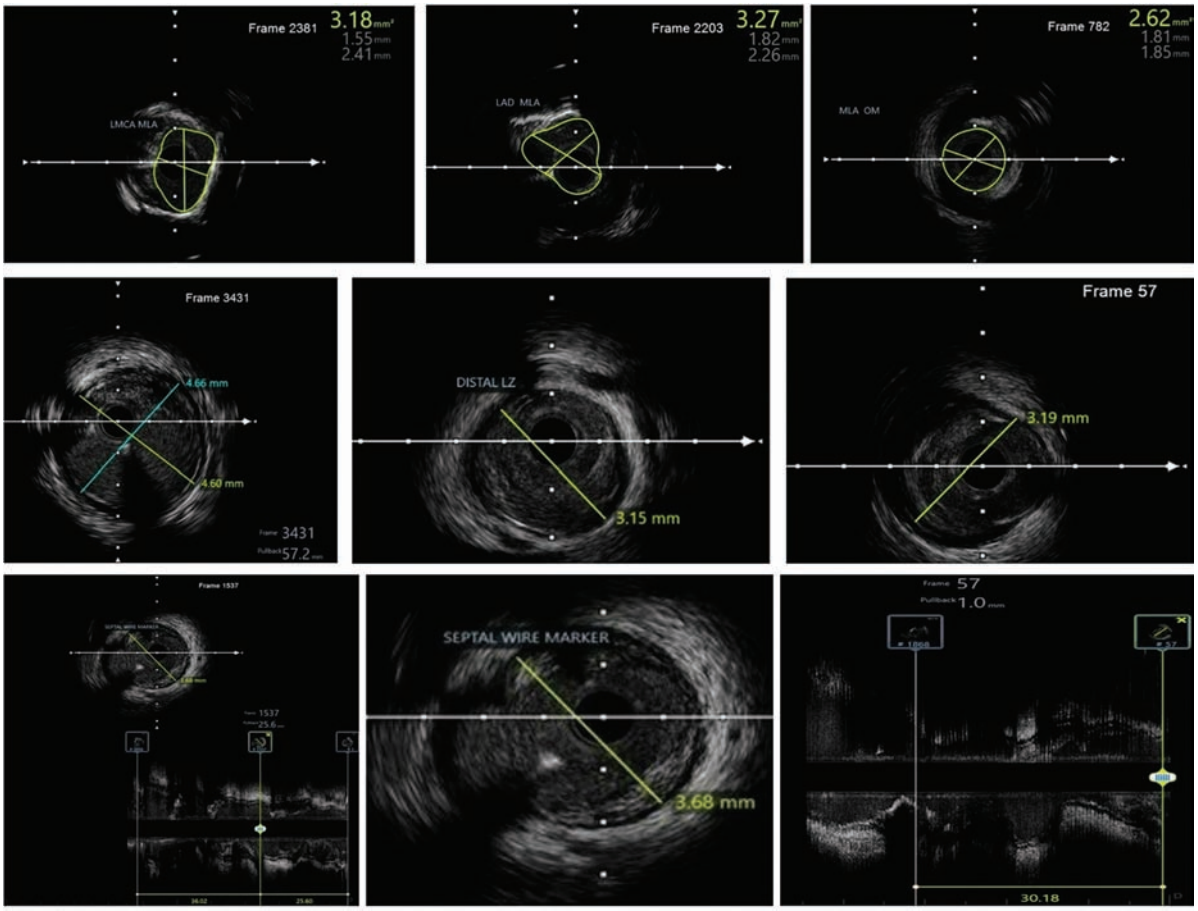

Figure 2: IVUS analysis before stenting:

Top row shows MLA at distal LMCA, LAD and OM as 3.18mm^2, 3.27mm^2 and 2.62mm^2 respectively.

Middle row shows vessel diameters at LMCA, distal LAD and OM as 4.6mm, 3.1mm and 3.19mm respectively.

Bottom row shows length measurements in LAD and OM. **Bottom left** image shows the length from LMCA ostium to septal marker wire as 36mm and septal marker wire to distal landing zone as 26.5mm. Similarly, **bottom right** image shows the length from ostial LCX to distal landing zone at OM as 30.1mm.

used at the ostial LCX. Then a 3x33mm DES was deployed at LCX-OM keeping the LAD wire as a marker to locate LCX ostium. The LCX stent was crushed using 3.5x12mm & 4x 8mm NC balloons and it was recrossed with Fielder-FC wire. First kissing balloon inflation was done using 3.5x12mm & 3.5x8mm NC balloons. Then the LCX wire was removed and it was kept in the left aortic sinus as a marker for the LMCA ostium. Then a 3.5x 38mm DES was deployed from the ostial LMCA-LAD, till the septal marker wire. After LMCA POT with a 4.5x8mm NC balloon, a 3x28mm DES was deployed from the distal end of the LMCA-proximal LAD stent with a 2mm overlap. LCX was recrossed again and the second kissing balloon inflation was done using 4x8mm & 3.5x8mm NC balloons. The final POT was done using a 4.5x8mm NC balloon. Then IVUS runs were done from LAD-LMCA and OM-LMCA and the parameters are given below (**Table 2 & Figure 3**). IVUS showed adequate stent expansion without edge dissection or malapposition. The entire procedure was done without contrast usage and the guide catheter was flushed with saline intermittently to avoid thrombus formation. Hydration with normal saline was started 6 hours prior to the procedure at the rate of 1.5ml/kg/hr and it was continued till 12 hours after the procedure. After the procedure, serial echocardiogram was done to rule out pericardial effusion and there was no significant rise in serum creatinine level. On 3 months follow-up, the patient remains symptom free.

Table 2: IVUS analysis after stenting:

Mid LAD MSA	5.25mm^2
Proximal LAD MSA	7.69mm^2
Distal LMCA stent area	11.02mm^2
Proximal LMCA stent area	11.53mm^2
LCX MSA	5.71 mm^2

Figure 3: IVUS images after stenting

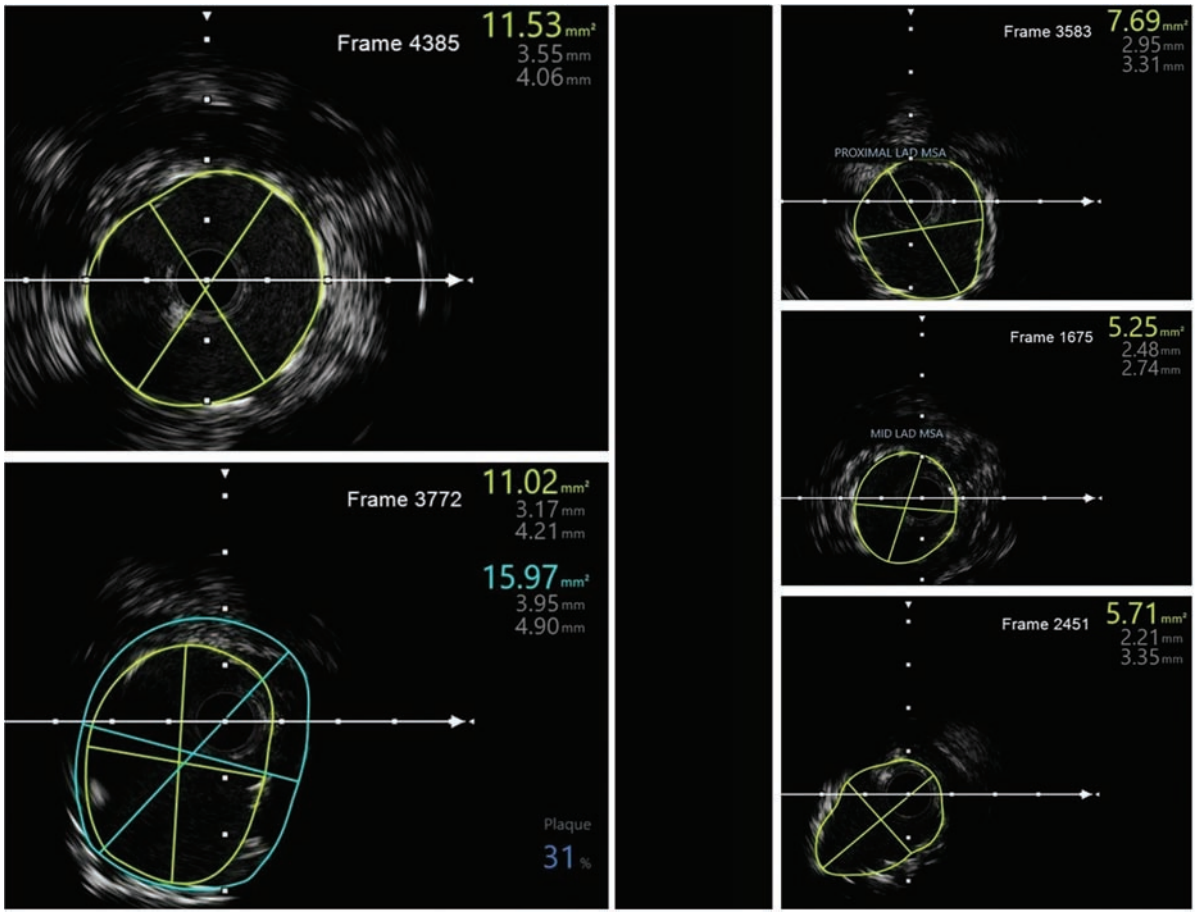

Figure 3: IVUS images after stenting: **Left upper and lower images** show MSA at proximal and distal LMCA as 11.53mm^2 and 11.02mm^2 respectively. **Right panel** shows MSA at proximal LAD, mid LAD and OM as 7.69mm^2, 5.25mm^2 and 5.71mm^2 respectively.

DISCUSSION

IVUS guided Zero-contrast PCI is feasible and safe in most of the patients who are at high risk of CI-AKI and studies have shown that even complex cases can be done without complications[3]. Hydration with normal saline should be started at least 3 hours before the onset of the procedure in elective procedures and it should be continued for the next 12 hours. In emergency procedures, hydration may be started as soon as possible according to the hemodynamic status of the patient. Some studies advocate hydration based on the hemodynamic condition of the patient, to avoid fluid overload and LVEDP or central venous pressure-based fluid administration are the commonly used methods. Statins should be continued in all cases and nephrotoxic medications like NSAIDs should be discontinued before the procedure. Though an immediate PCI after the coronary angiogram is safe in zero-contrast PCI, it should be performed in a staged manner after the initial angiogram in stable cases. The femoral arterial approach allows us to use larger guiding catheters with better support for complex PCI, though the radial approach is also feasible in most cases. After guiding catheter engagement, a metallic silhouette of the vessel is created using multiple wires as markers for side branches and the ostium of the main vessel. LCX wire acts as a marker to locate LAD ostium and LAD wire acts as a marker to locate LCX ostium. The LMCA ostium is located by a floating wire in the aortic sinus. It is important to note that the guidewire insertions should be done in the same fluoroscopic projections as that of the previous angiogram and the IVUS run confirms the luminal position of the guidewires. After metallic silhouette creation, an IVUS run is done to select the appropriate strategy for lesion preparation, to select the stent size and to identify the landing zones. Proximal and distal landing zones are identified fluoroscopically by their distances from the nearest marker wires and these distances are measured during analysis of the initial IVUS run. After stenting, an IVUS run is done again to identify the complications and for stent optimisation. During the procedure, strict monitoring of patient's symptoms, ECG changes and echocardiogram is required. If complications are suspected, check angiogram using minimal contrast should be taken immediately to avoid serious consequences. After procedure, serial echocardiographic monitoring is essential to rule out pericardial effusion. Operator experience in understanding the coronary anatomy, tactile feedback of guidewires and IVUS interpretation are essential for the successful completion of this procedure.

REFERENCES

1. Kidney Disease: Improving Global Outcomes (KDIGO) Acute Kidney Injury Work Group. KDIGO clinical practice guideline for acute kidney injury, Kidney Int. Suppl. 2 (2012) 1–138.
2. Bugani G, Ponticelli F, Giannini F, Gallo F, Gaudenzi E, Laricchia A, Fisicaro A, Cimaglia P, Mangieri A, Gardi I, Colombo A. Practical guide to prevention of contrast-induced acute kidney injury after percutaneous coronary intervention. Catheter Cardiovasc Interv. 2021 Feb 15;97(3):443-450.
3. Kumar P, Jino B, Roy S, Shafeeq A, Rajendran M. Absolute zero-contrast percutaneous coronary intervention under intravascular ultrasound guidance in chronic kidney disease patients - From despair to hope? Int J Cardiol Heart Vasc. 2022 May 16;40:101052.

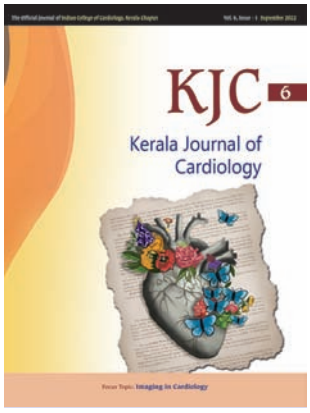

Survival Analysis

V. Raman Kutty

Research Director, Amala Cancer Research Centre, Thrissur, Kerala.

Former Professor,
Achutha Menon Centre for Health Science Studies, SCTIMST, Thiruvananthapuram.

In many clinical situations, a group of patients with similar clinical features and the same diagnosis are followed up for some time. The objective of this exercise is often to see the frequency of occurrence of an event- a complication, recovery, worsening of disease, or very often, death. The occurrence of this signal event gives us an idea about the progression of the disease, and whether our treatment has made any difference.

However, this is not as straightforward as it sounds. If we recruit every patient on the same day, it is easy to see how long it takes before the event of interest happens. This is like starting a marathon: everybody lines up on the same line and starts at the same time. We can easily identify how far a person has run, before dropping out.

But patients who we need to follow up may come at various points in time, sometimes even spread out over months or years. We cannot get very far if we design a study where we recruit only people who reported on the same day- our sample would be very small indeed. So, the recruitment takes place over a long time. At any point in the future, when we decide to stop the study, we may have people who have been followed up for varying lengths of time- one month, eight months, two years etc. It is impossible to conclude that a person who had a six-month event-free survival is like another with an event-free survival of two years. To complicate matters further, some people never develop the event at all during the period of our surveillance: can we conclude from this that they will never develop the event in their lifetime?

The statistical answer to this is to look at the 'median' period of event-free survival: the period by which 50% of the group has developed the event. It gives us an idea of what to expect in the group. We use a statistical approach called 'Survival Analysis' to look at this.

Address for correspondence: Dr. V. Raman Kutty, MD, M Phil, MPH (Harvard), L 51, LIC Lane, Pattom, Thiruvananthapuram-695004, Kerala, India.
Phone: +919847060199, E-mail: kuttyr@gmail.com

Survival curve of colon cancer- grouped by AJCC (American Joint Committee on Cancer) **criteria**

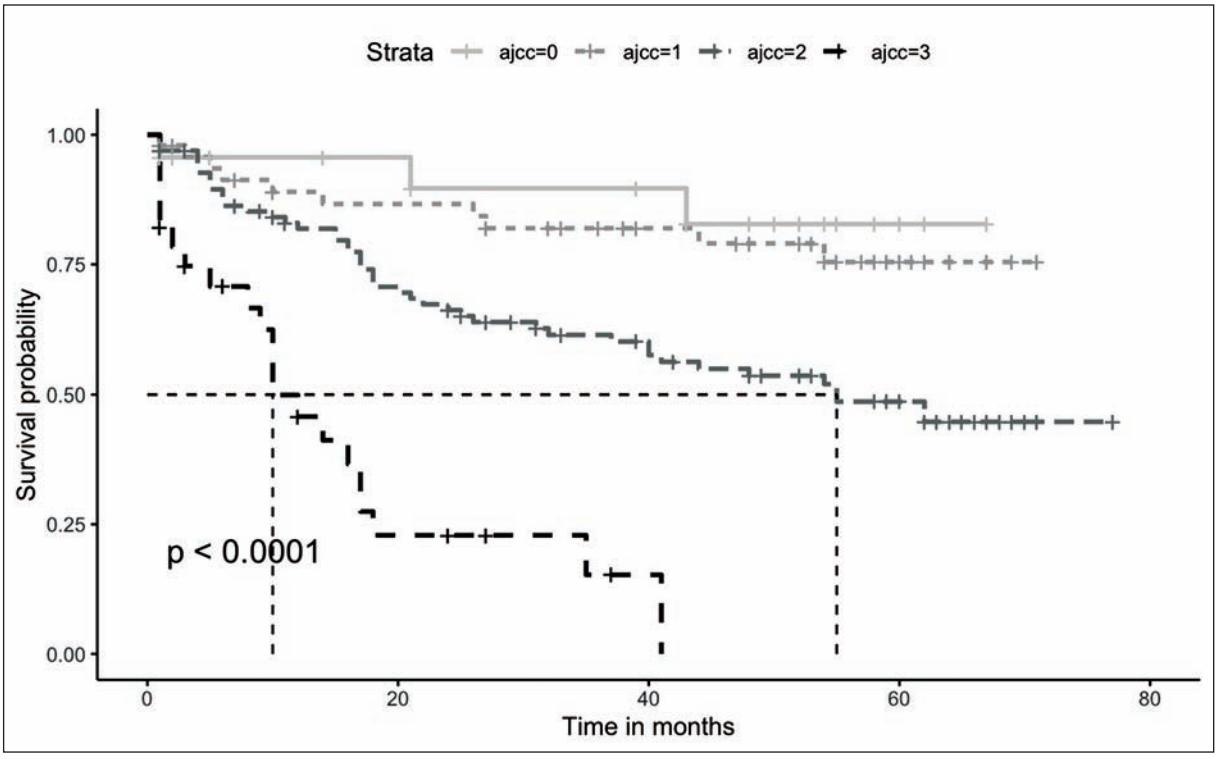

The survival plots show four groups by AJCC criteria. Two of the groups- 1 & 2- clearly show better survival, and many patients survive the observation period of around 80 months. Groups 2 & 3 clearly show poor survival, with median survival in group 2 hardly greater than 10 months. Overall, median survival is different in the four groups, as indicated by the p value for the Log-Rank test.

(*Data by kind courtesy of Dr Sunu Cyriac, Department of Oncology, Amala Institute of Medical Sciences, Thrissur.*)

DOI: 10.1001/virtualmentor.2013.15.1.mnar1-1301.

In the commonly used format, we plot event free survival against time in the group. This means that we have a graph with time on the X- axis, and the probability of event-free survival on the Y-axis. ('Probability of event-free survival' is just a fancy name for the proportion of the patients who have not developed the event yet). 'Zero' time, or the starting point of the X-axis, corresponds to 1 (or 100%) on the Y-axis, as the event has not occurred in anyone yet. At points in time when events happen, the probability dips sharply down, indicating that the event has already happened in some subjects and can only happen to the rest. If we join such points, we get a 'step' like graph which starts parallel to the X-axis from the zero point and drops down every time events happen. If the event happens to everyone in the group during the period of observation, the graph dips down to zero; if there are subjects in the group in whom the event has not happened even at the last point of observation, the line remains horizontal at that point. The information on the people in whom the event has not occurred during the period of observation is said to be 'right-censored', as it is incomplete.

FINDING THE MEDIAN

Now that we have the graph, it is easy to find the median survival. We draw a horizontal line parallel to the X-axis from the point in the Y-axis indicating 0.5 (or 50%); where this line meets the survival line, we drop a vertical line to the X-axis. The point where it crosses the X-axis will indicate the median period of survival.

One thing may be pertinent to point out here: the median survival indicates the time point at which 50% can be expected to have the event. This may be very asymmetrical: if 50% of the group develops the event in two years, it does not mean that the other 50% will develop the event in the next two years. It may take a much longer time, usually, for everyone to develop the event. This is a point that is easily overlooked, sometimes leading to tragic miscommunication between patient and doctor. (This has been beautifully illustrated in the essay 'The median isn't the message' by Stephen Jay Gould, eminent paleontologist. Gould was diagnosed with a form of cancer around the age of 40 and found

out that the median survival was only eight months. He took this to mean that he would die in that time. However, he survived to the age of sixty! In the essay, he writes about how he understood the meaning of the statistical term the hard way)*

COMPARING GROUPS

The approach of survival analysis can be extended to compare two or more groups. If we want to ask the question, 'is event-free survival better or worse in group A compared to group B?' we can construct the survival plots for the two groups and look at the median survival in them. We can construct 95% confidence intervals on the two survival curves: if there is overlap between them, it indicates that event-free survival in the two groups is similar (Please see the note on 'confidence intervals' in this series).

Another way to compare two groups is to use the 'Log-Rank' test: it is a statistical test which compares the event-free survival in two groups. The null hypothesis in this comparison would be that there is no difference between the groups. When we perform the Log-Rank test, if the 'p' value turns out to be below 0.05, we can reject the null hypothesis and conclude that the two groups are different. The 'Log-Rank' test is also called the 'Kaplan-Meier' test and the survival curve is often called the 'Kaplan-Meier' (or KM) plot.

WHEN WE HAVE MANY VARIABLES

We have looked at the situation comparing two groups identified by a single grouping variable, such as whether treated or not, male or female, old or young etc. In most situations, event-free survival would be affected by a variety of such factors. In this case, we need to 'control' for the effect of other variables when we look at the influence of one variable. We use the Cox's Proportionate Hazard (PH) regression to analyze this. Cox's regression tells us which of the variables are affecting event free survival in the group, holding the other variables constant.

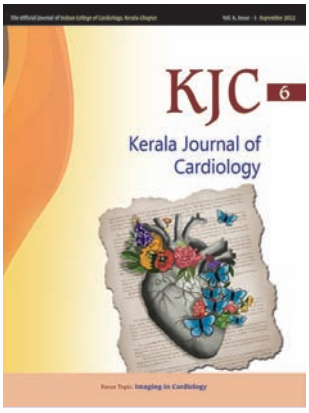

Saline Contrast Echocardiography
– *a Forgotten Tool in Cardiology*

Arun Gopalakrishnan

Associate Professor, Department of Cardiology, Division of Pediatric Cardiology, Sree Chitra Tirunal Institute for Medical Sciences and Technology, Thiruvananthapuram, Kerala, India.

INTRODUCTION

The application of microbubbles generated by agitated saline for contrast echocardiography is a proven, inexpensive yet underutilized tool in Cardiology. Saline contrast echocardiography (SCE) was initially developed to visualize functioning of the cardiac valves and adjoining structures[1]. The more reflective acoustic properties of saline microbubbles present an enhanced echocardiographic backscatter in the chamber opacified by saline. This tool can often obviate the need for additional expensive imaging modalities and can be diagnostic in several conditions.

In most cases, SCE involves injection of agitated saline from a large bore peripheral venous cannula. 5 – 10ml of 0.9% saline is mixed with 1 – 2ml of air and agitated using two 10ml luer lock syringes and a three – way stopcock for one minute[2]. The effluent air should then be discarded, and care taken to remove macrobubbles. The agitated saline is then injected rapidly into the vein under continuous ECG-gated echocardiography commencing exactly upon injection and focused on the area of interest. Repeated injections should be done only after waiting for sufficient time to ensure clearance of all microbubbles from both the right and left heart.

The application of SCE will be delineated henceforth using case – based illustrations.

CASE 1

A nine-month-old baby girl, weighing 7kg was referred to us for systemic desaturation (92%) noted during a routine immunization visit. The child had no cardiac symptoms and an uneventful past history. The arterial pulse was normal and there was no cardiomegaly. The first heart sound was normal, and the second heart sound had a wide fixed split. A short grade 2 mid-systolic murmur was noted at the left upper sternal border. Echocardiography revealed a 7mm ostium secundum atrial septal defect with left-to-right shunt. Pulmonary venous drainage was normal. The right superior caval vein and the inferior caval veins drained normally to the right atrium. A persistent left superior caval vein was noted. Saline contrast echocardiography was done from a left antecubital venous access. The first chamber to opacify was the left atrium, followed by filling of the right atrium through the atrial septal defect and the ventricles downstream (**figure 1**). Thus, SCE confirmed the diagnosis of persistent left superior caval vein to unroofed coronary sinus (Raghib syndrome).

Address for correspondence: Dr. Arun Gopalakrishnan, Associate Professor, Department of Cardiology, Division of Pediatric Cardiology, Sree Chitra Tirunal Institute for Medical Sciences and Technology, Thiruvananthapuram, Kerala, India - 695011. Email: arungopalakrishnan99@gmail.com

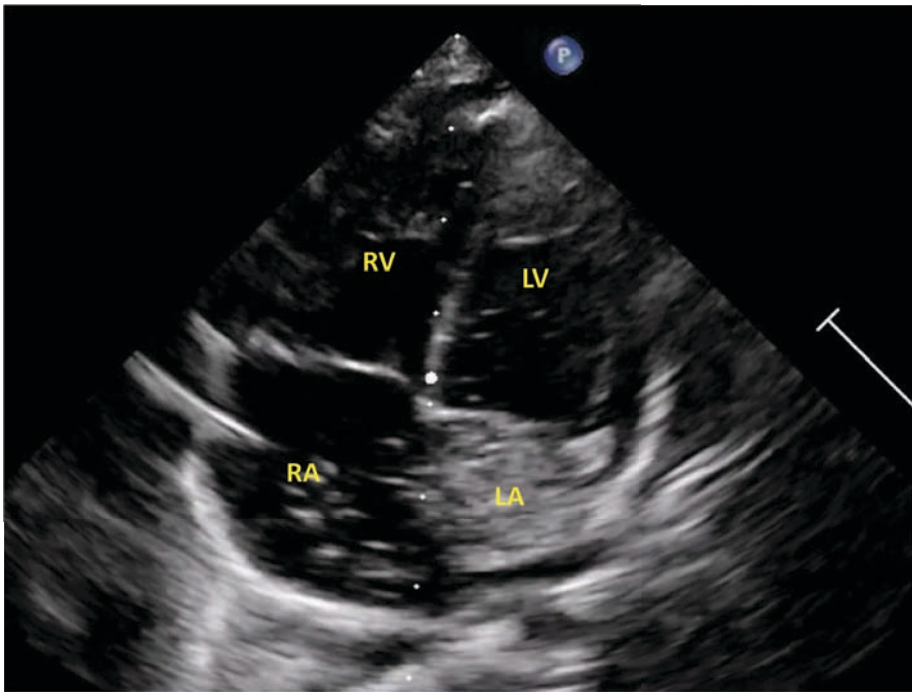

Figure 1: Saline contrast echocardiography from the left antecubital venous access, apical 4-chamber view, showing initial dense opacification of the left atrium (LA) followed by filling of right atrium (RA) through the atrial septal defect, and left ventricle (LV) in Raghib syndrome with additional ostium secundum atrial septal defect. RV – right ventricle

CASE 2

A 10-year-old boy presented to the Neurosurgery department with brain abscess and underwent burr-hole drainage surgery on antibiotics. He was referred to Cardiology in view of an oxygen saturation of 84% on room air. He had no past history of cyanotic spell, effort intolerance or heart failure and the parents had not noted any bluish discoloration of the body. Cardiovascular examination revealed normal peripheral pulses, no cardiomegaly and unremarkable heart sounds with no murmur. Chest X-ray and electrocardiography were unremarkable. Echocardiography confirmed usual arrangement of the atrial appendages and normally positioned cardiac apex. The interatrial and ventricular septa were intact and there was no shunt at the arterial level. The left heart chambers appeared slightly larger than the right sided chambers, but not unduly dilated (z-score of left atrium +1.58, left ventricular end diastolic diameter +0.77). Saline contrast echocardiography from the right anterior cubital venous access showed that the right superior caval vein drained to the left atrium, explaining the desaturation.

CASE 3

A 48-year-old lady was referred for evaluation of recurrent ischemic strokes over two years. She had no history of diabetes mellitus, systemic hypertension, dyslipidemia, family history of stroke or premature coronary artery disease. Thrombotic work-up was negative for protein C, protein S, factor V Leiden mutation, antiphospholipid antibodies, antinuclear antibody. Serum homocysteine level was 12 mmol/L (normal). Cardiovascular examination and electrocardiography were normal, and no structural heart disease or clot was identified on transthoracic echocardiography. She had no history of palpitations, and a 3-day Holter ruled out atrial fibrillation. Transesophageal echocardiography showed thin interatrial septum around the fossa ovalis but no atrial septal defect. The redundancy of the interatrial septum was 8mm, not mounting to the definition of an atrial septal aneurysm (>10mm). Thereafter SCE was done from a right antecubital venous access with Valsalva maneuver. Upon release of the Valsalva, 20 – 25 microbubbles were documented to traverse the patent foramen ovale (PFO) suggestive of a transient intracardiac right-to-left shunt. Thereafter, the patient underwent PFO device closure with a 30mm Amplatzer™ PFO occluder (St Jude Medical, Plymouth, MN, USA).

CASE 4

A 24-year-old lady was referred for an incidentally detected atrial septal defect (ASD) during a routine health check-up for a visa application. Though she was asymptomatic and past history insignificant, the oxygen saturation on room air was 85%. The arterial

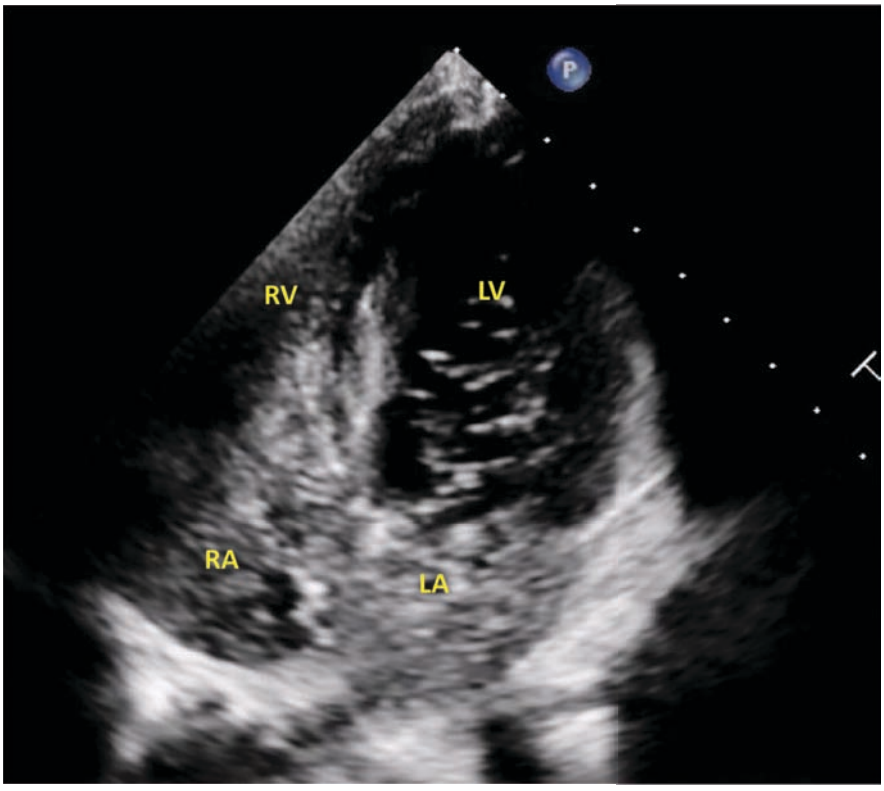

Figure 2: Saline contrast echocardiography from the right antecubital venous access, apical 4-chamber view, showing filling of the left atrium (LA) besides the right atrium (RA) and right ventricle (RV) suggestive of an atrial level right-to-left shunt. LV – left ventricle

pulses were normal, blood pressure 116/70 mmHg and jugular venous pressure was not elevated. Transthoracic echocardiography showed usual arrangement of the atrial appendages, normally positioned cardiac apex, concordant atrio-ventricular-arterial connections and normal connection of the pulmonary veins and systemic veins to the corresponding atria. The ostium secundum ASD measured 22 x 20mm. There was moderate tricuspid regurgitation, and the derived right ventricular systolic pressure was 32mmHg. A prominent Eustachian valve was noted to guard the entry of the inferior caval vein to the right atrium. Saline contrast echocardiography done from a femoral venous access showed dense contrast opacification of the left atrium from the right (**figure 2**), directed by the prominent Eustachian valve. Transesophageal echocardiography delineated adequate rims for the ASD. The defect was closed with a 24mm septal occluder following which the peripheral oxygen saturation improved to 100% on room air.

CASE 5

A 26-year-old lady was referred for evaluation of systemic desaturation identified during a routine evaluation. She had history of nasal bleeds in the past which were managed conservatively. The oxygen saturation on room air was 76%. She had uniform central cyanosis and pan-digital grade 2 clubbing. The arterial pulses, blood pressure and precordial cardiovascular examination were normal. Electrocardiography was unremarkable and echocardiography also suggested a structurally normal heart and no pulmonary hypertension. Thereafter, SCE was done from the right antecubital venous access. Dense filling of the left heart chambers was noted in the fourth cardiac cycle suggesting intrapulmonary right-to-left shunt. Invasive pulmonary angiography showed multiple globular pulmonary arteriovenous fistula (PAVF) in the right and left lungs. She underwent staged closure of the PAVF with improvement in saturation to 94%.

CASE 6

A 10-year-old boy with tricuspid atresia with pulmonary atresia presented with a saturation of 68%. He had been palliated with Blalock – Taussig shunt at two months of life, and thereafter with bidirectional Glenn shunt at 2 years of life with takedown of the prior shunt. He had been advised Fontan completion earlier but was lost to follow up after the second surgery. For six months prior to the latest presentation, he developed decline in effort tolerance and easy fatiguability. He had deep uniform

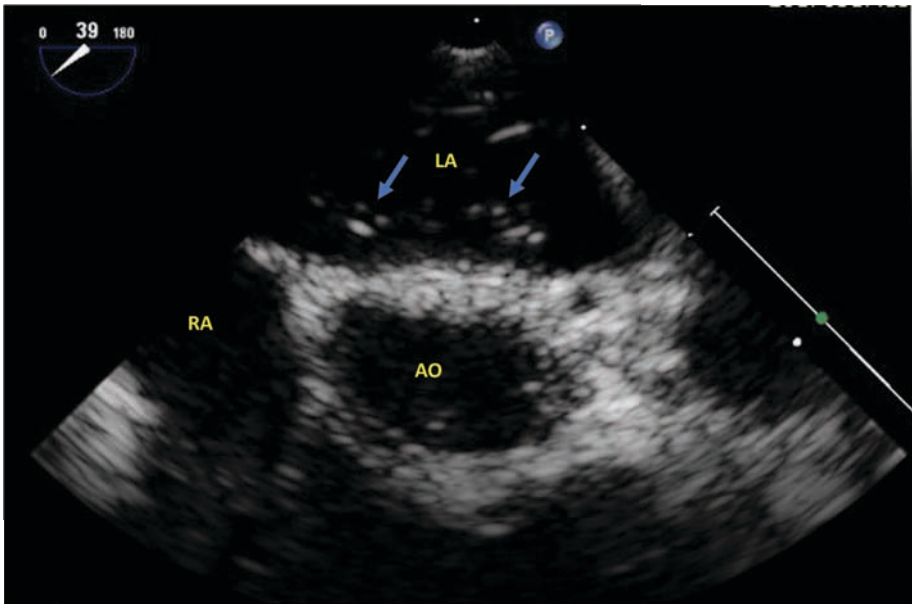

Figure 3: Saline contrast echocardiography from left pulmonary artery injection in post BDG patient with transesophageal echocardiography at 38-degree mid-esophageal position showing saline bubbles (blue arrows) in the left atrium (LA) suggestive of left pulmonary arteriovenous fistula. AO – aortic valve, RA – right atrium

central cyanosis, grade 3 clubbing and the conjunctivae were congested. The arterial pulse volume was normal. There was no cardiomegaly or cardiac murmur. Chest X-ray showed a cardiothoracic ratio of 0.52 and reticular pulmonary vascular pattern in both lung fields. He was taken up for cardiac catheterization and transesophageal echocardiography to evaluate for candidacy for Fontan completion. The mean pressure in the Glenn circuit and pulmonary arteries was 14mmHg. Transesophageal echocardiography probe was positioned at the mid-esophageal level to interrogate the pulmonary venous return. Agitated saline was injected into the right pulmonary artery using an NIH angiographic catheter advanced from the right internal jugular venous approach. More than 25 bubbles were imaged in the left atrium within five cardiac cycles suggestive of grade 3 pulmonary arteriovenous fistula (PAVF) in the right lung[3]. Thereafter SCE was done from the left pulmonary artery and 15 – 20 bubbles were imaged in the left atrium within five cycles suggestive of grade 2 PAVF(**figure 3**). The right lower and left upper pulmonary venous saturation were 91% and 94% respectively confirmative of right-to-left shunt at the pulmonary venous level. Angiogram in the Glenn circuit revealed diffuse mottled pattern in both lungs, most prominent in the right lower lobe, characteristic of diffuse PAVF.

DISCUSSION

Saline contrast echocardiography is a readily available bedside investigation in the diagnosis of several structural heart diseases as illustrated above. Besides its most popular use in the detection of patent foramen ovale, the next most common application of SCE is in the detection of systemic venous anomalies and pulmonary arteriovenous fistula. SCE is an invaluable tool in the evaluation of unexplained cyanosis. The identification of PAVF by SCE in the absence of any other cardiac pathology may occasionally suggest the presence of congenital porto-systemic shunts (Abernethy malformation)[4]. However, it must be performed cautiously so as to prevent SCE is also extremely useful in separately identifying the posteroinferior rim of ASD for device closure when the Eustachian valve is prominent[5].

In the postoperative setting, SCE may be useful to screen for systemic baffle leaks in patients post atrial switch (Senning / Mustard / Hemimustard). The patency of a surgical fenestration in the Fontan circuit may also be evaluated by SCE from a lower limb venous access.

Saline contrast echocardiography may also be useful in the identification of a right-to-left shunt at the great artery level, as in Eisenmenger syndrome with a large aortopulmonary window or patent arterial duct in patients with poor parasternal or suprasternal echo windows[2].

Careful clinical examination and echocardiography is mandatory before choice of venous access for SCE. The 3-to-5 beat rule is not a foolproof criterion for distinguishing intracardiac and extracardiac shunts on SCE[6]. Various systemic venous anomalies including

coronary sinus septal defects[7] and anomalous drainage of the caval veins[8] could be missed by a wrong choice of venous access. Pre-procedure instructions and training of the patient to perform a proper Valsalva are cardinal for the diagnosis of PFO by SCE.

REFERENCES

1. Gramiak R, Shah PM. Echocardiography of the Aortic Root. Invest Radiol. 1968 Oct;3(5):356–66.
2. Gupta SK, Shetkar SS, Ramakrishnan S, Kothari SS. Saline Contrast Echocardiography in the Era of Multimodality Imaging--Importance of "Bubbling It Right." Echocardiogr Mt Kisco N. 2015 Nov;32(11):1707–19.
3. Kartik SV, Sasidharan B, Gopalakrishnan A, Kurup HKN, Krishnamoorthy KM, Sasikumar D, et al. A Comparative Study of Invasive Modalities for Evaluation of Pulmonary Arteriovenous Fistula after Bidirectional Glenn Shunt. Pediatr Cardiol. 2021 Dec;42(8):1818–25.
4. Raghuram KA, Bijulal S, Krishnamoorthy KM, Tharakan JA. Regression of Pulmonary Vascular Disease After Therapy of Abernethy Malformation in Visceral Heterotaxy. Pediatr Cardiol. 2013 Dec 1;34(8):1882–5.
5. Krishnamoorthy KM, Gopalakrishnan A, Kumar DS, Sivasankaran SS. Eustachian valve-Masquerading ASD rim. Indian Heart J. 2017 Jun;69(3):422–3.
6. Freeman JA, Woods TD. Use of saline contrast echo timing to distinguish intracardiac and extracardiac shunts: failure of the 3- to 5-beat rule. Echocardiogr Mt Kisco N. 2008 Nov;25(10):1127–30.
7. Gopalakrishnan A, Menon S, Sasikumar D, Kurup HKN, Krishnamoorthy KM. Hemianomalous pulmonary venous drainage and type IIb coronary sinus septal defect - Utility of subxiphoid and right parasternal views. Echocardiogr Mt Kisco N. 2021 Oct;38(10):1833–5.
8. Desai M, Talwar S, Kothari SS, Jagia P, Airan B. Inferior vena cava to left atrium shunt presenting with polycythemia and stroke three decades following closure of atrial septal defect. Congenit Heart Dis. 2013 Aug;8(4):E102-105.

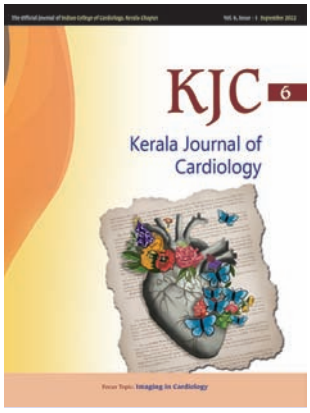

History of Echocardiography
— *An Odyssey of Tragedy, Hope and Glory*

Zulfikar Ahamed M.
Chief of Pediatric Cardiology, KIMS Hospital,
Thiruvananthapuram, Kerala.
Former Professor and Head, Department of Pediatric Cardiology,
SAT Hospital, Government Medical College, Thiruvananthapuram.

"Sweet Echo, Sweetest Nymph
That liv'st unseen
Within thy airy shell"

– John Milton

It all started probably with the sinking of the unsinkable Titanic. Titanic (in full, *RMS Titanic*) with its 2200 passengers and crew left on the maiden voyage from Southampton on 10th April 1912. It stuck an iceberg on 14th April near New Foundland and sank leaving behind 1500 dead. This was a major blow to the Western psyche. [Fig 2]

"Deeply regret advise you Titanic sank this morning fifteenth after collision iceberg resulting serious loss life; further particular matters later".

Bruce Ismay
Chairman, White star

People began seriously thinking of detecting icebergs early enough to avoid such catastrophe. They succeeded and the technique was even used for war. This was the beginning of a beginning - a search for a medical diagnostic tool using *'unheard'* sound, which we now call ultrasound. A search which continued across two world wars and extended beyond 1950s. A truly remarkable journey of intuitive thinking, serendipity, innovative techniques and boundless patience.

Figure 1. Echo, the cursed Nymph

Address for correspondence: Dr. Zulfikar Ahamed, MD, DM, 'Sajan', T.C. 1072/4, Pazhaya Road, Medical College P.O., Thiruvananthapuram - 695011
E-mail: zulfikarahamed@gmail.com

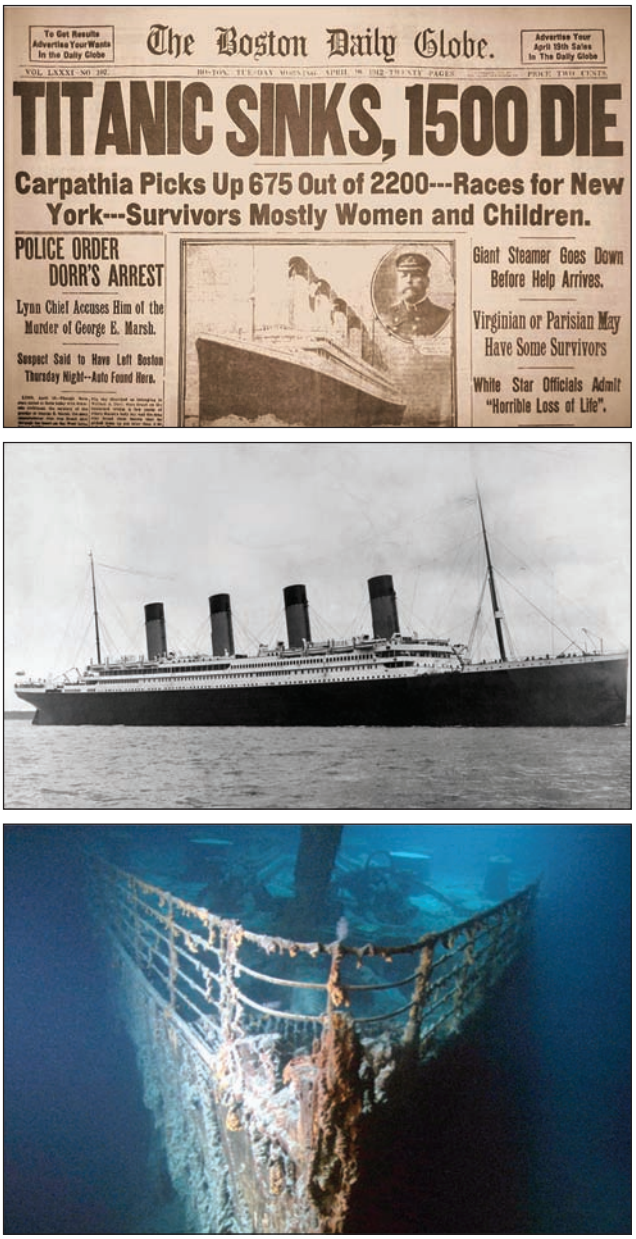

Figure 2. The Tragedy. Sinking of the Titanic

Of Pythagoras, Bats and Ultrasound

Pythagoras, a Greek mathematician and philosopher was probably the first human being to speak about sound and echo. However we had already heard about Echo, a nymph in Greek mythology and her infamous curse. According to Greek mythology, Zeus, the King of Olympian Gods used to come down to earth and consort with nymphs. Zeus had ordered Echo to hold on to Hera, his wife for a longer time by talking to her, to avoid being caught red handed by Hera. The angry and jealous Hera came to know this and cursed Echo. [She will] *'Only able to speak the last words spoken to her'*. The rest of the story is truly tragic to Echo.

On a more scientific note, even if bats can see during day light, they can seek and find others and food by a mechanism known as *'Echolocation'*. They emit high frequency sound pulses through their mouth and nose and can listen to the echo and assess the size, shape and texture of the objects. They emit sound in a very high frequency – 14000 hertz to 100,000 hertz. (The human ear can appreciate sound only when it is between 20 hertz and 20000 hertz). The knowledge regarding this phenomenon was first discovered by an Italian scientist, Lazzaro Spallanzoni (1729-1799). He described 'reflected echoes of inaudible sounds from Bats' which enabled them to navigate at dark (***'Opus Coli di fiscica'***).

Of Sound, Ultrasound and Echoes

The Greeks, the Chinese and the Egyptians were sound on acoustics. Aristotle taught that air movement caused sound. Pythagoras discussed pitch and frequency of sound and introduced a *sonometer*. Later, Da Vinci, the quintessential genius, stated that sound travelled in waves. Coming very close to our theme, Sir. Francis Galton invented the electronic ultrasound whistle – the dog whistle. The frequency of sound is measured as cycle per second (cps) and is called hertz (Hz) after Heinrich Rudolf Hertz (1857-1894) who was a physicist who died young and has a trans-generational link to our history of the echocardiography.

Ultrasound in Medicine

Perhaps the initial key event in this saga is the invention of piezoelectricity by Jaques Curie and Pierre Curie in 1880 (Production of Ultrasound Waves from Quartz crystals).

Immediately after the dreadful Titanic disaster, scientists began searching for a technique to detect icebergs. Quite naturally, a Briton, Lewis Richardson came up with an echo ranging technique to pick up submerged objects. Paul Langevin from France came up with the same technique in 1915 and it was then developed by U.S. Navy as SONAR (Sound Navigation and Ranging). [Fig 3] It was used to detect submarines in WW1. Later the same equipment was used by allies to detect German U boats in WW2. This definitely made a difference in naval warfare between the allies and Germans during WW2. [Fig 4]

Towards the end of WW2 (in 1941), Wild and Reid introduced ultrasound for possible medical / peaceful purposes. In 1947, K.T.Dussik imaged brain using ultrasound and he is quite justifiably called *'The Father of the Ultrasound'*.

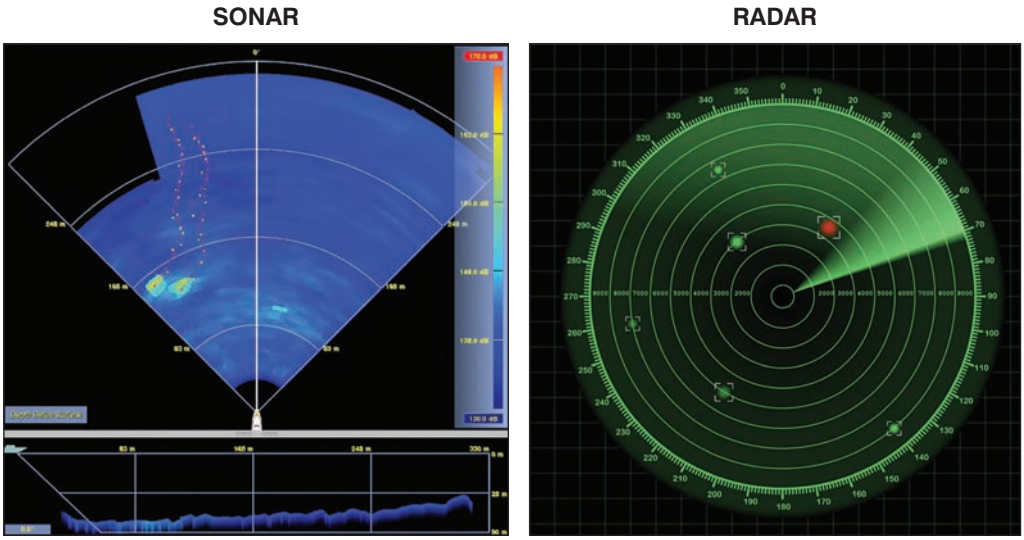

Figure 3. Averting the tragedy …more uses. The SONAR & RADAR

Figure 4. Ultrasound & The Wars. The U Boats. WW1, WW2.

In 1944, Floyd Firestone developed a system called Reflectoscope in which the same transducer generated the waves and detected reflected waves.

After the end of WW2, there was a progressive, synchronized interplay among SONAR, RADAR, development of Mitral Valve Surgery, Collaboration between Cardiologists and physicists , plain luck and of course perseverance in the genesis of cardiac ultrasound, what we now call as Echocardiography. There was a happy cohesion of elements of pursuing a definite goal, use in wars, accidental findings and sagacity of scientists.

Seeing The Heart With Sound

And finally the culmination of work on echoes arrived. The first real approach to a cardiac ultrasound and invention is credited, with unarguable justification to **Inge Edler and Hellmuth Hertz** who published their seminal paper in 1954, having first used it on a human being in 1953. [Fig 5]

"The use of ultra-sonic Reflectoscope for the continuous recording of the movements of the heart walls"

This was amplitude mode (A-mode) echocardiography. Edler accurately identified signals originating from the mitral valve from his later work in the 1960's. [Fig 6] The first term used to describe the innovative technique was 'Ultrasound Cardio Graphy' (UCG). Then Bernie Segal suggested the term echocardiography, strongly supported by Harvey Feigenbaum which has since then stood the test of time. Feigenbaum was the one who introduced the mono dimensional (M-mode) echo techniques and brought it to US and the rest of the world in 1968. He is also credited with the first ever text book on echocardiography published in 1972.

The next giant step was introduction of two dimensional echocardiography (2D-Echo), originally developed by Gramiak from M-mode tracings and later by Bom who in the1970s developed 2D-real time images.

Interestingly, even though use of Doppler in assessing cardiac physiology in echo, came in the late 1950s and 60s and even going up to 1980's, the Doppler

Figure 5. 'The Gentlemen From Lund' Hellmuth Hertz, Inge Edler.

Effect and its physical properties are attributed to a 19th century scientist, Johann Christian Doppler, an Austrian mathematician (1842). The major players who introduced Doppler technics to echocardiography were, Sato Mura (1956) and Kalmanson (1969). But it took its own time to convince clinicians of the tremendous use

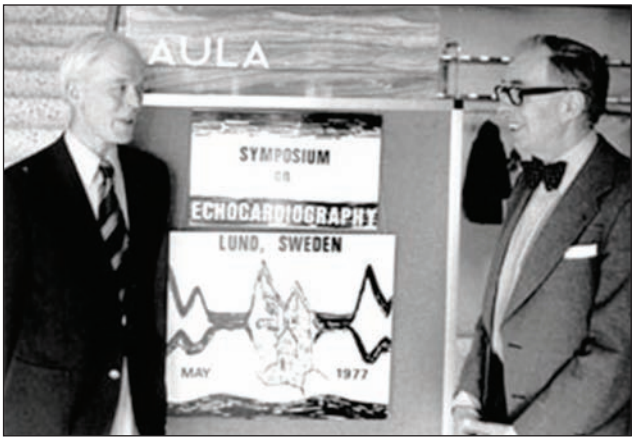

Figure 6. Hellmuth Hertz. Inge Edler. With ' the Images ' 1977

of Echocardiography. Color Doppler echocardiography, which was more user friendly was introduced by Bommer and Namekawa.

Later on further refinement and modification of Doppler came through Tissue Doppler Imaging, Speckle tracking strain imaging (non-Doppler)

Currently echocardiography has been on a process of evolution which has led to development of trans esophageal echocardiography, epicardial echocardiography and intracardiac echocardiography. So the imaging tool has become *closer to heart, on to the heart and even inside the heart*!

TEE, which took its first footsteps in the 1980's has become a formidable imaging tool. Epicardial echocardiography was first introduced in 1972 and has now become a famous meeting point for the cardiac surgeon and the cardiologist. ICE has now complemented TEE and is useful in EPS, TAVR etc.

3D reconstruction of 2D images began in 1974 and has now ushered in an era of 3D TTE as well as 3D TEE.

'Small is beautiful'

Smaller echo machines, lap top format machines and even pocket sized hand held devices are all now ready for use. Currently 'pocket' echo machines can complement clinical evaluation, help in intensive care units, triages and community screening settings.

'In Conclusion'

The development of echocardiography involved so many varied events and opportunities. It encompassed a good timing, surgical needs, proximity to shipyards, the chance link forged between Edler and Hertz, luck as exemplified by their connection to Siemens, receptive minds, clever thoughts, collaboration between clinical and non-clinical scientists and of course the perseverance of the protagonists. *It was a tale which opened with a human tragedy and ultimately ended in one of the most rewarding and unique practices of diagnostic cardiology.*

ECHOCARDIOGRAPHY & 'The Two Gentlemen From Lund'

Inge Elder; The Father of Echocardiography: 1911-2001

Inge Edler was born in Berlin on 17 th March, 1911, He had wanted to be a scientist but chose Medicine is it was less competitive! He went on to become the medical director of cardiovascular lab in the University of Lund. He started collaborating with a young Hellmuth Hertz in the late fourties and the rest is history.

Edler was recipient of Lasker Award which is considered American equivalent Nobel in Medicine, in 1977 along with Hertz. He was recognized as the *'Swedish Cardiologist of the 20th century'*. Many times nominated for Nobel Prize for physiology and medicine, never awarded. A pity.

At the age of 81, Edler took an adventurous journey along old Silk Road (Islamabad to Peking) and succeeded in his second attempt in the perilous adventure! He died on March 7th 2001.

Hellmuth Hertz: 1920 -1990

Carl Hellmuth Hertz was the son of Gustav Hertz who was a Nobel Prize winner in physics in 1925. He was born in 1920. Hellmuth Hertz had this 'Hertzonian' genes inherited from his grand uncle Heinrich Hertz (1857-1894) after whom, the term Hz (hertz) as S1 unit of frequency is measured. His father Gustav Hertz received 1925 Nobel Prize for Physics for his work on inelastic electron collisions in gases (1887-1975). [Fig 7] His association with a then 42 year old Edler ultimately brought about ***'one of the truly ground breaking and remarkable innovations of the 20th century'***.

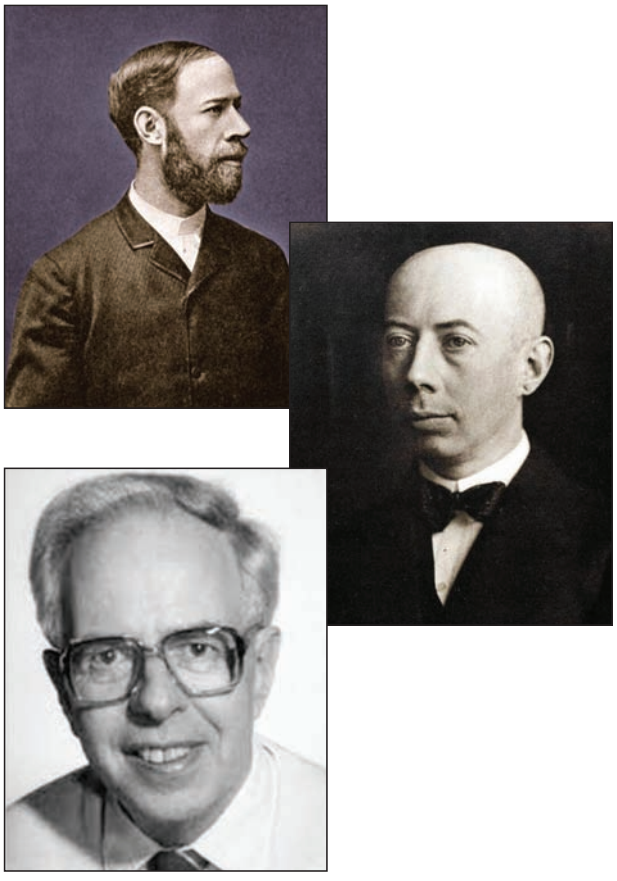

Figure 7. Heinrich Hertz, Gustav Hertz, Hellmuth Hertz. 'The Triumvirate' in Physics

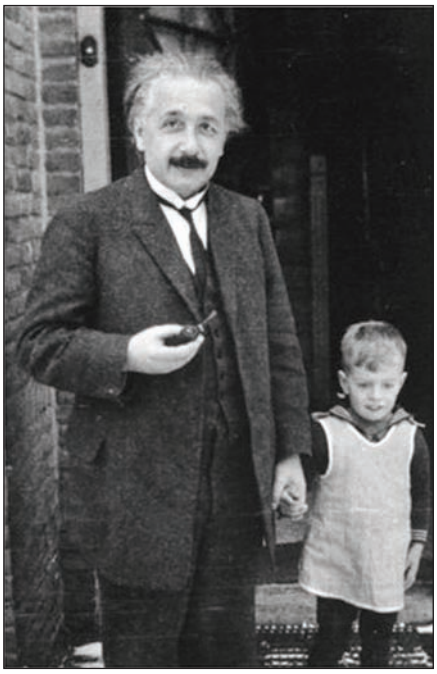

Figure 8. Hellmuth Hertz. With Albert Einstein. 'The Kid'.

Hertz, later created new technique of 2D echocardiography which interestingly was considered as lacking in medical and commercial interest! Hertz then moved on to new pastures and developed ink jet printer. [Fig 8]

Hertz died in 1990 in Lund.

ANECDOTES AND PEARLS IN THE HISTORY

Origin of the term, echocardiography

Initially it was named Ultrasound Cardio Graphy [UCG]. Dr. Bernie Segal suggested the term echocardiography but as its abbreviation would be ECG, it was initially rejected. Echoencephalography used to be practiced which later went into oblivion. So people embraced the current term Echocardiography with the Echo as its abbreviation

Great Minds Dampening the spirit of invention of echocardiography.

Paul Dudley White visited Lund to observe Edler's work and was less than impressed. Also was Cournand who had earlier received Nobel Prize for cardiac catheterization. It was then the insight and work of Harvey Feigenbaum which resurrected the echocardiography from possible demise in early 1960's.

'From Sweden, with Love'

Edler's work on the 'Reflectoscope' was reviewed in Rome, during the 3rd European Congress of cardiology in 1960 and later published in 1961 in **Acta Medica Scandinavia**. The movie featured ultrasound examination of Mitral stenosis, Aortic valve disease, Left ventricle and pericardial effusion.

Harvey Feigenbaum and Modern Echocardiography [Fig 9]

Even though work of Edler and Hertz was introduced to USA in the early sixties, America was skeptical of the new technology. However Feigenbaum and his colleagues steadily but surely presented the new imaging technic to cardiologists, highlighting its role in cardiac anatomic diagnosis. The term 'Echocardiography' and 'cardiac sonographer' (non physician) were probably due to the influence of Feigenbaum.

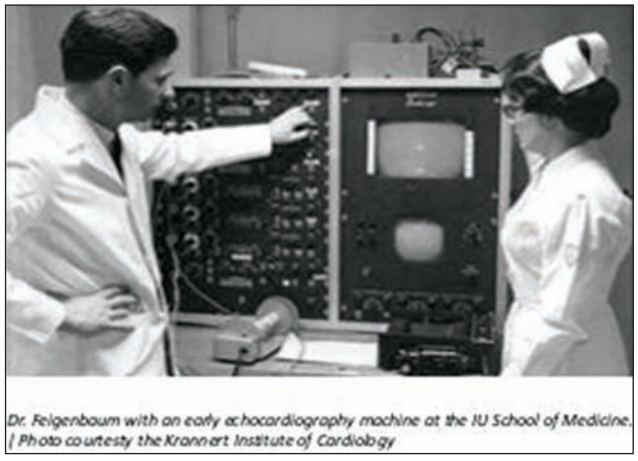

Dr. Feigenbaum with an early echocardiography machine at the IU School of Medicine. | Photo courtesy the Krannert Institute of Cardiology

Figure 9. Harvey Feigenbaum.
Harvey Feigenbaum is widely recognized as the "Father of modern Echocardiography" for pioneering the most widely used cardiac imaging technique in the world. He has been a leading scientist in this field for decades.

A Brief History of Cardiac Ultrasound In India

Echocardiography entered India as M mode echocardiographic machines which could deliver only a single dimensional 'ice pick' views. This was in 1975, specifically in Mumbai and Delhi and later in Chennai. The pioneers in M-Mode were K.D.Shah, Lakshmikanthan, Alagesan and S.K. Parashar. The first text book in India on echocardiography was published in 1979-1980 by Lakshmikanthan and Alagesan.

2D echocardiography ushered in a new era in cardiac imaging. Many congenital and acquired heart diseases were diagnosed.

G. Vijayaraghavan introduced one of the first 2D echo machines into Trivandrum, Kerala. This was in 1978. He vividly remembers how for recording the images, he borrowed photographic paper from the famous cinematographer Shaji N Karun. Later on phased array probes were introduced and in the mid-80s Doppler machines came into existence for diagnosis in India. Color Flow Mapping was introduced for the first time in USA in 1984 and in 1985 a workshop on CFM was held in Delhi. Navin Nanda, Natesa Pandian and Bijoy Khanderia were the prominent 'teachers'.

From mid 1990s's the entire spectrum of echocardiography was available to cardiologists in India. The continuing process of teaching and learning culminated in the formation of Indian Academy of echocardiography in 1994.

Committed pediatric echocardiography was pioneered from AIIMS Delhi and spread all over the nation. TEE was started in 1991 in Delhi.

The overall acceptance, spread and utilization of various modalities of Echo in our country nearly coincided with whatever was happening elsewhere and this fast paced development has helped assess cardiac maladies non-invasively and with no ionizing radiation and offer curative solutions. Now Fetal Echo has become a major filter in recognizing critical CHD in the unborn all over India, particularly in Kerala.

HISTORY OF ECHOCARDIOGRAPHY

Time Line One

Before 1900		
570 - 490 BC	Pythagoras	Sound and Bats
1588 – 164 g	Mersenne	Speed of sound
1627 – 1691	Robert Boyle	Sound needs a medium
1727 – 1799	Spallanazi	Echolocation by bats
1803 – 1853	Johann Doppler	Doppler shift [Fig 10]
1880	Pierre Curie	Piezo electrical
	Jaques Curie	Crystal [Fig 11]

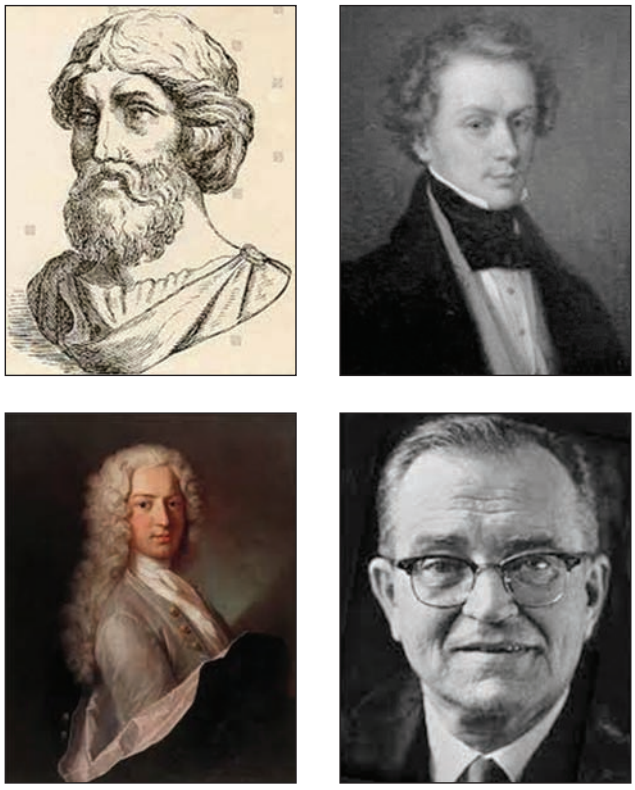

Figure 10. Pythagoras, Doppler, Bernoulli, Dussik. The Ancient Warriors of Science and One New

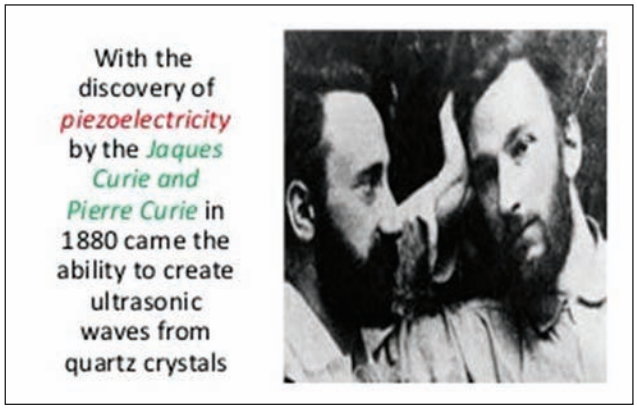

Figure 11. Concept of piezo electricity

Time Line Two: 20th Century

Echocardiography is a 20th century breakthrough in cardiac imaging, a quantum leap.

1912	Sinking of RMS Titanic	
1912	Development of SONAR	Lewis Richardson
1915	'Hydrophone'	Paul Langevin
1941	Ultrasound for possible medical uses	John Wild, John Reid
1942	Brain ultrasound	Karl Dussik
1944	Reflectoscope – generating receiving reflected sound	Floyd and Firestone
1951	B mode ultrasound	John Reid John Homes
1953	First Cardiac Ultrasound Echocardiogram	Inge Edler Hellmuth Hertz [Fig 9]
1954	First Paper on Echocardiography published	Inge Edler Hellmuth Hertz
1960	Movie on Echocardiography in Rome during conference of European Society of Cardiology [Fig 10]	Edler Hertz
1963	M-mode echo introduced in USA	Claude Joyner
1964	First real time 2D	Nicholas Bom
1966	Doppler ultrasound (PWD)	Don Baker Denis Watkins
1968	Electronic Phased Array [Fig 12]	J.C. Somer John Reid
1970's	Continuous Wave Doppler Color Doppler	Sata Mura Kalmanson
1968	Contrast Echocardiography	Gramiak Shah
1974	Electronic Phased array	Thurstone Van Ram
1979	Echo assessment across valves	Hatle Holen
1982	Color Flow Mapping	C. Kasai
1977	TEE	K. Hisanga
1982		J. Sauquet
1980's	3D Echocardiography	Kazumori
1990's	RT 3D 4D Echocardiography	Van Romm
2000's	Hand held echocardiography	

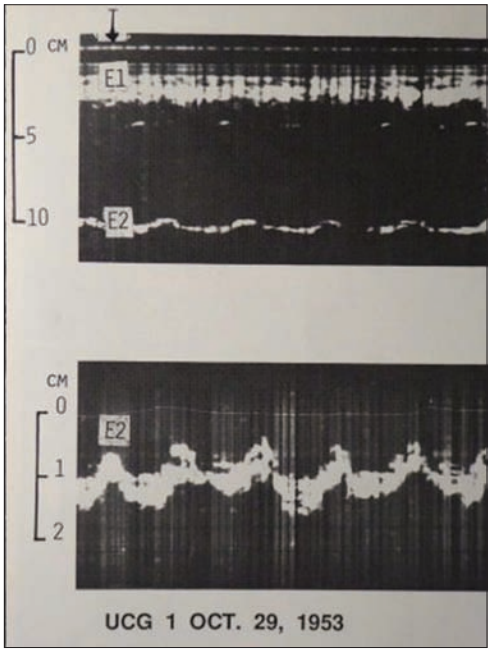

Figure 12. The first recorded echocardiogram from 29 October 1953. Upper panel echo from anterior chest wall (E1) to the posterior wall of the left ventricle (E2). Lower panel echo (E2) of the posterior left ventricular wall recorded at a larger scale (cm). Image from the South Swedish Society of Medical History

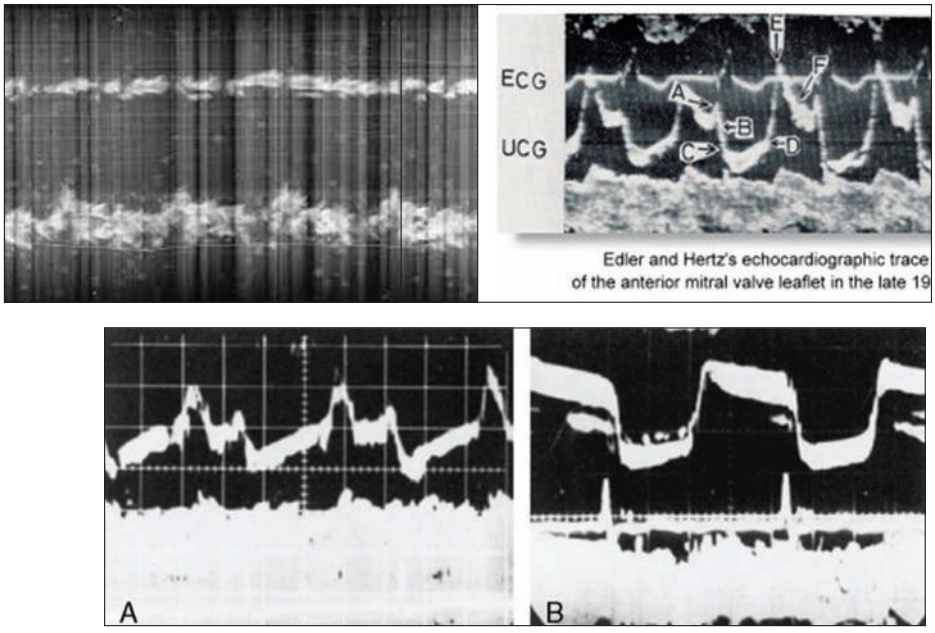

Figure 13. The First Epoch making Visuals !

Timeline post Edler / Hertz

2D real time echocardiography	1960's	Bom
Contrast echocardiography	1968	Gramiak Shah
First Phased Array probe	1968	Somer
First electronic phased array probe	1974	Turstone Van Ramm

Echo assessment across valves	1979	Holen Hatle
Real time color flow	1978	Brandestini
Color Flow Mapping	1982	Kasai
Trans Esophageal Echocardiography	1977/ 1982	Hisanga J.Souquet

Figure 14. Jan Somer with his Phased Array probe

Figure 15. Thomas Alva Edison. First Gramaphone.

FURTHER READING

1. S. Singh, Abha Goyal, The Origin of Echocardiography, A Tribute to Inge Edler, Text Heart Inst J, 2007; 34 : 431-438.
2. H. Feigenbaum, Evolution of Echocardiography Circulation 93, 7: 1996: 1321-1327.
3. Inge Edler and the Origins of Clinical Echocardiography. Eur. J. Echocardiography 2001; 3-5.
4. S.K. Parashar. History behind development of echocardiography in India. J. of the IAE and Cardiovascular Imaging 2008; 3: 2: 110-122.
5. W.F. Armstrong, T. Ryan. History of Echocardiography in 'Feigenbaum s Echocardiography. 7th edn. Philadelphia, Lippincott William and Wilkins p. 1-8.
6. A. D. Franco, L.B. Ohme , M.Gaudino et al. Serendipity and innovation: history and evaluation of transthoracic echocardiography. J. of Thoracic Disease 2017; 9 (Suppl): 257-263.
7. G. Weltrell. Echocardiograph: the first ultrasound picture of the moving heart. Hektoch International Journal, 2009.
8. I. Edler, C.H. Hertz. The use of ultrasonic reflectoscope for the continuous recording of the movements of the heart walls. 1954. Clin Physiol Funct Imaging 2004; 24: 118-136.
9. S. Satomura. Study on examining the heart with the ultrasonic Doppler method. Jpn. Circ. J 1956; 20: 227-228.
10. W. Bommer, L. Miller. Real time two D color flow Doppler; enahanced Doppler flow imaging in the diagnosis of Cardio Vascular disease. AJC 1982; 46: 944.
11. I. Edler. The diagnostic use of ultra sound in heart disease. Acta Medica Scandinvica 1955; 152 (9) : 32-63.
12. I. Edler, A. Gustafson, T. Karlefors, et al. The movements of Aortic and Mitral Valves recorded with ultrasonic echo technique (Motion Picture). Presented at III ECS, Sept 18-24, 1960, Rome, Italy.
13. J. Holen, S. Simmonsen. Determination of pressure gradient in MS with Doppler echocardiography BHJ 1979; 41: 529-535.
14. CR Joyner, JM Reid, JP Bond. Reflected Ultrasound in the assessment of mitral valve disease. Circulation 1963; 191: 711-714.
15. N.R Lundstrom, I. Edler. Ultrasound cardiography in infants and children Acta Pediatrica Scand 1971; 60: 117-128. [Fig 15]

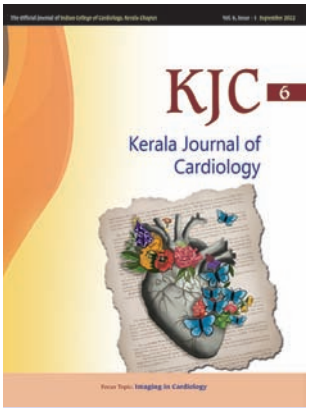

Left Ventricular Noncompaction

Manjunath K.M.
Inderjot Kaur
DM Senior Residents,
Pushpagiri Medical College, Thiruvalla,
Kerala.

INTRODUCTION

Non compaction of the left ventricular myocardium (LVNC) is being increasingly recognized and its diagnosis has moved from autopsy table or previously poorly recognized entity into a widely recognized cardiomyopathy. Advances in non invasive diagnostic technologies aid better delineation of morphology. It is a rare entity (2 in 10,000; Male : Female - 1 : 1).

CASE REPORT

A 70 year old male, farmer, with no previous cardiac history and no known comorbidities, presented with angina and breathlessness of 1 day duration. Troponin I and BNP were elevated. He was admitted in CCU for further evaluation and management. Antiplatelets and antianginals were given from outside hospital and was referred here. Echo showed Global LV hypokinesia severe LV systolic dysfunction-EF 30%, moderate MR, LV diastolic dysfunction. Multiple LV trabeculations were seen - Non compacted to compacted layer ratio of 3.3 suggestive of LV Non compaction. He was started on standard heart failure measures. In view of elevated troponin and angina, coronary angiogram was done which showed normal epicardial coronary arteries. Cardiac MRI was done - Severe LV systolic dysfunction-EF 30%, Non Compacted to Compacted myocardium ratio - 4.2 -s/o LV non compaction. It was a rare case of LV non compaction presenting for the first time at an elderly.

HISTORY

First described in association with other congenital abnormalities.

Dusek first described the postnatal persistence of spongy myocardium in 1975 pathologically.

Engberding and Bender made the first clinical recognition with 2-D echocardiography in 1984.

MORPHOLOGY

LV noncompaction will show prominent trabeculae and deep intertrabecular recesses. Myocardium will have two layers - outer thin compacted layer and inner thick noncompacted layer. Blood will be filling between the trabeculae.

LVNC presents with either structural CHD -sporadic and familial (examples: Atrial septal defect, Ventricular septal defect, Ebstein's anomaly, Tetralogy of Fallot, Transposition of great arteries, Barth syndrome, Charcot Marie Tooth, Nail patella syndrome) or isolated LV non compaction which is seen in pediatric age group or adults showing late presentation(adult pattern-3rd or 4th decade).

Address for correspondence: Dr. Manjunath K.M., DM Senior Resident, Pushpagiri Medical College, Thiruvalla, Kerala.
Phone: +91 9591712310, Email: manjunathkm12310@gmail.com

EMBRYOLOGY

Foetal heart initially receives blood from recesses. After 5th week, coronary arteries develop and recesses regress. This process is gene mediated - thick non compacted layer becomes thin compacted layer.

Mutations in the genes leads to premature arrest. Compaction takes from epicardium to endocardium and from base of the heart to apex. In case of premature arrest, the endocardium near the apex remains non compacted leading to spongy myocardium.

Various genes responsible for LVNCC are Fbkp1a/Notch pathway, G4-5gene/TAZ protein, 14-3-3 deletion, ZASP protein, TNNT2 protein, MYH7 protein, TPM1 protein, MYBPC3 protein, ACTC1[1].

CLINICAL MANIFESTATIONS

Patients of LV noncompaction usually present with heart failure, arrythmias, embolic episodes (Fig 1) . Heart failure is due to poorly functioning spongy myocardium. Abnormal myocardium may trigger arrythmias. Poorly contracting myocardium aids to thrombus formation leading to embolic events. Patients of LV noncompaction can develop microthrombi inside the crypts. These thrombi may dislodge causing coronary artery embolism resulting in small areas of infarction. Such events may have elevated troponin.

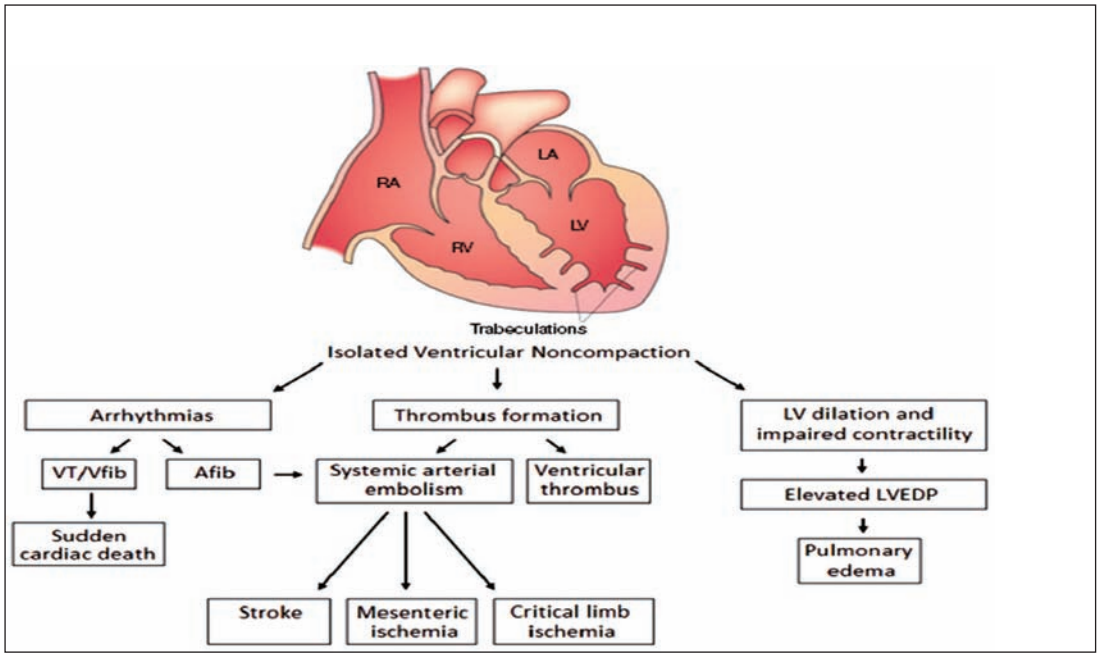

Fig 1: Pathophysiology of LVNC

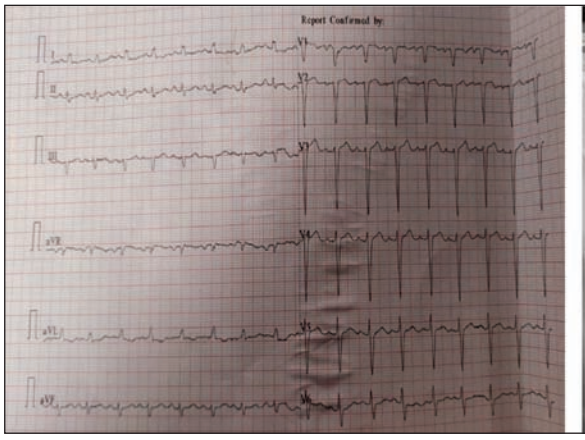

Fig: 2: ECG

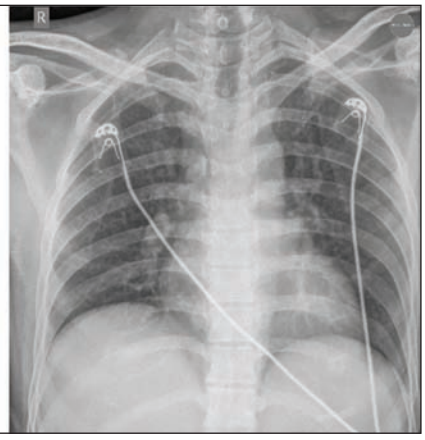

Fig: 3: CXR

Diagnosis

Diagnosis is mainly based on Echo and cardiac MRI (Cardiac MRI being the gold standard).

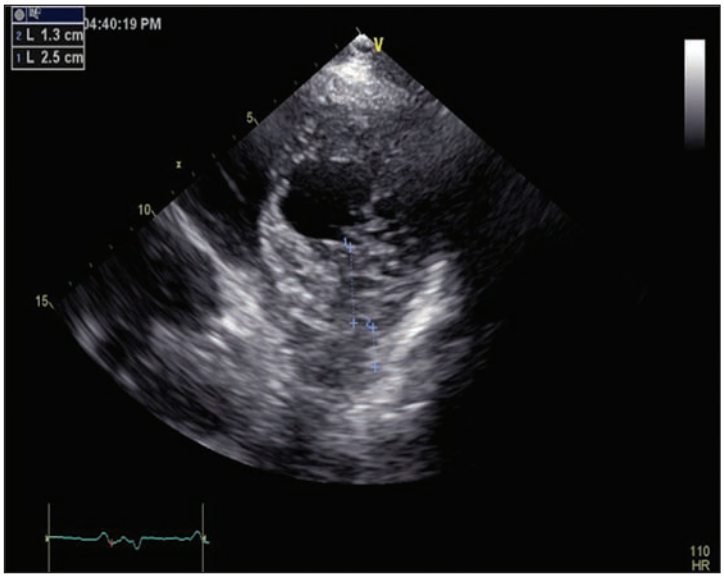

Fig: 4

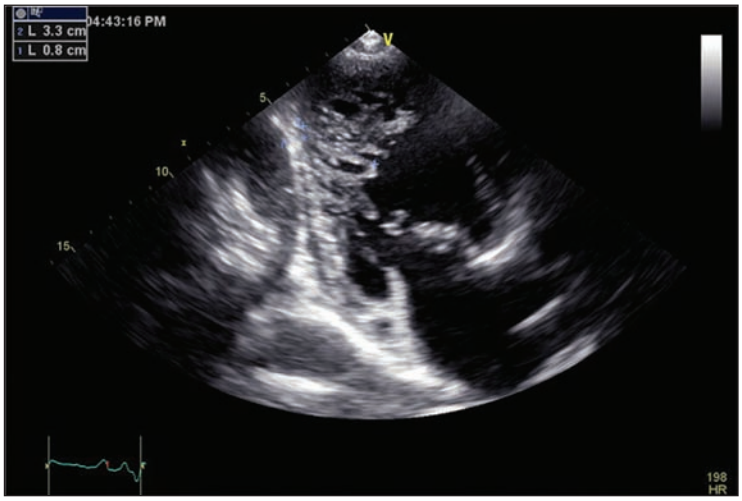

Fig: 5

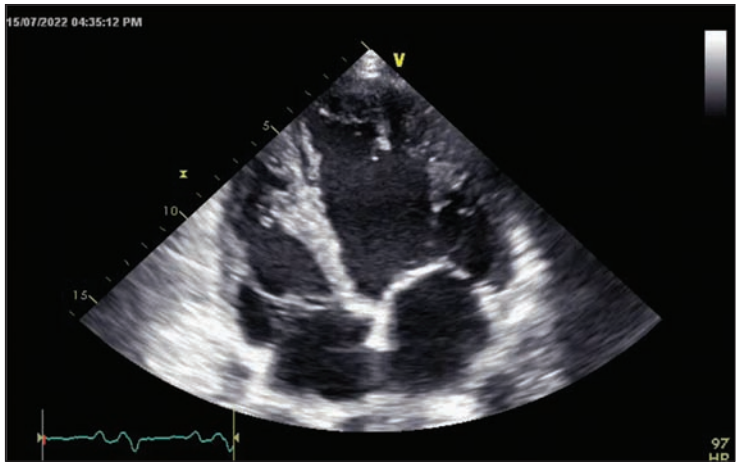

Fig: 6

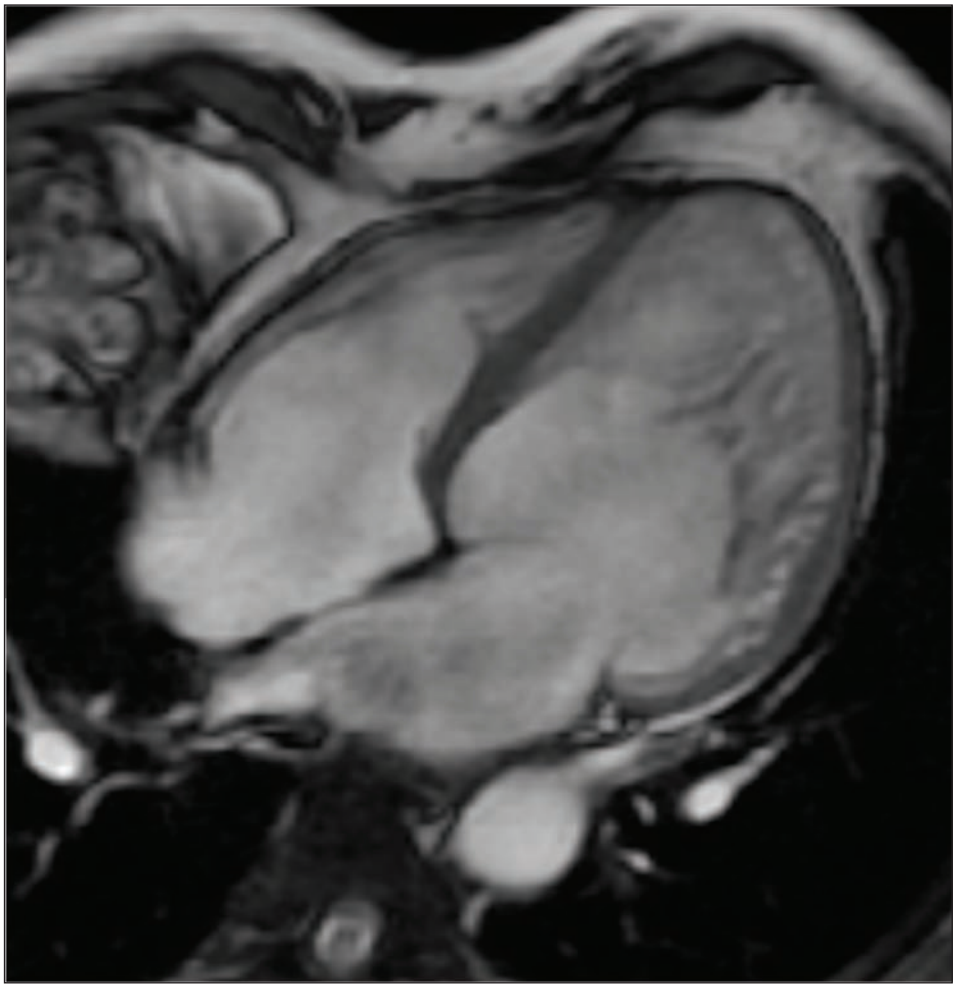

Fig: 7: Cardiac MRI

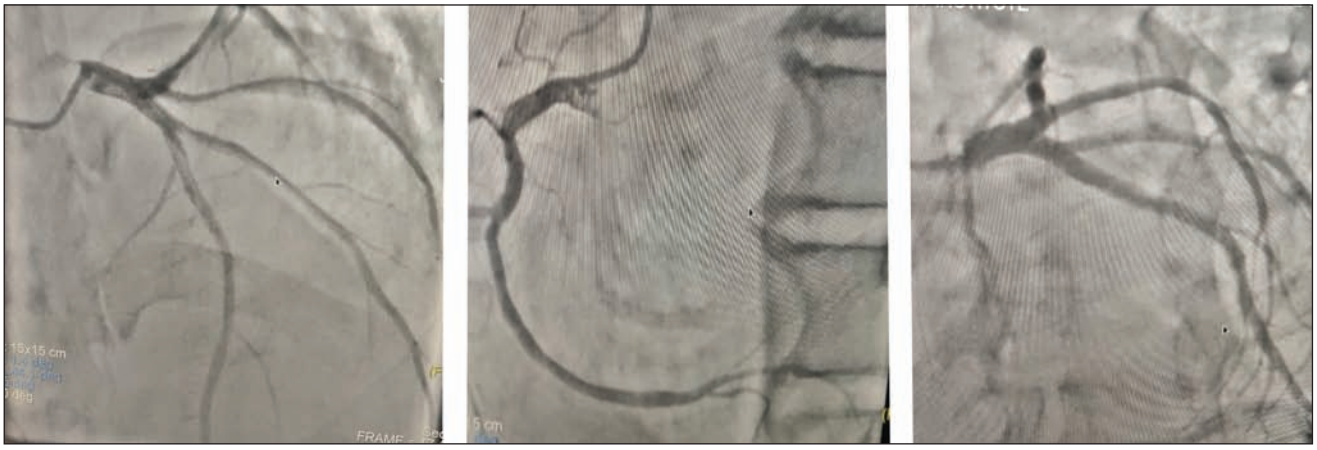

Fig: 8: Coronory angiography

ECHO AND MRI CRITERIA

There are three echo criteria and two MRI criteria for the diagnosis of Left ventricular non compaction [2]

ECHO CRITERIA	Chin	Jenni	Stollberger
	1. Numerous excessively prominent trabeculations with deep intertrabecular recesses 2. Progressive decrease in the ratio of myocardial thickness from epicardial surface to tough trough(X) and epicardial surface to peak(Y) of the trabeculations at the mitral valve and papillary muscle level(PLAX view) and apex 3. Progressive increase in the LV free wall thickness(Y) from the mitral valve level to apex	1. No coexisting cardiac abnormalities. 2. Two layered myocardial structure with a compacted (C) thin epicardial band and a thick non compacted (NC) endocardial layer of trabecular meshwork with deep endomyocardial spaces. Measurement of maximal NC/C layer. 3. Non compaction predominantly in mid lateral, mid inferior, and apical segments. 4. Color doppler evidence of deep perfused inter trabecular recesses.	1. >3 trabeculations protruding from LV wall, apical to the papillary muscles visible in one image plane. 2. Perfused inter trabecular spaces by color doppler. 3. Two layered myocardial structure with non compacted endocardial layer usually but not necessarily thicker than the compacted layer in the end systole
Cardiac phase	End diastole	Systole	-
Ratio/ Other	-	NC/C > 2.0	-

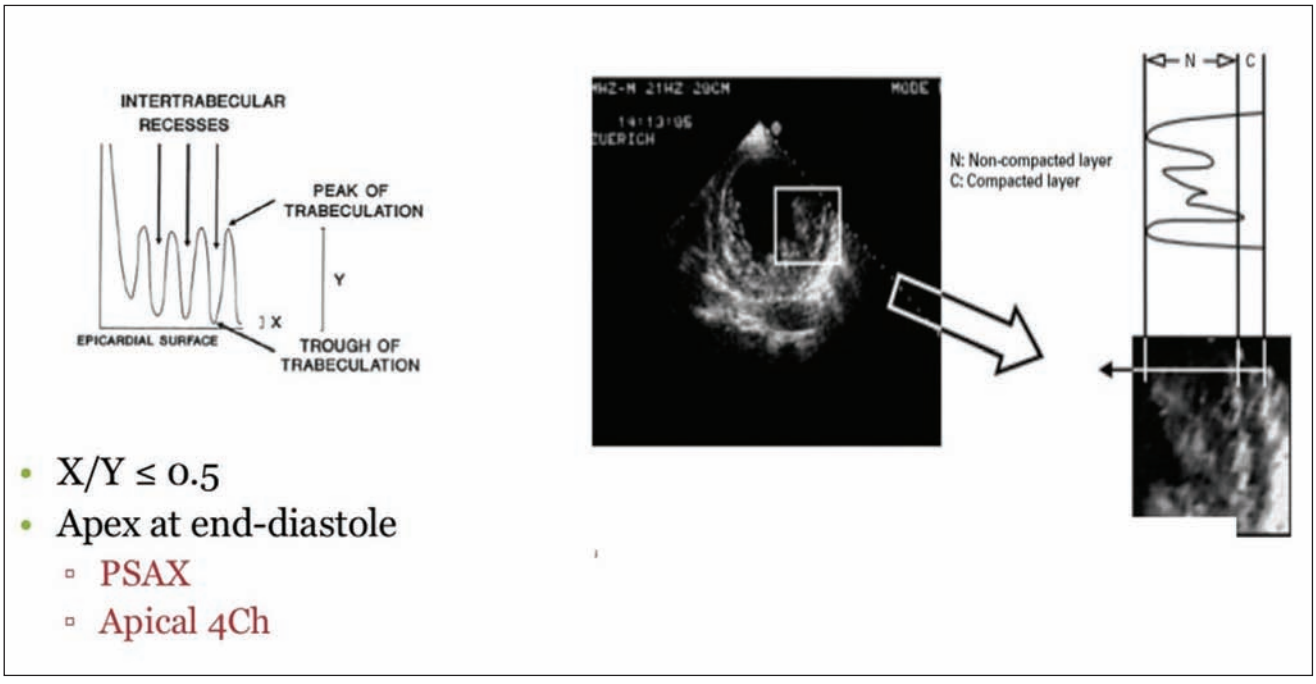

CMR		
	Petersen	**Jacquier**
Criteria	1. Two layered myocardium. 2. Compacted and non compacted segments measured from long axis SSFP cines at a site with the most prominent trabeculations. 3. Measurement should be perpendicular to the compacted myocardium (Apical segment 17 should not be used)	1. Short axis SSFP cines used to obtain total LV mass (tips of trabeculae to epicardium) 2. Same used to obtain compacted myocardial mass(epicardium to compacted endocardium) 3. Difference between first and second measurement provides trabecular mass. 4. Papillary muscles should be included in the compacted myocardial mass.
Cardiac Phase Ratio / others	Diastole NC/C 2.3	End diatole Trabecular mass >20%

MANAGEMENT

- Management strategies in LVNC are focused on genetic screening, prevention, both primary and secondary, of the major complications of LVNC cardiomyopathy, namely stroke and sudden cardiac death, secondary malignant ventricular arrhythmias, ventricular tachycardia and fibrillation, and guideline directed medical therapy (GDMT) for symptomatic congestive heart failure in the setting of systolic and or diastolic dysfunction.

- **Genetic and family screening**: Genetic evaluation, both testing and counselling, is recommended for patients with LVNC, those with one of the genetic syndromes associated with LVNC, and for patients in whom LVNC is incidentally discovered during routine medical screening . For family members in whom hypertrabeculation or LVNC is identified, close clinical surveillance should be recommended. Whereas CMR is the gold standard for diagnosing LVNC, echocardiography is used for screening the same.

- **Anticoagulation:** Hypertrabeculation and LVNC are associated with an increased risk of cardioembolic events. Current evidence supports the use of prophylactic anticoagulation for the primary prevention of thromboembolic events in patients with LVNC, HfrEF and AF and patients with intracardiac thrombi identified on ECHO or another cardiac imaging modality.

- **Sudden cardiac death**: Hypertrabeculation and LVNC are associated with increased risk of conduction abnormalities and tachyarrhythmia and systolic dysfunction secondary to LV dyssynchrony. The main indication for ICD implantation is primary prevention of sudden cardiac death. Patients with the risk of ventricular fibrillation and tachycardia in LVNC, patients who develop malignant ventricular tachyarrhythmia should undergo ICD implantation for secondary prevention[3,4].

CONCLUSION

Advances in imaging has increased recognition of the disorder. Clinical manifestations include heart failure, arrythmias and thromboembolism. Diagnosis can be made by echocardiography or CMR. LVNC has a variable prognosis. Treatment is based on clinical manifestations. It is a rare scenario to see LVNC in an elderly patient.

REFERENCES

1. van Waning JI, Caliskan K, Hoedemaekers YM, van Spaendonck-Zwarts KY, Baas AF, Boekholdt SM, van Melle JP, Teske AJ, Asselbergs FW, Backx AP, du Marchie Sarvaas GJ. Genetics, clinical features, and long-term outcome of noncompaction cardiomyopathy. Journal of the American College of Cardiology. 2018 Feb 20;71(7):711-22.
2. Wengrofsky P, Armenia C, Oleszak F, Kupferstein E, Rednam C, Mitre CA, McFarlane SI. Left ventricular trabeculation and noncompaction cardiomyopathy: a review. EC clinical and experimental anatomy. 2019 Aug;2(6):267.
3. Arbustini E, Favalli V, Narula N, Serio A, Grasso M. Left ventricular noncompaction: a distinct genetic cardiomyopathy?. Journal of the American College of Cardiology. 2016 Aug 30;68(9):949-66.
4. Udeoji DU, Philip KJ, Morrissey RP, Phan A, Schwarz ER. Left ventricular noncompaction cardiomyopathy: updated review. Therapeutic advances in cardiovascular disease. 2013 Oct;7(5):260-73.

Bempedoic Acid – "Unboxing A New Giant"

Krishna Mohan M.

Consultant Interventional Cardiologist,
CM Hospital, Pandalam, Kerala.

INTRODUCTION

Bempedoic acid is a novel, non-statin, lipid lowering therapy approved by USFDA for secondary prevention in ASCVD or primary prevention in patients with Heterozygous Familial Hypercholesterolemia as an add on to diet and maximally tolerated statin therapy.[1] It is an oral inhibitor of adenosine triphosphate (ATP)-citrate lyase (ACL) enzyme involved in cholesterol synthesis.[2,3] It has been approved in India on the lines of USFDA.

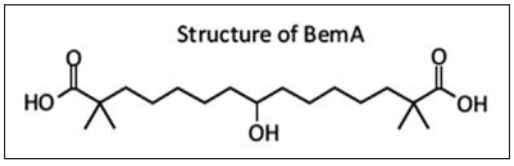

Mechanism of Action and Pharmacodynamics

Mechanism of bempedoic acid activation, metabolism, and clearance are shown in Fig.1. Bempedoic acid is a prodrug and is converted to its active form, bempedoyl CoA, by the enzyme Very long-chain acyl-CoA synthease-1 (ACSVL1).[4,5] The activity of bempedoic acid is exclusively confined to the liver[4,5] as the ACSVL1 enzyme is expressed mainly in the liver and not in the skeletal muscle. Hepatic cholesterol lowering upregulates expression of LDL-R, permitting an increased uptake of plasma LDL-C and results in lowering of LDL-C levels.

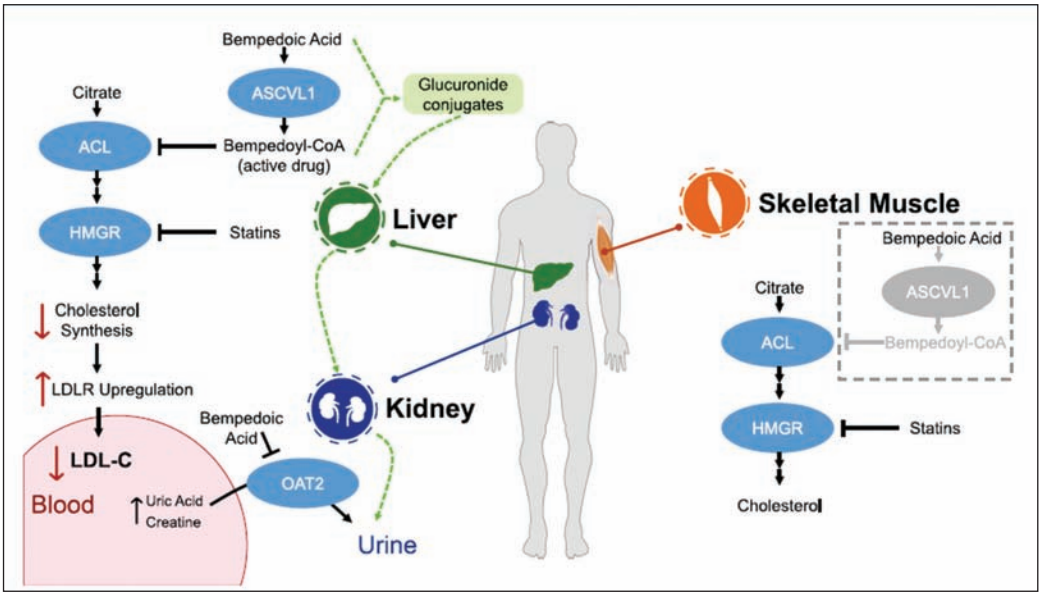

Figure:1 Adapted from: Role of Bempedoic Acid in Clinical Practice Christie M. Ballantyne & Harold Bays & Alberico L. Catapano & Anne Goldberg & Kausik K. Ray & Joseph J. Saseen Cardiovascular Drugs and Therapy. https://doi.org/10.1007/s10557-021-07147-5

Address for correspondence: Dr. Krishna Mohan M, MD, DM, Consultant Interventional Cardiologist, C M Hospital, Pandalam, Kerala.
Email: drkrishnamohanm@gmail.com

Pharmacokinetics

Bempedoic acid (prodrug) is well absorbed by the GIT and is reversibly converted to active metabolite (ESP15228). With a high plasma protein binding of 99%, it has a long plasma half-life (approx 21 hours), allowing once daily dosing.[6] The glucuronide metabolites of BA and ESP15228 are inactive and mainly excreted by the kidney (70%).[6]

No dosage adjustment is necessary. in patients with renal and hepatic impairment and are not expected to affect the efficacy or safety profile of bempedoic acid.[6]

Drug-Drug Interactions: Bempedoic acid doesn't interact with cytochrome P450 enzymes. The most important drug-drug interactions are those with simvastatin and pravastatin and doses of simvastatin >20 mg and pravastatin >40 mg should be avoided.[7]

Bempedoic Acid: Phase III clinical trials data

Four Phase 3 clinical trials have been conducted to determine the effect of bempedoic acid in patients with dyslipidemia known as the CLEAR [Cholesterol Lowering *via* ETC-1002, an ACL (ATP-citrate lyase)-Inhibiting Regimen] Trials. The CLEAR studies can be classified into two main groups based on the studied population.[6]

- The first group is the use of bempedoic acid add-ons to statins in patients who had failed to achieve LDL-C targets (*i.e.*, the CLEAR Harmony and CLEAR Wisdom).
- The second group is the use of bempedoic acid in patients with statin intolerance (*i.e.* CLEAR Serenity and CLEAR Tranquility).

Table 1: Major outcomes of the CLEAR trial[6]

Summary of phase 3 clinical studies of Bempedoic acid			
Study Name	Population Studied	Intervention	LDL-C reduction (placebo corrected difference) at 12 weeks
Bempedoic acid add-on to statin			
CLEAR Harmony	ASCVD and/or HeFH Taking maximally tolerated statin with or without other lipid-lowering agents LDL-C ≥ 70 mg/dL	Bempedoic acid 180 mg (n = 1488) *versus* placebo (n = 742)	- 18.1%
CLEAR Wisdom	ASCVD and/or HeFH Taking maximally tolerated lipid lowering therapy LDL-C ≥ 70 mg/dL	Bempedoic acid 180 mg (n = 522) *versus* placebo (n = 257)	- 17.4%
Bempedoic acid in statin-intolerant patients			
CLEAR Serenity	History of statin intolerance to ≥ 2 statins LDL-C ≥ 130 mg/dL for primary prevention LDL-C ≥ 100 mg/dL for secondary prevention in ASCVD or for HeFH	Bempedoic acid 180 mg (n = 234) *versus* placebo (n = 111) Using low-dose statin (10%) Using other lipid-lowering agents (30%) Never used lipid-lowering agents (57%)	- 21.4%
CLEAR Tranquility	History of statin intolerance with or without use of low low-dose statin LDL ≥ 100 mg/dL	Bempedoic acid 180 mg plus ezetimibe 10 mg (n = 181) *versus* placebo plus ezetimibe 10 mg (n = 88) Using low-dose statin (30%)	- 28.5%

The CLEAR Outcomes trial will evaluate the incidence of major cardiovascular events in both groups,[8] and results are expected to be reported in 2023.

In CLEAR trials, ‚Bempedoic acid was consistently associated with significant decreases in LDL-C at week 12 and reduction in hsCRP was also observed without additional adverse events.[9-12] Table 1 summarizes the major outcomes of the CLEAR trials.

Bempedoic acid - Adverse reactions

Adverse reactions reported with bempedoic acid are displayed by system organ class and frequency in table 2.

Frequencies are defined as: very common (>1/10); common (>1/100 to < 1/10); uncommon (> 1/1000 to < 1/100); Rare (> 1/10000 to <1/1000); very rare (<1/10000); and not known (cannot be estimated from the available data.

Table 2: Adverse reaction

System Organ Class	Adverse reactions	Frequency categories
Blood and lymphatic system disorders	Anemia Hemoglobin decreased	Common Uncommon
Metabolism and nutrition disorders	Gout Hyperuricemia	Common Common
Hepatobiliary disorders	AST Increased ALT Increased LFT Increased	Common Uncommon Uncommon
Musculoskeletal and connective tissue disorders	Pain extremity	Common
Renal and urinary disorders	Serum creatinine increased Blood urea increased GFR decreased	Uncommon Uncommon Uncommon

Tendon ruptures or injuries (rotator cuff, biceps or achilles tendon) were reported in 0.5% patients with bempedoic acid within weeks to months, commonly in patients more than 60 years of age.[13] Corticosteroids / fluoroquinolones / renal failure / and previous tendon disorders adds to the risk of tendon rupture.

The decrease in hemoglobin levels with bempedoic acid within the first 4 weeks of treatment, was stable over time, and reversible on discontinuation of the drug.

The incidence of new-onset or worsening diabetes is lower with bempedoic acid.[14]

Contraindications[15]

- Hypersensitivity to the active substance or any of the inactive ingredients
- Pregnancy and lactation
- Concomitant use with simvastatin > 40 mg daily

Special considerations[15]

- No dose adjustment is necessary in elderly patients.
- The safety and efficacy of BA in children aged less than 18 years have not yet been established.
- No dose adjustment is necessary in patients with mild or moderate renal and hepatic impairment.

Conclusion

Bempedoic acid provides an important alternative to ezetimibe and PCSK 9 inhibitors for further LDL-C lowering in statin-intolerant patients or in those

requiring further LDL-C reduction despite maximally tolerated statin therapy. 2018 ACC/AHA/MS Cholesterol guideline was published prior to data from CLEAR trials and hence bempedoic acid was not officially included as a non-statin option.

2019 European Society of Cardiology/ European Atherosclerosis Society (ESC/EAS) guideline for the management of dyslipidemias have included bempedoic acid as a potential novel therapy for LDL-C lowering.[16] Data on the impact of bempedoic acid on cardiovascular outcomes is awaited in the ongoing CLEAR Outcomes trial.

REFERENCES

1. Niman S et al. A Review of the Efficacy and Tolerability of Bempedoic Acid in the Treatment of Hypercholesterolemia. Am J Cardiovasc Drugs. 2020 Dec;20(6):535-548
2. Nexletol. Package insert. Esperion Therapeutics, Inc; 2020.
3. NILEMDO. Summary of product characteristics. Daiichi Sankyo Europe GmbH; 2020.
4. Pinkosky SL, Filippov S, Srivastava RA, Hanselman JC, Bradshaw CD, Hurley TR, et al. AMP-activated protein kinase and ATPcitrate lyase are two distinct molecular targets for ETC-1002, a novel small molecule regulator of lipid and carbohydrate metabolism. J Lipid Res. 2013;54:134–51.
5. Pinkosky SL, Newton RS, Day EA, Ford RJ, Lhotak S, Austin RC, et al. Liver-specific ATP-citrate lyase inhibition by bempedoic acid decreases LDL-C and attenuates atherosclerosis. Nat Commun. 2016;7:13457.
6. Wichaiyo S et al. Bempedoic Acid: A New Non-statin Drug for the Treatment of Dyslipidemia. Clin Drug Investig. 2021 Oct;41(10):843-851
7. Emery M, Hanselman JC, MacDougall D, Amore B, Sasiela W. A phase 1 drug-drug interaction study assessing the effects of steady state (SS) probenecid (PB) on single-dose bempedoic acid (BA) pharmacokinetics (PK) in healthy subjects. Presented at: American Society for Clinical Pharmacology and Therapeutics
8. Nicholls SJ, Lincoff AM, Bays HE, Cho L, Grobbee DE, Kastelein JJP, et al. Rationale and design of the CLEAR-Outcomes trial: Evaluating the effect of bempedoic acid on cardiovascular events in patients with statin intolerance. Am H J. 2020; 235:104–112.
9. Ray KK, Bays HE, Catapano AL, Lalwani ND, Bloedon LT, Sterling LR, et al. Safety and efficacy of bempedoic acid to reduce LDL cholesterol. N Engl J Med. 2019; 380:1022–32.
10. Goldberg AC, Leiter LA, Stroes ESG, Baum SJ, Hanselman JC, Bloedon LT, et al. Effect of Bempedoic acid vs placebo added to maximally tolerated statins on low-density lipoprotein cholesterol in patients at high risk for cardiovascular disease: the CLEAR Wisdom randomized clinical trial. JAMA. 2019; 322:1780–8.
11. Laufs U, Banach M, Mancini GBJ, GaudetD, Bloedon LT, Sterling LR, et al. Efficacy and safety of bempedoic acid in patients with hypercholesterolemia and statin intolerance. J Am Heart Assoc. 2019;8: e011662.
12. Ballantyne CM, Banach M, Mancini GBJ, Lepor NE, Hanselman JC, Zhao X, et al. Efficacy and safety of bempedoic acid added to ezetimibe in statin-intolerant patients with hypercholesterolemia: a randomized, placebo-controlled study. Atherosclerosis. 2018;277: 195–203.
13. Yang Y, Lu H, Qu J. Tendon pathology in hypercholesterolaemia patients: epidemiology, pathogenesis and management. J Orthop Translat. 2019; 16:14–22.
14. Preiss D, Seshasai SR, Welsh P, Murphy SA, Ho JE, Waters DD, et al. Risk of incident diabetes with intensive-dose compared with moderate-dose statin therapy: a meta-analysis. JAMA. 2011;305: 2556–64.
15. Bempedoic Acid Prescribing Information accessed on 21st April 2022
16. Mach F, Baigent C, Catapano AL, et al. 2019 ESC/EAS guidelines for the management of dyslipidaemias: lipid modification to reduce cardiovascular risk. Eur Heart J 2020; 41:111-88

KJC Focus Issues

(Available online at www.icckeralachapter.org)

KJC 1 - Congenital Heart Diseases

KJC 2 - Valvular Heart Diseases

KJC 3 - Interventions of Inter Atrial Septum

KJC 4 - Pulmonary Hypertension

KJC 5 - Hypertrophic Cardiomyopathy

KJC 6 - Imaging in Cardiology

KJC 7 - The Future Beckons

Write, and find your own Space ...

Team KJC invites articles

(Original research, Review articles, Case reports, Images, Perspective).

Email: sajanahmad@gmail.com

The Official Journal of Indian College of Cardiology, Kerala Chapter